Auditory Neural Oscillations and Excitation/Inhibition Balance in Emerging Psychosis

Hanna E Å Thuné (MSc)

A thesis submitted in fulfilment of the requirements for the Degree of

Doctor of Philosophy

Institute of Neuroscience & Psychology

College of Medical, Veterinary and Life Sciences

University of Glasgow

June 2019

Abstract

Chronic schizophrenia (ScZ) is associated with impaired gamma oscillations, reflected by robust alterations in 40 Hz ASSR. Oscillatory deficits may arise from changes in the cortical E/I-balance. However, it is unclear whether aberrant oscillations and potential underlying mechanisms are present also in early and clinical high risk (CHR) stages of psychosis.

In this thesis, data from a multimodal CHR study were used to explore auditory oscillatory alterations in CHR individuals, assessed using MEG-recorded 40 Hz Auditory Steady State Response (ASSR) measures, with the aim to establish how deficits may account for early alterations in neural circuits in emerging psychosis. To further map such changes, a group of first episode of psychosis (FEP) participants were also studied, and oscillatory measures were compared with H1-MRS measures of neurotransmitter levels as well as with clinical measures.

The thesis first presents a meta-analysis of ASSR findings in ScZ so far, showing that the response is impaired in chronic patients. Each of the following four chapters respectively present separate data analyses, focusing on baseline ASSR data, connectivity analyses, proton magnetic resonance spectroscopy (1H-MRS) analyses, and data assessing longitudinal outcomes.

Through these investigations, the thesis demonstrates impairments in RSMG 40 Hz spectral power and ITPC in CHR and FEP, with bidirectional connectivity impairments present between RSMG and primary auditory cortex in CHR participants. In addition, strong beta frequency reductions in power were observed in CHR and FEP participants relative to controls. No clear impairments were detected in 1H-MRS data, but a trend deficit in right auditory GABA levels was seen in FEP patients. Finally, investigations of longitudinal parameters revealed that RSMG oscillatory impairments are related to functioning at the time of scanning, but not to functioning at the one-year follow-up. Moreover, beta frequency power was found to be selectively impaired in individuals with sustained CHR symptoms and low GAF scores (at both baseline and 12 months).

Combined, the results of this thesis provide evidence for complex, subtle neural circuit alterations in emerging psychosis, which can be captured non-invasively using the 40 Hz ASSR paradigm.

Table of Contents

List of Tables

List of Figures

Acknowledgement

I would like to thank my supervisor Professor Peter Uhlhaas for his help and guidance over the past four years. A special thank you also to Dr Tineke Grent-t'Jong, as this PhD journey would have been much more difficult without her. Thank you for your support through the ups and downs!

Next, I would like to thank all the members working as part of the YouR-study research team. Thanks particularly to Emmi Mikanmaa, who worked on her PhD project alongside me and provided both moral and practical support along the way, to Lingling Hua and Dr Marc Recasens who collected MEG data and discussed analyses with me, to Kelly Chung and Dr Frauke Schultze-Lutter who trained me to perform psychological assessments and to Frances Crabbe who taught me to operate the MRI-scanner. These are just some of all the researchers, students and interns who helped on both a personal and professional level throughout the years. Thank you all!

Finally, I sincerely thank my friends and family for their endless encouragement. Thanks especially to my greatest supporters, my parents Maria and Michael and my love Phil. You kept me going and reminded me of what matters in life.

Author’s declaration

I declare that this thesis represents my own work unless indicated in the text, and that it does not include work forming part of a thesis presented for another degree.

_____

Hanna Thuné

Published articles

The findings presented in Chapter 3 have been published:

Thuné, H., Recasens, M., & Uhlhaas, P. J. (2016). The 40-Hz Auditory Steady State Response in Patients with Schizophrenia. JAMA Psychiatry, 73(11), 1145–1153. http://doi.org/10.1001/jamapsychiatry.2016.2619

Abbreviations

1H-MRS	Proton Magnetic Resonance Spectroscopy
AAL atlas	Automated Anatomical Labelling atlas
ASSR	Auditory Steady State Response
BACS	Brief Assessment of Cognition in Schizophrenia
BLIPS	Brief Limited Intermittent Psychotic Symptoms
CAARMS	Comprehensive Assessment of At-Risk Mental States
CHR	Clinical High Risk
DSM	Diagnostic and Statistical Manual of Mental Disorders
DTI	Diffusion Tensor Imaging
EEG	Electroencephalography
E/I	Excitation/Inhibition
ERP	Event-Related Potentials
FEP	First Episode of Psychosis
Fdr	False Discovery Rate
FFT	Fast Fourier Transformation
GABA	γ-Aminobutyric Acid
GAF	Global Assessment of Functioning
Glx	Glutamate-Glutamine Complex
GM	Grey Matter
HC	Healthy Controls
ICD	International Statistical Classification of Diseases and Related Health Problems
ITPC	Inter-Trial Phase Coherence
LCMV	Linearly Constrained Minimum Variance
MEG	Magnetoencephalography
MRI	Magnetic Resonance Imaging
NAA	N-acetyl aspartate
NMDA	N-methyl-D-aspartate
PV	Parvalbumin
RT	Reaction Time
ScZ	Schizophrenia
SOM	Somatostatin
SPI-A	Schizophrenia Proneness Instrument (Adult version)

Chapter 1 A General Introduction to Schizophrenia and Psychosis Risk States

1.1 Aim

Schizophrenia (ScZ) patients show robust impairments in neural oscillations (Uhlhaas & Singer, 2011; Uhlhaas & Singer, 2010), thought to reflect changes in the cortical excitation/inhibition (E/I) balance. Neural oscillations arise from the interaction between excitatory glutamatergic and inhibitory GABAergic signals (Bartos, Vida, & Jonas, 2007) and appear to play an important role in both cognitive and sensory functions (Fries, 2015; Siegel, Donner, & Engel, 2012; Ward, 2003). Thus, the oscillatory impairments in ScZ may reflect a core pathophysiological mechanism that could account for the severe cognitive and sensory dysfunctions in the disorder (Shin, O'Donnell, Youn, & Kwon, 2011; Uhlhaas & Singer, 2010).

The 40 Hz auditory steady state response (ASSR) is an oscillatory measure assessed using electroencephalography (EEG) or magnetoencephalography (MEG), which is impaired in chronic ScZ patients (Thuné, Recasens, & Uhlhaas, 2016). Likewise, magnetic resonance spectroscopy (1H-MRS) measures of glutamate and GABA have indicated altered E/I-balance in ScZ patients (Wijtenburg, Yang, Fischer, & Rowland, 2015). However, a direct link between the 40 Hz ASSR-deficits and alterations in GABAergic/Glutamatergic transmission has not been systematically explored. Furthermore, it is still unclear whether the 40 Hz ASSR could be a candidate marker for the detection of first-episode psychosis (FEP), or even participants at clinical high risk (CHR) for the development of ScZ, since it is unknown when 40 Hz ASSR impairments first emerge.

The available data from early-stage psychosis remain limited compared to the chronic ScZ literature. So far, one group has explored the 40 Hz ASSR in CHR individuals (Koshiyama et al., 2018a; Tada et al., 2016). Moreover, several groups have reported measures of GABA and glutamate levels in CHR samples (Bossong et al., 2018; Fuente-Sandoval, Leon-Ortiz, Favila, Stephano, & Mamo, 2011; Fuente-Sandoval et al., 2016; Fusar-Poli et al., 2011; Menschikov et al., 2016; Modinos, Şimşek, et al., 2018; Natsubori et al., 2014; N. Tandon et al.,

2013; Wood et al., 2010; Yoo et al., 2009), but to the author's knowledge nobody has yet attempted to look directly at the relationship between these measures in CHR.

Hence, the overarching aim of this thesis is to explore neuromagnetic 40 Hz ASSR and 1H-MRS measures of cortical GABA and Glx (Glutamate + Glutamine) in a large cohort of CHR individuals, with the objective to identify the nature of potential early oscillation and E/I changes. The a priori hypotheses were based on findings in ScZ populations:

1. CHR individuals will show reduced 40 Hz ASSR power and inter-trial phase coherence (ITPC) compared to healthy controls.

2. CHR individuals will show altered network connectivity compared to healthy controls.

3. CHR individuals will show impaired balance between Glx and GABA compared to healthy controls.

In addition, an FEP group was included in the analyses to allow comparisons with CHRs and controls, and to replicate previous FEP findings. CHR participant measures were hypothesised to be intermediate between controls and FEPs, with the FEP patients showing more pronounced impairments.

Furthermore, the relationship of oscillatory and neurochemical measures with psychological and neurocognitive data was explored, with the aim to establish if and how cortical oscillatory data may reflect clinical characteristics.

The following introductory sections serve to provide an overview of ScZ, focusing particularly on the postulated role of gamma oscillations and their association with the cortical E/I balance.

1.2 ScZ Prevalence

ScZ is a severe psychotic disorder with a typical age of onset in late adolescence or early adulthood (McGrath et al., 2016). Compared to women, men have an

earlier onset of approximately 4-5 years (Angermeyer & Kühn, 1988). The life-time prevalence is estimated to be approximately 1% worldwide (Millan et al., 2016) with highest prevalence among males, in urban areas and migrant communities (McGrath et al., 2004), highlighting the complex influence of social and environmental factors on the disorder.

Psychotic disorders, such as ScZ, are associated with substantial economic costs (Gustavsson et al., 2011). In Europe alone, ScZ and other psychotic disorders cost € 93.9 billion in 2010 (Gustavsson et al., 2011). These costs are explained by the long-term functional impairment experienced by ScZ patients, resulting in productivity loss and the need for continuous treatment and healthcare support (Jin & Mosweu, 2017).

Moreover, the personal costs of illness are also high. ScZ contributed 13.4 million years of life lived with disability to burden of disease globally in 2016 (Charlson et al., 2018) and is associated with a shorter life-span (Rössler, Joachim Salize, Van Os, & Riecher-Rössler, 2005) and a high risk of suicide (Gottesman, 1990). Furthermore, attempts to measure the quality of life experienced by ScZ patients (Bobes, Garcia-Portilla, Bascaran, Saiz, & Bousoño, 2007) suggest that patients experience an overall lower life quality not only compared to healthy individuals, but also lower than people with other chronic illnesses. Crucially, the quality of life declined progressively in relation to the duration of the disorder (Bobes et al., 2007), highlighting the importance of developing better and earlier treatments and intervention methods.

1.3 Conceptual Evolution and Clinical Symptoms of ScZ

While diagnostic criteria of ScZ have changed over time, the disorder is widely defined as a chronic condition with poor outcome (Schultz, North, & Shields, 2007; R. Tandon et al., 2013). The condition is associated with three distinct symptom groups (R. Tandon et al., 2013), including negative (avolition, anhedonia, affective blunting, alogia etc.) (Millan, Fone, Steckler, & Horan, 2014), positive (hallucinations and delusions) (Schultz et al., 2007), and cognitive symptoms (Schaefer, Giangrande, Weinberger, & Dickinson, 2013).

The concept of ScZ emerged as the result of early clinical observations (Jablensky, 2010). The French physician Morel observed characteristic psychotic symptoms in his young patients and labelled the condition démence précoce. Kahlbaum and Hecker described the conditions hebephrenia and catatonia which also shared features with ScZ (Adityanjee, Aderibigbe, Theodoridis, & Vieweg, 1999). Eventually, reports were integrated by the German psychiatrist Emil Kraeplin to describe a condition called dementia praecox (Jablensky, 2010).

Kraeplin's work on dementia praecox formed the foundation for the modern-day understanding of ScZ. He put emphasis on the chronic nature of the disorder, and highlighted avolition and poor prognosis as key clinical features (Andreasen, 1997; R. Tandon et al., 2013). In addition, he attempted to map the underlying aetiology, including factors such as age of onset, family history and premorbid behavioural patterns (Adityanjee et al., 1999). He also proposed a biological framework for the condition, involving serious cerebral cortical lesions (Adityanjee et al., 1999).

The term schizophrenia was coined by the Swiss psychiatrist Eugene Bleuler. He was influenced by psychoanalytic as well as neurological ideas and aimed to understand individual patient experiences of ScZ in the context of an underlying disease process (Hoff, 2015). His description of the illness focused primarily on four features which he considered fundamental to the disorder: loosening of associations, affective flattening, autism and ambivalence. Other symptoms such as hallucinations, delusions and changes in speech were considered accessory or secondary as they varied between patients (Adityanjee et al., 1999).

Subsequently, the concept was further advanced by the contributions of Kurt Schneider, who like Bleuler strived to identify and classify the main features of ScZ (Andreasen, 1997). He acknowledged both long- and short-term features of the disorder and introduced a list of "first-rank symptoms", which allowed for more unified diagnostic procedures (Adityanjee et al., 1999). In the symptom list, Schneider highlighted hallucination and delusion symptoms which Kraeplin and Bleuler had considered of less importance, with the aim to identify the most clinically meaningful characteristics (Andreasen, 1997; Jablensky, 2010).

Diagnosing ScZ remains a largely subjective process, based on patient reports of and clinical consensus (R. Tandon, Keshavan, & Nasrallah, 2008). A diagnosis is established using the current versions of the Diagnostic and Statistical Manual of Mental Disorders (DSM) (DSM-V American Psychiatric Association, 2013) or the International Statistical Classification of Diseases and Related Health Problems (ICD) (World Health Organization, 2018). In the DSM-V, a patient is diagnosed with ScZ if they have experienced two or more positive and/or negative symptoms continuously for one month (or shorter if successfully treated), and a notable impairment and functional decline for a duration of six months (R. Tandon et al., 2013). For an ICD-11 diagnosis of ScZ, persistent symptoms of delusions, hallucinations, thought disorder, experiences of influence, passivity, or control must have persisted for at least one month (World Health Organization, 2018).

Positive symptoms include hallucinations and delusions (Fletcher & Frith, 2009). Hallucinations are false perceptions and can occur in any sensory modality, while delusions are beliefs and convictions which are highly unlikely and which cannot be explained by the individuals cultural background (Fletcher & Frith, 2009). These symptoms are generally improved or fully treated by the administration of antipsychotic medication, but patients' functioning tends to remain low even after drug treatment due to the limited effect of medications on the remaining two symptom categories (Chue & Lalonde, 2014; Fusar-Poli, Papanastasiou, et al., 2015).

Negative symptoms of psychosis are debilitating and include widespread functional impairments, such as social withdrawal, avolition, anhedonia, affective flattening, as well as poverty of speech and thought (Andreasen, 1982; Crow, 1976). While the symptom features of ScZ are diverse and tend to vary between patients, around 40% of patients have been found to have two or more negative symptoms (Patel et al., 2015), with symptom severity associated with likelihood of hospital admission (Patel et al., 2015) and long-term functional outcome (Milev, Ho, Arndt, & Andreasen, 2005). As such, negative symptoms are a prominent feature of ScZ and may indicate clinical vulnerability.

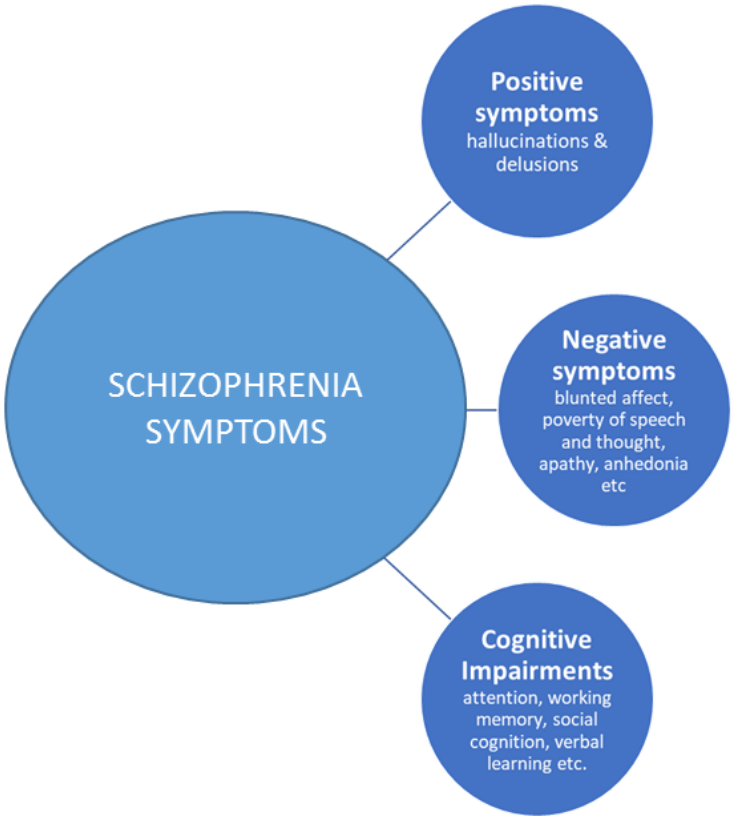

Figure 1 Overview of the Main Symptom Categories Observed in ScZ

Cognitive impairments have been recognized as the third core symptomatic feature of ScZ since the disorder was first described (Moskowitz & Heim, 2011), and are detrimental for patients' overall functioning, affecting areas such as social relationships, work performance and recreational activities (Bowie & Harvey, 2006; Green, Kern, Braff, & Mintz, 2000; Milev et al., 2005). Neurocognitive abnormalities are widespread, including domains such as attention (Luck & Gold, 2008), working memory (McGurk et al., 2004), and verbal memory (Bowie & Harvey, 2006; Guimond, Chakravarty, Bergeron-Gagnon, Patel, & Lepage, 2016).

In addition, social cognitive functions such as social cue perception, experience sharing, inferring other people's thoughts and emotions and emotional response regulation are also affected in ScZ patients (Green, Horan, & Lee, 2015). Importantly, cognitive abnormalities are understood to be among the first occurring symptoms, typically preceding the onset of psychosis (Fusar-Poli et al., 2012), and tend to be stable over time in contrast to other symptoms of psychosis which typically go through periods of improvement and relapses (Bowie

& Harvey, 2006). However, current antipsychotic drugs are inadequate for the treatment of these symptoms (Bowie & Harvey, 2006).

Cognitive and social cognitive impairments are thought to be closely linked to abnormalities in basic sensory processing (Hamilton et al., 2018). Low level sensory processing was previously thought to be intact in ScZ, yet research from recent decades has detected sensory processing abnormalities in all sensory modalities (Javitt, 2009).

1.4 Auditory Symptoms in ScZ

Auditory function is adversely affected in ScZ (Javitt & Sweet, 2015). Auditory hallucinations are a prominent feature of ScZ (Shergill, Murray, & McGuire, 1998), occurring in 60-80% of patients (A. Lim et al., 2016). Moreover, ScZ is associated with impaired basic auditory processing mechanisms and deficit auditory cognitive functions (Javitt & Sweet, 2015). As such, auditory impairments contribute to impairments across all major symptom domains of ScZ.

Auditory dysfunction is reflected by neuroimaging measures, providing empirical evidence for impairments in auditory sensory gating mechanisms as well as salient stimulus detection and oscillatory steady state response patterns in ScZ (Javitt & Sweet, 2015). Deficits in the fundamental sensory processes reflected by these measures may be closely linked to cognitive difficulties, possibly through faulty information filtering (Hamilton et al., 2018). Hence, auditory processing measures may be clinically useful for understanding and detecting early impairments in psychosis and could potentially constitute candidate biomarkers.

1.5 The At-Risk State

The clinical view of psychosis has developed over the past couple of decades to now recognize the importance of the pre-psychotic phase (Fusar-Poli et al., 2013). Individuals who go on to develop a psychotic disorder typically experience a prodromal period during which they begin to experience subtle changes in their experience of the world (Parker, 2006). This involves the onset of mild

symptoms such as subjective difficulties in concentration, perception, speech and thought patterns (basic symptoms) (Schultze-Lutter, 2009), and may eventually lead to attenuated psychotic symptoms, including delusions that are not held with complete conviction and not fully formed hallucinations (Yung, Yuen, Phillips, Francey, & McGorry, 2003).

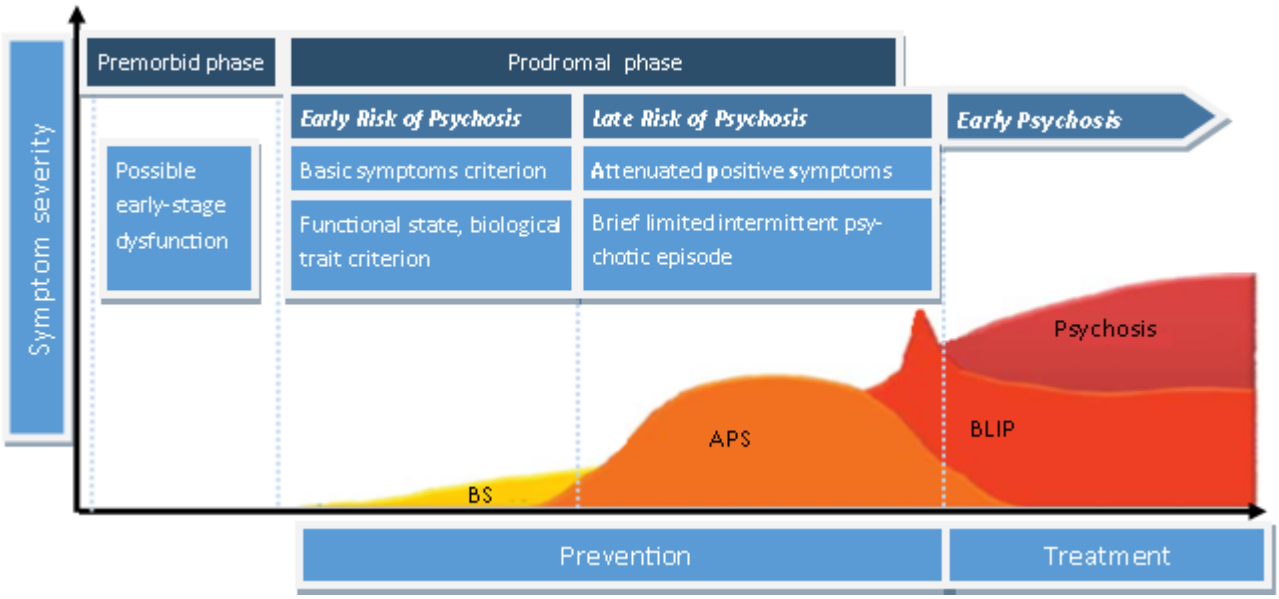

Figure 2 Psychosis Onset Trajectory, Adopted from Fusar-Poli et al., 2013

The earliest concept of prodromal psychosis was coined in the early 1900's and marked the start of a large research field focused on the study of individuals at-risk for psychosis (Fusar-Poli et al., 2013). Prodromal psychosis refers to patients who proceed to transition to psychosis. However, individuals may be considered at-risk regardless of later onset of psychosis if they meet a specific set of clinical criteria ("clinical high risk" – CHR, or "ultra-high risk" – UHR). In addition, individuals who have a first-degree relative suffering from a psychotic disorder form a separate high-risk group ("genetic high risk") (Fusar-Poli et al., 2013).

An important motivation for studying these groups is to map differences and similarities compared to psychotic patients, to identify mechanisms underlying the disorder, differentiate disorder impairments from side-effects caused by long-term medication, and to allow for earlier interventions (Fusar-Poli et al., 2013). The latter is thought to be of high importance in light of the observed

association between duration of untreated psychosis and poor long-term functional outcomes (Marshall et al., 2005).

To date, a number of interview measures have been developed with the purpose of detecting individuals in the at-risk state: The ScZ Proneness Instrument – Adult/Child and Adolescent versions (SPI-A or SPI-CY) was developed to detect the subtle subjective basic symptoms which typically present first (Schultze-Lutter, 2009), while the Comprehensive Assessment of At-Risk Mental States (CAARMS) (Yung et al., 2005), the Structured Interview for Prodromal Symptoms (SIPS) (including the companion Scale of Prodromal Symptoms [SOPS]) (Miller et al., 2003), and the Basel Screening Instrument for Psychosis (BSIP) (Riecher-Rössler et al., 2007) are all used to detect the later attenuated psychotic symptoms. Furthermore, the latest DSM manual (DSM-V) recognizes the at-risk Attenuated Psychosis Syndrome as a clinical state which in itself warrants diagnosis and treatment (Fusar-Poli et al., 2017). However, low specificity has limited the clinical use of at-risk measures, with meta-analysis results indicating transition in 18-36% of at-risk participants depending on duration of follow-up from 6 months to 3 years)(Fusar-Poli et al., 2013). In addition, prior to the inclusion of the Attenuated Psychosis Syndrome in the DSM-V, experts debated the usefulness and potential harmfulness of such a diagnosis (Shrivastava et al., 2011), with some raising concerns about ethical issues such as the possibility that the label could lead to unnecessary stigma (Yang, Wonpat-Borja, Opler, & Corcoran, 2010) , while others argued that even CHR individuals who did not convert were ill and would benefit from treatment (Ruhrmann, Schultze-Lutter, & Klosterkötter, 2010). Later evaluations have indicated that the clinical recognition of the CHR state can have beneficial effects for help-seeking patients (Fusar-Poli et al., 2017).

Currently, CHR diagnosis relies on psychological assessments (Fusar-Poli et al., 2013), yet identification of objective methods to detect CHR individuals could aid early detection and interventions. Since chronic ScZ patients show debilitating impairments in cognition, efforts have been made to map whether cognitive deficits could serve as a risk-marker. Robust widespread impairments were seen in CHR compared to healthy controls across several cognitive domains (De Paula, Hallak, Maia-de-Oliveira, Bressan, & Machado-de-Sousa, 2015; Fusar-

Poli et al., 2012), with impairments in verbal fluency and memory associated with subsequent transition to psychosis (Fusar-Poli et al., 2012) and normal verbal fluency in CHR being predictive of later remission from the at-risk state (Simon et al., 2012). Notably, CHR cognitive capacity was intermediate between that of healthy controls and psychosis patients (Fusar-Poli et al., 2013). Thus, evidence indicates that cognitive impairments are present but less pronounced in CHR and that cognitive performance may be useful for assessments of long-term outcome.

Functional neuroimaging methods have been utilized to study aberrant activity patterns in CHR. EEG and MEG measures of event-related potentials (ERPs) have revealed impaired auditory P50 and N100 sensory gating in chronic and first episode ScZ patients (Javitt & Sweet, 2015), with one study also reporting deficit P50 but not N100 suppression in CHR (Brockhaus-Dumke et al., 2008). The P50 peak is thought to be pre-attentive and linked primarily to stimulus filtering, while the N100 is affected by attention and appears to be functionally related to passive attention switching (Kisley, Noecker, & Guinther, 2004; Rosburg, Trautner, Elger, & Kurthen, 2009), suggesting that basic auditory sensory gating but not auditory attention switching is impaired in the CHR state. Another ERP implicated in ScZ is the mismatch negativity (MMN) response (Mikanmaa et al., 2017), elicited by the detection of change (Näätänen & Kähkönen, 2009). The MMN has been linked to the framework of predictive coding (Wacongne, 2016), and impairments in ScZ indicate a reduced ability to detect and adjust to unexpected changes in sensory input (Erickson, Ruffle, & Gold, 2015). However, CHR findings have varied, and several reports suggest that the impairment on group level is driven specifically by individuals who eventually transition to psychosis (Bodatsch, Brockhaus-Dumke, Klosterkotter, & Ruhrmann, 2015).

Functional EEG and MEG measures have also been used to map neural oscillatory patterns in patients. This could provide essential information about disease mechanisms, yet the knowledge about neural oscillations in the CHR population remains limited. In Chapter 4, new data from an oscillatory ASSR paradigm in a large CHR sample are presented, with the aim to shed more light on oscillatory changes in this important clinical group.

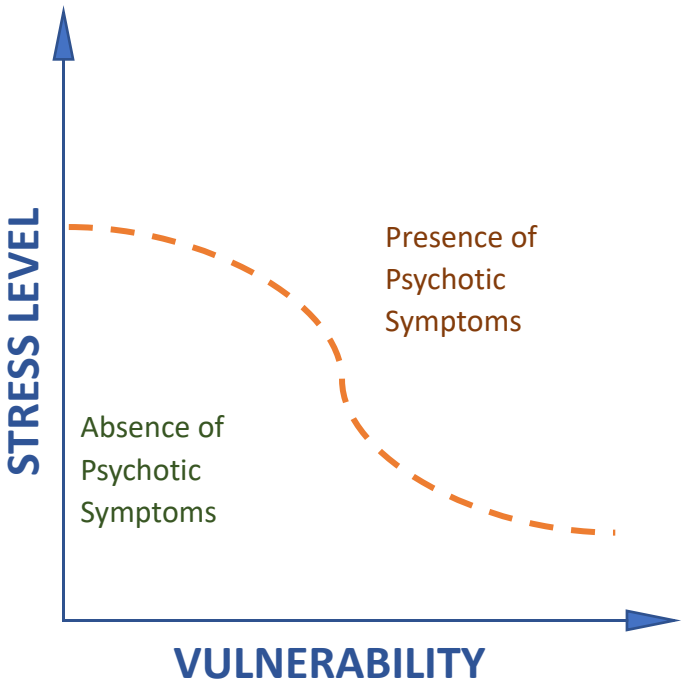

Figure 3 The Stress Vulnerability Model of ScZ Assumes that Increased Vulnerability to stress Increases the Likelihood of Experiencing a Psychotic Episode

1.1 Neurobiology of ScZ

Despite more than a century of research, ScZ is still only partially understood. It is thought that the disorder arises through the interplay of genetic risk factors, developmental abnormalities and external stressors (Gomes, Rincón-Cortés, & Grace, 2016; Howes & McDonald, 2004; Selemon & Zecevic, 2015). ScZ risk has a clear genetic component, with over 100 identified risk genes (Ripke et al., 2014), and high heritability (Hilker et al., 2018). Yet, external disruptions in early brain development during gestation and early infancy (for example maternal infection or malnutrition), and during later cortical maturation in adolescence (such as cannabis abuse) is also strongly linked to ScZ risk (Selemon & Zecevic, 2015). The combination of genetic risk and aberrant neural development may render patients more vulnerable to stressors (Figure 3), such as early trauma (Howes & McDonald, 2004). This framework is supported by in-vivo work: Animals exposed to a combination of neonatal excitotoxic lesions of the medial prefrontal cortex (mPFC) and cannabis in adolescence showed severely impaired social behaviour, similar to social impairments seen in psychotic patients (Schneider & Koch, 2005). Similarly, the MAM model is a rat stress vulnerability model, created through exposure to the mitotoxin

methylazoxymethanol acetate (MAM) during gestational day 17, and results in animals showing ScZ like behavioural, neurochemical and anatomical features (Gomes et al., 2016).

Neurochemical models of ScZ provide potential frameworks to explain how impairments may be mediated on a neurotransmitter level. For a long time, the dominant hypothesis postulated that ScZ emerges from alterations in dopaminergic signalling. The dopamine hypothesis stems from the early observation that drugs effective for alleviating positive symptoms acted on the dopaminergic system by increasing dopamine metabolism (Carlsson & Lindqvist, 1963; Howes, McCutcheon, & Stone, 2015). Subsequent work demonstrated that clinical antipsychotic efficacy was directly related to dopamine receptor binding (Creese, Burt, & Snyder, 1976), adding further support for the notion that hyperdopaminergic activity caused symptoms of ScZ. However, later post-mortem, lesion and PET studies indicated more complex alterations, involving striatal increases but frontal decreases in dopaminergic activity, proposed to each reflect positive and negative symptoms respectively (Howes & Kapur, 2009). While further research has provided additional evidence for this framework, the most recent formulation of the hypothesis highlights that these dopamine alterations are mostly presynaptic, may be caused by a range of contributing factors including genetic predisposition, environmental stress and drug use, and that the result of the dysregulation is psychosis rather than a specific diagnosis (such as ScZ) (Howes & Kapur, 2009).

The link between dopamine and ScZ has guided research and clinical approaches, but antipsychotic drugs targeting dopamine impairments are inefficient for treatment of negative and cognitive symptoms (Chue & Lalonde, 2014; Moghaddam & Javitt, 2012). Later work indicates that these symptom domains may be more linked to alterations in the glutamatergic system (Chue & Lalonde, 2014; Moghaddam & Javitt, 2012). The glutamate hypothesis of ScZ was originally formed as drugs of abuse acting on the glutamate system were found to trigger psychotic-like symptoms (Lahti, Weiler, Michaelidis, Parwani, & Tamminga, 2001; Morris, Cochran, & Pratt, 2005). Empirical evidence for such alterations comes from post-mortem, pharmacological and neuroimaging studies (Howes et al., 2015). The glutamate system deficits are thought to be related to

NMDA receptor dysfunction (Stone, Morrison, & Pilowsky, 2007), and give rise to symptoms through effects on the cortical E/I balance (Gonzalez-Burgos & Lewis, 2012). The proposed mechanism for these abnormalities will be discussed in more detail later in this chapter.

Thus, there is now evidence for both the dopamine and glutamate hypotheses (Howes et al., 2015) and there is an overall consensus that both signalling pathways are implicated in the disorder and may account for slightly different symptoms and patient subtypes. Furthermore, a recent addition to the biological understanding of ScZ is the notion that increased oxidative stress plays a role in the disorder. Oxidative stress is a disruption of balance between oxidants (rest products from aerobic metabolism) and anti-oxidant molecules, in favour of the oxidants (Sies, 1996). Higher levels of oxidants have been measured in ScZ patients compared to healthy controls (Gonzalez-Liencres et al., 2014), suggesting elevated levels of oxidative stress. This alteration could constitute one of the factors contributing to disrupted brain development in childhood and adolescence (Do, Cuenod, & Hensch, 2015). Intriguingly, recent work has linked oxidative stress to N-methyl-D-aspartate (NMDA) glutamate receptor impairments, suggesting that oxidative stress could also explain some of the glutamate pathway impairments (Hardingham & Do, 2016).

Another important consideration in understanding the neural underpinnings of psychosis, is that most research has been done on medicated patients. While medications are still inadequate, with varied and limited cognitive benefits (Keefe et al., 2007; Keefe, Silva, Perkins, & Lieberman, 1999; Leucht et al., 2009), antipsychotic drugs cause significant physiological side-effects, including extra-pyramidal motor impairments and sexual dysfunction for first-generation antipsychotic drugs, and metabolic changes for newer drug alternatives (Rummel-Kluge et al., 2010). Furthermore, meta-analytic data indicate that brain volume abnormalities frequently reported in ScZ may result from antipsychotic medication treatment (Moncrieff & Leo, 2010), although alterations in brain morphology have also been observed in medication naïve patients (Cahn et al., 2002; Chua et al., 2007). Thus, the potential effects of medication are essential to consider in the interpretation of all ScZ studies.

1.1.1 Cortical Excitation and Inhibition

One proposed neural mechanism for ScZ is an impairment in the balance between excitation and inhibition (Gonzalez-Burgos & Lewis, 2012; Lisman, 2012). Synchronized neural oscillations are fundamental for integrated sensory processing and cognition (Siegel et al., 2012) and are generated through the interaction between glutamatergic and GABAergic signals (Carlén et al., 2012; Shin et al., 2011; Z. Zhang & Sun, 2011). An disturbance in E/I balance could underlie some of the cognitive and sensory impairments seen in patients with psychosis (Barch & Ceaser, 2012; Uhlhaas & Singer, 2010; Uhlhaas, 2013).

Glutamate is the primary excitatory neurotransmitter in the central nervous system and is involved in a broad spectrum of brain functions (Howes et al., 2015; Kew & Kemp, 2005). The human cerebral cortex contains excitatory glutamatergic pyramidal neurons extending from superficial layers to the deep subcortical areas, constituting 70-80% of all cortical neurons (Markram et al., 2004). These cells communicate with surrounding cells via metabotropic and ionotropic synaptic receptors. The latter includes a-amino-3-hydroxy-5-methyl-4-isoxazolepropionic acid (AMPA), kainate and N-methyl-D-aspartate (NMDA) receptors (Kew & Kemp, 2005). The NMDA subgroup of receptors is unique as its activation requires removal of a voltage gated Mg^{2+} block in addition to ligand binding, providing a further regulatory mechanism. This receptor type is thought to be crucial for a range of functions such as neuronal development, synaptic plasticity, learning, and cell integrity (K. Hashimoto, 2017) and is involved in the maintenance of E/I balance through its presence on inhibitory interneurons, allowing the activation of these (Carlén et al., 2012).

Excessive levels of glutamate result in excitotoxicity and ultimately cell death and the synaptic release is therefore tightly regulated (Magistretti & Pellerin, 1999). Multiple mechanisms are in place for monitoring glutamate, including glutamate transport proteins, glial uptake and conversion of glutamate (Magistretti & Pellerin, 1999). Moreover, the glutamatergic cells are regulated locally by different subtypes of interneurons, releasing the primary inhibitory neurotransmitter GABA (Markram et al., 2004). The regular interplay between inhibitory GABA and excitatory glutamate neurons is thought to form the foundation for the rhythmic neural activity (Carlén et al., 2012; Gonzalez-

Burgos, Hashimoto, & Lewis, 2010), detected as neural oscillations using MEG or EEG (Vohs, Chambers, O'Donnell, Krishnan, & Morzorati, 2012).

Glutamatergic cells are regulated locally by interneurons (Markram et al., 2004). Across cortical regions and layers, the interneurons are molecularly and functionally diverse, with the three largest subgroups being neurons expressing the Ca^{2+} binding molecule parvalbumin (PV+), neurons expressing the neuropeptide somatostatin (SOM) and neurons expressing the serotonin receptor 5HT3a (5HT3aR) (Rudy, Fishell, Lee, & Hjerling-Leffler, 2011). Among these, the largest proportion of GABAergic interneurons are made up by PV+ cells (Rudy et al., 2011), and these have thus been the focus of much of the recent work in ScZ (T. Hashimoto et al., 2003; Lewis, 2011; Lewis, Curley, Glausier, & Volk, 2013; Taylor & Tso, 2014). However, recent evidence suggests that also SOM GABA interneurons play an important and distinct role which may be implicated in the maintenance of healthy cortical function (Chen et al., 2017).

The PV+ GABA interneurons can be divided into two types of fast-spiking cells: basket cells and chandelier cells (Rudy et al., 2011). These cell types are involved in local cortical circuits and typically do not project across cortical layers (Markram et al., 2004). The primary distinguishing feature between the cell types is which area of cortical pyramidal cells they project to. Basket cells target the proximal dendrites/cell bodies and are therefore able to adjust the amplitude of synaptic signals passing through the neuron. In contrast, the chandelier cells synapse on the axon initial segments of pyramidal neurons, allowing them to edit action potential output (Lewis, 2011; Markram et al., 2004). The primary SOM interneurons are Martinotti cells (Rudy et al., 2011), found in layers 2-6 of the cortex. These are distinct from PV+ neurons as they specialise in projecting up to superficial layer 1 of the cortex where they inhibit dendrites of the pyramidal cortex in one or several adjacent columns (Markram et al., 2004). Separate optogenetic tagging of SOM and PV+ interneurons in mice showed that SOM interneurons are preferentially linked to cortical beta (≈12-30 Hz) oscillations, while stimulation of PV+ interneurons correlated stronger with gamma range oscillations (Chen et al., 2017). Thus, distinct inhibitory neuronal subtypes appear to play separate but complementary roles in the generation of oscillations.

There is evidence suggesting that both glutamatergic and GABAergic signalling pathways are impaired in psychosis. For instance, studies mapping ScZ risk genes have highlighted genes linked to the expression of NMDA receptor subunits (Ripke et al., 2014), and revealed altered cortical expression of GABA related genes (Hoftman et al., 2015). In line with these data, post-mortem findings have shown altered NMDA receptor expression, trafficking, and downstream signalling pathways (Hammond, Shan, Meador-Woodruff, & McCullumsmith, 2014), as well as deficits in the GABA synthesis pathway (Lewis et al., 2012; Taylor & Tso, 2014). Furthermore, pharmacological manipulation in-vivo and in humans, using NMDA receptor antagonists such as MK-801, phencyclidine and ketamine, has been found to result in immediate symptoms resembling psychosis (Howes et al., 2015; Moghaddam & Javitt, 2012).

Moreover, NMDA receptor dysfunction may involve GABAergic interneurons during neural development, causing impaired interneuron maturation and ultimately aberrant regulation of both glutamate and GABA cortical signalling (Nakazawa, Jeevakumar, & Nakao, 2017). Combined, such findings have resulted in the E/I imbalance hypothesis of ScZ. This notion fits with the well-established glutamate hypothesis and could better account for cognitive and negative symptoms than the dopamine hypothesis (Howes et al., 2015).

1.1.2 Neural Oscillations

Neural oscillations are typically categorized based on frequency, ranging from delta (0.5–3 Hz) and theta (3–8 Hz) , to alpha (8-12 Hz), beta (12-30 Hz) and gamma (> 30 Hz) frequencies (Bartos et al., 2007). Different frequency bands are thought to represent different neural functions (Uhlhaas & Singer, 2010). Through synchronised firing at different frequencies, brain regions interact locally and over long distances and enable functions such as perception, memory and attention (Siegel et al., 2012). The establishment of such large scale networks involves the interaction of gamma oscillations which contribute to synchronization in local functional brain networks, and beta oscillations (12-30 Hz) permitting long-range synchronisation (Phillips & Uhlhaas, 2015; Siegel et al., 2012). In contrast, the lowest frequency bands, alpha (8-12 Hz), theta (3-8 Hz) and delta (0.5-3 Hz) are implicated in inhibition of activity during rest and sleep states, but are also involved in a range of important processes during

waking, such as inhibition, attention and long-range synchronization (Lisman, 2016; Phillips & Uhlhaas, 2015).

EEG and MEG techniques allow the non-invasive study of neural oscillations through the detection of electrical/magnetic signals from groups of cortical neurones (Lopes da Silva, 2010). Neuronal signalling involves electrical action potentials, formed by transmembrane currents, travelling down the axons of neurones (Lopes da Silva, 2010). As the current moves, a weak magnetic field arises around the neuron's projections, and when groups of neurones fire in synchrony, the compound strength from the electrical/magnetic signals is sufficient for detection with EEG electrodes/MEG sensors (Lopes da Silva, 2010). As the two methods detect different forms of the same signal, they share common features. However, EEG measures are more affected by scalp tissue thickness and cannot be reconstructed in the source space as easily as MEG measures (Ramantani et al., 2006). In contrast, MEG sensors are blind to magnetic fields from completely radial neurons and the MEG method is therefore inferior at detecting signals from deep brain sources (Ramantani et al., 2006).

Impaired oscillatory patterns in several frequency bands have been observed in ScZ patients (Moran & Hong, 2011). Given that high and low frequency oscillations are thought to interact to establish local as well as long range networks (Uhlhaas, 2013), changes in multiple frequencies in ScZ support the view that the disorder affects large brain systems (Anticevic & Lisman, 2017).

The gamma band has been studied extensively in ScZ patients, and deficits in this frequency range are considered an important feature of ScZ pathology (Shin et al., 2011). In the auditory domain, ScZ gamma oscillations have been studied using ASSR paradigms (Thuné et al., 2016), and there is consistent evidence for impaired 40 Hz ASSR evoked spectral power and ITPC measures of signal phase synchrony between trials (Thuné et al., 2016). Moreover, there are data indicating that lower frequency ASSRs, such as beta and theta oscillations, may also be impaired in ScZ (Kirihara, Rissling, Swerdlow, Braff, & Light, 2013).

Furthermore, the ASSR paradigm has been used to study induced gamma power in ScZ (Edgar et al., 2014; Hirano et al., 2015; Kirihara et al., 2012; Krishnan et

al., 2009; Roach, Ford, Hoffman, & Mathalon, 2013; Teale, Collins, Maharajh, Rojas, & Kronberg, 2009). Induced power is a measure of power which, in contrast to evoked power, is not phase-locked to the periodic ASSR stimulation (Hirano et al., 2015). Two studies reported reduced induced power around 40 Hz in ScZ (Roach et al., 2013; Krishnan et al., 2009), while others found no difference (Kirihara et al., 2013) or an increase in 40 Hz induced power in ScZ-patients (Teale et al, 2008). Moreover, broadband evaluations of induced power indicated increases in ScZ, both for baselined (Edgar et al., 2014) and non-baselined data (Hirano et al., 2015), including the pre-stimulus period. The discrepancies in findings may be accounted for in part by differences in methodology, such as different approaches for computing induced power or selection of frequency of interest.

In line with observed increases in induced power (Edgar et al., 2014; Hirano et al., 2015), one group reported elevated left hemisphere baseline power during a 40 Hz ASSR experiment in ScZ patients compared to controls. The increase correlated with ASSR power reductions during the task, suggesting that some of the task effect was driven by the underlying baseline difference (Spencer, 2012). However, it remains unclear whether the 40 Hz ASSR baseline is affected in ScZ as this has not been widely investigated.

In the visual domain, presentation of moving grating stimuli gives rise to a strong gamma response in healthy subjects (Hoogenboom, Schoffelen, Oostenveld, Parkes, & Fries, 2006). While presenting such stimuli during MEG recordings, colleagues recently found impaired visual gamma power in chronic ScZ patients and first-episode psychosis sample (Grent-’t-Jong et al., 2016). This is in line with previous visual gamma reports (Spencer, 2008; Wynn et al., 2005) and stimulations with more complex visual stimuli, such as Mooney faces (Grützner et al., 2013). Furthermore, visual oscillatory impairments were found to coincide with behavioural impairments (Grent-’t-Jong et al., 2016; Grützner et al., 2013), suggesting a link between visual perceptual processing abnormalities and neural oscillatory deficits.

Oscillatory alterations have also been detected in the lower beta, alpha, theta and delta frequency ranges (Moran & Hong, 2011). Reduced alpha and/or beta

power and phase-locking was reported in ASSR studies (Brenner, Sporns, Lysaker, & O'Donnell, 2003; Krishnan et al., 2009; Vierling-Claassen, Siekmeier, Stufflebeam, & Kopell, 2008), while one ASSR study reported intact beta (Maharajh, Teale, Rojas, & Reite, 2010). Beta phase-synchrony impairments were seen in both a visual steady state task (Riečanskỳ, Kašpárek, Řehulová, Katina, & Přikryl, 2010), and a gestalt perception task (Uhlhaas et al., 2006). In the alpha range, multiple complex oscillatory alterations have been reported (Başar & Güntekin, 2013). Early visual steady state investigations reported reductions in alpha-power (Rice et al., 1989), and reduced alpha phase-locking has also been observed during visual steady state stimulation (Riečanskỳ et al., 2010). In addition, alpha-band suppression was impaired in a multisensory paradigm in ScZ compared to controls (Roa Romero et al., 2016) and alpha amplitude abnormalities in ScZ were observed during an ambiguous visual perception task (Basar-Eroglu, Mathes, Khalaidovski, Brand, & Schmiedt-Fehr, 2016). Furthermore, the topographical pattern of alpha oscillatory responses to visually evoked stimulation was found to be altered in ScZ (Basar-Eroglu, Schmiedt-Fehr, Marbach, Brand, & Mathes, 2008). However, others reported intact alpha power in ScZ during a visual grating processing task (Grent-'t-Jong et al., 2016), in a visual-steady state task (Krishnan et al., 2005) and in a resting-state paradigm (Hinkley et al., 2011).

Increased slow-frequency theta and delta oscillations during wakeful rest has been reported as one of the most robust oscillatory alterations in ScZ (Boutros, Arfken, Galderisi, Warrick, & Pratt, 2009). In addition, there is evidence that delta oscillatory power is decreased during sleep (Keshavan et al., 1998). Moreover, delta and theta induced and evoked oscillatory activity was reduced in several cognitive and sensory processing tasks (Başar & Güntekin, 2013). In contrast, theta range increases in power have been reported from an ASSR task (Kirihara et al., 2012), and altered spatial patterns with both local increases and decreases in theta were reported from a visual domain task (Basar-Eroglu et al., 2008). Alterations in the theta range are potentially important as these may influence gamma range activity through cross-frequency coupling (Kirihara et al., 2012).

This section has highlighted that there is empirical evidence for disrupted oscillations in ScZ in both the auditory and visual domains, particularly but not exclusively, in the gamma range. However, while both visual and auditory steady state stimulation approaches provide information about oscillatory neural activity, it should be noted that they are not equivalent measures (Zoefel & VanRullen, 2017). Visual gamma paradigms tap into the intrinsic synchronised oscillatory sampling of sensory neurones in the visual cortex, while the 40 Hz ASSR is an evoked response reflecting entrainment of auditory neurones to an external stimulus (Lakatos, Gross, & Thut, 2019). As such, both types of experiments reflect the capacity of neurones to elicit an oscillatory response, but the 40 Hz ASSR is externally driven (Brenner et al., 2009). Nevertheless, the ASSR measure could provide important indications about the capacity of auditory neurones to entrain to oscillating sources within the brain or body

1.1.3 Dysconnectivity in ScZ

Evidence from neuroimaging data suggests that ScZ is a disorder of neural dysconnectivity (Stephan, Friston, & Frith, 2009). Neural connectivity measures capture structural connectivity, reflected by the white matter axonal connections between regions, or functional connectivity assessed through statistical estimates of the likelihood of two regions communicating (Bowyer, 2016). Available evidence indicates that both structural and functional connections are impaired in ScZ (Fitzsimmons, Kubicki, & Shenton, 2013).

Diffusion tensor imaging (DTI) measures have been used to examine structural connectivity, while fMRI has frequently been used to evaluate functional connectivity (Fitzsimmons et al., 2013; Fornito, Zalesky, Pantelis, & Bullmore, 2012). However, the high temporal resolution and direct measures of brain activity make EEG and MEG data suitable alternatives for functional measures and an increasing number of EEG and MEG ScZ studies are therefore reporting connectivity measures (Maran et al., 2016).

Results from a meta-analysis of DTI voxel-based morphometry measures of fractional anisotropy (i.e. degree of restriction of diffusion), showed poor consistency between studies, yet multiple reports indicate abnormalities in several brain regions in psychotic patients (Melonakos et al., 2011). In the

context of auditory function it is relevant to note that one study found no overall difference in corpus callosum fractional anisotropy between FEP and healthy controls, yet patients experiencing complex auditory hallucinations in the form of two or more conversing voices showed an increase in fractional anisotropy in these tracts compared to patients without severe hallucination symptoms (Mulert et al., 2012).

One longitudinal study exploring DTI measures of fractional anisotropy in controls, FEP and UHR participants found differences both at baseline, where the FEP patients had the lowest and controls the highest fractional anisotropy measures, and at follow-up where fractional anisotropy values declined in UHR participants who eventually transitioned to psychosis, but not in non-converters (Carletti et al., 2012). Thus, there is some evidence that impaired white matter integrity could be a feature associated with psychosis onset.

Functional connectivity has been widely evaluated using fMRI resting-state paradigms (Woodward, 2014). Some inconsistencies in results exist, yet recent systematic reviews and alternative methodological approaches have revealed robust evidence for dysconnectivity in ScZ (Damaraju et al., 2014; Giraldo-Chica & Woodward, 2017). Specifically, patients show reduced prefrontal-thalamic connectivity, but increased thalamic-sensorimotor connectivity (Giraldo-Chica & Woodward, 2017), as well as abnormalities in the cortico-cerebellar-striatal-thalamic loop and task specific networks (Sheffield & Barch, 2016). Moreover, dynamic connectivity analyses indicate that ScZ patients spend less time overall in states of strong large-scale connectivity, and that it is while patients are in such states that most abnormal connectivity patterns occur (Damaraju et al., 2014). However, while it has been speculated that connectivity alterations may underly cognitive impairments seen in ScZ, literature reviews have not indicated a clear link between connectivity changes and a specific cognitive domain, but rather suggest that dysconnectivity results in general functional impairments which may affect general cognitive function (Sheffield & Barch, 2016). Thus, fMRI has contributed to an emerging awareness of the characteristics of dysconnectivity in ScZ, and how such disruptions may relate to clinical symptoms.

Importantly, the high temporal resolution of connectivity data from EEG and MEG studies (Maran, Grent-‘t-Jong, & Uhlhaas, 2016) allow an expansion of the current understanding of ScZ connectivity changes. Several groups reported increased delta and theta band resting state functional connectivity in ScZ patients compared to healthy controls (Andreou, Leicht, et al., 2015; Di Lorenzo et al., 2015; Kam, Bolbecker, Donnell, Hetrick, & Brenner, 2013; Lehmann et al., 2014). Moreover, CHR subjects were found to have intermediate levels of theta-band functional connectivity, falling between the levels seen in ScZ patients and controls (Andreou, Leicht, et al., 2015). In the alpha and beta bands, both increased (Di Lorenzo et al., 2015; Hinkley et al., 2011; Kam et al., 2013) and reduced resting-state functional connectivity (Di Lorenzo et al., 2015; Hinkley et al., 2011; Kam et al., 2013; Lehmann et al., 2014) has been reported. Finally, resting-state gamma range connectivity appears increased in ScZ (Andreou, Nolte, et al., 2015; Di Lorenzo et al., 2015), especially in patients with long disease duration (Lorenzo et al., 2015).

Crucially, EEG/MEG data also provide evidence for connectivity disruptions in ScZ sensory pathways. Disrupted connectivity measures have been reported during both auditory (Henshall, Sergejew, Rance, McKay, & Copolov, 2013; Winterer, Coppola, Egan, Goldberg, & Weinberger, 2003; Ying, Zhou, Lin, & Gao, 2015) and visual tasks (Griesmayr et al., 2014; Krishna, Neill, Sánchez-Morla, & Thaker, 2015; Popov, Rockstroh, Popova, Carolus, & Miller, 2014).

In summary, there is evidence for disruptions in both structural connections and functional connectivity patterns in ScZ and to some degree also in FEP and at-risk individuals. Data from EEG/MEG indicate connectivity abnormalities in ScZ both during rest and in tasks, and thus support the ScZ dysconnectivity framework.

1.1.4 Magnetic Resonance Spectroscopy

Proton magnetic resonance spectroscopy (1H-MRS) provides a non-invasive method for measuring levels of brain metabolites, by exploiting the unique molecular resonance frequency of different chemical substances. Specifically, 1H-MRS is a molecular imaging technique which utilises the unique resonance frequencies of molecules arising from the magnetic shielding on protons by local

electron clouds (Dager, Oskin, Richards, & Posse, 2008), to create a spectrum showing the relative concentrations of brain metabolites (Stefan Blüml, 2013). Importantly, refined scanning protocols, such as the MEGAPRESS (MEscher-GArwood Point RESolved Spectroscopy) sequence (Mescher, Merkle, Kirsch, Garwood, & Gruetter, 1998; Mescher, Tannus, O'Neil Johnson, & Garwood, 1996), have enabled the measure of molecules such as GABA and the compound Glx (Glutamate + Glutamine), despite the relatively low concentrations of these in the brain and the fact that their resonance frequency peaks overlap with other metabolites (Edden, Puts, Harris, Barker, & Evans, 2013).

Early 1H-MRS ScZ studies focused on high concentration brain metabolites such as N-Acetyl aspartic acid (NAA), creatine and choline (Jessen et al., 2006; Keshavan, Montrose, Pierri, & Elizabeth, 1997; Wood et al., 2003, 2010; Yoo et al., 2009), which can easily be detected and measured in the 1H-MRS spectrum (Wijtenburg, Yang, Fischer, & Rowland, 2015). However, more recent efforts have been directed primarily at measures of GABA and Glutamate/Glx (Egerton, Modinos, Ferrera, & McGuire, 2017; Merritt, Egerton, Kempton, Taylor, & Mcguire, 2016; Poels et al., 2014; Wijtenburg et al., 2015), due to the potential high relevance of these for ScZ pathology. The MEGAPRESS sequence allows the acquisition of such measures through 1H-MRS spectral editing, whereby molecular interactions within the GABA molecule, known as J-couplings, are exploited to alter the appearance of the metabolite spectrum (Mullins et al., 2014). MEGAPRESS collects two spectra through one un-edited and one edited scan sequence. The latter utilises radio frequency pulse editing of a coupled molecular spin within the GABA molecule, targeting the GABA peak at 1.9ppm to shift the peak at 3ppm (Mullins et al., 2014). This allows computation of a difference spectrum where only peaks for GABA and Glx (Glutamate+ Glutamine) are visible.

1.9 ppm (those directly affected by the pulses), the GABA signal at 3 ppm (coupled to GABA spins at 1.9 ppm), the combined glutamate/ glutamine/glutathione (Glx) peaks at 3.75 ppm (coupled to the Glx res- onances at approximately 2.1 ppm),

As comprehensively reviewed by Poels et al (2014), Wijtenburg et al (2015) and Merritt et al (2016), measures of glutamate or Glx in ScZ have resulted in inconsistent findings so far. Decreased levels of glutamate or Glx have been observed in medial prefrontal cortex and anterior cingulate cortex (Natsubori et al., 2014; Rowland et al., 2013; Théberge et al., 2003). However, several studies have reported elevated glutamate or Glx concentrations, with significant increases observed in both frontal and temporal regions, the basal ganglia (Merritt et al., 2016; Poels et al., 2014) and medial prefrontal cortex (Poels et al., 2014). Such increases in glutamate are consistent with findings of NMDA receptor hypofunction in-vivo (Nakazawa, Jeevakumar, & Nakao, 2017) and human ketamine studies showing that artificial increases in glutamate give rise to psychotic-like symptoms.

Critically, evidence is emerging indicating that impairments are present also in the CHR population (Merritt et al., 2016). A recent report highlighted the importance of the hippocampus in psychosis pathology and demonstrated that CHR subjects who transitioned to psychosis had higher hippocampal glutamate levels than the CHR subjects who did not transition (Bossong et al., 2018). Furthermore, significant increases were observed in the anterior cingulate cortex (Fuente-Sandoval et al., 2016), the pre-commissural dorsal-caudate (Fuente-Sandoval et al., 2011), thalamus and caudate (Tandon et al., 2013) in CHR. However, contradicting findings have also been reported. Wood et al. did not observe glutamate alterations in a UHR sample (Wood et al., 2010) and no significant effects were found in high genetic risk groups (Block et al., 2000; Capizzano, Toscano, & Ho, 2011; Keshavan et al., 2009).

1H-MRS studies of GABA in psychotic individuals are inconsistent (Egerton et al., 2017; Wijtenburg et al., 2015). In ScZ patients, reduced GABA levels were reported in dorsal anterior cingulate cortex (Marenco et al., 2016) and bilateral calcarine sulci (Yoon et al., 2010). In contrast, increased concentrations were observed in medial and dorsolateral prefrontal cortex, anterior cingulate cortex, occipital cortex and basal ganglia (Kegeles et al., 2012; Öngür, Prescot, McCarthy, Cohen, & Renshaw, 2010; Rowland et al., 2013; Tayoshi et al., 2010). In FEP patients, decreased levels of GABA/creatine compared to healthy controls have been reported in the left basal ganglia, parietal occipital lobe (Goto et al.,

2010) and the bilateral calcarine sulci (Kelemen, Kiss, Benedek, & Kéri, 2013), but not in the frontal cortex (Goto et al., 2010).

Similarly, one UHR study found increased GABA in bilateral dorsal caudate and medial prefrontal cortex (Fuente-Sandoval, 2016), while another reported reduced GABA and GABA/Glx concentrations in the left frontal lobe (Menschikov et al., 2016). Moreover, medial prefrontal cortical levels of GABA were found to be correlated with left hippocampal cerebral blood flow, and this relationship was found to differ between UHR participants who transitioned to psychosis and those who did not (Modinos, Şimşek, Azis, et al., 2018). Thus, while the data remain limited there is increasing empirical support for the notion that both glutamate and GABA may be abnormal already prior to psychosis onset.

1.2 Disease Detection and Biomarkers

Psychiatric research has long had low priority, and the lack of knowledge of underlying biological mechanisms meant that detection and diagnosis was done exclusively using clinical information (McGorry et al., 2014; Singh & Rose, 2009). Recent research has improved the understanding of physiological and psychological mechanisms involved in psychotic disorders, yet the assessment methods remain largely the same and rely primarily on individual clinicians' interpretation of clinical consensus (Jablensky, 2010; McGorry et al., 2014). Thus, there is a need to develop new sensitive psychosis detection methods, for example through biomarkers.

A biomarker can be defined as follows: "A characteristic that is objectively measured and evaluated as an indicator of normal biological processes, pathogenic processes, or pharmacologic responses to a therapeutic intervention" (Biomarkers Definitions Working Group, 2001). This concept is challenging for aetiologically complex disorders such as ScZ, as the pathophysiology is likely to be heterogeneous, involving genetic, neural and social risk factors (Selemon & Zecevic, 2015).

A primary issue in the development of biomarkers for risk- or early stages of psychosis is the relative lack of empirical data from FEP and CHR samples. Moreover, as highlighted early by Kraemer, a crucial feature of a biomarker is

that it should be present prior to the outcome of interest (Kraemer et al., 1997). Thus, for the development of biomarkers truly reflecting risk of transition, a measure which differs specifically between controls and those CHR individuals who do transition to psychosis is required (Gifford et al., 2016). However, an important consideration is whether transition is the most relevant outcome variable. Thus, biomarkers predicting psychological, cognitive and/or social and occupational functioning may be equally important.

Neuroimaging measures are attractive alternatives to biochemical measures (such as serum hormonal and neuromodulator levels (Bičíková et al., 2011)) as they are non-invasive and can be collected easily in clinical settings (Bowyer et al., 2015). Consequently, neuroimaging measures impaired in ScZ have been proposed as potential biomarkers of psychosis, and could aid not only early detection, diagnosis and intervention of psychosis, but also the identification of better treatment targets (Fusar-Poli et al., 2013). For instance, machine learning algorithms have been applied to MRI data in order to predict transition to psychosis in a large CHR project, demonstrating relatively reliable predictions especially for the contrast converters vs healthy controls (Koutsouleris et al., 2012).

MEG and EEG have been used to study whether evoked potentials such as P50 and N100 sensory gating (Patterson et al., 2008) or MMN (Erickson et al., 2015) could be suitable marker candidates. In particular MMN-studies have yielded promising results. While some have failed to detect a difference in MMN between CHR and control subjects (Brockhaus-Dumke et al., 2005; Higuchi et al., 2013), MMN impairments have been found to be more severe in CHR participants who eventually transition to psychosis (Bodatsch et al., 2015, 2011; Lavoie et al., 2018), suggesting that MMN measures may be sensitive to the true prodromal state.

However, MEG and EEG measures of oscillations have not been evaluated extensively for psychosis prediction. Recent resting state EEG data suggest that oscillations can be used for psychosis prediction in CHR (Ramyead et al., 2016), however the potential for using sensory related task measures for assessments of clinical prognosis is unknown. One group has published ASSR data from CHR

individuals (Koshiyama et al., 2018a; Tada et al., 2016), but have not explored the predictive power of the measure. However, data from chronic and first episode ScZ patients indicate a moderately robust impairment across studies (Thuné et al., 2016), motivating further study of this measure in CHR samples to further evaluate its biomarker potential.

Chapter 2 Participants and Methods

2.1 Recruitment

All data reported in this thesis were collected as part of the longitudinal Youth Mental Health Risk and Resilience (YouR) study (Uhlhaas et al., 2017). The study was approved by the West of Scotland Research Ethics Committee 5. FEP and CHR participants were recruited through clinical referrals from the NHS in the Greater Glasgow and Clyde and Mid Lothian districts, as well as from the general population in Glasgow and Edinburgh, using the YouR study recruitment website (www.your-study.org.uk). Healthy control participants were recruited using the University of Glasgow psychology department's online subject pool.

Individuals between 16 and 35 years old were invited via advertisements, GP recommendations and emails to complete a questionnaire on the study website (McDonald et al., 2018), consisting of (a) the 16-item Prodromal Questionnaire (PQ-16) (Ising et al., 2012) and (b) a nine-item scale of perceptual and cognitive anomalies which was developed to assess basic symptoms. Participants endorsing 6 or more items on the SPQ and/or 3 on the basic symptom scale were invited for screening assessments at the University of Glasgow or the University of Edinburgh. Between September 2014 and July 2018 there were 2853 entries on the YouR study website. Out of these, 2190 met cut-off criteria for CHR and 382 participants in Glasgow and 78 in Edinburgh attended screening assessments.

Further participants entered the study via direct referrals from NHS services such as the psychosis early intervention program in Glasgow, Esteem. Until July 2018, a total of 32 participants in Glasgow and 7 in Edinburgh entered the study via this route. Like participants recruited from the website, the referred subjects attended initial screening assessments to establish whether they met CHR criteria.

Three FEP patients' data were recorded as part of a different first-episode of psychosis study, with the participants subsequently consenting to the data being shared between studies.

Inclusion criteria for all groups were: 16-35 years old (inclusive), no ferromagnetic implants in body, not pregnant, normal/corrected to normal vision, no neurological disorders and no acute suicidality. In addition, control participant inclusion required no history of psychiatric illness and no first-degree relatives with ScZ.

Participants were recruited to the CHR-group if they met (a) the SPI-A Cognitive-Perceptive Basic Symptoms (COPER) or Cognitive Disturbances (COGDIS) criteria; (b) CAARMS criteria for the attenuated psychosis group; (c) CAARMS criteria for genetic risk and functional deterioration (family history of psychosis plus a 30% drop in Global Assessment of Functioning (GAF) scores); or (d) CAARMS criteria for Brief Limited Intermittent Psychotic Symptoms (BLIPS). Screened CHR-participants were excluded if they met criteria for current or past diagnosis with Axis I psychotic disorders. Other co-morbid Axis I diagnoses, such as mood or anxiety disorders, were not exclusionary (Uhlhaas et al., 2017).

Participants meeting CAARMS criteria for psychosis threshold and the diagnostic criteria for FEP on DSM-IV, assessed using the Structured Clinical Interview for DSM-IV-TR AXIS I disorders (SCID-I) (First, 2015) were included in the FEP sample.

After screenings, 113 participants in Glasgow and 41 participants in Edinburgh met CHR inclusion criteria. Furthermore, 15 (Glasgow) and 11 (Edinburgh) participants met FEP criteria.

Following screenings, participants attended additional clinical interviews (Appendix 1). CHR and control participants were assessed with the Premorbid Assessment Scale (PAS) (Cannon-Spoor, Potkin, & Wyatt, 1982) and the Mini International Neuropsychiatric Interview (MINI) (Sheehan et al., 1998). FEP participants were assessed with the Structured Clinical Interview – Positive and Negative Syndrome Scale (SCI-PANSS) (Kay, Fiszbein, & Opler, 1987). Moreover, all participants underwent a neuropsychological evaluation, completing the Brief Assessment of Cognition in Schizophrenia (BACS) (Keefe et al., 2004). Results from the neuropsychological assessments are presented elsewhere (Haining et al., 2019).

The fourth study visit involved MEG and MRI measurements. MEG data were recorded on a 4D Neuroimaging Magnes 3600 Whole Head 248 Channel system. The test battery included a resting-state task, and measures of visual gamma oscillations, auditory MMN, the 40 Hz ASSR and auditory sensory attenuation.

MRI data were recorded on a Siemens 3 t scanner. A 10-minute duration anatomical T1 weighted magnetic resonance imaging (MRI) scan was recorded with parameters: 192 slices, voxel size 1 mm^3, FOV=256256 176 mm^3, TR=2250 ms, TE=2.6 ms, FA=9°. In addition, 1H-MRS measures of GABA and Glx were collected using MEGAPRESS (see Chapter 6).

Following the neuroimaging session, CHR participants were invited for follow-up visits every six months for a duration of up to three years. Initial analyses based on follow-up data are presented in Chapter 7.

During the time period considered in this thesis, a total of 107 CHR participants, 49 healthy control participants and 19 FEP patients underwent scans (Appendix 2). Some data were lost due to poor quality or participants' inability to complete the paradigm. Hence, data from a total of 93 CHR, 17 FEP, and 46 healthy controls are presented in this thesis. At the time of data analysis, 4 of the CHR participants had transitioned to FEP.

2.2 Clinical Characteristics

This thesis addresses ASSR oscillatory data in CHR individuals (Chapters 3, 4, 5 & 7). Power calculations for the present analyses were performed based on an assumed ASSR Hedge's g effect size of -0.42 found through meta-analytic evaluations of ASSR findings in ScZ (Chapter 3) (Thuné et al., 2016). Assuming an effect of -0.42, the current sample sizes and an alpha limit of 0.05, it was estimated that a minimum power of 0.75 should be obtained even for the smallest group included (FEP).

A summary of demographic variables is given in Table 1. There was no significant difference in overall group age, yet as expected the FEP group had the overall highest mean age, while CHR participants had the overall lowest mean age. There was a significant difference in GAF scores between groups (Independent-

Samples Median Test statistic: 64.00, p<0.01, d=2.49), with highest scores in the control group (mean 87.62, sd± 6.50), intermediate scores for CHR (59.48, sd± 12.87) lowest scores in the FEP group (43.31, sd± 14.23).Moreover, there was a significant difference in GAF variance (Levene's stat=6.80, p <0.01), with the control group showing least and the FEP group most variance.

Table 1 YouR Study Sample Demographic Characteristics

Group [N]	Control [46]		CHR [93]		FEP [17]		Test statistic	Sig. (p)	Effect[d]
	Mean	*Std*	*Mean*	*Std*	*Mean*	*Std*			
Demographic									
Age (years)	22.48	3.44	21.62	4.37	23.77	4.69	4.45[a]	0.11	0.31 (d)
Education (years)	16.61	3.04	15.01	3.38	14.92	2.97	3.90[b]	0.02	0.46 (d)
Mother education (years)	15.31	2.57	14.87	3.30	14.33	2.87	0.47[b]	0.63	0.18 (d)
Father education (years)	15.66	2.20	14.20	4.47	15.38	3.66	1.89[b]	0.16	0.37 (d)
Total CAARMS severity	0.76	2.42	26.56	16.96	85.00	25.85	64.54[a]	<0.01	0.77 (d)
Total BACS	0.00	0.99	-0.82	2.12	-2.99	2.51	10.15[b]	<0.01	2.98 (d)
GAF score	87.62	6.50	59.48	12.87	42.31	14.23	64.00[a]	<0.01	2.49 (d)
Role Functioning Score	8.57	0.78	7.51	1.07	N/A		37.47[b]	<0.01	-1.08 (d)
Social Functioning Score	8.84	0.48	7.55	1.08	N/A		54.10[b]	<0.01	-1.39 (d)
PAS childhood	1.38	1.45	4.02	3.41	N/A		22.04[a]	<0.01	0.91 (d)
PAS early adolescence	2.30	1.76	6.41	4.32	N/A		37.16[a]	<0.01	1.12 (d)
PAS late adolescence	2.76	2.53	6.26	4.51	N/A		22.45[a]	<0.01	0.88 (d)
Gender (male)	15		24		8		3.27[c]	0.20	0.15 (V)
Righthanded	39		84		17		3.21[c]	0.20	0.14 (V)
Learning disability (N)	1		13		1		5.63[c]	0.60	0.21 (V)
First degree relative with ScZ (N)	0		8		1		5.55c	0.06	0.19 (V)
Medication free (N)	46		44		3		49.45[c]	<0.01	0.56 (V)
Admission to hospital (N)	0		3		3		14.25[c]	<0.01	0.31 (V)
Current smoker (N)	6		23		5		4.63[c]	0.10	0.18 (V)
Past smoker (N)	5		13		0		2.28[c]	0.32	0.12 (V)

a) Independent-Samples Median Test statistic

b) F statistic

c) Chi square statistic

d) Effect sizes reported as Cohen's d or Kraemer's V

Gender and handedness were explored as both may potentially affect ASSR measures (Melynyte et al., 2018). However, here no significant difference was found in proportions of gender and handedness in the three groups. Thus, these factors are unlikely to have confounded the analyses presented in Chapters 4-7.

A total CAARMS severity score was calculated for each participant, by multiplying the global score by the frequency score for each of the four symptom groups and calculating the sum of these four numbers (as suggested by Morrison & French, 2012). There was a significant group effect (Independent-Samples Median Test statistic: 64.54, $p<0.01$, $d=0.77$), representing lowest CAARMS severity scores for controls (mean: 0.76 ±sd 2.42), intermediate scores for CHR participants (mean: 26.56,±sd 16.96) and highest scores for the FEPs (mean: 85.00,±sd 25.85).

A composite BACS score index was computed from z-score standardized and gender corrected individual test component scores. There was a significant difference in global BACS performance ($F:10.15$, $p<0.01$, $d:2.98$), representing reduced composite BACS scores for both CHR ($t=-3.03$, $p<0.01$) and FEP ($t=-3.51$, $p<0.007$) participants compared to controls.

The three groups differed significantly in terms of the proportion of unmedicated subjects. No controls were prescribed medication for psychological complaints, while members of both the FEP and CHR groups received pharmacological treatment for psychotic or comorbid symptoms. Specifically, 3 FEP subjects were unmedicated, 2 were given anti-depressants, 1 antipsychotics, and 11 multiple long-term medications. The majority of CHR participants were unmedicated (n=44), 22 were prescribed antidepressants, 1 antipsychotics, 1 mood stabilizers, and the remaining were prescribed other types of long-term medication (including anti-anxiety drugs such as beta-blockers) or multiple medications.

2.3 Conclusion

Despite a heterogenous sample including both self-referred subjects from the general public and patients referred from clinical services, the analysis of demographic and psychological variables follow an expected pattern, with

functional impairments being evident in CHR and FEP and overall lower scores on PAS, BACS and GAF assessments. Furthermore, the FEP and CHR groups were to a greater extent prescribed medication. Importantly however, the groups did not differ with regards to the potentially confounding variables age, handedness and gender.

Chapter 3 The Auditory Steady State Response in Chronic Schizophrenia: A Meta-Analysis

3.1 Introduction

The auditory steady state response (ASSR) allows the study of high frequency neural oscillations in auditory areas (O'Donnell et al., 2013) and gives rise to a robust entrainment response in healthy individuals (Tan, Gross, & Uhlhaas, 2015a). The measure has been widely used for the study of auditory function (Herdman & Stapells, 2001; Tlumak, Rubinstein, & Durrant, 2007), and has been applied for the evaluation of oscillatory signatures in psychiatric disorders (Isomura et al., 2016; O'Donnell et al., 2013; Rass, Forsyth, & Krishnan, 2012; Rass et al., 2010; Wilson, Rojas, Reite, Teale, & Rogers, 2007), including in ScZ (Javitt & Sweet, 2015).

The 40 Hz ASSR is thought to be a right hemisphere dominant response (Ross, Herdman, & Pantev, 2005), arising from the brain stem and primary auditory cortex (Herdman & Stapells, 2001), with further input from secondary auditory regions (Gutschalk et al., 1999; Herdman et al., 2002). The sources are distinct from those linked to auditory evoked potentials (Draganova, Ross, Wollbrink, & Pantev, 2008; Pantev, Roberts, Elbert, Ross, & Wienbruch, 1996). In fact, the 40 Hz ASSR is thought to represent a cortical resonance frequency response linked both to activation in auditory cortex as well as cerebellar sources (Pastor et al., 2002).

The 40 Hz ASSR response reflects interactions between GABAergic and glutamatergic signalling (Vierling-Claassen et al., 2008). In-vivo work has supported this view through the observation that NMDA receptor antagonists alter the 40 Hz ASSR (Leishman et al., 2015; Sivarao, 2015; Sivarao et al., 2013; Sullivan, Timi, Hong, & O'Donnell, 2015; Vohs et al., 2012). However, the direction of change has been inconclusive, and it was recently suggested that the degree of NMDA receptor failure could determine in which direction oscillations are affected (Sivarao, 2015).

ASSR analyses in ScZ have focused primarily on two measures; evoked 40 Hz ASSR spectral power, and inter-trial phase coherence (ITPC) (O'Donnell et al., 2013). The MEG signal can be expressed as a complex number, represented as a vector in a coordinate system with a real and an imaginary axis (Bastos et al., 2015). The length of the vector reflects signal amplitude, while the angle indicates signal phase (Bardouille & Ross, 2008). The power of an oscillatory signal represents the signal amplitude squared (Izhikevich, Gao, Peterson, & Voytek, 2018), with evoked power being the change in power from baseline following stimulation (David, Kilner, & Friston, 2006). In contrast, computing signal phase from the complex vector angle at a particular time point and comparing across trials provides a measure of phase consistency, which is called either the ITPC (when amplitude is included in the calculation) or the phase-locking factor (PLF) (when the amplitude is not considered in the calculation), and which provides valuable information about the capacity of cortical neurones to coordinate their firing and respond to stimulation in a synchronised manner (Bastos et al., 2015). Signal phase coherence in particular is thought to be essential for neural communication within and across brain regions (Fries, 2015), and abnormalities could therefore be important for understanding clinical symptoms of ScZ.

Impaired 40 Hz ASSR power and ITPC has been observed in chronic ScZ patients (O'Donnell et al., 2013; Thuné et al., 2016). An ASSR impairment was first reported by Kwon et al., who found reduced 40 Hz ASSR averaged power and altered phase delay in ScZ compared to healthy controls (Kwon et al., 1999). Subsequently, the initial findings were replicated (Brenner et al., 2003; Edgar et al., 2014; Hamm et al., 2015; Hamm, Gilmore, & Clementz, 2012; Hamm, Gilmore, Picchetti, Sponheim, & Clementz, 2011; Hirano et al., 2015; Hong et al., 2004; Kirihara et al., 2012; Komek, Bard Ermentrout, Walker, & Cho, 2012; Krishnan et al., 2009; Rass et al., 2012; Roach et al., 2013; Spencer, Niznikiewicz, Nestor, Shenton, & McCarley, 2009; Spencer, Salisbury, Shenton, & McCarley, 2008; Tada et al., 2016; Teale et al., 2008; Tsuchimoto et al., 2011; Vierling-Claassen et al., 2008; Wilson et al., 2008), and expanded to include additional stimulation frequencies (Vierling-Claassen et al., 2008; Hirano et al., 2015; Spencer et al., 2008). However, abnormalities in the 40 Hz range remain the most frequently reported ASSR finding in ScZ. Furthermore, reports from two FEP samples (Koshiyama et al., 2018b; Spencer et al., 2008; Tada et al., 2016)

and one CHR sample (Koshiyama et al., 2018a; Tada et al., 2016) suggest that impairments may begin already early stages of psychosis.

Thus, the 40 Hz ASSR measure has been highlighted as a potential biomarker for ScZ, yet until recently the findings from ScZ patients had not been systematically evaluated, and the potential impact of methodology and sample characteristics had not been explored. Thus, in preparation for the empirical work presented in this thesis, the author performed a meta-analysis on the 40 Hz ASSR ScZ literature available at the time (Thuné et al., 2016). The main findings from this published report are presented in this chapter.

3.2 Methods

3.2.1 Sample

Relevant studies published from November 1999 to March 2016 were identified through searches on PubMed using the following search terms: (1) auditory steady state response, (2) ScZ, (3) 40 Hz, (4) EEG, (5) MEG, and (6) steady state response. The search yielded 42 reports which were included in the present meta-analysis if they met pre-determined inclusion criteria: human studies, presenting new data, using EEG or MEG to measure ASSRs, sufficient statistical information (sample sizes and mean values and/or raw data and/or p values and/or effect sizes), including at least one sample of patients with ScZ and one sample of healthy controls, and reporting measures of evoked spectral power and/or ITPC or PLF. In the subsequent analyses, ITPC and PLF measures were treated as equal, as the difference between the two measures is minimal; the overall phase consistency across trials is considered to be reliably detected irrespective of whether amplitude is included or excluded from the calculation (Bastos et al., 2015).

Based on the criteria, 25 studies were excluded (reviews [n=5], animal studies [n=6], studies without ScZ patients or which examined another sensory modality [n=8], studies that did not report measures of spectral power and/or ITPC [n=3], and studies that used a sample already included in the analysis [n=3]). The final sample included 20 studies; 17 from PubMed searches, 2 obtained through searches in reference-sections in the original 42 papers, 1 highlighted by a

reviewer. Additional statistical information was provided by the authors for three of the included studies, as insufficient detail was included in the original publications (Hamm et al., 2011; Krishnan et al., 2009; Rass et al., 2012).

3.2.2 Effect Size Calculations

Effect sizes were computed in the software Comprehensive Meta-Analysis (version 3.3.070) (Borenstein, 2005) Hedge's g effect sizes ($mean_1$-$mean_2/SD_{pooled}$) were calculated for each measure (spectral power and ITPC measures) in each study using sample sizes for each group and either a p value or Cohen d value. Hedge's g effect sizes were chosen for the comparison since the pooled standard deviation used to calculate Hedge's g values is weighted by the number of participants in each group (Erickson et al., 2015). Secondary analyses were performed to investigate the effect of outliers more than 2 standard deviations away from the mean effect size.

Computation of the I^2 index (Higgins & Thompson, 2002) for the resulting effects revealed heterogeneity between studies (Overall I^2=46.78). This was reduced when random as opposed to fixed effect sizes were considered (Overall I^2=6.72). Thus, the rest of this chapter reports estimated random-effect sizes.

Two studies included analyses of several conditions or time-windows respectively (Hamm et al., 2015; Tada et al., 2016). In these cases, overall effects across conditions were included in the analyses.

3.2.3 Evaluation of Reporting Bias

Potential reporting bias was evaluated first through visual inspection of funnel plots, then through statistical evaluation of funnel asymmetry using Egger's regression test (Egger, Smith, Schneider, & Minder, 1997). Finally, effect sizes were corrected using the "trim and fill" method (Duval & Tweedie, 2000), with the aim to ascertain the possible effect of unpublished studies. In 9 studies in which both phase and power measures were reported, we only included power-effects in this analysis (resulting in a total n=15 [power] and n=5 [phase]), as there was no significant difference between power and phase effect sizes.

3.2.4 Exploration of Influencing Factors

Further analyses of the effect of sample and study design were performed using R (R Core Team, 2013) in R-studio. Selected covariates were explored using a mixed linear model approach in the R package nlme (Pinheiro, Bates, DebRoy, & RCoreTeam, 2011). The model was restricted to four independent fixed effect variables and one random effect variable. Because the majority of studies using MEG reported source level data and EEG-studies sensor/electrode level data, only one of these factors – analysis level (sensor/source) – was included in the model. The other selected variables were patient age, stimulus type (click trains vs amplitude-modulated tones) and stimulus duration. The r^2 values of the model were calculated using the package MuMIn (Barton, 2015), which allows the calculation of r^2 values adapted for mixed linear models (Nakagawa & Schielzeth, 2013).

Due to the low number of studies including FEP/CHR individuals, a comparison between FEP and chronic ScZ was not possible. Instead, the sample was divided into 2 age groups based on the median age (39.8 years). Likewise, since only 5 different stimulus durations have been reported (475, 500, 1000, 1024 and 1500 ms), durations were treated as categorical variables in the mixed linear model and were defined as either brief (≤500 ms) or long (≥1000 ms) in post-hoc analyses. One study reported 2 stimulus duration conditions (Hamm et al., 2015) and these were both included in the post-hoc t test evaluation of stimulus duration effects.

Statistical results are presented rounded to two decimal points.

3.1 Results

3.1.1 Effect Size

The final sample included 606 ScZ patients and 590 healthy controls (Table 2 and Table 3). In total, 15 studies included 40 Hz ASSR evoked power measures, 14 included 40 Hz ASSR phase measures (reported as ITPC or PLF), and 9 studies included both measures.

Table 2 Patients and Healthy Controls in Meta-Analysis Sample

Author	HC (N)	Gender HC (M/F)	ScZ (N)	Gender ScZ (M/F)	HC Mean Age (y)	ScZ Mean Age (y)	Patient Group	Illness Duration[a]	Medication Status	Imaging Technique	Image Analysis Level
Kwon et al., 1999	15	15/0	15	15/0	44.6	43.3	Chronic	21.1	Mixed	EEG	Sensor
Brenner et al., 2003	22	13/9	21	18/3	39.7	45.6	Chronic		Mixed	EEG	Sensor
Hong et al., 2004	17	8/9	24	14/10	41.1	39.7	Chronic		All medicated	EEG	Sensor
Spencer et al., 2008	33	19/14	16	19/14	27.5	25.5	FEP	*13.6	All medicated	EEG	Sensor
Vierling-Claassen et al., 2008	12	12/0	12	18/0			Chronic	26.2	All medicated	MEG	Source
Teale et al., 2008	15	12/3	15	13/2	34.8	37.9	Chronic	12.6	All medicated	MEG	Source
Wilson et al., 2008	10	4/6	10	7/3	15.82	14.64	Early onset	3.4	Mixed	MEG	Source
Krishnan et al., 2009	21	11/10	21	13/8	40	42.6	Chronic		All medicated	EEG	Sensor
Spencer et al., 2009	16	16/0	18	18/0	44.4	39.8	Chronic		All medicated	EEG	Sensor
Hamm et al., 2011	18	13/5	18	16/2	39.7	40.7	Chronic	18.2	Mixed	MEG	Source
Tsuchimoto et al., 2011	22	9/13	17	6/11	37	35.6	Chronic	13.5	All medicated	MEG	Sensor
Hamm et al., 2012	16	9/7	17	11/6	39.5	41.5	Chronic		Mixed	EEG	Sensor
Komek et al., 2012	12	7/5	12	7/5	31.4	30.3	Chronic		All medicated	EEG	Sensor
Rass et al., 2012	56	26/30	42	23/19	38.75	36.86	Chronic		Mixed	EEG	Sensor
Kirihara et al., 2013	188	94/94	234	182/52	43.9	44.5	Chronic	22.7	Mixed	EEG	Sensor
Roach et al., 2013	25	14/11	18	21/7	36.1	39.3	Chronic		All medicated	EEG	Sensor
Edgar et al., 2014	29	22/7	39	33/6	37.9	40.87	Chronic		Mixed	MEG	Source
Tada et al., 2016	21	11/10	15	8/5	22.4	22.1	FEP		All medicated	EEG	Sensor
Hirano et al., 2015	24	20/4	24	20/4	44.1	46	Chronic	21.1	All medicated	EEG	Source
Hamm et al., 2015	18	11/7	18	9/9	40.8	45.6	Chronic		Mixed	EEG	Sensor

a) **mean years/*days since admission**

Hedge's g effect sizes ranged from 0.69 to -1.50. In total, 3 effect sizes were greater than 0, suggesting an increase in patients with ScZ compared to controls (g=0.20 for spectral power in Hong, 2004; g=0.53 for spectral power and g=0.69 for phase locking in Hamm, Gilmore, & Clementz, 2012). One of these effects was statistically significant (phase locking in Hamm et al., 2012). The remaining 26 negative effect sizes reflect a reduction in ASSR measures in ScZ. The average Hedge's g random effect size was -0.58 for power measures and -0.46 for phase

measures (Figure 4), indicating a moderately strong effect. However, initial analysis revealed that 3 effect sizes were more than 2 SD from the total mean effect size (i.e., the total [SD] mean effect size was −0.55 [0.46]), and, therefore, they were treated as outliers (both power and phase in Hamm et al (Hamm et al., 2012) and power in Vierling-Claassen et al. (2008). Without these outliers, the Hedge's g random effect sizes were -0.45 [phase n=13] and -0.59 [power n=13], suggesting a robust effect also in the absence of outliers.

Table 3 Meta-Analysis Sample Characteristics

Measure	All included studies[a]	Phase locking	Spectral power	p
N (studies)	20	14	15	
Mean N: ScZ	30.3	36.4	18.8	0.28
Mean N: Controls	29.5	35.6	21	0.26
Mean Age: ScZ	37.5	38.3	36.4	0.54
Mean Age: Controls	36.8	37.9	36.2	0.57
Stimulus duration	696.2	708.9	663.3	0.73

a) The characteristics were compared between the 14 articles reporting phase measures and the 15 articles reporting spectral power measures (9 studies were part of both groups).

The initial statistical comparison revealed no difference between phase and power measures (95% CI: −0.49 to 0.22; t(28)=−0.80; p=0.43), justifying the inclusion of one single effect size from each study in further explorations (15 studies with power measures and 5 studies with phase measures). Mixed linear model analyses revealed a significant effect of patient age (p=0.03) and a trend effect of stimulus duration (p=0.05) on the 40 Hz ASSR measures. There was, however, no effect of stimulus type (p=0.40) or analysis level (p=0.79). The conditional R^2 of this model was 0.94, indicating that the fixed and random variables combined explained more than 90% of the variance. The R^2 of the fixed variables alone (marginal R^2) was 0.54. When the same model was used to evaluate the data set without outliers, only the effect of age remained (patient age: p=0.04; stimulus duration: p=0.34; stimulus type: p=0.27; analysis level: p=0.84).

3.1.2 Post-Hoc Analyses

Post-hoc t tests were used to investigate these results further. None of the above effects remained statistically significant, but there was a trend toward

stronger ASSR reductions in studies with younger participants (t=1.41; p=0.18; 95% CI:−0.14 to 0.69, g[≤39.8 years]=-0.67, g[>39.8 years]=-0.40), and in studies with shorter stimulus durations (t=1.50;p=0.17; 95% CI:−0.18 to 0.90, g[short]=-0.72, g[long]=-0.37). One outlier each were identified for the post-hoc evaluations of the effects of analysis level (Hamm et al., 2012) and stimulus duration (Hong et al., 2004), and 2 for the age comparison (Hamm et al., 2012; Hong et al., 2004), but removing these studies from the respective analyses did not alter the outcome.

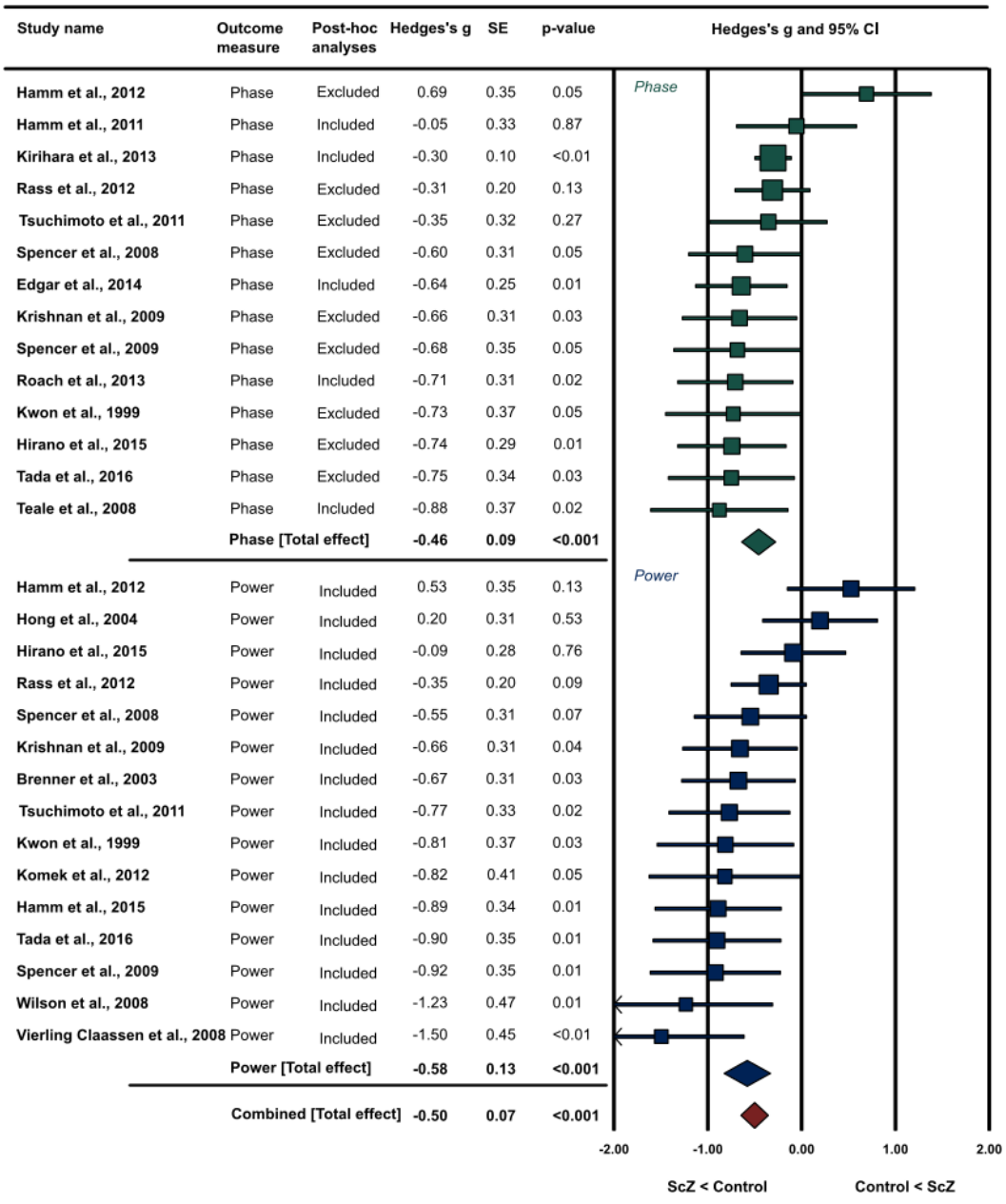

Figure 4 Effects of 40 Hz ASSR in Patients with ScZ vs Healthy Controls (HC). Meta-Analysis Hedge's g Random Effect Sizes, Showing Power and Phase Effects Separately. For Later Post-Hoc Analyses Only One Effect Size Value from Each Study was Included, Selecting the Value for Power in all Cases where both Measures were Reported.

3.1.3 Reporting Bias

Plotting one 40 Hz ASSR effect size from each study in a funnel plot revealed some asymmetry (Figure 5), suggesting that the sample could be affected by reporting bias (Egger regression test: t=2.20; p=0.04; 95% CI: −2.73 to −0.07). Using the "trim and fill" method of Duval and Tweedie(2000) we estimated 5 hypothetically missing studies, which suggests a slight bias in favour of studies reporting ASSR impairments in patients with ScZ. The addition of these studies adjusted the overall Hedge's g random model effect size to -0.42.

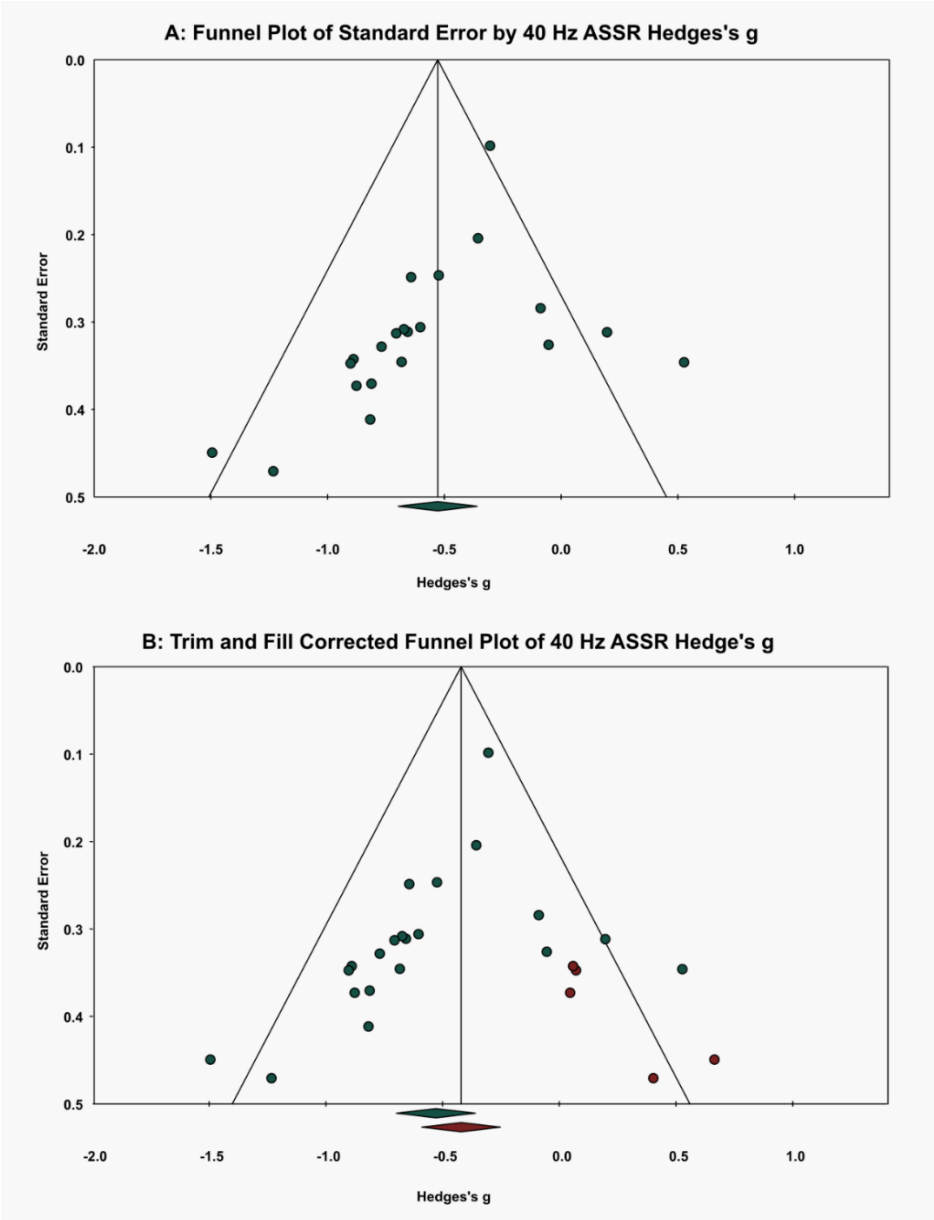

Figure 5 A) Hedge's g Effect Sizes for 40 Hz Auditory Steady State Response (ASSR) Measures from all Studies (n=20) Plotted Against Effect Size Standard Errors. The Plot Shows Some asymmetry. B)Trim and Fill–Corrected Funnel Plot with Additional Studies on the Right Side of the Mean, Showing an Adjusted Overall Hedge's g Random Effect Size of −0.42.

3.2 Discussion

This meta-analysis provides evidence for a moderate reduction in both spectral power and ITPC measures during 40 Hz stimulation in patients with ScZ, highlighting impairments in both the generation of high-frequency oscillations, and in the precise temporal coordination of rhythmic activity in response to entrainment of auditory neural circuits. Importantly, this effect remained significant after correction for potential publication bias.

Optogenetic and pharmacological findings indicate that disturbances in cortical E/I pathways may underlie 40 Hz ASSRs impairments (Sivarao, 2015; Sohal, Zhang, Yizhar, & Deisseroth, 2009). Thus, the observed pattern of 40 Hz ASSR deficits could inform the understanding of circuit impairments in ScZ, and emphasise the possible contribution of disrupted parvalbumin GABAergic interneuron signalling (Lewis, Curley, Glausier, & Volk, 2012) and/or dysfunctional NMDA receptors (Kantrowitz & Javitt, 2010) in ScZ.

The meta-analysis indicated a trend toward more pronounced impairments in the 40 Hz ASSRs in younger patients with ScZ compared with older patients. This contrasts with previous reports of progressive reductions in EEG evoked potentials in psychosis (Salisbury, Shenton, Griggs, Bonner-Jackson, & McCarley, 2003) and magnetic resonance imaging parameters (Kasai et al., 2003) during the course of ScZ. However, the majority of current 40 Hz ASSR studies have been conducted in patients with chronic ScZ, and further research is required to establish the pattern and strength of ASSR deficits in patients with a first episode of psychosis and in at-risk populations.

Due to the modest number of studies, further replication of the 40 Hz ASSR deficit in patients with ScZ is required; the effect size of the ASSR deficit is currently lower than other electrophysiological indices of auditory dysfunctions in ScZ, such as the mismatch negativity (Erickson et al., 2015) (Hedge's g=0.95 for all patients with ScZ and Hedge's g=0.81 for patients with chronic ScZ) and P50 (de Wilde, Bour, Dingemans, Koelman, & Linszen, 2007)(Cohen's d=1.28).

Based on the current data, the meta-analysis can only provide a preliminary indication regarding the potential impact of recording techniques (EEG vs MEG)

and analysis parameters (source vs sensor). However, the meta-analysis does highlight that source reconstructed data are available predominantly from MEG studies, suggesting that these reports may have superior sensitivity to detect subtle regional effects. In addition, further relationships with cognitive deficits as well as clinical parameters in patients with ScZ would significantly enhance the utility of the 40 Hz ASSR as an important index of auditory circuit functions in patients with ScZ. Finally, additional investigations focusing on early stages of psychosis are essential to establish the potential clinical usefulness of 40 Hz ASSR measures.

3.3 Conclusion

This systematic meta-analysis of the 40 Hz ASSR in ScZ indicates a moderately robust impairment in both evoked power and phase-locking measures in patients. However, further work in younger psychosis patients and CHR samples is required to build on the understanding of neurobiological circuit dysfunctions in psychosis, and to establish if 40 Hz ASSR measures could constitute a useful biomarker. Subsequent chapters will present data which provide a starting point for addressing these questions

Chapter 4 The 40 Hz Auditory Steady State Response in the Clinical High-Risk State and First Episode Psychosis

4.1 Introduction

The meta-analysis presented in Chapter 3 established that 40 Hz ASSR ITPC and spectral power are robustly impaired in chronic ScZ (Thuné et al., 2016). However, data from CHR participants and FEP patients remain limited. Preliminary findings indicate that alterations may occur prior to diagnosis (Koshiyama et al., 2018a; Tada et al., 2016), but the available studies are limited by the small number of CHR participants and the potentially confounding influence of antipsychotic medication.

To address these issues, this chapter presents analyses of MEG-measured ASSR data from the YouR study, with the aim to investigate further whether ASSR impairments are present in CHR individuals. In addition, analyses comparing the control and CHR data with data from a small FEP sample are presented. Due to the limited CHR 40 Hz ASSR reports available, a data-driven approach was used for selection of regions for analysis. However as stated in Section 1.1, the analysis was based on the hypothesis that CHR individuals would show reduced 40 Hz ASSR evoked power and ITPC compared to healthy controls. MEG-measured data were utilised as spatial reconstruction of cortical regions, which was a key component of the planned analysis, is easier with MEG than with EEG (Barkley & Baumgartner, 2003).

The clinical potential of the 40 Hz ASSR depends on whether abnormalities are robustly and reliably present in affected patients, but also on whether deficits can be detected in vulnerable undiagnosed individuals. Reports of ASSR measures in first-degree relatives of schizophrenia patients indicate that the 40 Hz ASSR is sensitive to genetic risk (Hong et al., 2004; Rass et al., 2012). In addition, 40 Hz ASSR impairments have been reported in Autism Spectrum Disorders and Bipolar Disorder (Maharajh, Abrams, Rojas, Teale, & Reite, 2007; Rass et al., 2010; Rojas et al., 2011; Wilson et al., 2007), suggesting that ASSR deficits may not be specific to schizophrenia, but reflect genetic vulnerability for psychosis and disorders with similar sensory processing deficits.

In psychosis research, initial reports indicated that impairments in both 40 Hz ASSR power and phase coherence are present in FEP patients (Koshiyama et al., 2018a; Spencer et al., 2008; Tada et al., 2016). Moreover, impaired 30 Hz ASSR power and phase-locking, measured using EEG, has been observed in FEP (Spencer et al., 2008), indicating potential deficits in high beta frequency oscillations in addition to gamma band deficits.

Similarly, one research group observed abnormal 40 Hz ASSR in the earliest component of the response (0-100ms and 200-300ms) in FEP, and impairments in both FEPs and CHR participants, during the later stimulation periods (300-500ms) (Tada et al., 2016). These findings were replicated with a larger sample size (Koshiyama et al., 2018a). Hence, available data suggest that sustained gamma oscillatory responses may be aberrant in CHR as well as in FEP. However, the meta-analysis presented in the previous chapter (Thuné et al., 2016) revealed some publication bias in the ScZ literature and it is possible that a similar bias is present for CHR and FEP studies. Accordingly, more data from larger samples are needed to clarify the nature of 40 Hz ASSR alterations at different stages of psychosis.

4.2 Methods

4.2.1 Data Collection

Analyses included data from the 93 CHR participants, 17 FEP patients and 46 healthy controls described in Chapter 2.

MEG data were recorded on a 4D Neuroimaging Magnes 3600 Whole Head 248 channel MEG scanner at a sampling rate of 1kHz. Auditory stimuli were 1000 Hz carrier tones amplitude-modulated at 40 Hz. One hundred tones were presented for 2000 ms, with an inter-trial interval of 2000 ms (± 500 ms jitter) through MEG compatible inner-ear tubes. In addition, a simple attention task consisting of the detection of non-amplitude modulated target 1000 Hz tones (N=10) was added in order to ensure that participants attended the auditory stimuli (Figure 6).

4.2.2 MEG Data Pre-Processing

Data were pre-processed and analysed in Fieldtrip (Oostenveld, Fries, Maris, & Schoffelen, 2011) in MATLAB (version 2013b). Raw data were epoched from 1000 ms prior to stimulus onset to 2400 ms post stimulus onset, linear trends were removed, data were 'de-noised' relative to reference MEG channel signals and down sampled to 500 Hz. Moreover, muscle, eye movement and cardiac artefacts were removed from data through visual inspection, principal component analysis and independent component analysis. Following pre-processing, the average number of trials available was 93.8 (± sd 3.9) and trial numbers did not differ significantly between groups ($p>0.05$).

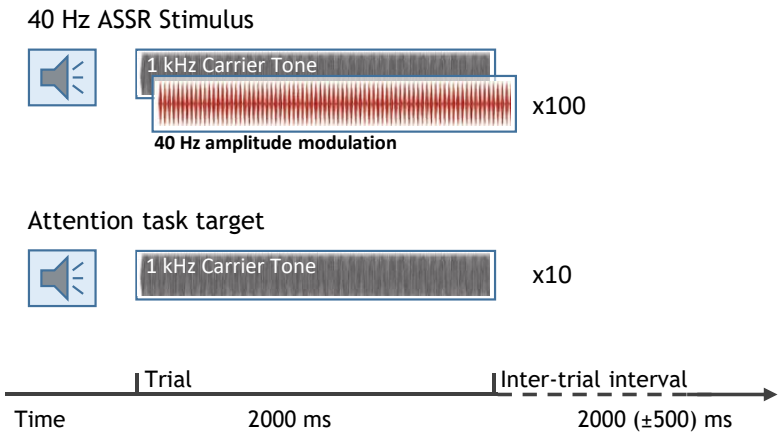

Figure 6 ASSR Stimulation Task Setup

Pre-processed cleaned MEG data were transformed from axial to planar orientation (Bastiaansen & Knösche, 2000), to aid subsequent plot interpretation. Next, grand average spectral power and ITPC data were calculated for each group during the stimulation period (0-2000ms). Cleaned baseline and task data were compared across groups to establish whether the stimulation paradigm successfully entrained brain regions to fire synchronously in the 40 Hz frequency range. In other words, the presence of an overall stimulation effect was explored. This analysis indicated that both evoked power and ITPC in the 38-42 Hz range evolved around 150 ms and were sustained until 1950 ms post-stimulus onset in the present sample. Thus, statistical evaluations of group effects were performed at 38-42 Hz and from 150-1950 ms, using non-parametric Monte-Carlo permutation based independent samples F-tests, which

were corrected for multiple comparisons using a cluster-based permutation approach.

4.2.3 Evoked Spectral Power and ITPC Analyses

Similar to the meta-analysis presented in Chapter 3, the main analyses focused on evoked spectral power, indicating the squared amplitude of the signal (Izhikevich et al., 2018), and the ITPC, reflecting phase consistency of oscillations across trials (Bardouille & Ross, 2008).

Time-frequency representations of data were obtained by convolving the planar preprocessed data with a complex wavelet, using a Hanning taper sliding window Fourier transform approach. The computation was done using a step-size of 25 ms across epochs, 4 s padding and smoothing ± 1Hz, including frequencies 1-100 Hz and keeping individual trials. Statistical group comparisons of evoked spectral power were performed on time-frequency data computed relative to baseline power (-600 to -100 ms prior to stimulus onset, relative change method).

Furthermore, post-hoc statistical tests of spectral power in the 15-25 Hz range, at 500-1500 ms, were performed. In addition, potential differences in baseline (-600 to -100 ms) 40 Hz power were explored between groups as previous work has indicated altered ASSR baseline power in ScZ (Spencer, 2012).

The ITPC index was computed in two steps. First, a fourier spectrum was computed using the time-frequency analysis approach described above. Next, the ITPC was estimated from the complex norm of the time–frequency decomposition by dividing by vector amplitude, summing vector angles, finding the absolute value and normalizing this and finally removing the singleton dimensions. The resulting ITPC values range in value from 0 to 1 and reflect the degree of phase consistency across trials. For statistical analyses, ITPC was computed across time (150-1950 ms), averaged over frequency (38-42 Hz) and expressed relative to baseline (-600 to -100 ms prior to stimulus onset, absolute change method).

All statistical group comparisons of sensor level data focused on grand average data calculated for each study group, and group effects at 38-42 Hz were explored both on whole brain data and on 12 selected sensors of interest (six sensors covering temporal and parietal regions of each hemisphere) identified based on analyses of overall effects of stimulation (see Section 4.3.2). A non-parametric montecarlo permutation-based approach was employed to perform independent samples F-tests and tests were corrected for multiple comparisons using a cluster-based permutation approach.

4.2.4 Source Reconstruction

A T1 weighted MRI scan was recorded on a Siemens 3T Trio Trim scanner using 3D MPRAGE sequences (192 slices, voxel size 1 mm^3, FOV=256x256x176 mm, TR=2250 ms, TE=2.6 ms, FA=9°), and converted to SPM8 format using MRIcron (Rorden & Brett, 2000). During the scan, a vitamin E pill was placed by the left ear to allow for detection of the left hemisphere in the MRI data. MEG head models were computed and aligned with the T1, first using the nasion, right and left ears as anatomical landmarks and subsequently fine-tuning the match using digitized MEG head shape points.

MEG data were reconstructed in the source space using Linearly Constrained Minimum Variance (LCMV) (Van Veen, Van Drongelen, Yuchtman, & Suzuki, 1997) beamformer spatial filters and the standardized Automated Anatomical Labelling (AAL) brain atlas (Tzourio-Mazoyer et al., 2002). Coordinates for the centroids of 116 AAL regions were specified in each subject brain from an MNI template and used to model signals at each brain region. Source modelling at the 116 AAL centres was done using a grid size of 5 mm, individual subject head models and normalised lead fields. Next, the AAL source estimations from individual subject grid-points were normalized to an MNI template brain with dimensions 91x109x91 mm, to allow averaging data from different subject grids despite individual differences in brain anatomy data. Subsequent statistical group comparisons were based on data averaged for each experimental group.

Similar to sensor level data, successful activation of brain regions following ASSR stimulation (a stimulation effect) was confirmed prior to the performance of any further analyses. This was done by comparing two stimulation time-windows

(500-1000 ms and 1000-1500 ms) with the baseline (-600 to -100 ms) across groups, using a non-parametric Monte-Carlo permutation based dependent samples t test. Following this initial statistical inspection of the data, auditory, subcortical and cerebellar nodes significantly activated during ASSR stimulation were selected as regions of interest (ROI). For the ITPC measure, only nodes with a t value >5 were considered, given the large number of activated nodes. Group effects were evaluated statistically in the 38-42 Hz range, both averaged over frequency and time (150-1950 ms) and averaged over frequency but not time.

4.2.5 Behavioural and Clinical Data

Behavioural data (reaction times (RTs) and response accuracy), were analysed in SPSS. Differences in reaction times were evaluated using a Welch test, as differences in group variance were detected. Response accuracy was determined by computing d' scores for each participant and subsequently analysing group differences using a Kruskal-Wallis H-test. Post-hoc tests were performed using Mann Whitney U-tests.

Correlations between clinical and demographic measures (see Chapter 2) and ASSR data were performed using Spearman correlations. In the CHR group, the relationship between ITPC and spectral power, composite BACS scores, total CAARMS scores and GAF scores was explored. In addition, CAARMS perceptual abnormality scores were included, as auditory gamma-band oscillations may also be relevant for the generation of hallucinations (Spencer et al., 2009).

The potential impact of demographic variables age and gender on the 40 Hz ASSR-measures was explored in separate analyses. Results indicated that neither variable likely affected the outcome of the main ASSR analyses, as no significant relationship was found with ASSR measures in the ROIs. Thus, these variables were not corrected for in the main analyses.

4.3 Results

4.3.1 Behavioural Data

Mean RTs were not different between groups (Welch $F(2)=1.06$, $p=0.36$), but differed in group variance (Levene statistic=4.22, $p=0.02$). Furthermore, there was a significant group difference in response accuracy, expressed as d' ($H(2)=6.88$, $p=0.03$). This difference represented a significantly poorer response accuracy in CHR ($U=1651.50$, $p=0.01$, $N=135$), and FEP ($U=441.00$, $p<0.001$, $N=57$) compared to controls.

4.3.2 Effect of Stimulation Across Groups

Data recorded during baseline and 40 Hz stimulation were compared across groups to establish whether the paradigm elicited a statistically significant evoked response (stimulation effect). A statistically significant evoked increase spectral power was observed in sensor MEG data ($t(155)=9.01$, $p<0.001$, cluster correction), as well as for 40 Hz ITPC ($t(155)=14.78$, $p<0.01$, cluster correction), primarily over temporal regions. In addition, a wide-spread whole brain beta power activation at 15-25 Hz was also observed ($t(155)=0.86$ to 6.37; $p=6.66e-04$ to 0.17). Across groups, this beta response emerged around 350 ms over frontal, temporo-parietal and occipital areas (Figure 7B), with particularly pronounced activation over the left-hemisphere.

The sensor level effects were reflected in virtual channel source data, where significant false discovery rate (fdr) corrected effects were observed for 40 Hz ASSR power and ITPC (Table 4). A significant stimulation effect for spectral power in the beta 15-24 Hz range was also found on virtual channel level, across all nodes (all $p \leq 0.002$, fdr corrected)

4.3.3 40 Hz Spectral Power: Sensor Analysis

Group comparisons of sensor level data revealed no significant difference in 40 Hz ASSR power (38-42 Hz) ($F(2)=3.49e-05$ to 9.54; $p=0.41$ to 1.00) (Figure 7A). Moreover, no significant difference was found in a separate analysis focusing only on CHR and control participants ($t(138)=-3.91$ to 3.48; $p=0.41$ to 1.00).

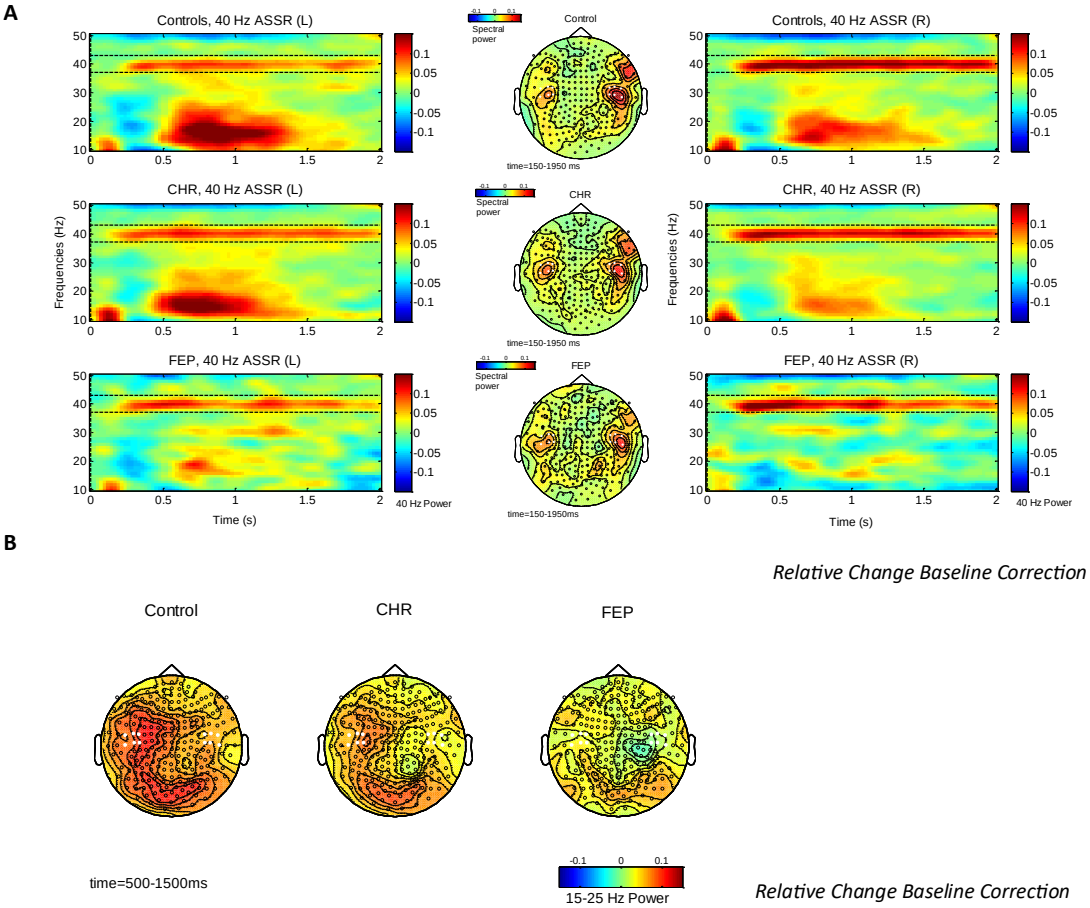

Figure 7 Evoked Spectral Power Measured during 40 Hz ASSR Stimulation, in Control Participants, CHR Participants and FEP patients. Showing A) Time-Frequency Plots and 40 Hz Topographies, B) Beta (15-25 Hz) Post-Hoc Topographies

4.3.4 Beta Spectral Power: Sensor Analysis

A strong beta band activation in the 15-25 Hz range was observed across groups at sensor level (Figure 7B), warranting post-hoc investigation. However, there was no difference in beta power between groups in sensor data (F(2)=3.13e-04 to 5.80, p=0.14 to 1.00), measured from 500-1500 ms.

4.3.5 Inter-Trial Phase Coherence: Sensor Analysis

Sensor level analyses comparing the 40 Hz ASSR ITPC between groups revealed no significant effect ($F(2)=5.76x10^5$ to 9.97, p=0.55 to 1.00). Planned post-hoc tests between CHR and controls (t(138)=3.88 to -3.42, p=1.00 to 0.28) and

between FEP and controls (t(62)=3.66 to -4.01, p=1.00 to 0.15) also did not reveal significant differences between groups.

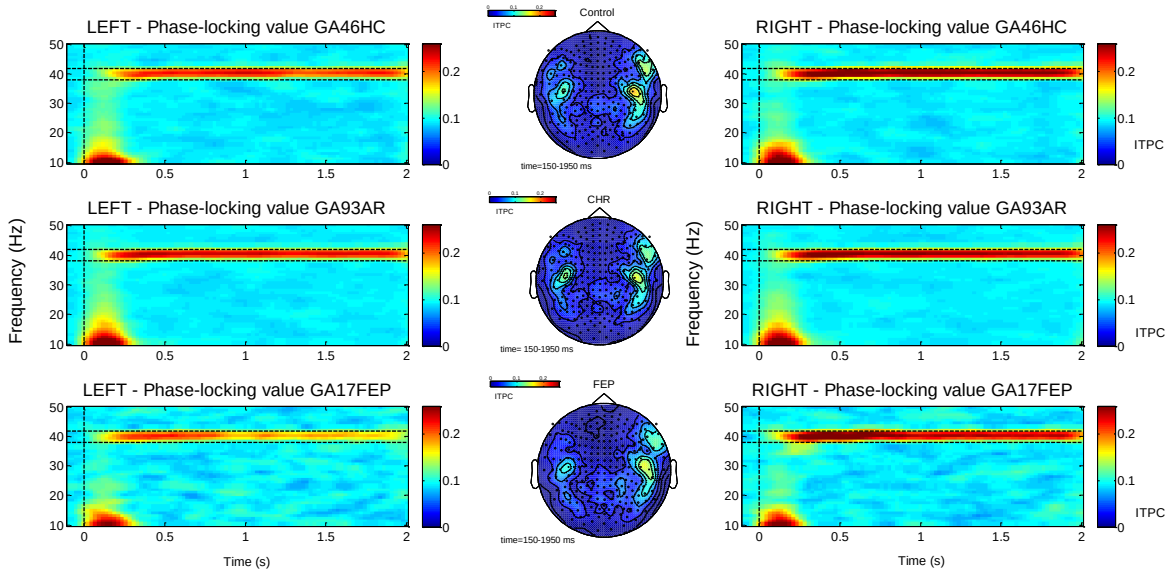

Figure 8 Sensor Level ITPC Data Recorded During 40 Hz ASSR Stimulation. Absolute Baselined Data.

In addition to sustained 40 Hz activity, a low-frequency evoked response in the 0-20 Hz range was observed from stimulus onset to 250 ms post-stimulus (Figure 8). Analyses of this evoked response revealed no significant differences between groups at sensor level (F(2)=0.003 to 8.41, min p=0.34).

4.3.6 40 Hz ASSR Power: Source Analysis

Nine ROI nodes were selected for spectral power analyses, identified by selecting auditory, subcortical and cerebellar nodes significantly activated during ASSR stimulation (Table 4).

Group analyses revealed no effect in primary auditory areas, but a statistical trend was found in the RSMG (F(2)=2.77, p=0.06) (Table 5). Post-hoc tests showed a significant reduction for both the CHR and FEP-groups. A transient reduction was also seen the right cerebellar areas 4-5 (Figure 9). The effects did not survive fdr correction for multiple comparisons.

No statistical group difference in 40 Hz ASSR baseline power was detected (F(2)=0.11 to 2.05; p=0.13 to 0.91).

Table 4 Brain Regions of Interest Selected for 40 Hz ASSR Analyses

Brain Region	Local Maxima MNI Coordinates (right, anterior, superior) [a]	ITPC ROI	Spectral power ROI
Left Supramarginal Gyrus (LSMG)	-55.79 -33.64 30.45	✓	
Right Supramarginal Gyrus (RSMG)	57.61 -31.5 34.48	✓	✓
Left Heschl's Gyrus (LHES)	-41.99, -18.88, 9.98	✓	
Right Heschl's Gyrus (RHES)	45.86, -17.15, 10.41	✓	✓
Left Superior Temporal Gyrus (LSTG)	-53.16, -20.68, 7.13	✓	
Right Superior Temporal Gyrus (RSTG)	58.15, -21.78, 6.8	✓	✓
Left Medial Temporal Gyrus (LMTG)	-55.52, -33.8, -2.2	✓	
Right Medial Temporal Gyrus (RMTG)	57.47, -37.23, -1.47	✓	✓
Left Inferior Temporal Gyrus (LITG)	-49.77, -28.05, -23.17	✓	
Right Inferior Temporal Gyrus (RITG)	53.69, -31.07, -22.32	✓	✓
Left Hippocampus (LHIP)	-25.03, -20.74, -10.13	✓	
Right Hippocampus (RHIP)	29.23, -19.78, -10.33	✓	✓
Left Thalamus (LTHA)	-10.85, -17.56, 7.98	✓	✓
Right Thalamus (RTHA)	13, -17.55, 8.09	✓	✓
Right Cerebellar areas 4-5 (RCRBL45)	17.20, -42.86, -18.15	✓	✓
Right Cerebellar area 10 (RCRBL10)	25.99, -33.84, -41.35	✓	

a) Coordinates from Tzourio-Mazoyer et al. 2002

Table 5 40 Hz Spectral Power Analyses

Brain region	Group Analysis		CHR vs HC			FEP vs HC		
	F	p	t	p	d	t	p	d
RSMG	2.77	0.06	-2.23	0.02*	-0.45	-1.41	0.06	-0.39
RHES	0.12	0.89	0.41	0.35	0.08	-0.04	0.49	-0.01
RSTG	0.12	0.89	0.05	0.47	0.02	-0.37	0.42	-0.10
RMTG	1.08	0.35	-1.15	0.12	-0.20	0.34	0.35	0.10
RITG	0.08	0.91	-0.05	0.46	-0.00	-0.39	0.37	-0.10
RHIP	0.04	0.96	0.61	0.28	0.05	-0.39	0.37	0.00
LTHA	0.45	0.66	0.23	0.42	0.04	-0.05	0.50	0.22
RTHA	0.32	0.74	0.12	0.45	-0.10	0.73	0.25	-0.19
RCRBL45	0.47	0.61	-0.61	0.26	0.13	-0.67	0.25	-0.10

a) Data averaged across trial time-window

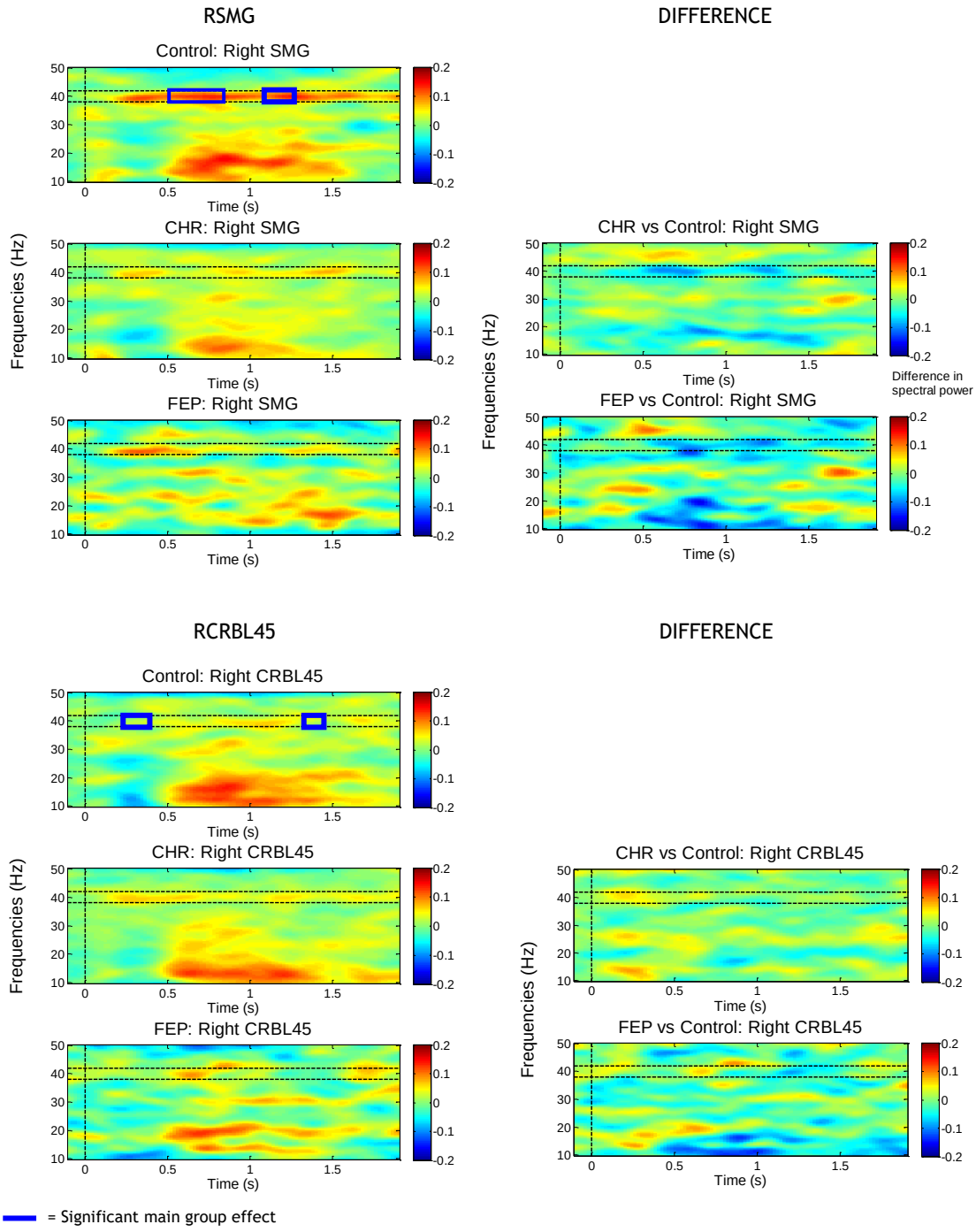

Figure 9 40 Hz ASSR Spectral Power Group Effects Across Trial in RSMG and RCRBL45. Including Group Difference Plots. Highlighted Regions Indicate Time Periods where Group Effect p<0.05 (uncorrected). No Effects Survived fdr Correction.

4.3.7 Beta Power: Source Analysis

Analyses of source reconstructed data in the beta (15-25 Hz) frequency band indicated whole brain increases in beta power during the 40 Hz ASSR stimulation compared to baseline . Group differences in 15-25 Hz power were detected in 7 AAL nodes (Table 6; Figure 10). The largest effect was observed in the RSMA

(F(2)=3.85, p=0.02) and the LROL (F(2)=5.51, p<0.01). In particular, 15-25 Hz power in the LROL was impaired in both CHR and FEP participants compared to controls, with a more pronounced reduction in the FEP-group compared to CHR participants.

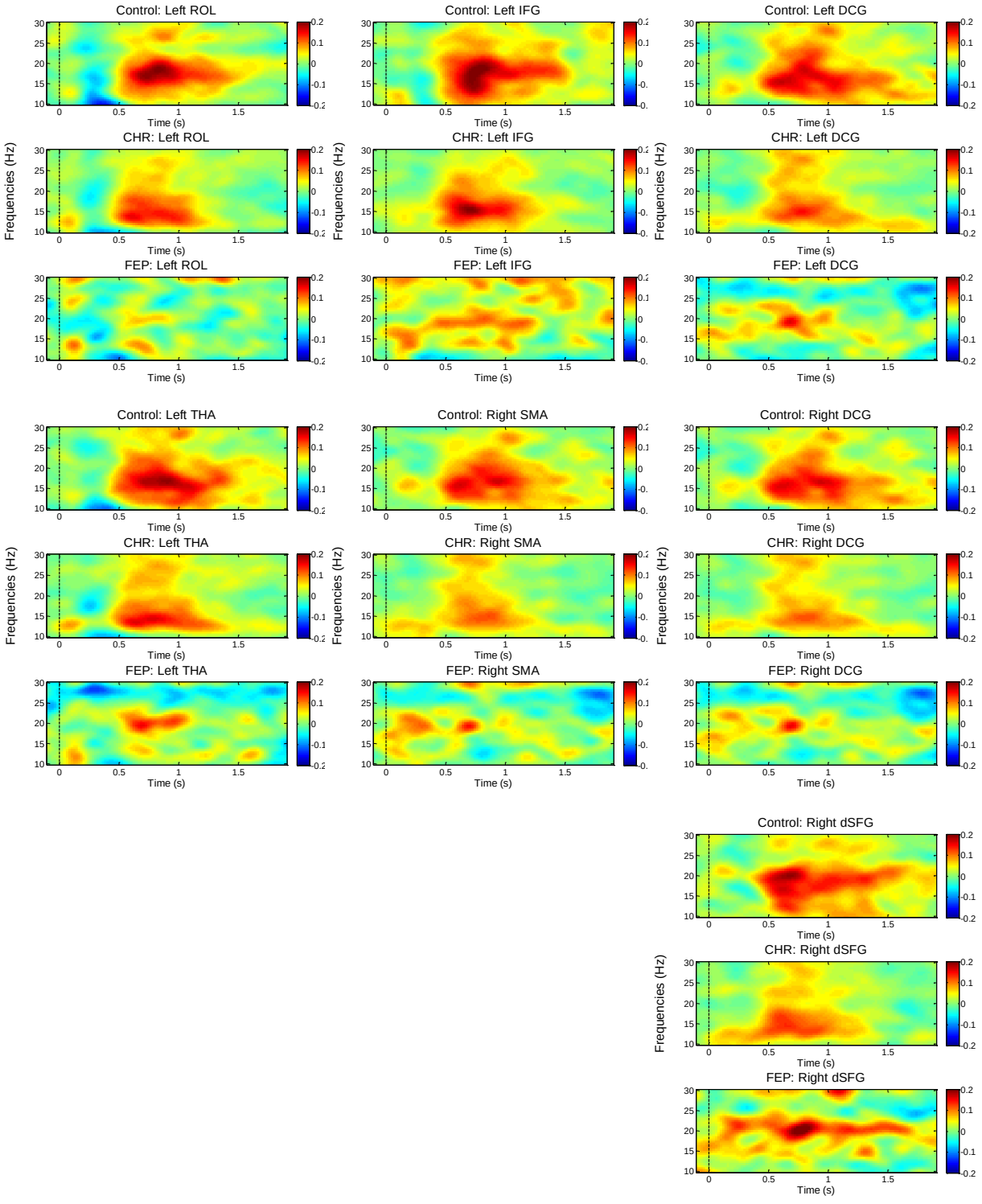

Figure 10 Nodes with Significant Beta Range (15-25 Hz) Spectral Power Group Differences between 500-1500 ms (all p<0.05, fdr corrected).

Table 6 Beta Spectral Power: Virtual Channels with Significant Group Effects

Brain Area	Group Effect		Post-Hoc								
			CHR vs HC			FEP vs HC			FEP vs CHR		
	F	p	t	p	d	t	p	d	t	p	d
Right Superior Frontal Gyrus (RSFG)	3.24	0.04*	-2.59	0.01*	0.47	-0.82	0.22	0.23	0.78	0.21	-0.21
Left Inferior Frontal Gyrus (LIFG)	3.18	0.04*	-2.11	0.02*	0.38	-2.32	0.01*	0.66	-0.73	0.24	0.19
Right Supplementary Motor Area (RSMA)	3.85	0.01*	-2.31	0.01*	0.42	-2.08	0.01*	0.59	-1.02	0.16	0.27
Left Dorsal Cingulate Gyrus (LDCG)	3.23	0.04*	-2.16	0.02*	0.39	-1.94	0.02*	0.55	-0.77	0.23	0.20
Right Dorsal Cingulate Gyrus (RDCG)	3.58	0.02*	-2.26	0.01*	0.41	-2.01	0.02*	0.57	-0.87	0.20	0.23
Left Rolandic Area (LROL)	5.51	0.01*	-2.00	0.02*	0.36	-3.17	0.00*	0.90	-2.17	0.02*	0.57
Left Thalamus (LTHA)	3.91	0.02*	-2.27	0.02*	0.41	-2.21	0.01*	0.63	-1.11	0.14	0.29

4.3.8 Inter-Trial Phase Coherence: Source Analysis

Sixteen auditory, subcortical and cerebellar regions showed a significant change in ITPC (with T> 5) during ASSR stimulation and were selected as ROI nodes (Table 4).

Source reconstructed time averaged ITPC data differed significantly between groups in the RSMG (Table 7; Figure 11). Moreover, in data not averaged across time, less sustained effects were seen in the LTHA, the LITG and the RCRBL10 (Figure 11). All effects were driven by reduced ITPC in the CHR group. However, the effects did not remain significant after false discovery rate correction.

Analyses of the early evoked ITPC response observed in the 0-20 Hz range at 0-250 ms post-stimulus revealed a group difference in LHES ($F(2)=3.10$, $p=0.02$), representing increased ITPC in CHR compared to controls ($t(138)=2.64$, $p=0.002$, $d=0.48$). A trend group difference was present in LMTG ($F(2)=3.07$, $p=0.05$), corresponding to decreased ITPC in FEP compared to controls ($t(62)=-2.20$, $p=0.01$, $d=-0.62$).

Table 7 40 Hz ITPC Source Analyses

Brain region	Group Analysis		CHR vs HC			FEP vs HC		
	F	p	t	p	d	t	p	d
LSMG	0.35	0.72	-0.83	0.21	-0.17	-0.04	0.50	-0.02
RSMG	3.62	0.03*	-2.69	0.00*	-0.49	-1.43	0.07	-0.41
LHES	0.10	0.92	-0.24	0.41	-0.04	0.23	0.40	0.07
RHES	0.47	0.63	-0.88	0.20	-0.16	0.03	0.48	0.01
LSTG	0.13	0.91	-0.17	0.41	-0.02	0.33	0.36	0.11
RSTG	0.20	0.82	-0.45	0.34	-0.09	-0.55	0.30	-0.16
LMTG	0.04	0.96	0.29	0.38	0.05	0.10	0.45	0.03
RMTG	0.50	0.62	-0.98	0.16	-0.17	-0.19	0.45	-0.05
LITG	0.87	0.43	1.16	0.13	0.21	0.96	0.16	0.28
RITG	0.79	0.46	-0.88	0.19	-0.16	-1.09	0.14	-0.30
LHIP	0.45	0.67	-1.05	0.15	-0.17	-0.16	0.44	-0.04
RHIP	0.95	0.38	-0.72	0.24	-0.14	-1.26	0.09	-0.37
LTHA	0.86	0.42	-1.33	0.10	-0.24	-0.06	0.50	-0.02
RTHA	0.37	0.69	-0.88	0.20	-0.16	-0.42	0.35	-0.12
RCRBL45	0.37	0.70	-0.46	0.32	-0.07	-0.75	0.23	-0.21
RCRBL10	1.01	0.36	-0.40	0.35	-0.07	-1.28	0.10	-0.37

4.3.9 Correlations

No significant correlation was found between 40 Hz ASSR power in ROI's and composite BACS scores across groups, or between 40 Hz ASSR power, composite BACS, total CAARMS scores or GAF scores within the CHR group alone. Likewise, there was no significant correlation between ASSR power and perceptual abnormality scores in CHR participants (Table 8).

A significant correlation was found across groups between 40 Hz ASSR ITPC and composite BACS scores in the LSTG (Rho=-0.176, p=0.040) (Table 9). In the CHR group, a significant correlation was found between ITPC and total BACS scores in the LSTG (Rho=-0.264, p=0.015), total CAARMS scores in the LMTG (Rho=0.247,

p=0.023) and LITG (Rho=0.230, p=0.034), and between ITPC and perceptual abnormality scores in the LITG (Rho=0.266, p=0.013) (Table 9, Figure 12). Following false discovery-rate correction for multiple comparisons the correlations did not remain significant, with the lowest corrected values being p=0.125, for the correlations between 40 Hz ASSR ITPC and total CAARMS scores in the RSMG, RSTG, RHES, and LITG.

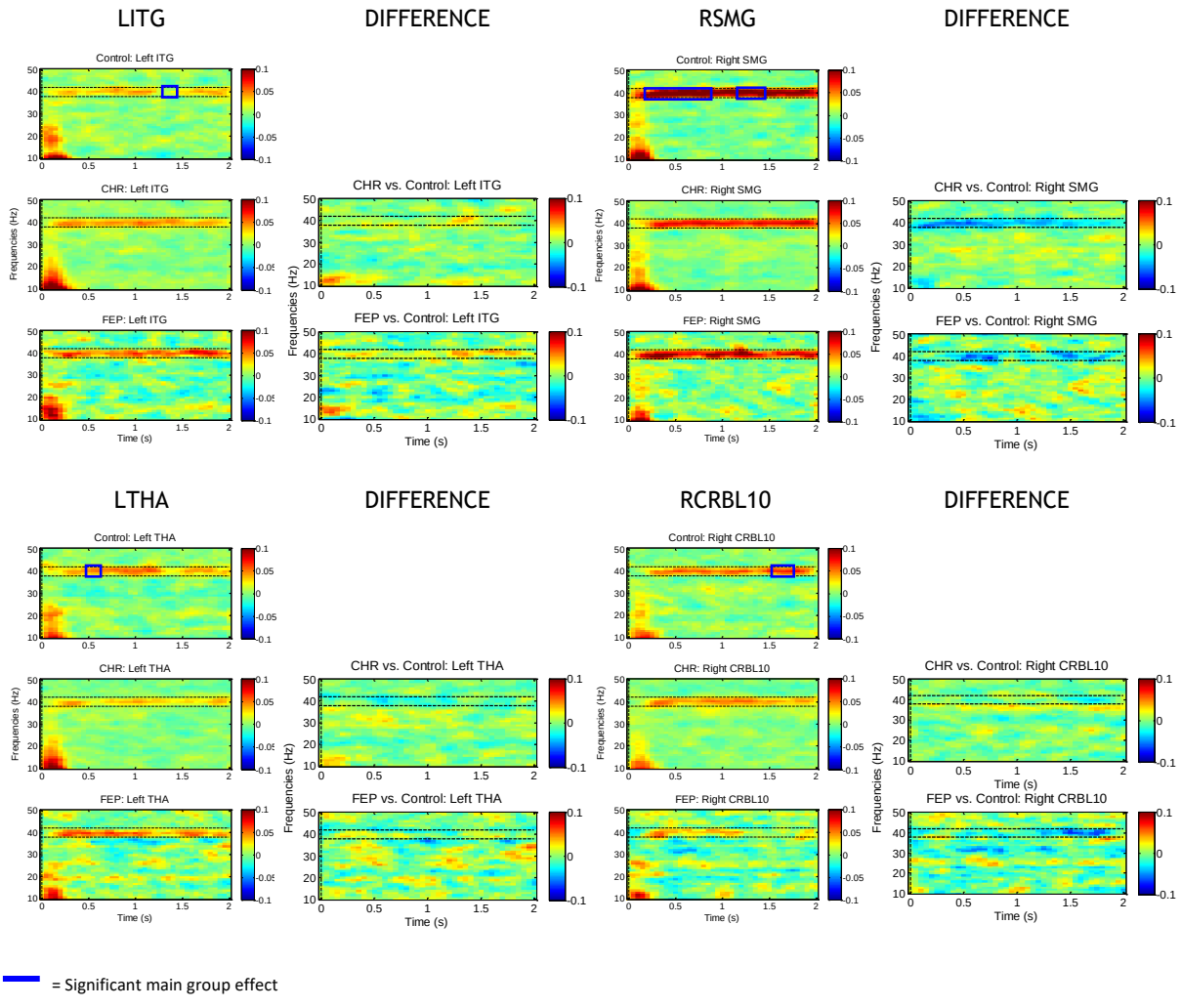

Figure 11 ITPC during 40 Hz ASSR: Group Effects across Trial in RSMG, RCRBL10, LITG and LTHA, Including Group Difference Plots. Highlighted Regions Indicate Time Periods where Group Effect p<0.05 (uncorrected). No Effects Survived fdr Correction.

Correlation analyses investigating relationships between beta range (15-25 Hz) spectral power and clinical measures demonstrated a positive relationship between GAF scores and power across all seven identified beta ROIs (Table 10, Figure 13). In the RSMA, RSFG and bilateral DCG, the correlations with GAF scores survived correction for multiple comparisons (fdr). A correlation was also

observed between total CAARMS scores and RDCG beta power in CHRs (Table 10, Figure 13).

Table 8 40 Hz Spectral Power: Spearman Correlation Coefficients

Brain Area	All groups	CHR only			
	Composite BACS[a]	Composite BACS	Total CAARMS	Perceptual Abnormalities[c]	GAF
RSMG	0.16[b]	0.05	0.11	0.11	-0.03
RMTG	0.04	0.1	-0.05	-0.06	-0.05
RSTG	0.04	0.09	0.00	-0.05	0.02
RHES	-0.05	-0.07	-0.11	-0.16	0.01
RITG	-0.04	-0.09	-0.13	-0.04	0.03

a) z-transformed and gender corrected BACS score

b) Spearman correlation coefficient

c) Perceptual abnormality score measured on the CAARMS scale

Table 9 40 Hz ITPC: Spearman Correlation Coefficients

Brain Area	All groups	CHR only			
	Composite BACS[a]	Composite BACS[a]	Total CAARMS	Perceptual Abnormalities[c]	GAF
RSMG	0.15[b]	0.16	-0.05	-0.13	-0.15
LSMG	-0.01	0.05	-0.02	0.05	0.04
RSTG	-0.01	0.03	-0.16	-0.10	0.06
LSTG	-0.18*	-0.26	0.16	0.21	-0.17
RMTG	0.07	0.09	-0.03	-0.10	-0.04
LMTG	-0.09	-0.07	0.25*	0.14	-0.07
RHES	0.00	0.01	-0.15	-0.16	0.09
LHES	-0.11	-0.19	0.08	0.15	-0.07
RITG	0.02	0.04	0.03	-0.01	-0.16
LITG	-0.13	-0.15	0.23*	0.27*	-0.07

a)z-transformed and gender corrected BACS score

b) Spearman correlation coefficient

C)Perceptual abnormality score measured on the CAARMS scale

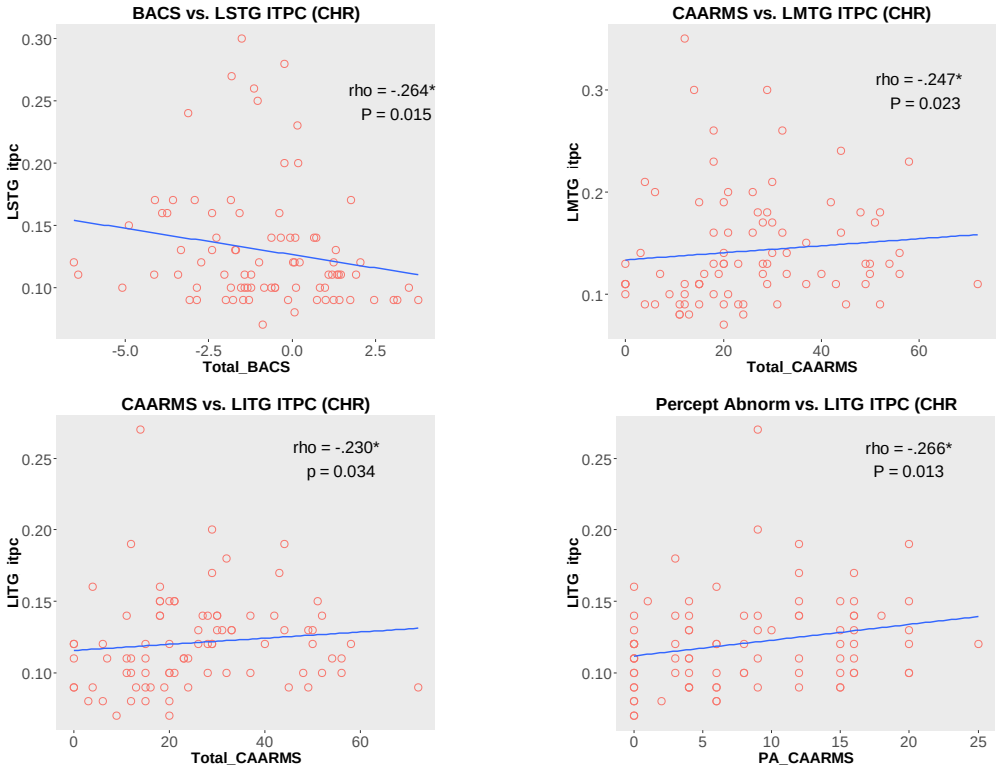

Figure 12 Spearman Correlations between ITPC and Psychological Measures in CHR Participants. No fdr Correction.

Table 10 Beta (15-25 Hz) Spectral Power: Spearman Correlation Coefficients

Brain Area	All groups	CHR only			
	Composite BACS[a]	Composite BACS	Total CAARMS	Perceptual Abnormalities[c]	GAF
RSMA	0.16[b]	0.16	-0.19	-0.05	0.35**
LROL	0.15	0.14	-0.15	0.03	0.21*
LTHA	0.12	0.16	-0.15	-0.04	0.25*
RSFG	0.09	0.06	-0.18	-0.09	0.30**
LIFG	0.10	0.06	-0.08	-0.08	0.22*
LDCG	0.10	0.14	-0.14	-0.06	0.32**
RDCG	0.12	0.19	-0.21*	-0.07	0.39**

a)z-transformed and gender corrected BACS score

b) Spearman correlation coefficient

c) Perceptual abnormality score measured on the CAARMS scale

***=p<0.05 (2-tailed); **=p<0.01 (2-tailed), effects survived fdr correction in RSMA, RSFG and bilateral DCG.**

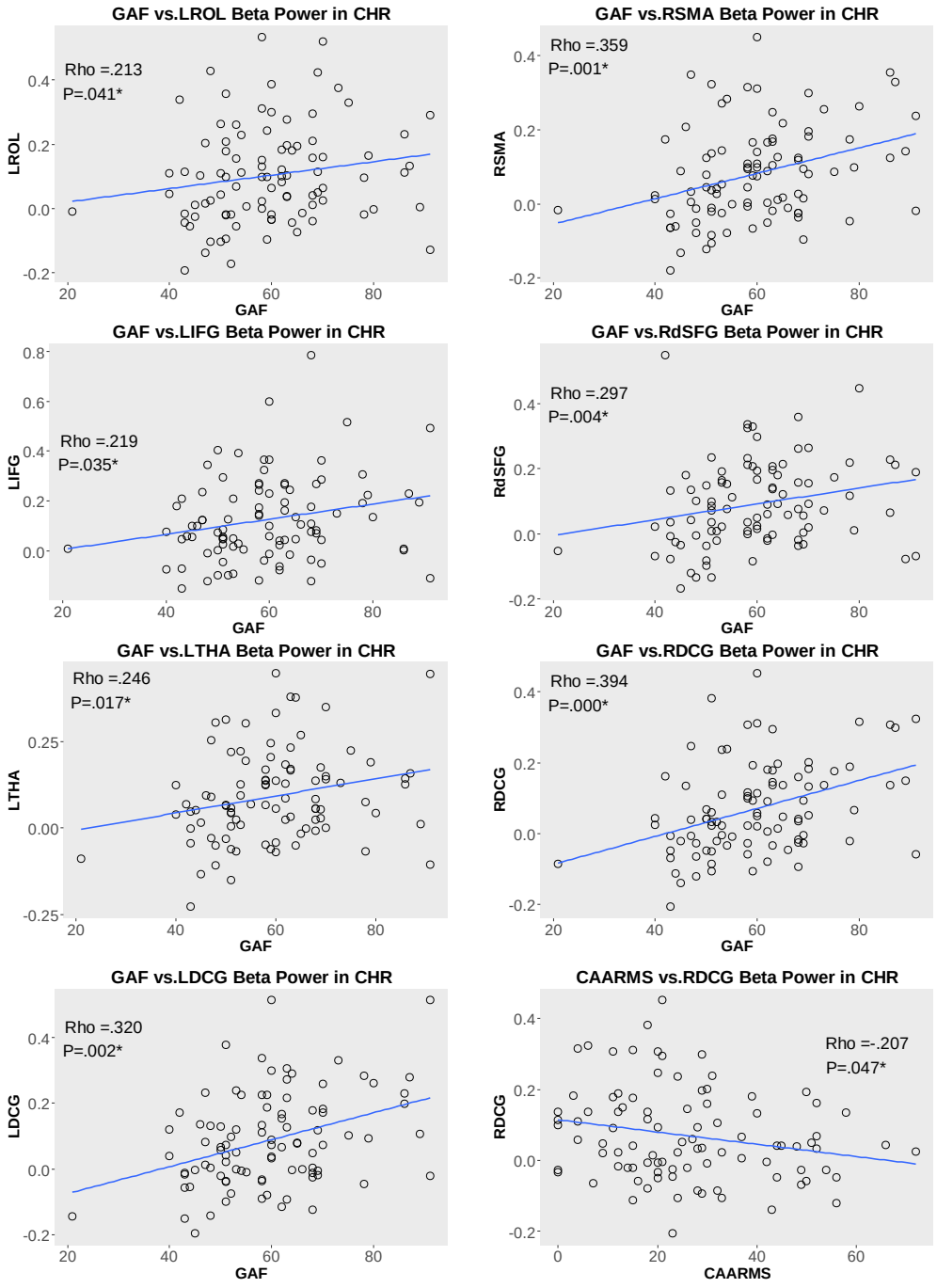

Figure 13 Spearman Correlations between Beta (15-25 Hz) Spectral Power, GAF and CAARMS Scores in CHR Participants. P-values for RSMA, RSFG and bilateral DCG survive fdr correction.

4.4 Discussion

The results indicate that changes in 40 Hz ASSR spectral power and ITPC were present in CHR and FEP, but these were only detected in source reconstructed MEG-data. The absence of group differences in sensor data could be attributed to field spread, causing the signal at each sensor to contain information from multiple neuronal sources (Schoffelen & Gross, 2009), thus diluting small local effects in individual ROIs. Hence, the results suggest that alterations in 40 Hz ASSR spectral power and ITPC are subtle in both the CHR and FEP states.

Behavioural analyses revealed no significant difference in RTs. However, response accuracy was reduced in CHR and FEP participants compared to controls. Thus, while overall response speed was equal across groups, performance was poorer in CHR and FEP, possibly reflecting attention impairments.

Both spectral power and ITPC data point to impairments in the capacity of auditory networks to generate synchronised 40 Hz neural oscillations in FEP and CHR individuals, but this abnormality stemmed from aberrant functioning in secondary (RSMG), as opposed to primary, auditory areas. Hence, the data indicate that basic auditory processing impairments reflected by 40 Hz ASSR oscillation measures first develop in higher level secondary regions before affecting primary auditory regions in later stages of psychosis.

The strongest impairments in both CHR and FEP participants were found in the RSMG. The SMG is part of the inferior parietal lobule, one of the last cortical regions to mature during development (Torrey, 2007). This area is involved in the integration of sensory data (Torrey, 2007), is closely linked to the auditory P300 event-related potential (Horovitz, Skudlarski, & Gore, 2002; Menon, Ford, Lim, Glover, & Pfefferbaum, 1997; Skosnik, Krishnan, & Donnell, 2007), and is also central in several complex auditory functions (Bangert et al., 2006; Niznikiewicz et al., 2000; Oberhuber et al., 2016; Rauschecker & Scott, 2009; Vines, Schnider, & Schlaug, 2006). Furthermore, an early study reported inferior parietal lobule involvement in the 40 Hz ASSR (Reyes et al., 2005).

In ScZ, the SMG has been highlighted as one of the regions involved in auditory hallucinations (Gaser, Nenadic, Volz, Büchel, & Sauer, 2004). In view of this potential role of the SMG in ScZ, future ASSR work should further explore impairments in this region, as the current findings suggest that such alterations may precede the onset of the first psychotic episode.

Existing evidence suggests that CHR subjects may fail to sustain the 40 Hz ASSR (Koshiyama et al., 2018a; Tada et al., 2016). However, the current results indicate impairments in RSMG throughout the stimulation period, indicating that also the initiation of the ASSR could be abnormal. It should be noted that none of the 40 Hz ITPC and spectral power reductions in FEP and CHR-groups survived corrections for multiple comparisons. Nevertheless, the fact that both ITCP and spectral power reductions were observed in the same ROI suggests that potentially these impairments reflect an important aspect of circuit dysfunctions during emerging psychosis.

An unexpected widespread increase in beta range power was detected during 40 Hz ASSR stimulation across groups. This activation was not seen in ITPC data, suggesting that beta oscillations were non phase locked. Moreover, the activation did not resemble a resonance response to 40 Hz stimulation as it spanned approximately 10 Hz. Thus, the next paragraphs discuss established roles of beta oscillations and speculate about the signal observed in the current data.

Beta oscillations play an important part in motor preparation and inhibition, manifested as a decrease in beta power immediately prior to a motor action, and a beta power increase, or rebound, during motor termination or inhibition (Kuhn et al., 2004; Y. Zhang, Chen, Bressler, & Ding, 2008). Thus, the observed beta response might reflect inhibition of motor activity (Heinrichs-Graham, Kurz, Gehringer, & Wilson, 2017; Wagner, Wessel, Ghahremani, & Aron, 2017), triggered as participants evaluated the ASSR stimulus and determined that it was not a “target” sound. This hypothesis is supported by the pattern of response, which was most pronounced in the left hemisphere, contralateral to the finger used for button presses in the attention task. Notably, spectral power at 15-25 Hz was impaired in CHR and FEP participants compared to controls in several

regions, including areas implicated in motor function, such as the LROL and the RSMA. This is consistent with reported motor impairments in ScZ patients (Morrens, Docx, & Walther, 2014) and CHR individuals (Bernard & Mittal, 2014a; Gschwandtner et al., 2006). Notably, pharmacological data suggest a close link between beta oscillations and GABAergic function in the motor system (Premoli et al., 2017). In vivo data have revealed a positive correlation between post-movement beta rebound power and GABA levels in motor cortex (Gaetz, Edgar, Wang, & Roberts, 2011). Thus, the present findings may reflect early GABAergic changes in CHR individuals.

Previous reports of beta oscillatory abnormalities in ScZ have also been linked to deficits in sensory and multi-sensory processing (Balz et al., 2016), as well as attention (Ghorashi & Spencer, 2015; Todorovic, Schoffelen, Ede, Maris, & De, 2016) and salience signalling (Liddle et al., 2016) abnormalities. Among the regions affected in the current analyses are frontal and subcortical regions known to be involved in such functions (Pratt et al., 2017; Rueckert & Grafman, 1996). Moreover, correlation analyses revealed a strong relationship between beta power and global functioning, whereby beta spectral power was positively related to GAF scores in the CHR group, suggesting that those assessed as lower functioning also showed weaker beta power activation. Hence, beta range group differences detected in CHR and FEP participants may represent early impairments in multiple functional domains.

Correlation analyses in the 40 Hz range revealed a negative association between composite BACS scores and LSTG ITPC across groups, indicating a weak significant relationship between neural activity and cognition. These results suggest a relationship between the capacity to elicit 40 Hz auditory oscillations and cognitive performance. Furthermore, in the CHR group ITPC measures were correlated to both BACS and CAARMS scores in several nodes, but these relationships did not survive correction for multiple comparisons. Few prior investigations have explored clinical correlates of the ASSR in psychosis, nor in the at-risk state, and future investigations should map potential relationships further.

Finally, potential baseline power group differences were explored, as increased left hemisphere baseline power has previously been reported in 40 Hz ASSR recordings in chronic ScZ patients, along with trend increases in left hemisphere broadband power (Spencer, 2012). However, the present analyses did not replicate this finding in FEP and failed to detect any differences in baseline power in CHR. Thus, the current data do not indicate that baseline power differences could account for the task related effects reported here.

The current results have limitations; 40 Hz ASSR abnormalities found in CHR and FEP were subtle, with small to moderate effect sizes, and did not survive stringent statistical correction. However, consistent impairments in RSMG in both spectral power and ITPC support the notion that the ASSR was impaired in this area. Furthermore, the study focused on CHR participants, resulting in a small FEP sample relative to the other two groups. However, power analyses indicated that the size of the FEP sample was sufficient to detect ASSR impairments with a power of 0.8. Furthermore, the CHR and FEP groups consisted of a mixture of unmedicated and medicated participants, including a variety of psychiatric medications ranging from anxiolytic to antipsychotic drugs. Future work should address the influence of various medications on the ASSR.

Finally, the use of a beamformer algorithm for source reconstruction is a crucial methodological limitation which might have hindered the detection of statistical effects. The beamformer methods rely on the assumption that no sources in the brain are strongly correlated (Hillebrand, Singh, Holliday, Furlong, & Barnes, 2005), yet in the case of 40 Hz ASSR stimulation where both hemispheres are entrained to the same auditory stimulus, the left and right auditory cortex are naturally correlated. This caused clear issues when whole-brain source data were explored using the LCMV algorithm compared to an alternative “exact low-resolution brain electromagnetic tomography” approach (eLoreta) (Pascual-Marqui et al., 2011; Pascual-Marqui, Michel, & Lehmann, 1994). However, when analyses focused on specific centroids of AAL ROIs, the results obtained using LCMV were equivalent to those from eLoreta. Thus, it was assumed that AAL ROI LCMV data were successfully reconstructed despite correlated auditory sources, and these data were therefore selected for analyses instead of eLoreta data due to the superior resolution of beamformer data (Hillebrand et al., 2005).

Nevertheless, it is possible that correlated signals may have caused some cancellation of sources, meaning that the effects seen in the present analyses may be weaker than if a more appropriate method had been employed.

4.5 Conclusion

Analyses provide evidence that the patterns of 40 Hz ASSR activation are aberrant in CHR and FEP participants, but effects were small to moderate. Furthermore, a strong relationship was seen between beta power elicited during 40 Hz ASSR stimulation and CHR participants' GAF scores. As such, the measure could help inform the understanding of oscillatory changes associated with auditory function in the CHR state, and highlight alterations leading to the transition to psychosis and functional deterioration. Follow-up data from the current sample will be important to further investigate these changes.

Chapter 5 Neural Connectivity During Auditory Steady State Response Stimulation in the CHR State

5.1 Introduction

A prominent theory of ScZ postulates that the pathophysiology involves widespread neural dysconnectivity (Stephan, Friston, & Frith, 2009). Moreover, altered connectivity may underlie both sensory impairments and hallucinations in psychosis (Ford et al., 2012). Neuroimaging methods have been used to evaluate this hypothesis by exploring both structural and functional connectivity in ScZ (Fitzsimmons et al., 2013; Maran et al., 2016) and more recently in clinical CHR populations (Andreou, Leicht, et al., 2015; Ramyead et al., 2015). MEG/EEG allow the study of dynamic interactions between multiple brain regions (Maran et al., 2016), and are thus ideally suited for the study of functional connectivity. However, the number of MEG/EEG-studies in psychosis/ScZ are limited (Maran et al., 2016). In this chapter, Granger Causality (GC) functional connectivity data estimated from auditory steady state response (ASSR) task data from CHR individuals, FEP patients and healthy controls are presented. The aim of the analyses was to address the following questions: 1) Is functional connectivity impaired during the ASSR paradigm in FEP? and 2) Are potential impairments also present in participants meeting CHR criteria?

Previous data suggest that ScZ patients have altered functional connectivity compared to control participants (Maran et al., 2016). Findings in resting state data indicate that alterations are present in all frequency bands from delta to gamma (Andreou, Leicht, et al., 2015; Di Lorenzo et al., 2015; Kam et al., 2013; Lehmann et al., 2014; Tauscher, Fischer, Neumeister, & Rappelsberger, 1998). Similarly, data from task based paradigms have revealed local changes in specific frequency bands (Griesmayr et al., 2014; Henshall et al., 2013; Krishna et al., 2015; Popov et al., 2014; Winterer et al., 2003). Moreover, there is some evidence that functional connectivity is altered also in CHR (Andreou, Leicht, et al., 2015).

In the visual domain, EEG/MEG data indicate that healthy controls have higher frontal-posterior phase synchronization in the beta and low gamma frequency

range during a remembered pursuit task studying smooth pursuit eye movements (Krishna et al., 2015). A similar pattern of aberrant frontal-posterior connections was observed in a cognitive visuospatial delayed match to sample task (Griesmayr et al., 2014). Furthermore, ScZ patients displayed altered power and connectivity in the alpha and beta range in a facial affect recognition experiment (Popov et al., 2014).

Notably, connectivity analyses of auditory data have revealed reductions in fronto-temporal coherence during an odd-ball paradigm in ScZ patients and their siblings (Winterer et al., 2003). Moreover, one study observed reduced interhemispheric coherence in four EEG electrode pairs in patients with auditory hallucinations compared both to healthy controls and patients with no recent auditory hallucinations (Henshall et al., 2013).

So far there is insufficient data on connectivity networks implicated in the ASSR task (Chapter 3). Two studies have reported measures of functional connectivity during ASSR stimulation in ScZ patients (Mulert, Kirsch, Pascual-marqui, McCarley, & Spencer, 2011; Ying et al., 2015). One reported impaired inter-hemispheric functional connectivity between primary, but not secondary auditory areas during the 40 Hz ASSR in ScZ relative to controls (Mulert et al., 2011). Others found disrupted connectivity in a fronto–temporal network in ScZ during ASSR stimulation (Ying et al., 2015). Thus, connectivity data from local auditory networks during 40 Hz ASSR stimulation are lacking, both for ScZ, FEP and CHR.

One measure of functional connectivity is Granger Causality (GC), a statistical measure of directed functional ("causal") interactions, first developed in economics (Granger, 1969). The method is widely used in neuroscience, as it allows the identification of functional connections from time-series data (Seth, Barrett, & Barnett, 2015). In brief, the algorithm determines to what degree time-series data in a region A at time point t can be used to estimate the time-series data in a region B at time point t+1. "Causal" connectivity is assumed if the signal at region B can be predicted better when the information from region A is included in the algorithm than when it is excluded (Granger, 1969), interpreted as signals in region A "causing" the time-course in region B.

Provided that data meet a set of assumptions (e.g. stochastic, stationary data), the GC method is efficient and has several benefits over other methods; In the frequency domain the GC index can be estimated both using a parametric and non-parametric method (Bastos & Schoffelen, 2016). The parametric approach is based on an autoregressive model, the selection of which is affected by individual subject data variability, task and data quality (Bastos & Schoffelen, 2016). However, the non-parametric alternative circumvents this issue by estimating GC using data points from the entire frequency spectrum (Bastos & Schoffelen, 2016). Furthermore, the GC index can be estimated both in the time and frequency space, and the effect of potential confounding factors, such as differences in signal strength, can be minimized (Seth et al., 2015). However, the analyses remain prone to bias when trial numbers are low or when groups are unequal in size (Bastos & Schoffelen, 2016).

In addition to evaluating strength of connections, recent findings suggest that GC data can provide an indication of whether a connection is primarily involved in feedforward or feedback signalling in terms of laminar connections (Michalareas et al., 2016). Interactions between feedforward and feedback signals are implicated in cognitive processing (Bubic, 2010; Clark, 2013; MacKay, 1954) and impairments in either type of pathway could account for impairments in cognition.

Anatomically, feedforward connections are thought to originate primarily in superficial layers of the cortex and project to the granular layer (Felleman & Van Essen, 1991). In contrast, feedback connections typically originate in infragranular layers (Markov et al., 2014) and target cortical layers 1 and 6 (Michalareas et al., 2016). These cellular divisions have been found to correlate with neural oscillation frequencies. Specifically, feedforward-associated layers show strong gamma-band synchronisation, while infragranular feedback layers appear associated with stronger alpha/beta oscillations (van Kerkoerle et al., 2014).

GC connectivity studies have provided further evidence for this framework (Bastos et al., 2015; Michalareas et al., 2016). A directed influences asymmetry index (DAI) was computed using GC neuroimaging data, and was found to

correlate with a supragranular labelled neuron index capturing the anatomical signature of the feedforward or feedback character of a projection (Bastos et al., 2015; Michalareas et al., 2016). Thus, it follows that computation of DAI from GC data may help elucidate how anatomical feedforward and feedback connections are involved in early deficits observed in psychosis

In the following sections of this chapter, connectivity data from the YouR study CHR and FEP samples are presented. The analyses aim to evaluate ASSR task related connectivity in this group and investigate whether connectivity alterations could account for the subtle changes in spectral power and ITPC reported in Chapter 3. In addition, exploratory analyses of DAI indices are performed.

5.2 Methods

5.2.1 Data Collection and Statistical Analyses

The analyses included ASSR data from 93 at risk participants, 17 FEP patients and 46 healthy controls outlined in Chapter 2. Detailed descriptions of psychological assessments and collection of MEG data are provided in Chapters 2 and 4. All analyses described below were performed in the MATLAB toolbox Fieldtrip (Oostenveld et al., 2011). Statistical group differences were evaluated using a non-parametric Monte-Carlo permutation-based approach on time- and group-averaged data, across the analysed frequencies. Results were corrected for multiple comparisons using a fdr method. All statistical output reported are rounded to two decimals.

5.2.2 MEG Data Analyses

MEG-data were pre-processed and reconstructed as described in Chapter 4, Section 4.2. T1 weighted MRI scans recorded on a Siemens 3T Trio Trim scanner with 3D MPRAGE sequences (192 slices, voxel size 1 mm^3, FOV=256x256x176 mm, TR=2250 ms, TE=2.6 ms, FA=9°), and converted to SPM8 format using MRIcron (Rorden & Brett, 2000) were used to create individual subject MEG headmodels and generate leadfields. MEG data were reconstructed in the source space using Linearly Constrained Minimum Variance (LCMV) (Van Veen et al., 1997)

beamformer spatial filters and the standardized Automated Anatomical Labelling (AAL) brain atlas (Tzourio-Mazoyer et al., 2002). Coordinates for the local maximum centroids of 116 AAL regions were specified in each subject brain from an MNI template and used to model signals at each brain region. Source modelling at the 116 AAL centroids was done on a grid size of 5mm, using the LCMV beamformer approach, individual subject head models and normalised leadfields. Next, the AAL source estimations from individual subject grid-points were normalized to an MNI template brain with dimensions 91x109x91 mm, to allow averaging data from different subject grids despite individual differences in brain anatomy data. The regions of interest (ROIs) selected for connectivity analyses were right Heschl's gyrus (RHES), right superior marginal gyrus (RSTG) and right supramarginal gyrus (RSMG) (Figure 14). These regions were chosen based on their functional roles and observations from power and ITPC analyses (see Chapter 4).

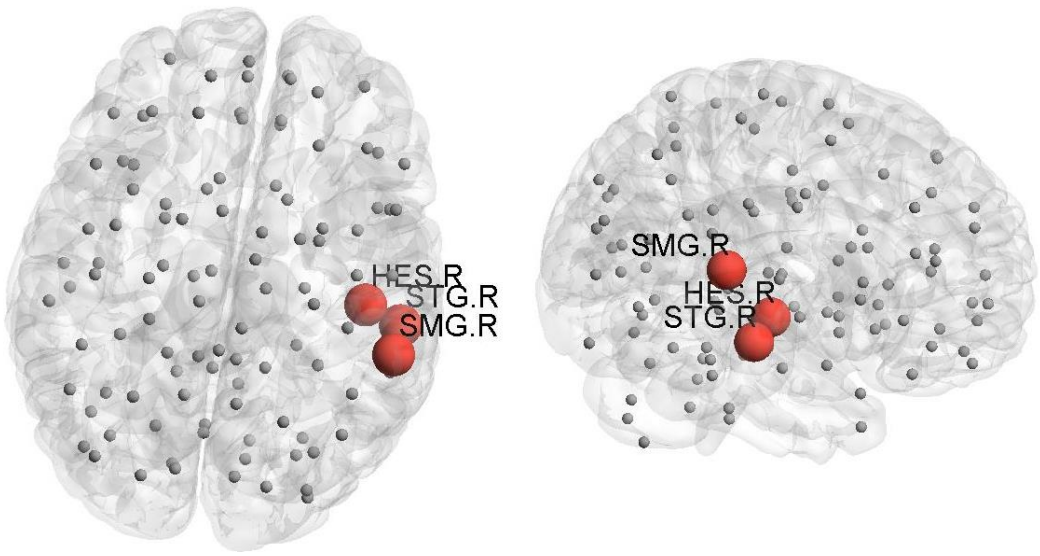

Figure 14 Nodes Included in GC Connectivity analysis

The data from selected AAL ROIs were rescaled to account for individual differences in data strength and variability, potentially biasing statistical analyses. The maximum and minimum amplitude per trial and channel for each participant were used to transform the data to values between 0 and 1

(formula=$X(t) - min_{amp}/(max_{amp}-min_{amp})$, where X(t)=raw amplitude at time t) (Grent-'t-Jong et al., 2018). Furthermore, prior to Fourier Transformation the data were down sampled from 500 Hz to 200 Hz (using ft_resampledata) to make connectivity computations more efficient.

Trials were cut into segments of 500 ms, starting at 350 ms to avoid evoked signals (analysis window: 350 ms – 1350 ms). This doubled the number of trials included in the analysis, improving the signal-to-noise ratio and thus making GC computations more reliable (Bastos & Schoffelen, 2016). A similar approach was adopted for the baseline analysis (-1000 ms - 0 ms).

Fast Fourier Transformation (FFT) of AAL ROI data was performed by convolving the data with a complex wavelet ('mtmconvol'), using a Hanning taper sliding window approach, 1 s padding, and smoothing of ±2 Hz, for frequencies 0-99 Hz. Measures of single subject GC connectivity between the 3 ROIs were computed using a non-parametric approach through matrix factorization and variance decomposition of the resulting Fourier spectrum. GC analyses were performed separately on data collected during stimulation and baseline data. GC data measured during ASSR stimulation was subsequently baseline corrected by subtracting GC baseline data.

Additional frequency specific GC analyses were performed on FFT data averaged around the 40 Hz frequency band (38-42 Hz), as pronounced GC-values in this frequency range were expected given the 40 Hz entrainment of auditory networks during the ASSR-stimulation.

As the FEP group was smaller (n=17) than the other two groups, this group was compared to a subset of randomly drawn control participants (Bastos & Schoffelen, 2016).

5.2.3 Directed Influences Asymmetry Index

Finally, the CHR and control 40 Hz specific GC data were studied further to clarify the degree to which each of the three GC connection pairs were feedforward or feedback. This was done using the DAI method which has been used recently in both in-vivo and human brain connectivity research (Bastos et al., 2015; Michalareas et al., 2016):

$$DAI(A - to - B) = \frac{(GC(A - to - B) - GC(B - to - A)}{(GC(A - to - B) + GC(B - to - A))}$$

The numerator captures the predominant net direction of the connection (i.e. whether the connection is primarily feedforward or feedback), while the denominator serves as a normalization factor to account for differences in connectivity strengths between areas (Michalareas et al., 2016).

5.2.4 Correlation Analyses

Associations between GC connectivity data and attenuated psychotic symptoms and cognitive impairments in CHR were investigated using Spearman correlation analyses. GC connectivity at 40 Hz (38-42 Hz) in each connection was correlated with total CAARMS scores, perceptual abnormality CAARMS scores, and BACS scores (z-scored and adjusted for gender).

5.3 Results

5.3.1 Broadband Baseline Analyses

Analyses of baseline connectivity across the 0 to 90 Hz range showed transient differences between CHR-participants and controls ($p<0.05$) in the connections RHES to RSMG around 80 Hz (CHR>Controls), RSMG to RHES around 40 Hz (Controls>CHR), RSMG to RSTG and RHES to RSTG (at 20, 30 and 40 Hz, Controls>CHR). Similar differences ($p<0.05$) were seen between the FEP-group and controls around 30-40 Hz for the connections RHES to RSTG and RSMG to RHES (Controls>FEP). Furthermore, stronger increases were seen around 20 and 40 Hz for RSTG to RSMG in FEP baseline data ($p<0.01$) (Figure 15B).

5.3.2 Broadband Stimulus Evoked Analyses

Analyses of stimulus-related GC data (baseline corrected) revealed significant ($p<0.01$) group differences for FEP compared to controls at 20 Hz for the connection RHES to RSTG (Control > FEP), and at 30 Hz for RSMG to RSTG (Control > FEP). There was also a weaker reduction in FEP GC compared to controls in RSMG to RSTG at 20 Hz ($p<0.05$).

There was a significant group difference ($p<0.01$) between CHR and controls at 30-40 Hz for RSTG to RSMG (Control > CHR) and at around 40-50 Hz for RSMG to RHES (Control > CHR) (Figure 15A). In addition, CHR GC was also reduced for RSMG to RSTG around 15, 30 and 70 Hz ($p<0.05$).

5.3.3 40 Hz Frequency Specific Analyses

When analyses were restricted to the 38-42 Hz range, no significant differences were found between FEP and controls. However, a network of reduced connectivity was found in CHR-participants (Figure 17), involving connections between the following nodes: RSTG to RSMG ($t(138)=-3.04$, $p=0.003$,$d=0.53$), RSMG to RHES ($t(138)=-2.23$, $p=0.01$, $d=0.39$) and RHES to RSMG ($t(138)=-1.94$, $p=0.03$, $d=0.33$) (Table 11A).

5.3.4 Directed Influences Asymmetry Index

Across groups, DAI values at 40 Hz indicated feedback connectivity for the RSMG to RHES connection, while the RSTG to RSMG and RSTG to RHES connections were predominantly feedforward (Table 11B).The DAI values were lower in CHRs, suggesting that the degree of feedforward or feedback directionality was less pronounced in the CHR group, but there was no statistically significant group difference.

A

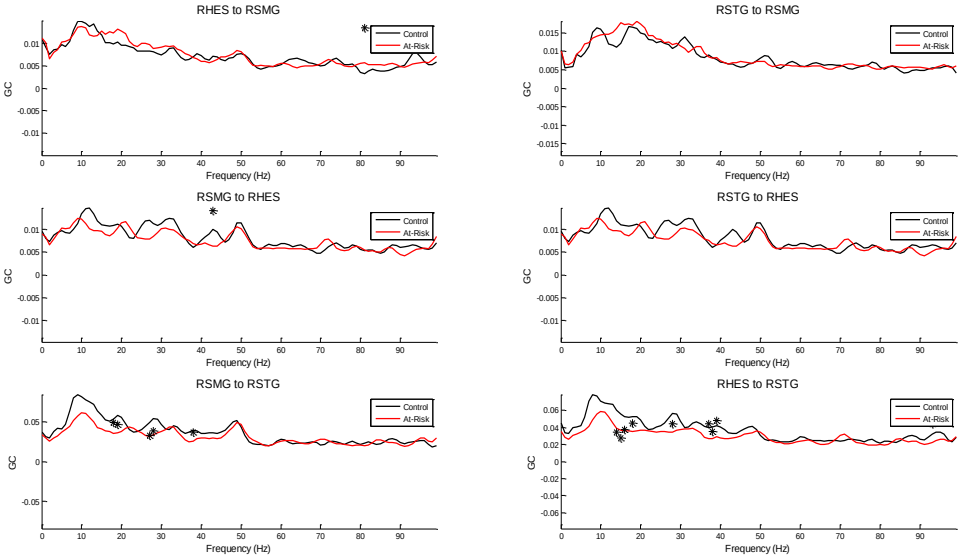

B

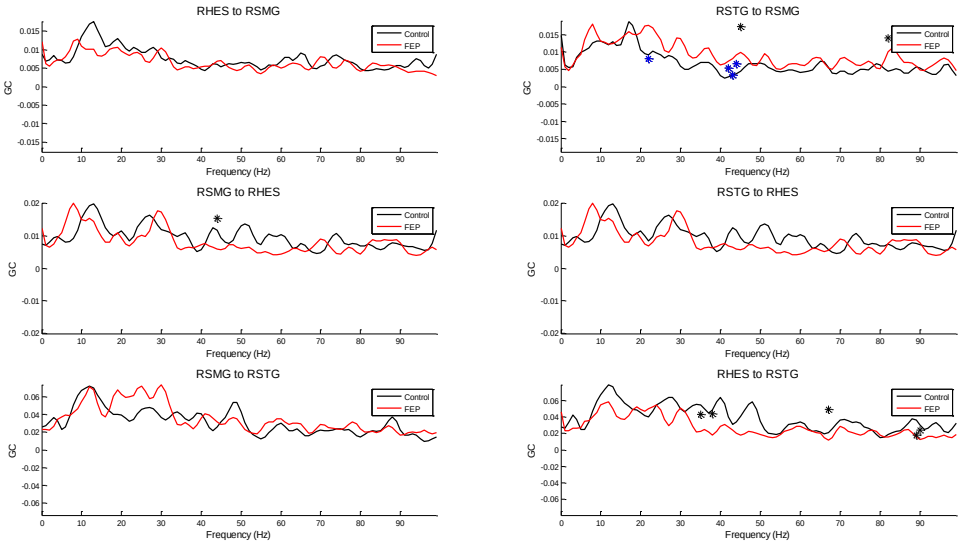

*p<0.05 (uncorr)
*p<0.01 (uncorr)

Figure 15 GC in Baseline Data for A) CHR vs Controls and B) FEP vs Random Subset of Controls. All p-values uncorrected.

5.3.5 Correlation Analyses

Correlation analyses between GC averaged at 40 Hz (38 – 42 Hz) and total CAARMS, CAARMS PA and total BACS scores did not reveal any significant relationships between symptom severity and connectivity measures in the CHR-group. Associations varied in strength from RHES to RSTG connectivity vs total

CAARMS scores (Rho=0.16, p=0.14) to RSMG to RSTG connectivity vs total CAARMS (Rho=0.01, p=0.94).

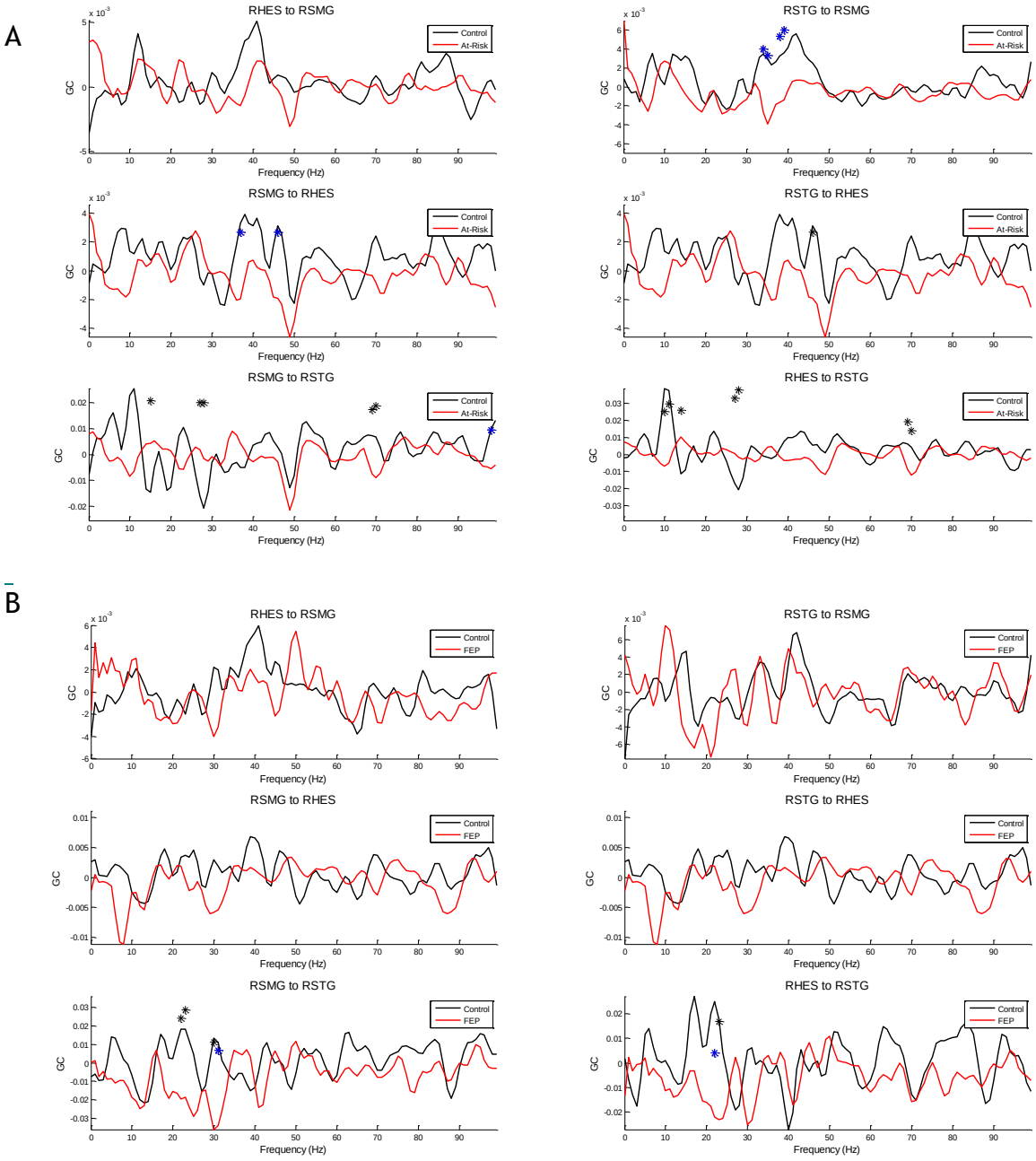

Figure 16 GC Data during ASSR Stimulation for A) CHR vs Controls and B) FEP vs Random Subset of Controls. All p-values uncorrected.

Granger Causality

At-risk vs. Controls

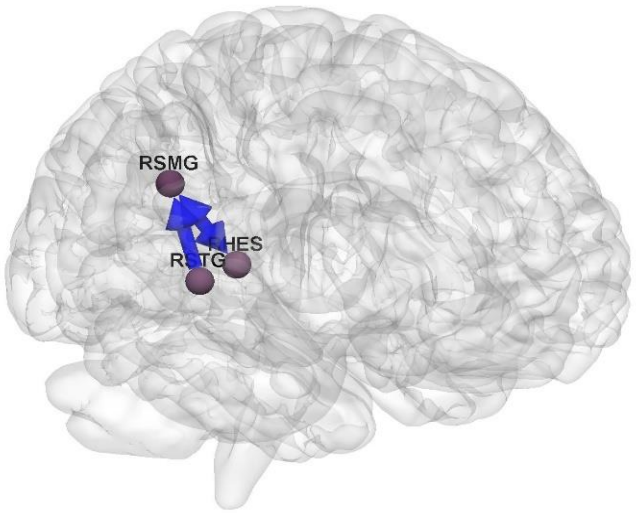

Figure 17 40 Hz GC Reduced Connectivity in CHR vs Controls. P-values uncorrected.

Table 11 A) Group Comparison of 40 Hz GC in CHR vs control participants. B) Directed Influence Asymmetry Index (DAI) at 40 Hz. All p-values uncorrected.

A	*Connection*	*t Statistic*	*95% Confidence Interval*	*p*	*d*
	RHES to RSMG	-1.95	-0.02 to 0.69	0.03*	0.33
	RSTG to RSMG	-3.04	0.17 to 0.89	0.00*	0.53
	RSMG to RHES	-2.23	0.04 to 0.75	0.01*	0.39
	RSTG to RHES	-1.58	-0.08 to 0.63	0.07	0.27
	RSMG to RSTG	-0.40	-0.27 to 0.44	0.36	0.08
	RHES to RSTG	-1.50	-0.09 to 0.62	0.08	0.26

B	*Connection*	*Control DAI*	*CHR DAI*	*Mann Whitney U*	*p*	*d*
	RHES to RSMG	-2.20	-0.32	1045.00	0.87	0.32
	RSTG to RSMG	10.56	3.13	939.00	0.37	-0.06
	RSTG-to-RHES	4.48	0.67	1050.00	0.89	-0.04

5.4 Discussion

The results suggest altered connectivity patterns in auditory pathways in FEP and CHR individuals compared to controls. The nature of these alterations differ between groups, with FEP participants showing baseline deficits in lower

frequency bands during the 40 Hz stimulation period, while CHR impairments were primarily seen in the 40-50 Hz range during stimulation.

Broadband analyses of the baseline data showed increased baseline connectivity in the FEP group compared to controls around 20 Hz and in the 40-50 Hz band in the RSTG to RSMG connection ($p<0.01$). No such elevations were detected in the CHR group. Hyperconnectivity has been highlighted as a potential mechanism underlying auditory hallucinations (Ford et al., 2012), through elevated connectivity between temporal and subcortical regions, as demonstrated by fMRI evidence (Hoffman, Hernandez, Pittman, & Hampson, 2011). Thus, baseline hyperconnectivity in FEP individuals may reflect emerging auditory hallucinations. This should be explored further through correlation analyses with auditory hallucination scores in a larger FEP group.

In contrast, baseline analyses also revealed connections with reduced GC ($p<0.05$) in CHR and FEP participants in both the beta and gamma frequency range. Paradoxically, hypoconnectivity could also be implicated in hallucinations (Ford et al., 2012), via resulting impairments in self-monitoring and self-recognition processes such as efference copy (Melloni et al., 2007). Moreover, hypoconnectivity is thought to contribute to basic attention deficits (Rosenberg et al., 2016), reflected in negative and cognitive symptoms of psychosis. Thus, the detected emerging connectivity alterations may interact to contribute to both perceptual and cognitive abnormalities.

Analyses of task data measured during 40 Hz ASSR stimulation showed reduced connectivity at 20 Hz from RHES to RSTG, and at 30 Hz from RSMG to RSTG for FEP patients, while GC-connectivity at 40 Hz was intact. Notably, one of the connections affected by this reduction was intact in the baseline (RSMG-RSTG). Hence, stimulation deficits are unlikely to be driven exclusively by underlying baseline differences. Thus, the data indicate that the FEP state is associated with auditory connectivity alterations both in baseline and during stimulation, primarily in the beta and low gamma frequency range.

Significant group differences in GC were also seen between CHR participants and controls, reflecting reduced connectivity between RSTG and RSMG at 30-40 Hz,

and between RSMG and RHES in the 40-50 Hz frequency range. Thus, the GC impairments in CHR were observed around the frequency range of the ASSR stimulus, indicating that emerging CHR symptoms may be associated with a reduction in the ability to entrain to the 40 Hz ASSR stimulation. Indeed, CHRs showed bidirectional connectivity impairments between lower- and higher-level auditory processing regions during 40 Hz ASSR stimulation, suggestive of abnormal network entrainment.

Frequency specific analyses of GC data averaged around 40 Hz (38-42 Hz) were performed for the CHR and control groups. In line with broadband analyses, results showed significantly lower connectivity from RSTG to RSMG and bi-directionally between RSMG and RHES in CHRs compared to controls.

Moreover, the 40 Hz specific GC data were used to compute DAI values for each participant in both CHR and control groups, with the aim to determine the degree to which each node pair represented a laminar feedforward or feedback connection in the 40 Hz range. This approach was based on previous work indicating a close link between DAI measures and a supragranular labelled neuron index (Bastos et al., 2015). Across controls and CHR participants, DAI indices indicated that 40 Hz GC connections between the RSTG and RSMG, and between RSTG and RHES were primarily feedforward, while the connection between RHES and RSMG represented primarily feedback laminar projections. The DAI values were lower in the CHR group across all three node pairs, potentially suggesting a less clear division between feedforward and feedback connections in this group. However, this group difference was not statistically significant.

Results presented in Chapter 4 suggest that spectral power and ITPC during 40 Hz ASSR stimulation were impaired in CHR individuals compared to controls, particularly in the RSMG. The present connectivity analyses provide a theoretical framework to explain these findings as the GC analyses reveal that the establishment of network connectivity at 40 Hz is impaired between primary auditory regions and RSMG, especially in the bottom-up direction, suggesting that the 40 Hz ASSR generated in RHES and RSTG could not successfully transfer to RSMG through these pathways. Subsequent DAI analyses revealed that the

affected connections represented both feedforward and feedback laminar projections, potentially pointing to bidirectional anatomical connectivity abnormalities between primary auditory regions and RSMG during ASSR stimulation. This has implications for the development of psychotic symptoms, as the SMG and surrounding areas are involved in a range of sensory and language processing functions, and have been highlighted as key regions in the emergence of hallucinations (Torrey, 2007).

Correlation analyses did not indicate a relationship between clinical data and connectivity measures in CHR. Contrary to the notion that connectivity deficits mirror hallucination symptoms (Ford et al., 2012), no relationship was seen between perceptual abnormality scores and connectivity measures.

In this study, the selected nodes were spatially close, which could pose problems due to field-spread (Schoffelen & Gross, 2009). One way to address this issue would be to use alternative connectivity measures such as the weighted phase lag index, imaginary coherence or orthogonalized envelope correlation, which all involve correction for source signal leakage (Colclough et al., 2016). However, in the present analysis the direction of connectivity and the possible differential alterations in top-down and bottom-up connectivity between groups was of interest. GC provides information about directed connectivity, while none of the previously mentioned alternatives do (Colclough et al., 2016). Therefore, attempts to deal with signal leakage issue were instead done by reconstructing the data in source space, which reduces signal leakage (Schoffelen & Gross, 2009). Assuming that any remaining field spread affected all experimental groups equally, the primary research question, whether there were connectivity differences between groups, could be addressed. Nevertheless, future studies should explore this SMG-HES and SMG-STG bilateral connections using both GC and other connectivity measures, in order to establish further to what degree signal leakage may have contributed to the present results.

5.5 Conclusion

This is the first report of GC connectivity during 40 Hz ASSR stimulation in a CHR sample and indicates impaired connectivity bidirectionally between higher and lower-level auditory regions during the stimulation period in the 40 Hz range.

Furthermore, similar patterns of connectivity deficits were seen in FEP, with additional observations of baseline hyper connectivity. Combined, the data reveal mechanisms potentially contributing to early psychotic symptoms and provide a novel insight into auditory connectivity during 40 Hz ASSR stimulation in CHR and FEP.

.

Chapter 6 Magnetic Resonance Spectroscopy Measures of GABA and Glx

6.1 Introduction

ScZ has been associated with impairments in glutamate and GABA signalling, indicating an abnormal cortical E/I balance (Anticevic & Lisman, 2017). Such deficits could account for gamma oscillatory abnormalities observed in patients (Uhlhaas & Singer, 2014), and could hence be a source of sensory processing deficits and cognitive impairments (Senkowski & Gallinat, 2015). Yet, the time of alteration onset is unclear, as studies exploring CHR participants remain relatively few in numbers and results have been inconclusive (Mikanmaa et al., 2017). Thus, the aim of the analyses presented in this chapter was to use 1H-MRS to explore E/I balance changes in a larger CHR sample. Specifically, 1H-MRS was used to collect measures of GABA and Glx, the latter being a molecular complex in the 1H-MRS metabolite spectrum containing the overlapping peaks of glutamate and glutamine (Merritt et al., 2016). Moreover, relationships between 1H-MRS data and MEG-measures of neural oscillations were investigated. Uniquely, the 1H-MRS data were collected from bilateral auditory cortex, which is a key region of interest in terms of ScZ symptoms (Javitt & Sweet, 2015).

As the major excitatory and inhibitory neurotransmitters in the central nervous system, glutamate and GABA are implicated in a vast number of neural functions, ranging from neural development and metabolic processes to higher cognitive functions (Newsholme, Procopio, Ramos Lima, Pithon-Curi, & Curi, 2003; Wu & Sun, 2015). Reliable and accurate measures are thus important to map illness mechanisms and to evaluate pharmacological responses (Keshavan, Lawler, Nasrallah, & Tandon, 2017). Accumulating 1H-MRS evidence supports the notion that glutamate and GABA are altered in ScZ.

The most consistently reported findings are elevated glutamate/Glx levels across multiple brain regions, including both temporal regions, the basal ganglia (Merritt et al., 2016; Poels et al., 2014) and frontal cortex (Poels et al., 2014). Notably, these observations are now also increasingly reflected in the CHR literature (Bossong et al., 2018; Fuente-Sandoval et al., 2011; Fuente-Sandoval et al., 2016; N. Tandon et al., 2013). In contrast, no significant effects were

found in relatives of ScZ patients (Block et al., 2000; Capizzano et al., 2011; Keshavan et al., 2009).

GABA 1H-MRS measures in psychosis have been inconclusive (Egerton et al., 2017; Wijtenburg et al., 2015), and the data available are limited. Reductions were noted in dorsal anterior cingulate cortex (Marenco et al., 2016) and bilateral calcarine sulci (Yoon et al., 2010) in ScZ, and in left basal ganglia, parietal occipital lobe (Goto et al., 2010) and the bilateral calcarine sulci (Kelemen et al., 2013) in FEP patients. In contrast, GABA elevations were observed in medial and dorsolateral prefrontal cortex, anterior cingulate cortex, occipital cortex and basal ganglia (Kegeles et al., 2012; Öngür et al., 2010; Rowland et al., 2013; Tayoshi et al., 2010) in ScZ. Changes in GABA have also been reported in CHR samples, suggesting that deficits may occur prior to diagnosis. Increased GABA was observed in bilateral dorsal caudate and medial prefrontal cortex (Fuente-Sandoval., 2016), while reduced GABA and GABA/Glx concentrations were seen in the left frontal lobe (Menschikov et al., 2016).

1H-MRS measures of GABA and glutamate/Glx show high test-re-test reliability (Greenhouse, Noah, Maddock, & Ivry, 2016; Jensen, Auerbach, Pisoni, & Pizzagalli, 2017). However, GABA concentrations are not consistent across the cortex but vary between brain regions (Greenhouse et al., 2016). In addition, depending on the brain area, voxels contain different proportions of grey matter, white matter and cerebrospinal fluid (CSF), which may contain different levels of metabolites of interest and thus influence the overall result (Harris, Puts, & Edden, 2015). Traditionally, large voxels were placed over the centre of the brain. However, increased scanner strengths combined with modern optimized techniques and shimming sequences make it possible to place voxels over more specific regions, thus avoiding CSF and allowing for higher signal strength from a smaller voxel volume (Harris et al., 2015).

In the present study, 1H-MRS data were collected from bilateral auditory cortex to allow correlations between 1H-MRS data with MEG-measurements of 40 Hz ASSRs. To the author's knowledge, these are the first reported 1H-MRS measures of GABA and Glx from auditory regions in psychosis. However, successful

recordings of 1H-MRS data from auditory cortex have been reported in other populations (Brown, Singel, Hepburn, & Rojas, 2013; Richards et al., 1997).

The data were recorded on a 3T MRI scanner, which does not provide sufficient resolution to study the glutamate peak alone (Wong, Schranz, & Bartha, 2018). Therefore, the Glx complex (the overlapping peaks of glutamate and the glutamate pre-cursor glutamine) were measured to obtain an estimation of neural glutamate levels. This approach is supported by existing data suggesting that glutamate is the primary contributor to the Glx peak (Shungu et al., 2013). Furthermore, measures of glutamine and changes in the glutamine-glutamate equilibrium are potentially also useful as they may reflect glutamate turnover rates (Merritt et al., 2016).

1H-MRS metabolite concentrations are measured relative to a reference molecule, typically the peak of water or of the metabolite creatine, since these are thought to be stable across disease states (Wijtenburg et al., 2015). However, empirical evidence suggests that creatine levels may be altered in psychotic patients compared to controls (Öngür, Prescot, & Jensen, 2009), and some papers reported a decrease (Bossong et al., 2018; Yoo et al., 2009) or speculated decrease (Wood et al., 2003) in creatine in high-risk populations. If true, using creatine as a reference could lead to misleading conclusions regarding Glx and GABA concentrations. Yet, others controlled for creatine group differences and found no significant effect (Fuente-Sandoval et al., 2016; Marenco et al., 2016), leaving the exact role of creatine in psychotic and CHR individuals unclear. In an attempt to clarify this question, a separate analysis was carried out on some data in this chapter, comparing measures done with water and creatine as reference respectively.

6.2 Methods

6.2.1 Sample

Participants were recruited as part of the YouR study (Chapter 2). 1H-MRS data from voxels in right and left auditory cortex were analysed separately. Right hemisphere analyses included data from 64 CHR, 11 FEP and 31 healthy control

participants. For the left voxel the final sample size was 39 CHR, 7 FEP and 22 healthy controls.

6.2.2 1H-MRS Data Collection

1H-MRS data were collected on a 3T Siemens Trio MRI scanner, using the MEGAPRESS+ sequence which is optimised for measures of GABA and has an inbuilt macro-molecule suppression. Voxels of 2 cm^3 were placed in the bilateral auditory cortex and in the right visual cortex. Measures in the left auditory cortex started after approximately 12 months of data collection. Results from the visual cortex voxel are reported elsewhere (Grent-‘t-Jong, 2019, in press).

Voxels were placed manually over Heschl’s gyrus and parts of the superior temporal cortex, using three planar views to identify anatomical landmarks and ensure optimal standardization across participants. Subsequently, the voxel was rotated to best fit the angle of the gyrus.

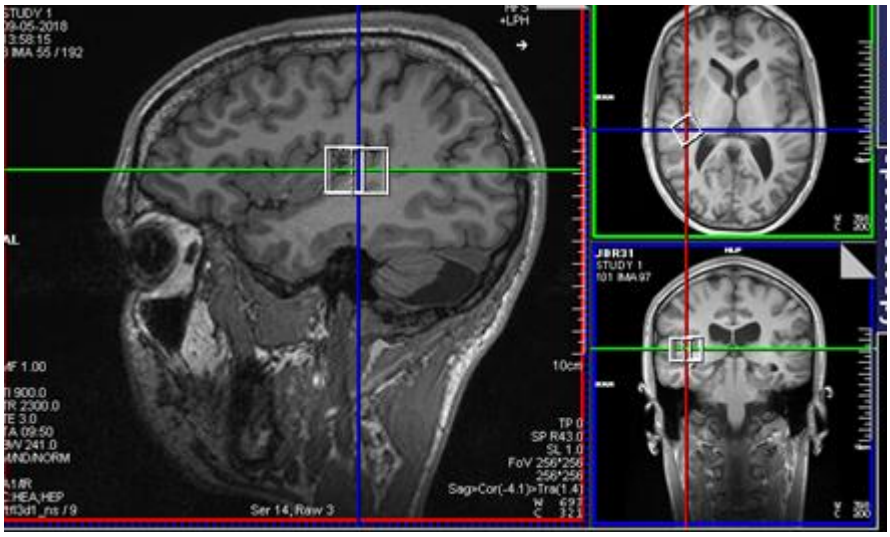

Figure 18 Representative Voxel Placement in Right Auditory Cortex Placed Using T1 Planar Slice Views.

FASTMAP shimming (Gruetter & Tkáč, 2000) of each voxel was applied to improve local-field homogeneity in ROIs. Next, three scans were acquired, including a full spectrum acquisition, a GABA-edited MEGAPRESS scan (128 trials) providing data on GABA and Glx concentrations, and an unsuppressed water scan (64 trials). The MEGAPRESS parameters were: TR/TE=1500/68 ms, 1.9 ppm ON- and 1.5 ppm OFF-resonance editing pulse frequencies (i.e., symmetric editing to suppress macromolecule contribution), 44 Hz editing Gaussian pulse bandwidth,

delta frequency of -1.7 ppm relative to water, 50 Hz water suppression, 90° flip angle, acquisition bandwidth of 1200 Hz, duration 426 ms, number of points 512.

6.2.3 1H-MRS Data Processing and Analysis

All 1H-MRS-data processing was performed in the open-source software Gannet (Gannet 2.1, Edden, Puts, Harris, Barker, & Evans, 2013). Water was used as the primary reference molecule for calculating GABA and Glx levels, but separate Glx analyses were also carried out with the metabolite creatine as reference. Levels of GABA were adjusted for voxel grey matter, white matter and cerebrospinal fluid content.

Data quality was judged by inspecting GABA and Glx peaks and baselines visually, and by computing H/Cr fit-errors and the water peak width. Generally, data were included in the analyses if the H/Cr fit-error was lower than 15 and the water peak width was 12 or lower.

Data were analysed statistically using SPSS statistics software (IBM Corp. Released 2013. IBM SPSS Statistics for Windows, Version 22.0. Armonk, NY: IBM Corp). The distribution and variance of the data in each group was determined for each of three variables (GABA, Glx and the ratio GABA/Glx measured relative to water). All statistical output is presented rounded to 2 decimal figures.

Initial analyses focused on CHR participants compared to controls, as the primary aim was to establish if differences exist between these groups. Due to non-parametric data the comparison was evaluated using Mann Whitney U non-parametric tests. Exploratory secondary group analyses including FEP patients were performed using Kruskal-Wallis non-parametric tests.

6.2.4 Correlation Analyses

Spearman correlation analyses were performed between 1H-MRS data and total CAARMS scores, composite BACS scores and 40 Hz ASSR oscillatory power and ITPC measures across groups. Oscillatory data were extracted from the Heschl's gyrus, superior temporal gyrus, medial temporal gyrus, supramarginal gyrus and

thalamus. The correlations were false discovery rate (fdr) corrected for multiple comparisons using the R stats package (version 3.1.2).

The relationship between H1-MRS data and gender, age and global functioning (GAF) scores were explored in separate analyses to determine the potential impact of these variables on H1-MRS measures. Age and GAF scores were explored using ANOVA analyses, while gender was analysed using Pearson's Chi^2 tests.

Table 12 Demographic Characteristics of Samples

Hemisphere	*Demographic variable*	*Control*	At Risk	*FEP*	*Group Statistic*	*p*
Right	*Age (±sd)*	22.33 (3.68)	21.85 (4.34)	23.73 (4.36)	0.98 (F)	0.38
	Gender (f:m)	1.73:1	3.57:1	0.57:1	6.89 (Chi^2)	0.03
	CAARMS total (±sd)	N/A	27.71 (16.64)	84.13 (27.81)	-8.22 (t)	<0.00
	GAF (±sd)	86.90 (7.28)	57.78 (12.57)	45.33 (14.38)	82.63 (F)	<0.00
Left	*Age (±sd)*	22.10 (3.06)	21.94 (4.52)	25.57 (5.13)	2.28 (F)	0.11
	Gender (f:m)	1.88:1	2.17:1	0.4:1	2.73 (Chi^2)	0.26
	CAARMS total (±sd)	N/A	28.17 (17.61)	90.67 (21.28)	-7.81 (t)	<0.00
	GAF (±sd)	89.75 (5.62)	56.69 (9.85)	41.14 (10.92)	119.02 (F)	<0.00

6.3 Results

6.3.1 Sample

Demographic characteristics are reported in Table 12. Neither the left nor right voxel samples differed significantly in age between groups. Gender proportions in each differed in the right (Pearson Chi^2=6.89, Cramer V=0.26, p=0.03), but not in the left hemisphere (Pearson Chi^2 =2.73, Cramer V=0.21, p=0.255). No association was found between any of the variables and the MRS measures in either the right or left hemisphere voxel.

6.3.2 1H-MRS Group Comparisons

There were no significant differences in 1H-MRS measures between CHR and controls in either hemisphere voxel (Table 13). Furthermore, secondary group analyses including the FEP group showed no statistical group difference in any of the measures (Table 13).

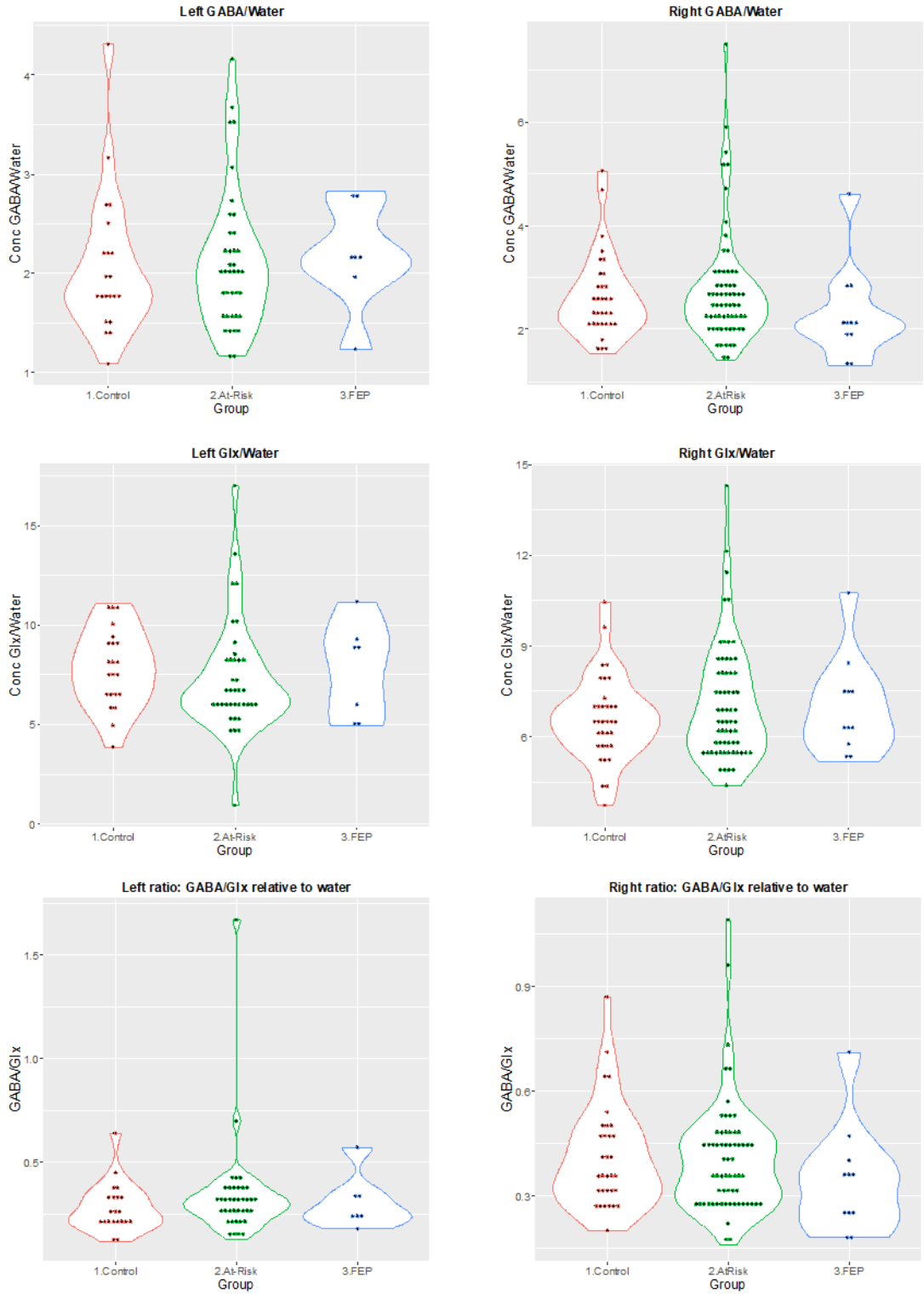

Figure 19 1H-MRS Measures of GABA, Glx and GABA/Glx Ratio in the Right and Left Auditory Cortex.

Table 13 Group Comparisons of 1H-MRS Data

Main Analyses: Controls vs CHR		*Control Mean*	*SD*	CHR Mean	SD	U[a]	p	d
Right	*GABA/Water)*	2.65	0.81	2.77	1.12	989.0	0.92	-0.08
	Glx/Water	6.68	1.44	7.08	1.91	1111.0	0.58	0.08
	Ratio	0.41	0.15	0.41	0.16	918.0	0.64	-0.13
Left	*GABA/Water*	2.06	0.74	2.31	0.96	406.5	0.32	0.33
	Glx/Water	7.74	1.90	6.95	3.00	270.5	0.10	-0.21
	Ratio	0.28	0.12	2.17	10.61	440.5	0.11	0.25

Additional Analyses: Including FEP		*Controls* Mean	SD	CHR Mean	SD	FEP Mean	SD	H[b]	p	d
Right	*GABA/Water)*	2.65	0.81	2.77	1.12	2.30	0.91	3.64	0.16	0.26
	Glx/Water	6.68	1.44	7.08	1.91	7.00	1.60	0.38	0.83	0.25
	Ratio	0.41	0.15	0.41	0.16	0.34	0.15	2.73	0.26	0.17
Left	*GABA/Water*	2.06	0.74	2.31	0.96	2.17	0.53	1.48	0.48	0.19
	Glx/Water	7.74	1.90	6.95	3.00	7.74	2.39	2.76	0.25	0.23
	Ratio	0.28	0.12	2.17	10.61	0.30	0.13	2.76	0.25	0.23

a) U statistic from Independent Samples Mann-Whitney U test
b) H-statistic from Kruskal-Wallis test

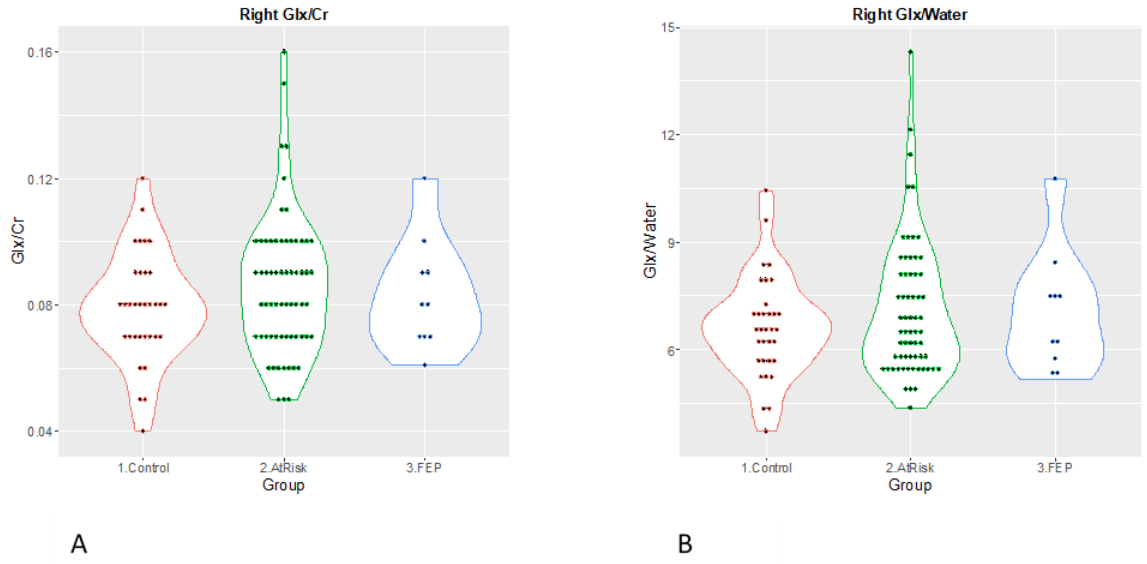

Figure 20 A) Right Hemisphere Glx Data Referenced by Creatine, and B) Right Hemisphere Glx Data Referenced by Water.

Post-hoc comparisons of FEP compared to controls confirmed that there was no group difference between these groups, however there was a trend reduction in right hemisphere auditory GABA in FEP relative to controls (Left: GABA U=89.00, p=0.29, d=0.33, Glx U=74.00, p=0.98, d=0.17, Ratio U=77.00, p=0.70, d=0.29; Right: GABA U=111.00, p=0.09, d=-0.43, Glx U=199.00, p=0.64, d=0.34, Ratio U=117.00, p=0.13, d=-0.43).

The distribution and spread of data were inspected graphically (Figure 19) and evaluated statistically. There was no difference in variance between groups in either voxel for measures of GABA (Left: Levene statistic=1.19, p=0.28; Right: Levene statistic=0.83, p=0.36), Glx (Left: Levene statistic=1.07, p=0.31; Right: Levene statistic =3.02, p=0.09), or ratio (Left: Levene statistic=2.28, p=0.14; Right: Levene statistic =0.02, p=0.90).

6.3.3 Role of Reference Molecule

The comparison of water- and creatine-referenced right voxel Glx revealed that the data distribution and difference between groups remained similar (Glx/creatine: F(2)=1.15, p=0.32; Glx/Water: F(2)=0.73, p=0.49) (Figure 20). Thus, there was no indication that creatine-levels in the CHR or FEP groups had an impact on differences in GABA/Glx levels.

6.3.4 Correlation Analyses

A negative correlation was found between composite BACS scores and right auditory voxel Glx levels (Table 14), indicating that individuals performing worse in the BACS assessment had higher levels of Glx (Figure 21). Moreover, left auditory 1H-MRS Glx/water was positively correlated with ASSR power in LHES and LSTG (Table 15, Figure 21). However, the correlations did not survive fdr correction for multiple comparisons.

Table 14 Psychological Variables: Spearman Correlations across Groups

Hemisphere	MRS Measure	BACS (Rho)	CAARMS (Rho)
Right	*GABA/Water*	-0.08	-0.09
	Glx/Water	-0.23*****	0.03
	Ratio	0.14	-0.06
Left	*GABA/Water*	0.12	0.15
	Glx/Water	0.14	-0.07
	Ratio	-0.01	0.07

P<0.05 = * (uncorr)

Table 15 Spearman correlation coefficients for correlations between 1H-MRS data and ipsilateral 40 Hz ASSR power and phase measures

ASSR Measure	Hemisphere	MRS measure	HES (Rho)	STG (Rho)	MTG (Rho)	SMG (Rho)	THA (Rho)
40 Hz Power	**Right**	**GABA/Water**	0.13	0.04	-0.03	-0.07	0.12
		Glx/Water	-0.00	-0.16	-0.16	-0.09	-0.04
		Ratio (GABA/Glx)	0.06	0.16	0.10	-0.00	0.07
	Left	**GABA/Water**	0.17	0.20	-0.03	0.19	-0.03
		Glx/Water	0.30*	0.29*	-0.00	0.23	0.11
		Ratio (GABA/Glx)	-0.11	-0.11	0.02	-0.09	-0.09
ITPC	**Right**	**GABA/Water**	-0.04	-0.01	-0.14	-0.13	-0.01
		Glx/Water	-0.05	-0.10	-0.11	-0.12	-0.04
		Ratio (GABA/Glx)	-0.03	0.06	-0.02	-0.01	0.01
	Left	**GABA/Water**	0.03	0.15	0.14	0.06	0.06
		Glx/Water	0.01	0.25	0.12	0.06	0.07
		Ratio (GABA/Glx)	0.08	-0.10	-0.01	-0.02	0.06

P<0.05 = * (uncorr)

6.1 Discussion

Based on the results presented in this chapter it is not possible to accept the hypothesis that E/I imbalances are present in the primary auditory cortex in CHR individuals. Earlier findings have varied, and in line with the present analyses several previous studies have failed to detect a difference in glutamate/Glx (Block et al., 2000; Keshavan et al., 2009; Wood et al., 2010, Cappizzano et al., 2011) or GABA (Modinos, Şimşek, Horder, et al., 2018; Wang et al., 2016) compared to controls. However, the current analysis is limited by several methodological problems, possibly contributing to the lack of significant results.

The preliminary results from FEP patients did not indicate prominent glutamate or GABA deficits compared to controls. However, a trend reduction in GABA levels was detected in the right auditory voxel, suggesting that subtle emerging deficits may be present. Potentially, this difference might be stronger in a larger sample. Here data could not be used or were missing from 6 (right voxel) or 8 (left voxel) participants, resulting in 11 and 9 included participants respectively and thus underpowered analyses (power for left voxel max effect=0.13; power

for right voxel max effect =0.22). Thus, further work is required to clarify the extent to which auditory 1H-MRS impairments are present in FEP.

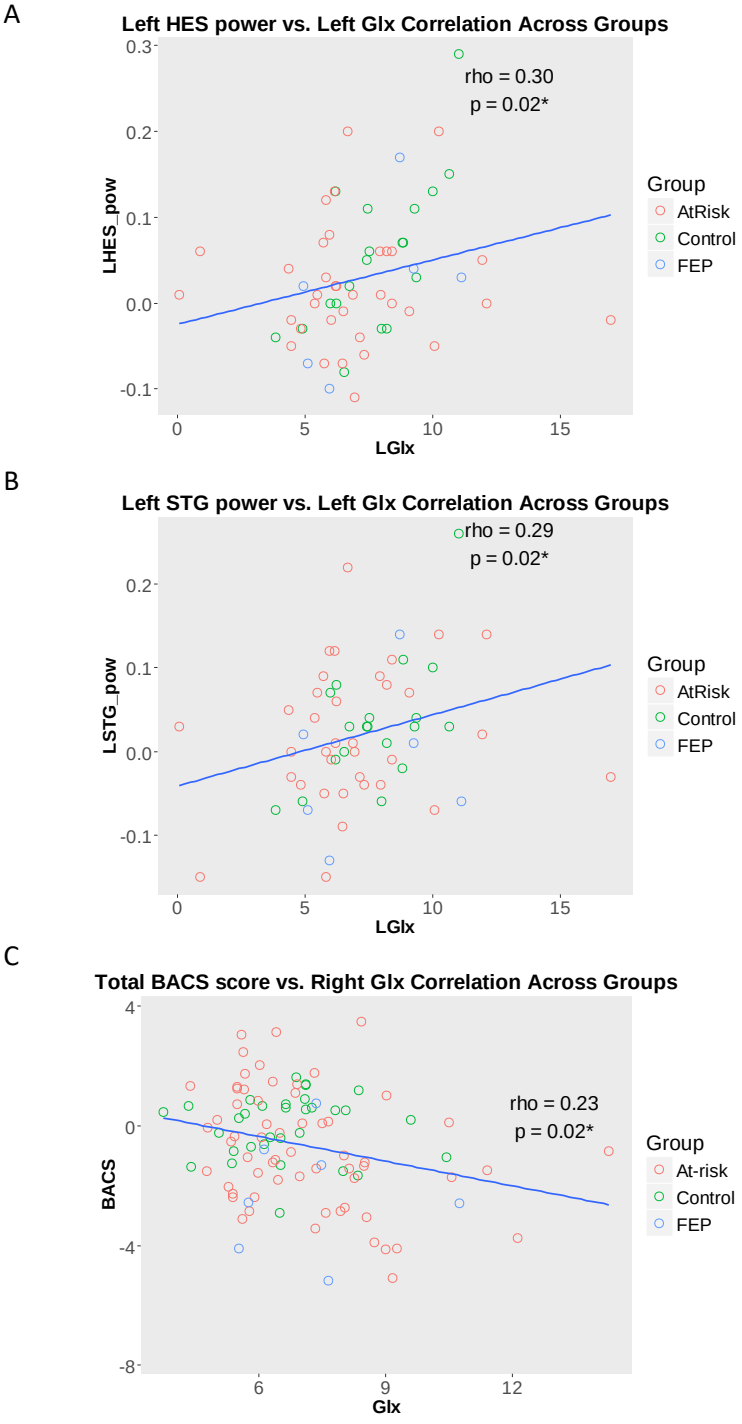

Figure 21 Relationship between A) Left Heschl's Gyrus 40 Hz ASSR Power and Left Hemisphere Glx Data, B) Left Superior Temporal Gyrus 40 Hz ASSR Power and Left Hemisphere Glx Data and C) Total BACS Scores and Right Hemisphere Glx Data, across the Three Study Groups. All p-values uncorrected.

Right hemisphere Glx measures were negatively correlated with composite BACS scores, indicating that 1H-MRS abnormalities may be present in participants with poorer cognitive capacity. The potential link between Glx and cognition could have further implications as cognition is closely linked to basic sensory and neural functions and is the strongest predictor of global functioning (Fusar-Poli , Papanastasiou, et al., 2015). However, the correlation was weak and did not survive correction for multiple comparisons.

One of the analysis objectives was to investigate the relationship between GABA and Glx measured through 1H-MRS, and oscillatory 40 Hz ASSR measures. Previous studies have reported correlations between 1H-MRS measures of GABA (Muthukumaraswamy, Edden, Jones, Swettenham, & Singh, 2009) and glutamate (Falkenberg, Westerhausen, Specht, & Hugdahl, 2012) with fMRI and MEG measures in controls. The present results revealed that left hemisphere Glx/water data were weakly correlated with 40 Hz ASSR oscillatory power in ipsilateral primary auditory regions (Heschl's gyrus and superior temporal gyrus) across groups, however this association did not survive correction for multiple comparisons. Hence, the current results are in line with others which failed to detect significant correlations between MEG and 1H-MRS measured GABA and glutamate in controls (Cousijn et al., 2014).

Water was selected as reference molecule in this analysis, primarily to enable correction for tissue composition in the computation of GABA, but also to circumvent potential group differences in creatine (Öngür et al., 2009). Early H1-MRS reports in ScZ highlighted alterations in creatine kinase, an enzyme which catalyses the conversion of creatine (Burbaeva, Savushkina, & Boksha, 2003), and indicated impaired creatine in patients (Öngür et al., 2009). However, the exploratory comparisons of water- and creatine-corrected Glx measures in the current study did not suggest significant differences in outcome depending on which reference molecule was used.

The auditory cortex poses challenges for 1H-MRS measurements due to its small size and the proximity to the scalp and cerebrospinal fluid, which can adversely affect the signal quality. Yet, the shimming and data quality parameters obtained from the 1H-MRS scans were within the normal range for the data

presented in this chapter, suggesting adequate quality. However, rejection of poor data and limited data availability resulted in relatively small groups and low statistical power, particularly for FEP participants. Accordingly, larger datasets are required to obtain more robust insights into the presence of E/I-abnormalities in early-stage psychosis.

Moreover, the present analyses focused on GABA and Glx rather than GABA and glutamate. Glx is assumed to provide an indirect indication of glutamate levels but is also affected by glutamine (Merritt et al., 2016). Consequently, any detected changes in Glx could be caused by alterations in glutamate, but also by altered glutamine levels, complicating the interpretation of results. Furthermore, it is important to note that glutamate has many roles in the human brain (McKenna, 2007), including non-excitatory metabolic functions and exact levels vary between individuals (Krause & Kadosh, 2014). Thus, the usefulness of cross-sectional group comparisons for identifying true clinically relevant differences between patients and controls is unclear. Potentially, longitudinal follow-up measures could provide more meaningful measures for the detection of neurotransmitter alterations associated with psychosis onset risk.

6.2 Conclusion

The present analyses suggest that merely meeting threshold criteria for CHR or FEP diagnoses may not in itself be indicative of changes in auditory cortical E/I balance. However, neurocognitive functional impairments may be linked to a change in the equilibrium between Glx and GABA, through elevations of Glx, as indicated by weak correlations in left primary auditory cortex.

Chapter 7 Longitudinal Data

7.1 Introduction

Traditionally, CHR intervention studies have focused on comparing CHR participants who transition to FEP versus those who do not (Fusar-Poli et al., 2013). However, 40-85% of participants meeting CHR criteria have been found to not convert within the time scope of studies (Addington et al., 2011), with declining transition rates in recent years (Fusar-Poli et al., 2013). Furthermore, the CHR state is fluid, with a proportion of participants typically remitting fully over time, while others continue to meet CHR criteria.

Previous work has highlighted that duration of symptoms as well as baseline global functioning are indicative of the functional prognosis (Fusar-Poli et al., 2009; Larsen, Moe, Vibe-Hansen, & Johannessen, 2000). Furthermore, MRI studies have revealed correlations between baseline grey matter (GM) volume and conversion risk among CHR participants (Cannon et al., 2015; Pantelis et al., 2003). Crucially, the relationship was not driven by antipsychotic medication (Cannon et al., 2015). Moreover, follow-up data revealed progressive GM loss in converted CHR individuals, while non-converters only showed GM impairments in the cerebellum at follow-up (Pantelis et al., 2003). Finally, the mismatch-negativity ERP measured has been found to differentiate between CHR remitters and non-remitters (Kim, Lee, Yoon, Lee, & Kwon, 2018), and between converting and non-converting CHRs (Bodatsch et al., 2011). Thus, there is evidence that both clinical and neuroimaging variables may be useful for the detection of individuals who may require early intervention to prevent a poor clinical outcome.

Attempts to develop individualised risk-predictors have employed computational modelling strategies and machine learning (Orrù, Pettersson-Yeo, Marquand, Sartori, & Mechelli, 2012). For instance, multiple demographic and clinical measures were combined to create a risk index calculator (Cannon et al., 2016), which showed reasonable prediction accuracy (Harrell's concordance index 0.71 and 0.79 respectively) in two separate samples (Cannon et al., 2016; Carrión et al., 2017).

Other investigators have employed machine learning strategies with structural (Koutsouleris et al., 2012, 2010; Sun et al., 2009) and functional (Shen, Wang, Liu, & Hu, 2010) MRI data in both CHR and established ScZ. These efforts yielded promising results (Orrù et al., 2012), but there is a lack of data from other imaging modalities such as EEG and MEG, which may be better suited for capturing subtle neural changes at early stages of psychosis.

Accordingly, the aim of this chapter was to explore potential relationships between baseline ASSR measures (see Chapter 4) and clinical variables, with the objective to establish whether MEG oscillation measures are predictive of long-term clinical outcomes. Four separate analyses were performed on contrasting CHR subgroup pairs, defined based on participant CHR state at follow-up, transitions to FEP, baseline and longitudinal measures of GAF.

7.2 Methods

7.2.1 Sample

Data from 93 CHR participants and 46 healthy controls (described in Chapter 2) formed the basis for the analyses in this chapter. Data available from the 12-month follow-up visit were used to explore the relationship between 40 Hz ASSR and beta power oscillatory data and longitudinal psychological/clinical outcomes.

7.2.2 ROI Selection

The present work was based on a data-driven approach whereby analyses were focused on source reconstructed 40 Hz power and ITPC-data from RSMG. Furthermore, analyses explored beta power (15-25 Hz) from seven nodes found to differ between CHR and controls in Chapter 4: Right Superior Frontal Gyrus (RSFG), Left Inferior Frontal Gyrus (LIFG), Right Supplementary Motor Area (RSMA), Left Dorsal Cingulate Gyrus (LDCG), Right Dorsal Cingulate Gyrus (RDCG), Left Rolandic Area (LROL), Left Thalamus (LTHA). Additional supplementary analyses of 40 Hz measures included all nodes from Chapter 4 (Appendix 3).

7.2.3 Statistical Comparisons

Analyses focused on CHR subgroups based on CHR status at the 12-month follow-up (sustained CHR n=14; resolved CHR n=36), transitions (Transitions n=4; Non-converters n=89) and GAF scores at baseline (high GAF scores ≥65: n=26; low GAF scores <65:n=61) and at the 12-month follow-up (high GAF scores ≥65: n=24; low GAF scores <65:n=26). High GAF scores represented no or mild functional impairment and low scores reflected moderate to severe impairments (Haining et al., 2019).

7.3 Results

At the 12-month follow-up, 14 of the included CHR participants met the CAARMS criteria for attenuated psychosis, while 36 did not meet criteria. Furthermore, at the time of analysis four CHR individuals had reached the FEP threshold. They were found to meet FEP criteria at their 6-month, 9-month and 12-month (two participants) follow-up visits respectively.

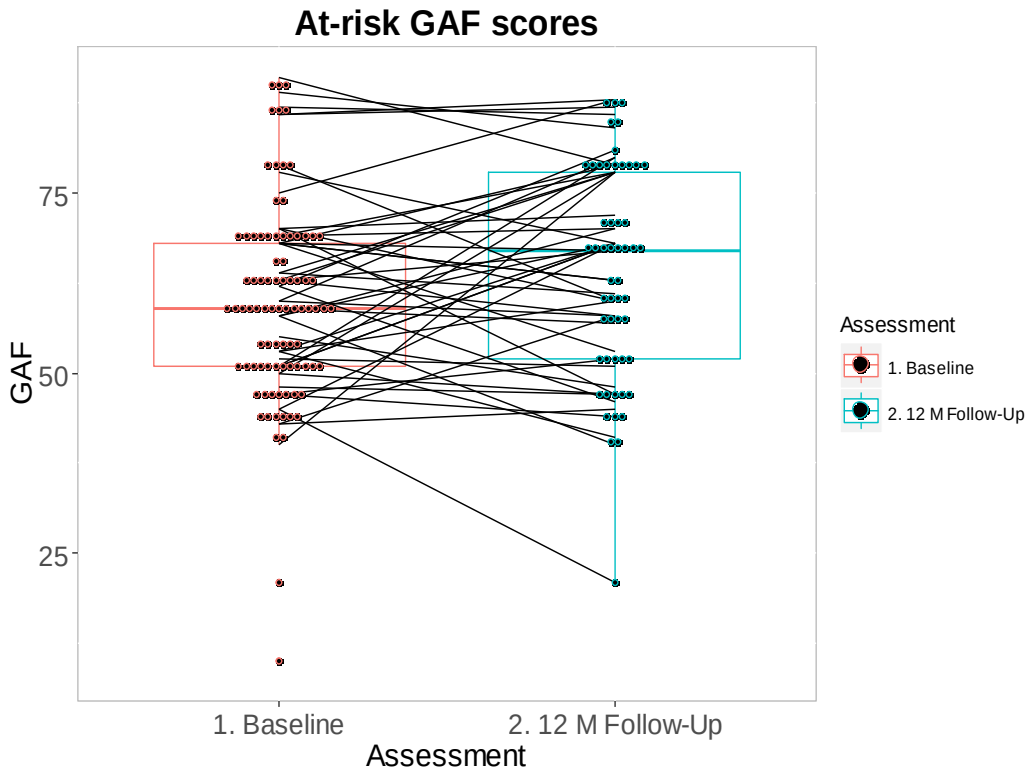

Figure 22 Global Assessment of Functioning in CHR Sample at Baseline and 12M Assessments.

GAF data from the 12-month follow-up visit was available for 50 CHR participants. Data loss relative to baseline was due in part to participant disengagement, but 13 participants had not yet reached the 12-month follow-up at the time of analysis. Twelve CHR participants had high GAF scores (≥65) at both baseline and 12-months, 19 CHR had low GAF scores at both time-points and the remaining 19 participants changed GAF level between baseline and the 12-month follow-up (Figure 22). At 12-months, the mean GAF score in the CHR group was 63.34 (sd±14.90).

Table 16 RSMG 40 Hz Power: Comparisons between CHR Subgroups and Healthy Controls

Groups based on	Group Analysis		Poor outcome[a] vs HC			Good outome[b] vs HC			Poor vs Good outcome		
	F	p	t	p	d	t	p	d	t	p	d
CHR status at 12 M	0.55	0.55	-0.42	0.34	-0.11	-1.06	0.15	-0.25	0.32	0.35	0.14
GAF at Baseline	2.92	0.05*	-2.39	0.01*	0.46	-0.88	0.20	0.20	1.11	0.13	-0.27
GAF at 12 M	2.26	0.12	-0.31	0.38	0.09	-2.18	0.02*	0.55	1.65	0.05*	-0.47
Transitions	2.48	0.09	-0.54	0.33	0.28	-2.22	0.02*	0.40	0.19	0.37	-0.10

a) **Sustained CHR; GAF<65, Converted CHR**
b) **Resolved CHR; GAF≥65, Non-converted CHR**

P<0.05 = * (uncorr)

Table 17 RSMG 40 Hz ITPC: Comparisons between CHR Subgroups and Healthy Controls

Groups based on	Group Analysis		Poor outcome[a] vs HC			Good outome[b] vs HC			Poor vs Good outcome		
	F	p	t	p	d	t	p	d	t	p	d
CHR status at 12 M	1.26	0.29	-0.90	0.19	-0.27	-1.52	0.06	-0.34	0.17	0.43	-0.05
GAF at Baseline	1.26	0.04*	-2.45	0.01*	0.48	-1.61	0.06*	0.40	-0.37	0.35	0.09
GAF at 12 M	1.79	0.17	-1.16	0.13	-0.28	-1.8	0.04*	-0.45	0.57	0.29	-0.16
Transitions	3.77	0.03*	-0.35	0.43	0.18	-2.75	0.00*	0.50	0.61	0.25	-0.31

a) **Sustained CHR; GAF<65, Converted CHR**
b) **Resolved CHR; GAF≥65, Non-converted CHR**

P<0.05 = * (uncorr)

7.3.1 RSMG 40 Hz ASSR

7.3.1.1 Risk status

Statistical comparisons showed no 40 Hz spectral power or ITPC group difference in RSMG (Figure 23, Figure 24).

However, supplementary analyses indicated an increase in 40 Hz ASSR spectral power in sustained CHR participants in the right cerebellar areas 4-5 (RCRBL45) compared to both controls and resolved CHR participants ($F=3.06$, $p=0.05$; post-hoc sustained CHR vs Controls $t=2.25$, $p=0.02$, $d=0.70$; post-hoc sustained CHR vs resolved CHR $t=2.21$, $p=0.01$, $d=0.63$) (Appendix 3). Considering small group sizes and modest statistical effects, this finding is preliminary and should be explored more, but it nevertheless highlights the cerebellum as a potentially important area in the CHR state.

7.3.1.2 Global functioning levels

Significant RSMG group effects were detected for both spectral power and ITPC measures, representing significant reductions in the CHR group with low GAF scores, and a trend for the CHR group with high GAF scores at baseline, relative to controls (Figure 23, Figure 24,Table 16; Table 17).

When follow-up GAF scores were used to form CHR subgroups, no overall group effect was seen, yet post-hoc comparisons revealed that 40 Hz spectral power and ITPC measures were significantly reduced in the CHR group with high follow-up GAF scores, relative to controls (Table 17). Furthermore, 40 Hz spectral power was reduced in CHR participants with high follow-up GAF scores compared to those with low follow-up GAF scores (Table 16). However, none of the observed effects survived fdr correction.

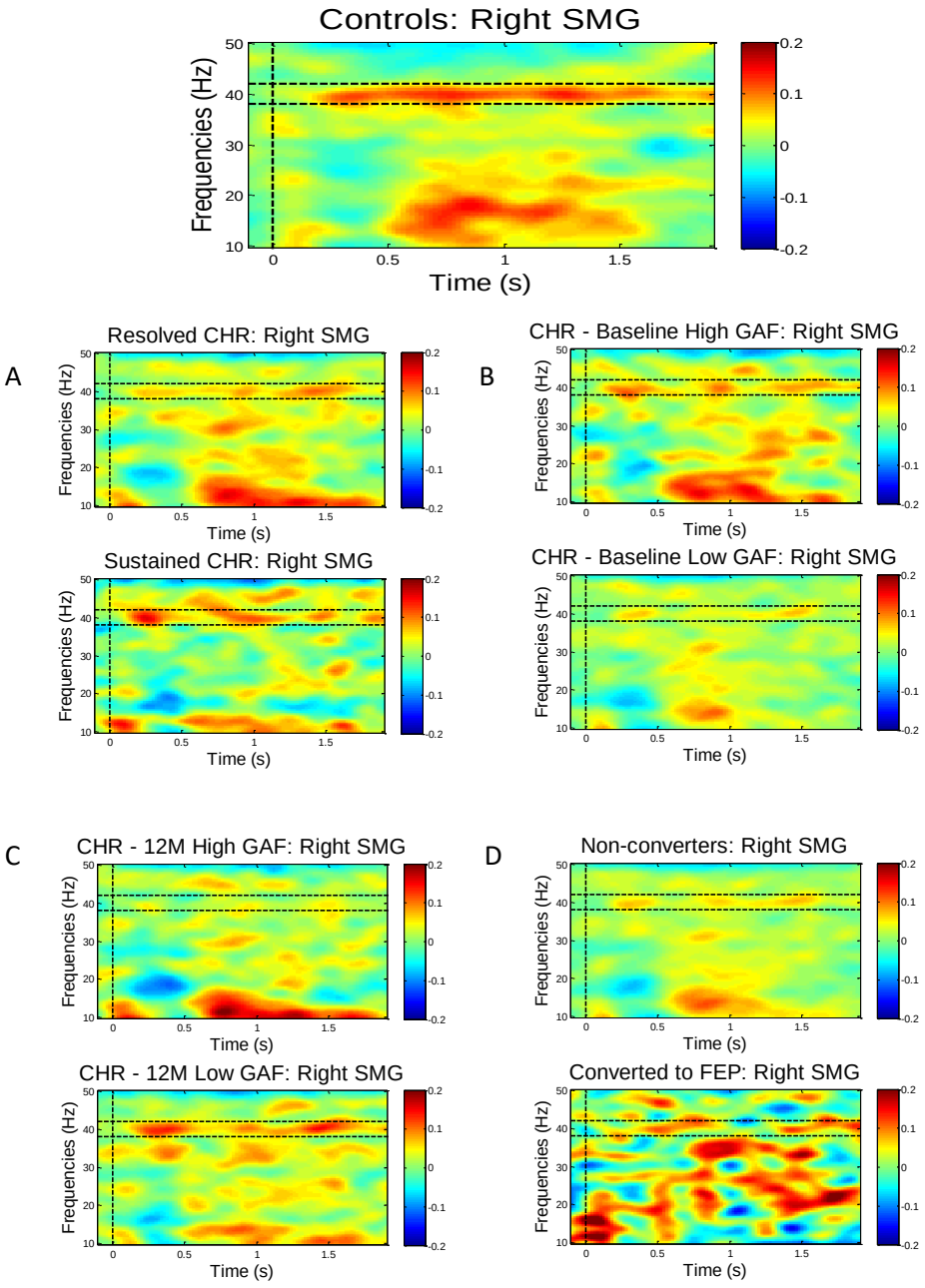

Figure 23 RSMG 40 Hz ASSR Power in Controls and CHR Subgroups Based on A) Risk Status at 12 Months Follow-Up, B) GAF Scores at Baseline, C) GAF Scores at 12 Month Follow-Up, D) Transitions

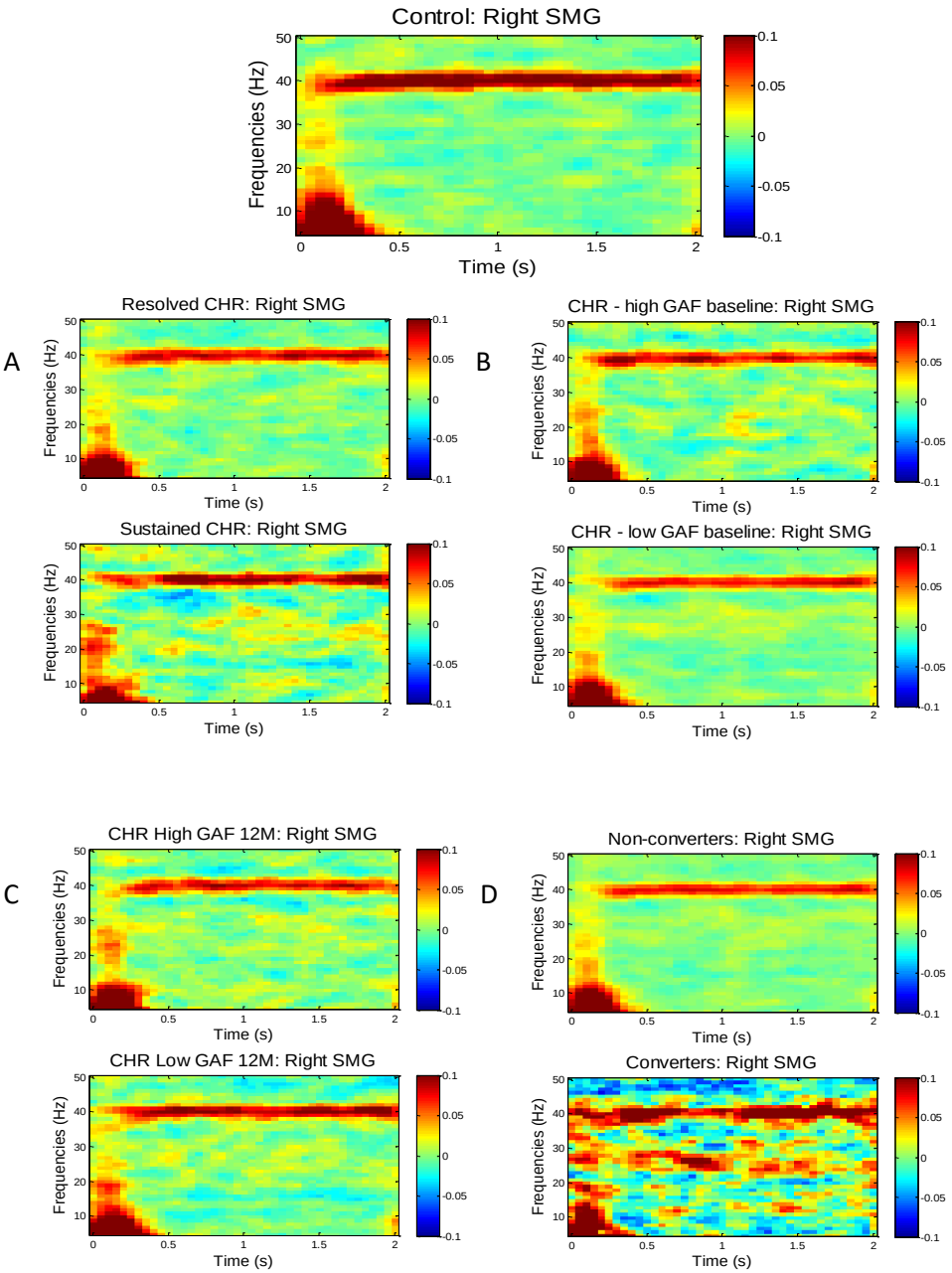

Figure 24 RSMG 40 Hz ASSR ITPC in Controls and CHR Subgroups Based on A) Risk Status at 12 Months Follow-Up, B) GAF Scores at Baseline, C) GAF Scores at 12 Month Follow-Up, D) Transitions

7.3.1.3 Transitions

Visual observation of data indicated that the four CHR participants who converted to psychosis had stronger spectral power activation during 40 Hz ASSR stimulation in several nodes than the 89 CHRs who did not transition. There was no overall group effect in neither spectral power nor ITPC data (Figure 23, Figure 24). However, post-hoc tests showed that both RSMG spectral power (Table 16) and ITPC (Table 17) differed significantly in non-transitioned but not in transitioned CHR participants.

7.3.2 Beta Frequency Nodes

7.3.2.1 Risk status

Trend group effects for the comparison between sustained and resolved CHR and healthy controls were detected for beta (15-25 Hz) spectral power in the right superior frontal gyrus (RSFG) and the left Rolandic area (LROL). These effects represented significant decreases in beta power in the sustained CHR group compared to controls in both regions and decreased LROL power in sustained CHR compared to resolved CHR (Table 18, Figure 25).

Table 18 Comparisons of Beta Power in CHR Risk Subgroups and Healthy Controls

ROI	Group Analysis		Sustained CHR vs HC			Resolved CHR vs HC			Sustained vs Resolved CHR		
	F	p	t	p	d	t	p	d	t	p	d
Right Superior Frontal Gyrus	2.86	0.06*	-1.98	0.01*	0.61	-1.69	0.05*	0.38	-0.91	0.17	0.28
Left Inferior Frontal Gyrus	1.34	0.29	-1.69	0.05*	0.52	-1.15	0.13	0.24	-0.50	0.31	0.17
Right Supplementary Motor Area	2.02	0.14	-1.90	0.03*	0.58	-0.95	0.17	0.19	-1.38	0.08	0.45
Left Dorsal Cingulate Gyrus	1.28	0.30	-1.49	0.07	0.46	-1.01	0.14	0.19	-0.73	0.24	0.27
Right Dorsal Cingulate Gyrus	1.89	0.18	-1.91	0.03*	0.58	-0.77	0.22	0.15	-1.43	0.06	0.48
Left Rolandic Area	2.72	0.07*	-2.38	0.01*	0.73	-0.87	0.18	0.17	-1.66	0.04*	0.55
Left Thalamus	1.56	0.22	-1.65	0.05*	0.50	-1.03	0.14	0.17	-0.95	0.17	0.36

P<0.05 = * (uncorr)

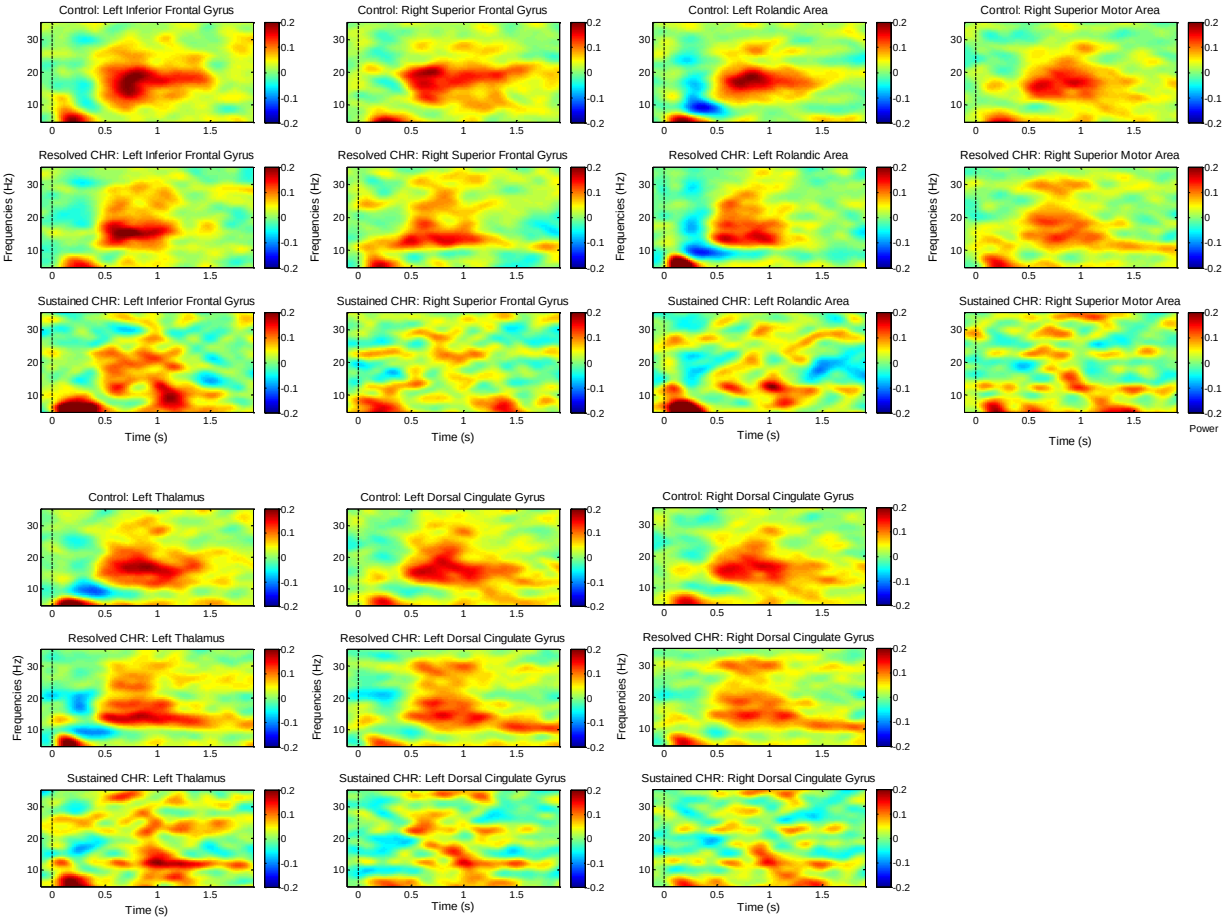

Figure 25 Beta Power (15-25 Hz) in Seven ROIs where CHR Differ Significantly from Healthy Controls; Subgroups Based on Risk Status at 12 Month Follow-Up.

7.3.2.2 Global functioning levels

Group effects were observed in all seven ROI's for comparisons of controls and baseline GAF CHR subgroups. Post-hoc analyses revealed a strong reduction in power across all nodes for CHR participants with low baseline GAF (<65) compared to controls (fdr corrected), while individuals with high baseline GAF (≥65) did not differ from controls. Moreover, the low baseline GAF CHR group showed significantly reduced beta power relative to the group with high baseline GAF in the RSFG, RSMA, RDCG, and LROL. In addition, trend impairments were seen in the LIFG, LDCG and LTHA (Figure 26, Table 19).

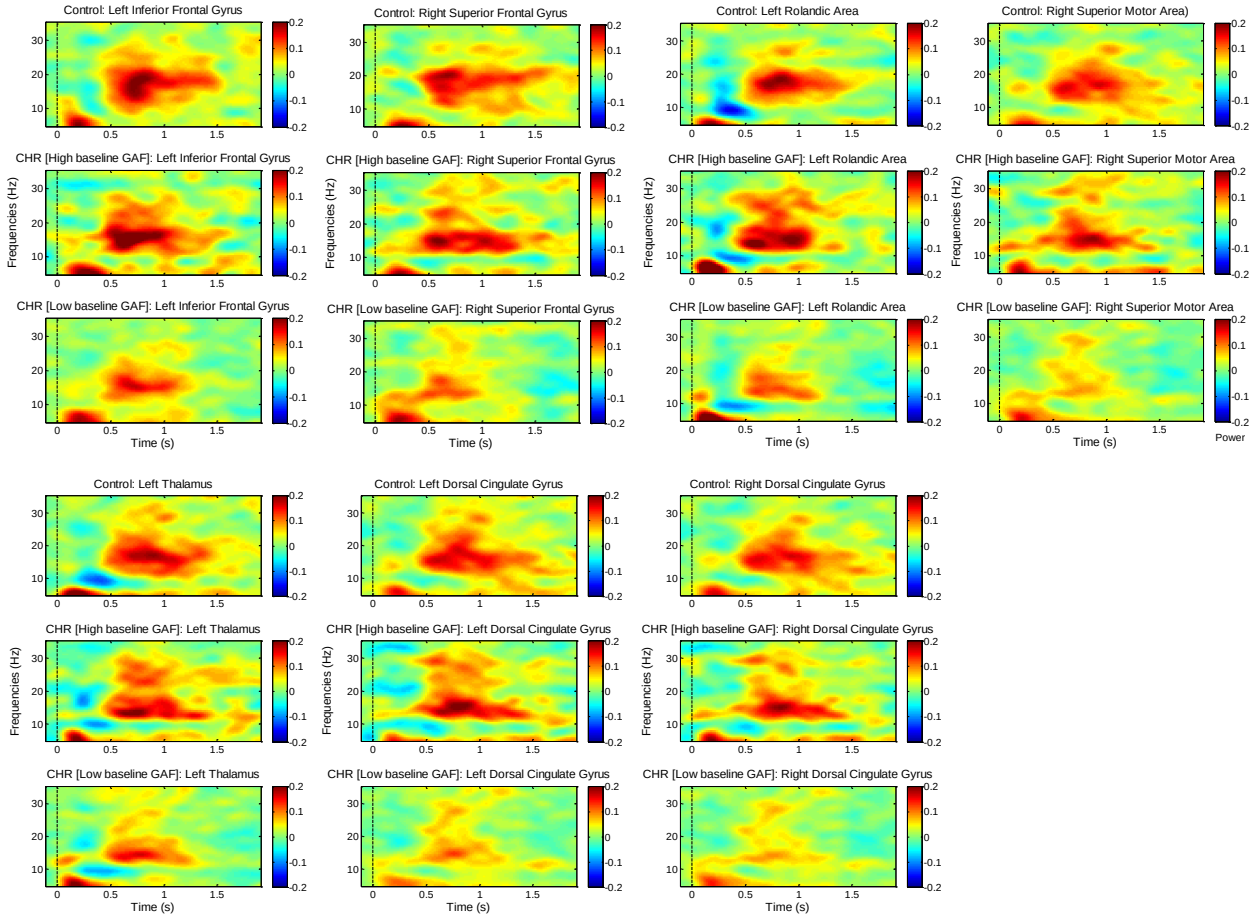

Figure 26 Beta Power (15-25 Hz) in Seven ROIs where CHR Differ Significantly from Healthy Controls; Subgroups Based on CHR GAF Score at Baseline.

For CHR subgroups divided based on the 12-month follow-up GAF score, significant group effects were detected in LIFG, bilateral DCG and LTHA, and trend effects were observed in remaining nodes. These reflected significant impairments in the CHR group with low follow-up GAF scores across nodes (fdr corrected in LIFG, LDCG and RDCG) compared to controls, and impairments relative to CHR participants with high follow-up GAF scores in all nodes except in the right superior temporal gyrus (Figure 27,Table 19).

7.3.2.3 Transitions

Statistical evaluations revealed a significant group effect in right superior frontal gyrus, reflecting reduced beta power in non-converters compared to controls. Furthermore, trend group effects were present in the remaining six ROIs, reflecting significant reductions for both converters and non-converters relative to controls in the LIFG and the LROL, and significant reductions in non-converters vs controls in the RSMA, bilateral DCG and the LTHA. No group

differences were observed between converted and non-converted CHRs (Figure 28, Table 20).

Table 19 Comparisons of Beta Power in CHR GAF Subgroups and Healthy Controls

ROI	Group Analysis		Low GAF vs HC			High GAF vs HC			Low vs High GAF		
	F	p	t	p	d	t	p	d	t	p	d
Baseline[a]											
RSFG	5.35	0.00*	-3.13	0.00*	0.61	-0.70	0.23	0.17	-2.12	0.02*	0.50
LIFG	3.16	0.04*	-2.59	0.01*	0.51	-0.41	0.34	0.10	-1.50	0.07	0.35
RSMA	4.69	0.01*	-3.02	0.00*	0.59	-0.67	0.21	0.17	-1.92	0.03*	0.45
LDCG	3.58	0.03*	-2.64	0.01*	0.52	-0.58	0.26	0.14	-1.62	0.07	0.38
RDCG	4.17	0.01*	-2.84	0.00*	0.55	-0.62	0.24	0.15	-1.79	0.05*	0.42
LROL	4.52	0.01*	-2.72	0.00*	0.53	0.09	0.47	-0.02	-2.40	0.01*	0.56
LTHA	3.64	0.03*	-2.62	0.01*	0.51	-0.59	0.27	0.15	-1.65	0.06	0.39
12 Months Follow-up[b]											
RSFG	2.69	0.07	-2.16	0.01*	0.53	-1.34	0.10	0.34	-0.76	0.21	0.21
LIFG	4.30	0.02*	-3.08	0.00*	0.76	-0.21	0.41	0.05	-2.13	0.02*	0.60
RSMA	2.73	0.06	-2.38	0.01*	0.58	-0.59	0.30	0.15	-1.66	0.05*	0.47
LDCG	3.39	0.04*	-2.62	0.00*	0.64	-0.06	0.49	0.02	-2.24	0.02*	0.63
RDCG	3.33	0.04*	-2.58	0.00*	0.63	-0.22	0.44	0.06	-2.17	0.02*	0.61
LROL	2.86	0.06	-2.45	0.01*	0.60	-0.41	0.34	0.10	-1.72	0.05*	0.49
LTHA	3.47	0.04*	-2.57	0.01*	0.63	-0.11	0.48	0.03	-2.31	0.02*	0.65

a) P<0.05 = * (All significant results survived fdr correction)

b) P<0.05 = * (fdr corrected in LIFG, LDCG and RDCG)

Table 20 Comparisons of Beta Power in CHR Transition Subgroups and Healthy Controls

ROI	Group Analysis		Converted vs HC			Non-converters vs HC			Converters vs Non-converters		
	F	p	t	p	d	t	p	d	t	p	d
RSFG	3.32	0.04*	-0.81	0.20	0.43	-2.53	0.00*	0.46	-0.07	0.49	0.04
LIFG	2.58	0.08	-1.67	0.04*	0.87	-1.98	0.02*	0.36	-0.82	0.21	0.42
RSMA	2.65	0.07	-0.76	0.22	0.40	-2.26	0.01*	0.41	-0.11	0.48	0.06
LDCG	2.37	0.10	-0.94	0.17	0.49	-2.08	0.03*	0.38	-0.33	0.38	0.17
RDCG	2.60	0.08	-0.97	0.15	0.51	-2.18	0.02*	0.40	-0.38	0.37	0.19
LROL	2.64	0.08	-1.69	0.03*	0.88	-1.83	0.04*	0.33	-1.17	0.13	0.60
LTHA	2.78	0.07	-1.26	0.08	0.66	-2.15	0.02*	0.39	-0.72	0.26	0.37

a) P<0.05 = * (uncorr)

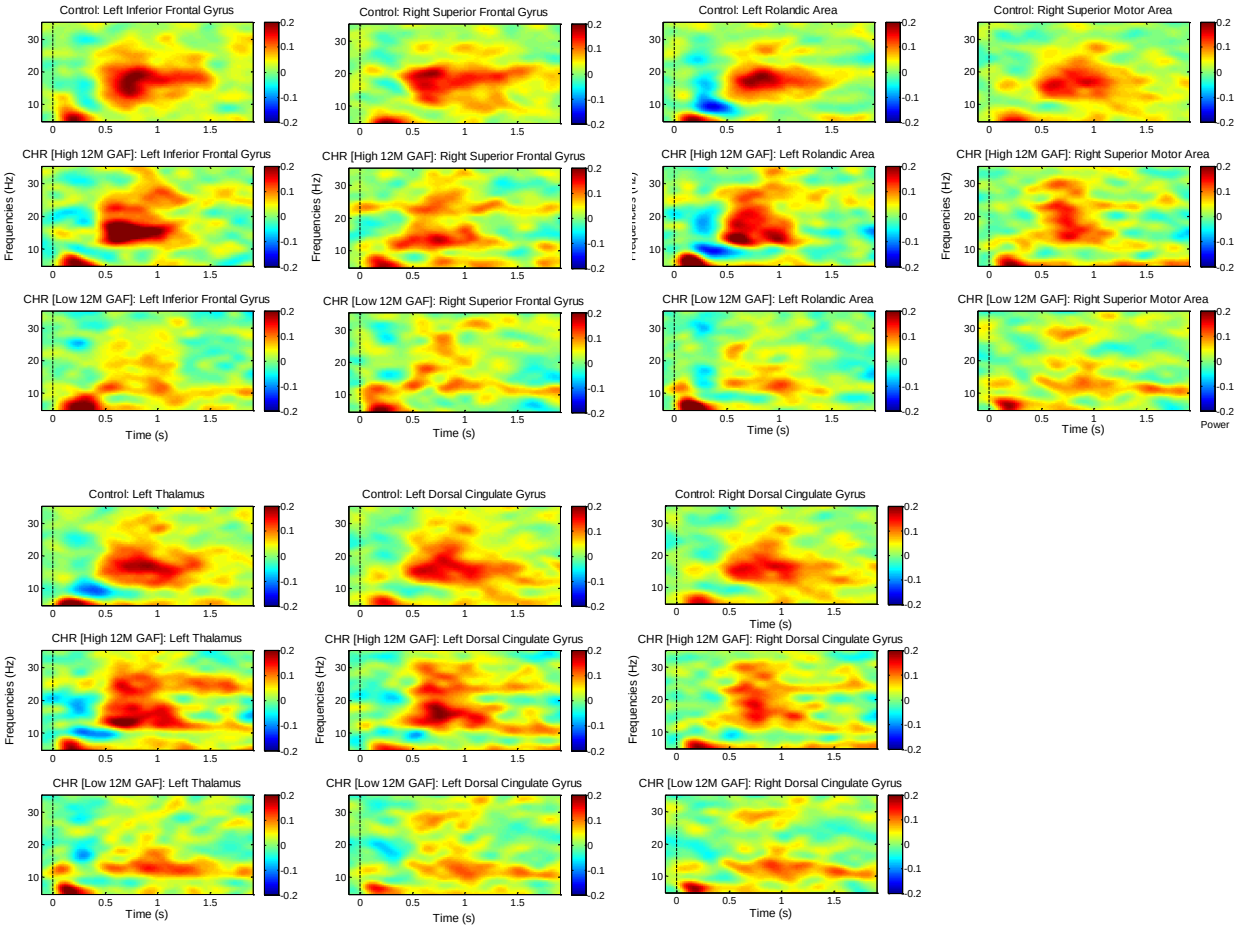

Figure 27 Beta Power (15-25 Hz) in Seven ROIs Where CHR Differ Significantly from Healthy Controls; Subgroups Based on CHR GAF Scores at 12 Month Follow-Up.

7.4 Discussion

The results provide tentative evidence that RSMG 40 Hz ASSR measures may reflect functional vulnerability in CHR individuals. However, these preliminary analyses did not indicate a specific relationship between long-term presentation of attenuated psychotic symptoms and RSMG deficits. In contrast, beta (15-25 Hz) power measures in ROIs selected based on results in Chapter 4, were found to be selectively impaired in individuals with sustained CHR symptoms and low GAF scores (at both baseline and 12 months), suggesting that ROI power measures in this frequency range may be potentially useful for prognosis prediction.

Impairments in both RSMG 40 Hz ASSR power and ITPC were found to be more pronounced in the CHR group with low baseline GAF scores, suggesting that RSMG deficits may reflect functional vulnerability. However, analyses based on follow-up GAF scores showed no overall group effects, and only the high GAF group differed from controls. Thus, 40 Hz ASSR impairment reflected the degree of functional impairment at the time of scanning to some degree but does not appear clearly related to future functioning levels. This is in line with recently published findings showing that baseline ASSR measures predicted functioning at the 1-2 year follow-up assessments in FEP participants, but not in CHR subjects (Koshiyama et al., 2018a)

Notably, supplementary analyses (Appendix 3) indicated that the sustained CHR group had significantly higher 40 Hz spectral power in the right cerebellar areas 4-5. This is a preliminary result as comparison groups were small, but abnormalities in cerebellum are in line with previous findings in CHR and psychosis (Pantelis et al., 2003; Shen et al., 2010). Thus, the present finding highlights that further investigation of cerebellar oscillatory changes in CHR is warranted, as impairments appear potentially specific to individuals with long-term presence of attenuated psychotic symptoms.

Chapter 4 revealed seven nodes where CHR and FEP participants showed significant reductions in 15-25 Hz beta power, and a positive relationship between beta power and GAF scores was found across these nodes in the CHR group. In line with this observation, a clear difference was detected here

between control participants and CHR participants with low GAF scores at both baseline and the 12-month follow-up assessment, while no difference was detected between controls and CHR participants with high GAF scores. Crucially, the results also revealed more pronounced impairments in individuals with sustained CHR symptoms at the 12-month follow-up. Thus, these findings highlight the possibility to employ beta power measures for predictions of long-term functioning.

The functional relevance of the observed beta response was discussed in Chapter 4, highlighting motor function as a likely candidate. In CHR individuals and first-degree relatives, neurological soft sign deficits have been the most frequently reported motor impairments (Mittal et al., 2014). Importantly, previous studies reported that neurological soft signs predicted negative but not positive symptoms in a small CHR sample (Mittal et al., 2014). Furthermore, a link between neurological soft sign symptoms and neuropsychological impairments has been reported in FEP (Mohr et al., 2003). Both cognitive and negative impairments have been found to be associated with global functioning (Milev et al., 2005). Thus, if beta abnormalities observed in the current sample are indeed related to motor function, potential deficits in motoric neurological soft signs could account for the clear relationship seen with global functioning scores.

The present analyses were restricted by the limited amount of follow-up data available at the time of analysis. In addition, only four individuals had transitioned to FEP, resulting in low statistical power for analyses including this group, and noisy plots. However, while the results should be viewed with this limitation in mind and interpreted cautiously, the findings provide insight into relationships between the ASSR measure and long-term clinical profiles. Thus, the present results can provide guidance for future analyses, and possibly for the development of clinical test batteries.

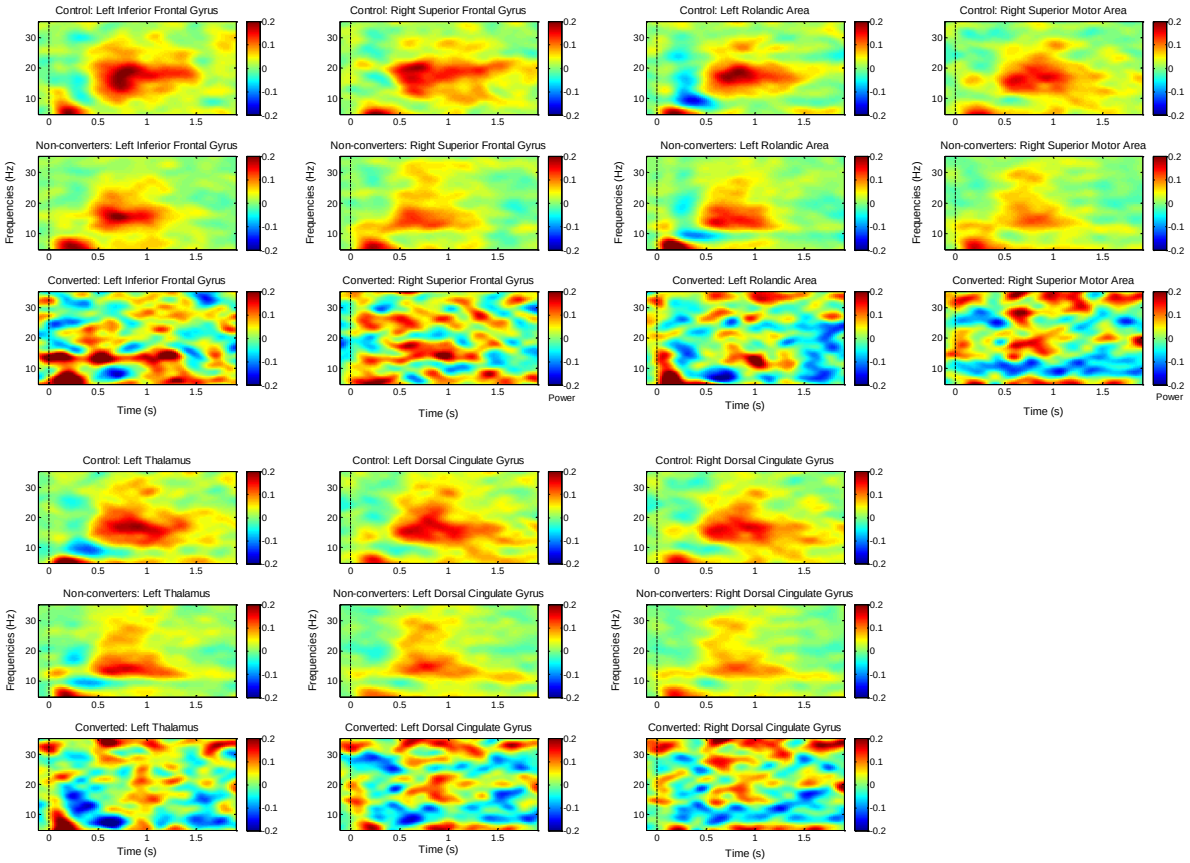

Figure 28 Beta Power (15-25 Hz) in Seven ROIs where CHR Differ Significantly from Controls; Subgroups Based on CHR Conversion to FEP.

Moreover, it is controversial whether MEG can detect signals from deep brain regions such as the cerebellum (Dalal, Osipova, Bertrand, & Jerbi, 2013). Supplementary analyses (reported in detail in Appendix 3) indicated that subjects with sustained CHR symptoms had significantly higher 40 Hz spectral power in the right cerebellar areas 4-5. However, the cerebellum is located deep in the back of the skull, close to the neck (Dalal et al., 2013), and it is therefore possible that measures may be affected by differences in muscle tension. However, it is worth noting that magnetometers used for measures in the present study, while sensitive to artefact activity, also are superior to gradiometers for detection of deep brain signals (Vrba & Robinson, 2000). Furthermore, previous reports indicate that cerebellar measures using MEG are possible provided sufficient signal-to-noise ratio (Attal & Schwartz, 2013; Kirsch et al., 2003; Wibral et al., 2011). Here, data were cleaned carefully prior to analysis in order to avoid influence from muscle artefacts, which combined with extensive evidence for cerebellar involvement in ScZ from other modalities (Picard, Amado, Mouchet-Mages, Olié, & Krebs, 2008), support the notion that the results observed reflect true differences in brain activity. Nevertheless, it

cannot be ruled out that muscle artefacts contributed to the statistical group difference.

7.5 Conclusion

Analyses in this chapter and supplementary findings (Appendix 3) reveal a possible link between both 40 Hz ASSR alterations and beta power deficits and long-term clinical prognosis, measured through assessment of both attenuated psychotic symptoms and GAF levels.

Chapter 8 General Discussion

This thesis focused on auditory high frequency oscillations in CHR and FEP individuals, using a MEG ASSR paradigm. Furthermore, MEG-data were explored in the context of clinical variables as well as MRS-measured Glx and GABA levels. Finally, the potential relationship between ASSR measures and CHR outcome was addressed.

8.1 40 Hz ASSR

Results from the 40 Hz ASSR data analysis revealed a modest but consistent impairment in RSMG in both 40 Hz spectral power and ITPC. At source level, this effect was significant and sustained (uncorrected) in CHR and reached a trend level in the FEP sample. Furthermore, Chapter 5 explored connectivity between right primary auditory areas (HES and STG) and the RSMG during 40 Hz ASSR. Analyses revealed both bottom-up (RSTG to RSMG and RHES to RSMG) and top-down (RSMG to RHES) reductions in connectivity at 40 Hz in CHR participants.

The SMG in the inferior parietal lobule is involved in a range of functions, including complex auditory functions, such as auditory language processing (Niznikiewicz et al., 2000; Oberhuber et al., 2016; Rauschecker & Scott, 2009), auditory pitch memory (Vines et al., 2006) and auditory-motor multisensory processing (Bangert et al., 2006). In addition, the SMG has been implicated in basic auditory target detection and is thought to be closely linked to the auditory P300 ERP (Horovitz et al., 2002; Menon et al., 1997; Skosnik et al., 2007). Notably, impairments in these functional domains have been observed in ScZ (Bambini et al., 2016; Bernard & Mittal, 2014a; Javitt & Sweet, 2015; Morrens et al., 2014).

Both structural and functional abnormalities have been documented in ScZ in the inferior parietal lobule, including the SMG (reviewed by Torrey, 2007). Crucially, the SMG is involved in self-awareness and self-reflection (Shad et al., 2012; Van Der Meer et al., 2013), the cognitive processes required to differentiate between the self and non-self and the recognition of self-generated feelings and actions (Van Der Meer et al., 2013). Accordingly, inhibition of the right inferior parietal lobule, using repetitive transcranial magnetic stimulation, disrupts

performances in a self-others discrimination task in healthy volunteers (Uddin, Molnar-Szakacs, Zaidel, & Iacoboni, 2006). Consistent with this observation, degree of insight in ScZ patients has been found to correlate with inferior parietal lobule activation (Van Der Meer et al., 2013). Moreover, machine learning investigations identified the SMG as part of a network with pronounced impairments and strong discrimination power in a comparison between controls and chronic ScZ patients (Guo, Kendrick, Yu, Wang, & Feng, 2014).

Notably, the SMG is also implicated in aberrant ScZ sensory integration (Torrey, 2007) and auditory hallucinations (Gaser et al., 2004). Structural findings have indicated a link between auditory hallucinations and left SMG GM volume loss in chronic ScZ (Gaser et al., 2004), while fMRI data highlighted bilateral SMG in auditory verbal hallucinations (Sommer et al., 2008). Furthermore, inter-hemispheric synchronization between auditory regions appears crucial for conscious auditory perception (Steinmann et al., 2014), and interhemispheric 40 Hz ASSR connectivity deficits were found to correlate with auditory hallucinations in ScZ (Mulert et al., 2011). In the current findings no direct link was found between RSMG MEG-data and overall perceptual abnormalities, yet the findings support SMG involvement in aberrant sensory processing. Specifically, the present data indicate that the basic auditory response to stimulation in primary auditory cortex is intact in CHR, but that the propagation of the oscillatory entrainment response to the SMG is impaired, potentially reflecting deficits that could account for sensory integration and auditory perceptual abnormalities.

Two studies reported inferior parietal lobule involvement in the 40 Hz ASSR (Koenig, van Swam, Dierks, & Hubl, 2012; Reyes et al., 2005). It was suggested that the response involves the activation of a temporally dispersed network including the temporal lobe, medial frontal, frontal parietal, inferior parietal, contralateral cerebellum and temporal cortices (Reyes et al., 2005). Crucially, Koenig et al (2012) observed impaired 40 Hz phase-coherence in the inferior parietal lobule in ScZ patients with auditory hallucinations. However, to the author's knowledge there are no other investigations of inferior parietal lobule involvement in the ASSR in ScZ as studies have primarily focused on sensor level data or source reconstructed data from primary auditory regions (Thuné et al.,

2016). In contrast, the present data-driven ROI selection approach supports the notion that a wider network of regions is activated through ASSR stimulation and reveals that ASSR deficits in emerging psychosis do not appear to involve primary auditory regions.

The oscillatory response captured by ASSR stimulation is thought to reflect the underlying neural circuitry (Spellman & Gordon, 2015) through activation of interacting glutamatergic and GABAergic signals. Specifically, evidence suggests that glutamate released from pyramidal neurons acts on NMDA receptors on GABAergic interneurons to trigger inhibition through subsequent GABA release, resulting in a rhythmical excitation-inhibition pattern (Carlén et al., 2012).

The crucial role of both GABA and glutamate in the generation of gamma oscillations has been demonstrated in previous investigations. Optogenetic work has revealed that blockage of GABAergic PV+ inhibitory interneurons prevents gamma activity, while stimulation of these cells significantly enhances gamma oscillations (Sohal et al., 2009). Furthermore, in-vivo work has demonstrated the involvement of glutamate through pharmacological manipulations with ketamine (Sigurdsson, 2016) and MK800 (Sivarao, 2015). Administration of NMDA glutamate receptor antagonists has revealed altered gamma oscillations, including both increases (Rebollo, Perez-zabalza, Ruiz-mejias, Perez-mendez, & Sanchez-vives, 2018; Sivarao et al., 2013) and decreases (Sullivan et al., 2015; Vohs et al., 2012). Evidence suggests that the direction of gamma oscillatory abnormalities can depend on the degree of NMDA receptor blockage (Sivarao, 2015; Sivarao et al., 2016).

In-vivo work has indicated the possibility that NMDA receptor dysfunction begins on GABAergic interneurons during neural development, causing impaired interneuron maturation and ultimately aberrant regulation of both glutamate and GABA cortical signalling (Nakazawa, Jeevakumar, & Nakao, 2017). A relatively novel addition to this neural model of ScZ is the role of oxidative stress (Ng, Berk, Dean, & Bush, 2008). Recent work has demonstrated that disrupted oxidant/anti-oxidant balance, resulting in elevated oxidative stress, is a candidate mechanism explaining such early developmental NMDA receptor deficits (Hardingham & Do, 2016).

Notably, the SMG matures late in neural development (Leroy et al., 2011; Torrey, 2007), extending until mid-late adolescence (Paus, 2005). Moreover, there is evidence for sex differences in the development of this area, with a hypothesized earlier maturation in males than females (Raznahan et al., 2010). Combined with findings discussed above, one interpretation of the observed RSMG oscillatory deficit in CHR individuals is thus that aberrant neural development of NMDA receptors on GABAergic interneurons, occurring during adolescence around the time of SMG maturation, could account for early auditory impairments and attenuated psychotic symptoms in emerging psychosis. The earlier maturation of this brain region in males provides a potential explanation for the typically earlier age of psychosis onset in men (Angermeyer & Kühn, 1988). Furthermore, 1H-MRS findings in the current investigation provide preliminary evidence for a trend reduction of GABA in right primary auditory areas in FEP patients. This suggests a potential spread of impairments from higher inferior parietal areas to auditory cortex with increasing psychotic symptoms.

Potential long-term implications of observed RSMG deficits in the CHR group were explored in longitudinal analyses, revealing a relationship between RSMG impairments and baseline GAF scores. However, the preliminary longitudinal analyses did not indicate a direct link between RSMG measures and acute psychosis risk.

In addition, longitudinal analyses including supplementary nodes provide preliminary support for an increase in cerebellar 40 Hz ASSR power in the right cerebellar areas 4-5 (from AAL atlas), corresponding to the lateral lobules (4 and 5) of the cerebellum. Interestingly, these alterations appear specific to prolonged attenuated psychotic symptoms. These findings may be in line with a model suggesting that ScZ arises through abnormal connections in the cortico-cerebellar-thalamic-cortical circuit, associated with both higher-order mental and motor functions (Andreasen & Pierson, 2008). Furthermore, meta-analysis data (fMRI and PET) of measures in five functional domains (language, working memory, emotion, executive processing/attention and motor) found alterations in the cerebellar functional topography in ScZ, with areas of both increased and decreased activation (Bernard & Mittal, 2014b). Thus, cerebellar alterations

contributing to ASSR abnormalities in emerging psychosis should be explored further.

At a circuit level, elevated cerebellar gamma oscillations may also be accounted for by NMDA receptor blockage/hypofunction (Rebollo et al., 2018; Sivarao et al., 2016, 2013). As discussed above, increases in 40 Hz ASSR power and ITPC may reflect partial NMDA receptor hypofunction (Sivarao et al., 2016). Thus, the current data imply that in the CHR group, NMDA receptor impairments were more pronounced in the RSMG, where a reduction in ASSR measures was found, than in the RCRBL4-5 area where 40 Hz oscillation measures were augmented.

Finally, an important question is whether ASSR impairments in ScZ are riding on underlying oscillatory baseline changes (Spencer, 2012). Reports of increased baseline power in the 40 Hz range (Spencer, 2012), in line with a notion that NMDA receptor deficits cause increases in non-stimulus evoked gamma power independent of degree of receptor impairments (Sivarao et al., 2016), have given rise to a debate about whether ASSR impairments truly reflect abnormal evoked gamma entrainment. To address this issue, baseline data in the current analysis were compared between groups. No statistically significant differences were found, demonstrating that at least in CHR and FEP individuals, ASSR deficits are unlikely to be influenced by underlying baseline differences. Moreover, the present findings also do not indicate global NMDA receptor deficits in CHR and FEP but suggest that any NMDA receptor alterations are regionally specific to a limited brain area, notably the RSMG.

8.2 ASSR Data Analysis

Statistically significant group differences in ASSR measures were found in source reconstructed data, but not at the sensor level. The ASSR has been found to be robust using both MEG (Tan et al., 2015b) and EEG measures (Legget, Hild, Steinmetz, Simon, & Rojas, 2017) in healthy controls, and the meta-analysis performed in preparation of this PhD project (Chapter 3) revealed no difference between chronic ScZ measures from source or sensor level analyses (Thuné et al., 2016). However, the regional specificity of sensor level data is compromised by field spread through input from multiple neural sources to each sensor (Schoffelen & Gross, 2009). Combined with the generally small-moderate effect

sizes seen in the present analyses and in previous CHR studies (Koshiyama et al., 2018b), it is not surprising that regionally specific group differences may be diluted at sensor level and thus not detected.

Both MEG and EEG allow the reconstruction of data on source level (Darvas, Pantazis, Kucukaltun-Yildirim, & Leahy, 2004), but methodological challenges have resulted in the majority of ASSR studies reporting source analyses using MEG (Chapter 3; Thuné et al., 2016), with only two studies exploring source reconstructed EEG measures of ASSR in ScZ (Koenig et al., 2012; Spencer et al., 2009). The methods share similarities, but while MEG has the advantage of being resistant to confounding effects from tissue conductivity (Darvas et al., 2004), EEG enables superior capture of radial sources (Ahlfors, Han, Belliveau, & Hämäläinen, 2010). Thus, for a full picture of CHR deficits, evaluations of both MEG and EEG source reconstructed data may be valuable.

8.3 Beta Oscillations

In addition to 40 Hz findings, analyses of oscillatory data in Chapter 4 revealed a group effect of power in the beta frequency range (15-25 Hz) in seven nodes, including two frontal (Right Superior Frontal Gyrus, Left Inferior Frontal Gyrus), two motor (Right Supplementary Motor Area, Left Rolandic Area) and three subcortical regions (Left Dorsal Cingulate Gyrus, Right Dorsal Cingulate Gyrus, Left Thalamus). This effect represented impaired beta power in CHR and FEP compared to controls across regions, and impaired beta power in FEP compared to CHR in LROL.

Increased contralateral beta power is an established feature of motor inhibition after movements (“beta rebound”) (Y. Zhang et al., 2008) and during the withholding of motor actions (Solis-Escalante, Müller-Putz, Pfurtscheller, & Neuper, 2012). In the present ASSR paradigm, participants were instructed to press a button with their right index finger when hearing a deviant non-ASSR stimulus. Therefore, each trial involved the active evaluation of stimuli to determine whether a response was appropriate or not. Hence, it is possible that the beta signal observed in the current sample represents a beta motor evaluation and subsequent suppression of a prepared motor action.

Thus, the current findings provide further tentative evidence for abnormal motor processing in both CHR and FEP. Motor impairments have been reported in ScZ, CHR populations and first-degree relatives of patients (Schäppi, Stegmayer, Viher, & Walther, 2018), highlighting motor dysfunction as a potential endophenotype for ScZ (Chan & Gottesman, 2008). Notably, neurological soft signs, which have been reported as the most prominent motor impairment in CHR (Mittal et al., 2014), are potentially related to deficits in the inferior parietal lobule and specifically in the SMG (Torrey, 2007). However, while beta analyses highlight possible motor suppression deficits in CHR and FEP, clarification through further explorations of relationships between beta oscillations and motor performance tasks are required to test this speculative hypothesis.

Beta power oscillations are implicated in a range of functions (Engel & Fries, 2010) and the observed changes may also mirror abnormalities in other functional domains. One proposed hypothesis is that beta deficits in ScZ reflect impaired salience signalling (Liddle et al., 2016), whereby high neural significance is attributed to insignificant external and internal experiences, proposed to contribute to both positive (Kapur, 2003) and cognitive symptoms (Palaniyappan & Liddle, 2012). Beta power deficits seen in CHR and FEP participants could thus potentially represent an emerging aberrant attribution of salience to repetitive neural activation elicited by ASSR stimulation.

Moreover, there is intriguing evidence that beta frequency abnormalities may be implicated in auditory hallucinations (van Lutterveld et al., 2012). Specifically, left temporal cortex beta power was found to correlate with auditory verbal hallucination severity (van Lutterveld et al., 2012). This possible role is noteworthy firstly as the beta power topographies in the present study suggested pronounced left hemisphere impairments in CHR and FEP, and secondly considering the clearly established role of the SMG in hallucinations. However, further investigation is needed to establish how the detected beta power impairments in CHR and FEP may contribute to these symptoms.

8.4 1H-MRS Measures

The 1H-MRS study investigated the relationship between oscillatory findings and possible neurotransmission deficits in GABA and Glx, with the aim to further elucidate potential E/I balance alterations in emerging psychosis. In addition, possible effects of the selection of 1H-MRS reference molecule on Glx measures were explored in a separate analysis.

While no significant impairments were seen in CHR compared to controls, a trend impairment in right auditory cortical GABA was seen in the small FEP group ($U=111.00$, $p=0.09$, $d=-0.43$). This analysis was underpowered, but highlights a potential deficit driven by GABA reductions in auditory cortex in early psychosis and demonstrates that further work in this brain region is warranted.

Additional analyses explored correlations between 1H-MRS measures and both clinical parameters and 40 Hz ASSR measures. In contrast to previous reports from healthy volunteers (Falkenberg et al., 2012; Muthukumaraswamy et al., 2009), only weak correlations were seen here between left voxel Glx and 40 Hz ASSR power in left HES and STG, but neither relationship survived correction for multiple comparisons. Importantly, the auditory cortex is a small folded region with high individual anatomical variability (Da Costa et al., 2011), and thus the 1H-MRS voxel covered not only primary auditory regions, but some adjacent regions as well. This was adjusted for by correcting for GM/WM and CSF content, but overlap with surrounding brain regions could nevertheless account for the limited correlations observed. In addition, the present 1H-MRS analyses had relatively low statistical power due to small sample size (Control $N=31_{right}$, 22_{left}; CHR $N=64_{right}$, 39_{left}; FEP $N=11_{right}$, 7_{left}). However, the findings are in line with other reports which also failed to replicate 1H-MRS correlations with neuroimaging measures (Cousijn et al., 2014). Thus, the present analyses constitute evidence for a relationship between 1H-MRS measures and gamma oscillations assessed through a 40 Hz ASSR paradigm in the auditory cortex.

Correlation analyses with psychological measures revealed a weak negative relationship between right auditory cortical Glx and composite BACS scores, representing superior cognitive performance in individuals with lower auditory Glx concentrations.

Correlations between clinical parameters and 1H-MRS measures have not previously been explored in auditory voxels. One previous study reported a positive correlation between dorsolateral prefrontal cortex Glx and performance on an auditory verbal learning test in chronic ScZ patients (Ohrmann et al., 2007). However, correlations between Glx and cognitive measures have been inconsistent, with some reporting positive and some negative relationships in frontal regions and cingulate cortex (Merritt, Mcguire, & Egerton, 2013). Moreover, prefrontal 1H-MRS GABA was positively correlated with negative symptoms in CHR (Modinos, Şimşek, Horder, et al., 2018), while anterior cingulate GABA was positively correlated with performance on a cognitive coding test and an attention task (Rowland et al., 2013). Thus, the timing and implications of Glx and GABA alterations in emerging psychosis may depend on the brain regions measured.

Moreover, in the current study, right auditory 1H-MRS measures were computed twice, using first water and subsequently creatine as reference molecule. This was done in order to establish whether the chosen reference molecule could influence results, as has been suggested previously (Öngür et al., 2009). However, in this sample the results did not differ significantly depending on reference, indicating that if deviations in creatine levels are present in emerging psychosis, they were not substantial enough to affect group comparisons here.

8.5 Sample Characteristics

Chapter 2 presented demographic and clinical features of the sample. Analyses of clinical variables confirmed that the sample was adequately matched in terms of age, gender and handedness. This is critical as differences in these variables could potentially confound results (Edgar et al., 2014; Melynyte et al., 2018; Thuné et al., 2016). Furthermore, CHR and FEP participants were impaired compared to controls in GAF score ratings, composite BACS scores, total CAARMS scores and childhood functioning, demonstrating deficits in line with existing knowledge of the CHR and FEP states (Fusar-Poli , Rocchetti, et al., 2015; Riley et al., 2000).

A consideration when interpreting the data is that both the FEP and CHR samples studied here were relatively high functioning; a majority of participants were

non-help-seeking individuals recruited from the community, and the average global functioning scores were higher than an estimated average in a recent meta-analysis (Fusar-Poli , Rocchetti, et al., 2015). Notably, higher overall risk of conversion to psychosis has been observed in samples recruited from clinical services than in samples recruited from the public (Fusar-Poli et al., 2016). However, individuals with lower functioning levels were also represented in the present sample, including individuals referred from NHS services. Accordingly, these data suggest that the online recruitment method is not only a valid approach, but also a useful method to identify a functionally and clinically diverse sample of CHR individuals.

8.6 Correlations between ASSR and Clinical Parameters

Potential relationships between 40 Hz ASSR oscillatory data and clinical variables were explored. Links between clinical symptoms and 40 Hz ASSR measures in patients with ScZ are potentially important for understanding the behavioural/clinical relevance of oscillatory changes. In the current sample, ROI specific positive correlations were seen for CHR participants between 40 Hz ASSR ITPC and global CAARMS severity scores in the LITG and LMTG, and between 40 Hz ASSR ITPC and perceptual abnormality ratings in the LITG. These results constitute a replication of previous findings, suggesting a link between left hemisphere 40 Hz ASSR synchrony and positive symptoms, particularly auditory hallucinations (Spencer et al., 2009). However, a recent contrasting publication reported a negative correlation between 40 Hz ASSR synchrony and hallucinations, but in contrast to previous findings and the present analyses, that observation was based on sensor level EEG data analyses which did not differentiate between hemispheres (Zhou et al., 2018).

Given the role of gamma-band oscillations in facilitating cognition and perception (Fries, 2015; Uhlhaas & Singer, 2010) correlations may be expected between the 40 Hz ASSR impairments and cognitive deficits in patients with ScZ. A modest relationship was noted between working memory performance and 40 Hz ASSR ITPC in ScZ patients (Light et al., 2006). However, Kirihara et al (2012) examined this relationship in a larger ScZ group, and found that only total theta (4-8 Hz) amplitude reductions were correlated with deficits in verbal

memory in patients with ScZ, whereas no relationship was found with 40 Hz ASSRs. In the current thesis, only a weak negative correlation between composite BACS scores and 40 Hz ASSR ITPC in LSTG was detected across the three groups and no correlation was seen in the CHR group alone. These conflicting results suggest that ASSR measures are not directly related to overall cognitive performance, \but could potentially reflect performance in specific cognitive domains.

No measure of negative symptoms was explored here. However, global functioning has been found to be predicted by this symptom category (Wittorf, Wiedemann, Buchkremer, & Klingberg, 2007), and analyses of GAF scores did not indicate a direct correlation between 40 Hz ASSR measures and baseline global functioning levels. This is in line with previous work, which has only demonstrated a relationship between high gamma (80-Hz) ASSR amplitude and negative symptoms. However, recent evidence suggests a significant correlation between 40 Hz ASSR and community functioning (Zhou et al., 2018), highlighting a need to further investigate potential associations to specific functional domains.

In addition to replication of previous findings, the current investigation also revealed novel correlations. Unexpectedly, a strong robust association in CHR was found between beta power (15-25 Hz) and GAF scores across the seven nodes where beta deficits were detected in the CHR group. While no such observation has previously been published, knowledge about the functional implications of beta oscillations allow for speculations about the nature of this relationship. As mentioned previously, beta oscillations are implicated in a range of motor functions, including neurological soft signs which are impaired in CHR (Mittal et al., 2014). Neurological soft signs include deficits in sensory integration, and in motor inhibition and coordination (Chan & Gottesman, 2008). Moreover, beta oscillations have been implicated in salience signalling (Liddle et al., 2016) as well as basic attention (Wróbel, 2000). Thus, lower GAF ratings in individuals with deficit capacity to elicit beta oscillations could reflect severity of impairments in several domains important for global functioning.

8.7 Predicting Psychosis

As discussed in Chapter 7, promising attempts to assess individual risk levels have involved the development of risk indices based on combinations of measures known to be impaired in ScZ (Cannon et al., 2016). This method has the potential advantage of capturing risk based on data from a single individual, which would be required in a clinical setting (Gifford et al., 2016). One such risk-calculator was found to have a moderate to strong ability to separate psychosis converters from non-converters (Harrell's concordance index 0.71 and 0.79 respectively) in two separate samples (Cannon et al., 2016; Carrión et al., 2017). Such compound risk scores may provide a way to capture more of the underlying biological changes and constitute a more reliable marker than one stand-alone measure.

A similar potentially useful approach is to combine neuroimaging measures with computational modelling strategies and machine learning (Orrù et al., 2012). So far, the method has been applied primarily on structural (Koutsouleris et al., 2012, 2010) and functional (Shen et al., 2010) MRI data. These efforts have yielded promising results (Orrù et al., 2012), but there is a lack of machine learning based prediction data from other imaging modalities such as EEG and MEG which may be better suited for capturing subtle neural changes at early stages of psychosis.

However, focusing solely on psychosis transition is unhelpful since transition rates are declining (Lim et al., 2018), but many participants remain in a low functioning CHR state for a substantial period of time and may benefit from interventions (Addington et al., 2011). Instead, developing methods to predict long-term functional impairments may be more meaningful. Thus, future work should focus on the development of prediction batteries designed to detect individuals with a poor long-term functional prognosis.

An important issue for risk and prognosis predictions is whether measures are specific to psychosis or merely sensitive to a general state of vulnerability. Notably, ScZ shares many pathological similarities with bipolar disorder (Cardno & Owen, 2014; Meda et al., 2012; Schretlen et al., 2007) and autism spectrum disorder (ASD) (Radeloff et al., 2014; Sheitman, Kraus, Bodfish, & Carmel, 2004)

and previous work has demonstrated 40 Hz ASSR impairments in both bipolar disorder (Rass et al., 2010) and ASD (Wilson et al., 2007). However, the work presented in this thesis highlights that ASSR measures analysed using regionally and frequency specific approaches potentially allow the detection of differential, functionally distinct alterations. For example, general impairments in functioning appear linked to RSMG 40 Hz ASSR deficits, which may be similar to abnormalities seen in bipolar disorder and ASD patients. In contrast, increased 40 Hz power in the right cerebellar areas 4-5 (demonstrated in supplementary analyses) could potentially reflect deficits specific to attenuated psychotic symptoms. Such differential functional roles should be evaluated further and considered in future developments of prediction tools.

8.8 Considerations and Future Work

The project set out primarily to study CHR individuals, with a lower number of FEP patients recruited in order to compare CHR and FEP findings and to replicate existing FEP findings. However, the smaller FEP sample size poses a limitation for data interpretation: The trend level statistical results seen for FEP participants in several analyses (compared to significant results for CHR in many of the same analyses) could reflect either underpowered analyses or a true trend. Further recruitment of FEP participants to the YouR study will help clarify this issue.

Moreover, due to the size of the YouR study and the longitudinal nature of recruitment and data collection, only some participants had attended the 12-month follow-up visit when this thesis was prepared. Data available from the 24- and 36-months follow-up assessments were insufficient for meaningful analysis. However, ongoing collection of data will provide additional data for important evaluations of long-term symptom development in future analyses. These data will also be important to further clarify the predictive value of baseline imaging measures such as the 40 Hz ASSR. Moreover, as resources were focused on exploring the CHR group, follow-up assessments were only performed for this group. This means that CHR longitudinal changes cannot be compared to potential changes in FEP over time. However, for the current research questions

longitudinal changes in CHR in relation to baseline measures were the key focus for analyses.

A majority of subjects were still within the first year of their participation in the study at the time of analysis, and future follow-up assessments will establish how many will convert to psychosis within three years. At the time of analysis, transition rates in the current sample were modest compared to numbers reported in early CHR studies (Lim et al., 2018; Mason et al., 2004; Yung et al., 2007). However, the number of transitions seen here are similar to recent findings, reflecting an overall decline in transition rates in recent years (Hartmann et al., 2016; Lim et al., 2018; Yung et al., 2007). This decline could be due to factors such as earlier referrals to services and the presence of comorbidities (Lim et al., 2018).

Impairments in selective attention are a characteristic of psychosis (Gold et al., 2018), and one of the earliest emerging deficits evident in the CHR state (De Paula et al., 2015). This justified the inclusion of an attention task during the recording of 40 Hz ASSR data, as there is evidence for an effect of attention on ASSR measures (Hamm et al., 2015). Selective attention enhances ASSR measures in both controls and patients (Hamm et al., 2015). Hence, differential attention between study groups could confound results.

Analyses demonstrated equal response speed across groups, suggesting that all individuals were paying attention to sounds presented. However, a few individuals in the FEP and CHR groups had increased error-rates (missed responses or responded to non-targets), making these groups perform significantly worse overall. Impaired target detection has previously been observed in ScZ samples, and could relate to an overall sensitivity to incoming stimuli, possibly linked to deficits in the inhibition of salience processing networks (Jimenez et al., 2016). Thus, the observed performance deficit could be associated with the same hyperarousal mechanisms hypothesized to give rise to increased ASSR measures in the sustained CHR group.

A continuous discussion in psychosis research is the degree to which findings in chronic samples may be confounded by long-term use of antipsychotic

medication (Goff et al., 2017). Here, a wide range of medications were prescribed for psychotic and co-morbid symptoms in both the CHR and FEP group. Most previous ASSR studies have not focused on addressing this issue, but the reported presence of ASSR deficits in CHR (Koshiyama et al., 2018b; Tada et al., 2016), FEP (Koshiyama et al., 2018b; Spencer et al., 2008) and early onset ScZ (Wilson et al., 2008) indicate that long-term medication is unlikely to be a major contributor to the observed deficits. However, Hong et al. (2004) reported differential ASSR effects in patients on first and second generation antipsychotics and Rass et al. (2010) found that bipolar disorder patients medicated with any of a range of psychotropic medications had lower 40 Hz ASSR phase locking than unmedicated patients. Furthermore, in-vivo work has revealed ASSR alterations following pharmacological manipulations (Sivarao, 2015; Vohs et al., 2012). Thus, medication was considered, but no statistical correction was performed, due to the variety of drugs and limited availability of information about exact dosages.

Some MEG and 1H-MRS data were lost due to poor data quality. This was a problem particularly for the 1H-MRS measures. However, all analyses focusing on the primary group of interest (CHR) relative to controls had adequate statistical power for meaningful comparisons (>0.40 power).

Finally, future work should further explore the beta frequency signal reported here to clarify whether it reflects a motor-inhibition evoked beta response. In addition, further investigations should aim to clarify the elevated cerebellar ASSRs in sustained CHR participants (Appendix 3), by exploring whether connectivity alterations are present between the cerebellum and/or thalamus and auditory cortex.

8.9 Final Conclusion

The search for early neural mechanisms involved in the emergence of CHR symptoms is essential to progress the understanding of early psychosis. The data presented in this thesis reveal the subtlety and complexity of such changes and highlight that multimodal approaches may help construct a framework for neural mechanisms contributing to emerging psychotic illness.

The findings indicate specifically that poor functional outcome in CHR, potentially representing a general vulnerability state, may be reflected by impaired RSMG 40 Hz power and ITPC, and reduced connectivity between RSMG and primary auditory areas. Furthermore, the analyses provide evidence of a robust beta frequency power deficit in CHR and FEP, strongly related to CHR functioning both at baseline and follow-up assessments. Thus, the current work demonstrates that ASSR measures provide a potential method for capturing alterations in the oscillatory domain, in both the beta and gamma range. Each should be studied further in future work and may provide candidate measures for machine learning projects attempting to assess individual risk levels.

Appendix

Appendix 1

YouR-Study Assessment Checklist

At-Risk Group

Participant ID: _____

Visit 1: Date: _____
_____ At-risk Consent
_____ At-Risk Information sheet
_____ Demographics (including substance use, family history and risk asset.)
_____ Positive scale, CAARMS
_____ COGDIS/COPER, SPI-A

Visit 2: Date: _____
_____ Debrief

Visit 3: Date: _____
_____ COGDIS/COPER, SPI-A (Opt)
_____ Positive scale, CAARMS (Opt)
_____ M.I.N.I
_____ Scale for Premorbid Adjustment
_____ Social role scale
_____ Functional role scale

Visit 4: Date: _____
_____ Brief Assessment of Cognition in Schizophrenia Battery (BACS)
_____ Neuropsychological Testing Battery
_____ Edinburgh Handedness Inventory
_____ National Adult Reading Test
_____ Visual Acuity test
_____ Beliefs About Paranoia Scale (BAPS)
_____ Brief Core Schema Scale (BCSS)
_____ Psychosis Attachment Measure (PAM-SR)
_____ Adverse Childhood Experience Scale (ACES)
_____ The Rust Inventory of Schizotypal Cognitions (RISC)

Visit 5: Date: _____
_____ MEG
_____ MRI
_____ Blood sample (opt)
_____ Urine sample (opt)
_____ Inventory of Interpersonal Problems
_____ Significant Others Scale
_____ International Positive and Negative Affect Schedule (I-PANAS-SF)
_____ Social Interaction Anxiety Scale
_____ Assessment of Musicality
_____ Assessment of Video Gaming
_____ The Autism Symptom SElf-ReporT for adolescents and adults (ASSERT)
_____ Early Symptomatic Syndromes Eliciting Neurodevelopmental Clinical Examinations (ESSENCE)
_____ Adult ADHD Self-Report Scale (ASRS)

Month 3: Date: _____
_____ Positive scale, CAARMS
_____ Inventory of Interpersonal Problems
_____ Significant Others Scale
_____ I-PANAS-SF

Month 6: Date: _____
_____ Positive scale, CAARMS
_____ SCID I & II
_____ IIP
_____ SOS
_____ I-PANAS-SF
_____ Social role scale
_____ Functional role scale

Month 9: Date: _____
_____ Positive scale, CAARMS
_____ IIP
_____ SOS
_____ I-PANAS-SF

Month 12: Date: _____
_____ Positive Scale, CAARMS
_____ SCID I & II
_____ IIP
_____ SOS
_____ I-PANAS-SF
_____ Social role scale
_____ Functional role scale

Month 15: Date: _____
_____ Positive scale, CAARMS
_____ IIP
_____ SOS
_____ I-PANAS-SF

Month 18: Date: _____
_____ Positive scale, CAARMS
_____ IIP
_____ SOS
_____ I-PANAS-SF

Month 21: Date: _____
_____ Positive scale, CAARMS
_____ IIP
_____ SOS
_____ I-PANAS-SF

Month 24: Date: _____
_____ Positive Scale, CAARMS
_____ SCID I & II
_____ IIP
_____ SOS
_____ I-PANAS-SF
_____ Social role scale
_____ Functional role scale

YouR-Study Assessment Checklist

FEP Group

Participant ID: _____

Visit 1: Date: _____
_____ At-risk Information sheet
_____ At-risk Consent
_____ Demographics info (including substance use, family history and risk assessment)
_____ Positive scale, CAARMS
_____ COGDIS/COPER, SPI-A

Visit 2: Date: _____
_____ Debrief
_____ Potential referral to services

Visit 3: Date: _____
_____ SCID I & II
_____ PANSS
_____ Visual Acuity
_____ Potential referral to services

Visit 4: Date: _____
_____ MEG
_____ MRI
_____ Blood sample (opt)
_____ Urine sample (opt)
_____ Assessment of musicality
_____ Assessment of video gaming

Month 3: Date: _____
_____ Brief Assessment of Cognition in Sz battery
_____ Neuropsychological battery
_____ PANSS
_____ Edinburgh Handedness Inventory
_____ National Adult Reading test

YouR-Study Assessment Checklist

Control Group

Participant ID: _____

Visit 1: Date: _____
_____ Control consent form
_____ Control information sheet
_____ Positive scale, CAARMS
_____ COGDIS/COPER, SPI-A
_____ M.I.N.I
_____ Premorbid Adjustment Scale
_____ Social role scale
_____ Functional role scale

Visit 2: Date: _____
_____ Brief Assessment of Cognition in Sz battery
_____ Neuropsychological testing battery
_____ Edinburgh Handedness Inventory
_____ National Adult Reading Test
_____ Beliefs about Paranoia Scale
_____ Brief Core Schema Scale (BCSS)
_____ Psychosis Attachment Measure
_____ Adverse Childhood Experience Scale (ACES)
_____ Rust Inventory of Schizotypal Cognitions (RISC)
_____ Inventory of Interpersonal Problems – 32 items (IIP)
_____ Significant Others Scale (SOS)
_____ The International Positive and Negative Affect Schedule – short form (I-PANAS-SF)
_____ Social Interaction Anxiety Scale

Visit 3: Date: _____
_____ MEG
_____ MRI
_____ Blood sample
_____ Urine sample
_____ Assessment of musicality
_____ Assessment of video gaming

Follow-up: Date:_____
_____ Psychophysical assessment
_____ MEG

Appendix 2

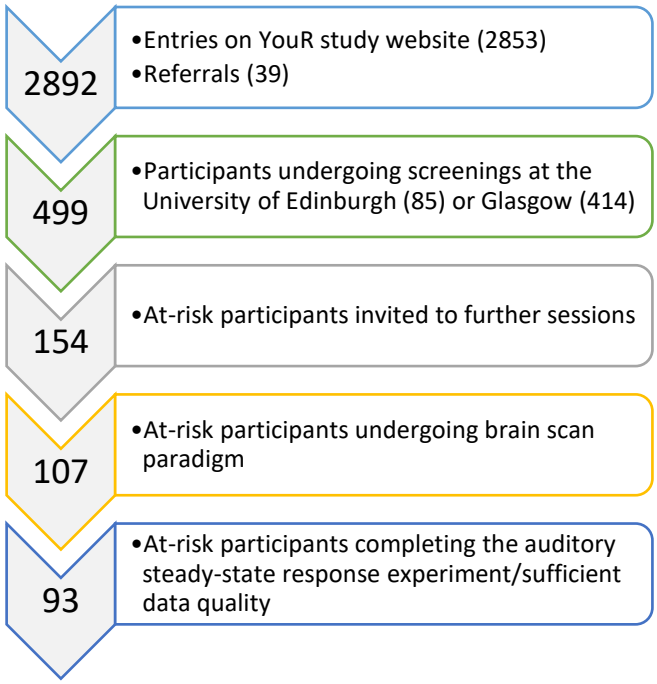

Flow of YouR study at-risk participant recruitment from September 2014 to July 2018, for the auditory Steady State response task, recorded as part of the neuroimaging battery.

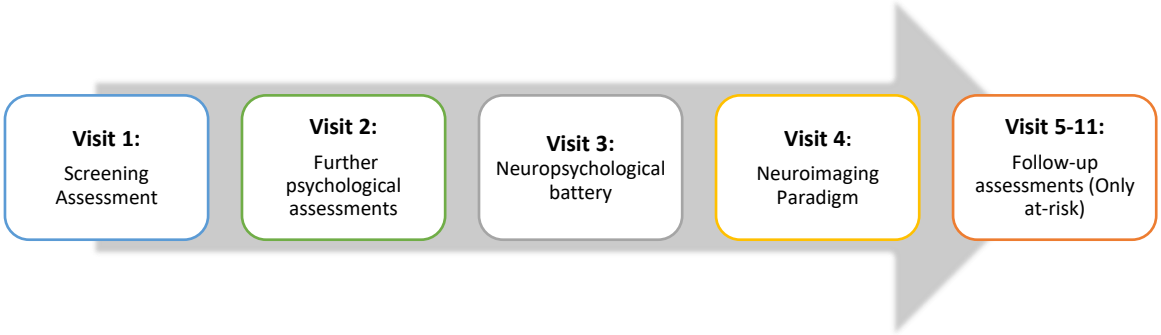

YouR-study assessment timeline from the first face-to-face screening visit to at-risk participant follow-up assessments

Appendix 3

Supplementary longitudinal analyses.

At the 12-month follow-up, individuals with sustained CHR symptoms had significantly higher 40 Hz ASSR spectral power in the right cerebellar areas 4-5 (RCRBL45) than both controls and participants with resolved CHR symptoms (Table A). A significant group effect was also seen in ITPC data in the RCRBL45, but this effect was not significant in any of the post-hoc comparisons (Table B).

Table A 40 Hz power in sustained and resolved CHR to controls

Brain region	Group Analysis		Sustained CHR vs Control			Resolved CHR vs Control			Sustained vs Resolved CHR		
	F	p	t	p	d	t	p	d	t	p	d
RSMG	0.55	0.55	-0.42	0.34	-0.11	-1.06	0.15	-0.25	0.32	0.35	0.14
RHES	0.16	0.85	0.11	0.44	0.04	0.55	0.28	0.20	-0.28	0.37	-0.16
RSTG	0.06	0.95	0.12	0.38	0.04	-0.25	0.42	-0.01	0.42	0.35	0.08
RMTG	0.98	0.37	-0.04	0.46	-0.00	-1.28	0.10	-0.23	1.10	0.17	0.28
RITG	0.04	0.97	0.27	0.37	0.09	-0.03	0.49	0.08	0.30	0.41	0.01
RHIP	0.47	0.62	0.28	0.40	0.09	0.99	0.15	0.26	-0.40	0.33	-0.16
LTHA	0.04	0.96	0.25	0.39	0.08	0.24	0.41	0.11	0.07	0.48	-0.03
RTHA	0.27	0.76	0.68	0.24	0.22	0.28	0.39	0.07	0.55	0.29	0.174
RCRBL45	3.06	0.05*	2.25	0.02*	0.70	0.69	0.24	0.22	2.21	0.01*	0.63

P<0.05 = * (uncorr)

Table B ITPC in sustained and resolved CHR compared to controls

Brain region	Group Analysis		Sustained CHR vs Control			Resolved CHR vs Control			Sustained vs Resolved CHR		
	F	p	t	p	d	t	p	d	t	p	d
LSMG	0.26	1.36	0.32	0.37	0.10	-1.55	0.06	-0.35	1.41	0.08	-0.45
RSMG	0.29	1.26	-0.90	0.19	-0.27	-1.52	0.06	-0.34	0.17	0.43	-0.05
LHES	0.23	1.58	1.01	0.15	0.31	-0.98	0.16	-0.22	1.93	0.03	-0.61
RHES	0.17	1.81	-1.89	0.03	-0.58	-0.71	0.24	-0.16	-1.38	0.07	0.44
LSTG	0.46	0.81	0.85	0.18	0.26	-0.54	0.29	-0.12	1.33	0.10	-0.42
RSTG	0.71	0.36	-0.76	0.23	-0.23	-0.43	0.35	-0.10	-0.57	0.28	0.18
LMTG	0.74	0.34	0.73	0.23	0.22	0.10	0.46	0.02	0.86	0.20	-0.27
RMTG	0.62	0.48	-0.45	0.35	-0.14	-0.95	0.17	-0.21	0.23	0.41	-0.07
LITG	0.21	1.57	1.63	0.06	0.50	0.55	0.29	0.12	1.56	0.07	-0.49

RITG	0.67	0.41	-0.31	0.41	-0.10	-0.90	0.18	-0.20	0.36	0.35	-0.11
LHIP	0.45	0.78	0.09	0.44	0.03	-1.12	0.13	-0.25	0.93	0.19	-0.29
RHIP	0.63	0.47	-0.16	0.47	-0.05	-0.98	0.16	-0.22	0.57	0.28	-0.18
LTHA	0.67	0.42	0.05	0.46	0.01	-0.85	0.19	-0.19	0.75	0.23	-0.24
RTHA	0.69	0.36	-0.03	0.49	-0.01	-0.84	0.19	-0.19	0.57	0.26	-0.18
RCRBL45	0.95	0.05*	0.28	0.37	0.09	0.19	0.43	0.04	0.18	0.42	-0.06
RCRBL10	0.85	0.15	0.00	0.47	0.00	-0.51	0.29	-0.11	0.44	0.32	-0.14

P<0.05 = * (uncorr)

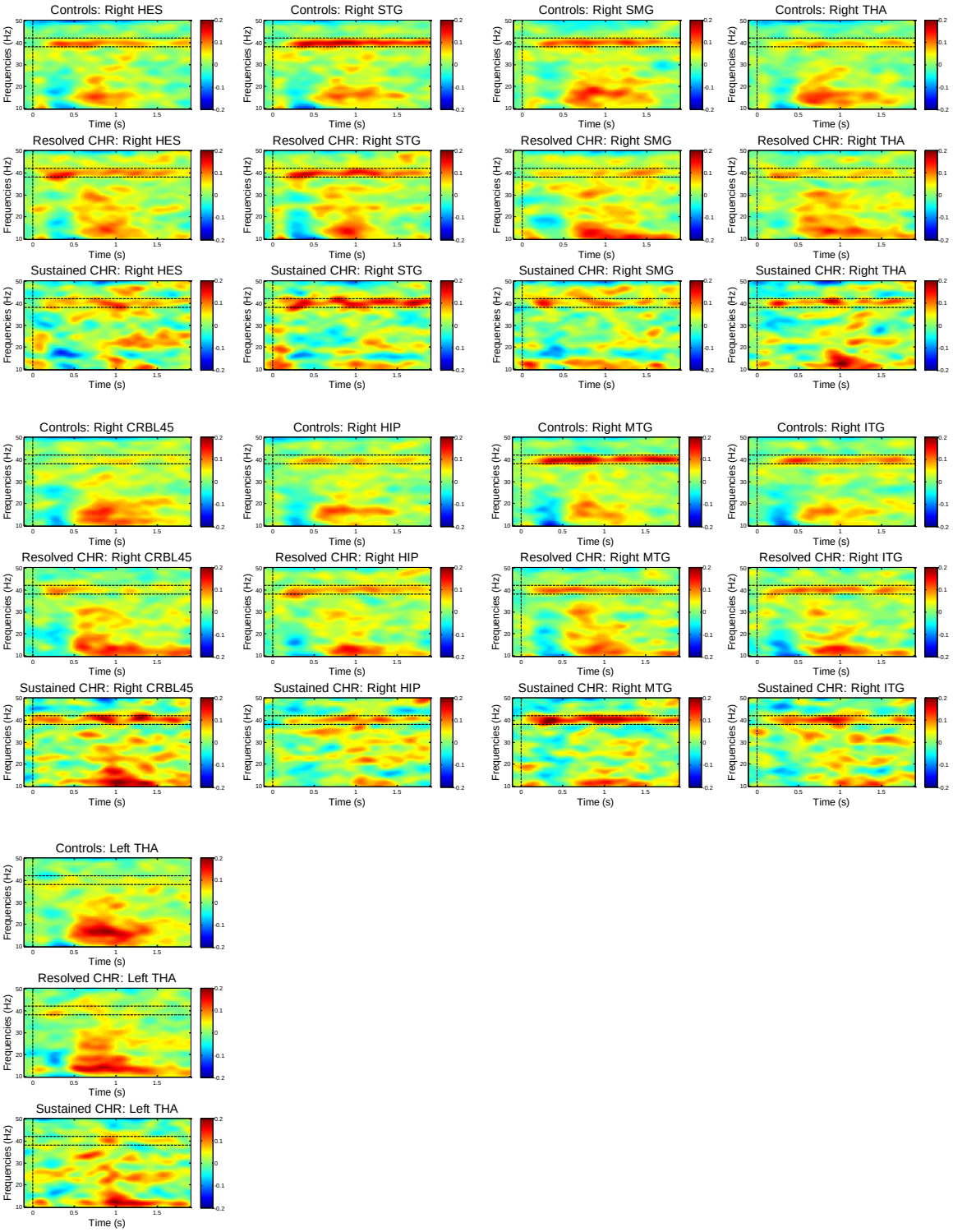

Figure A ASSR time-frequency plots for power ROIs - Grouped according to CHR status at 12 months follow-up

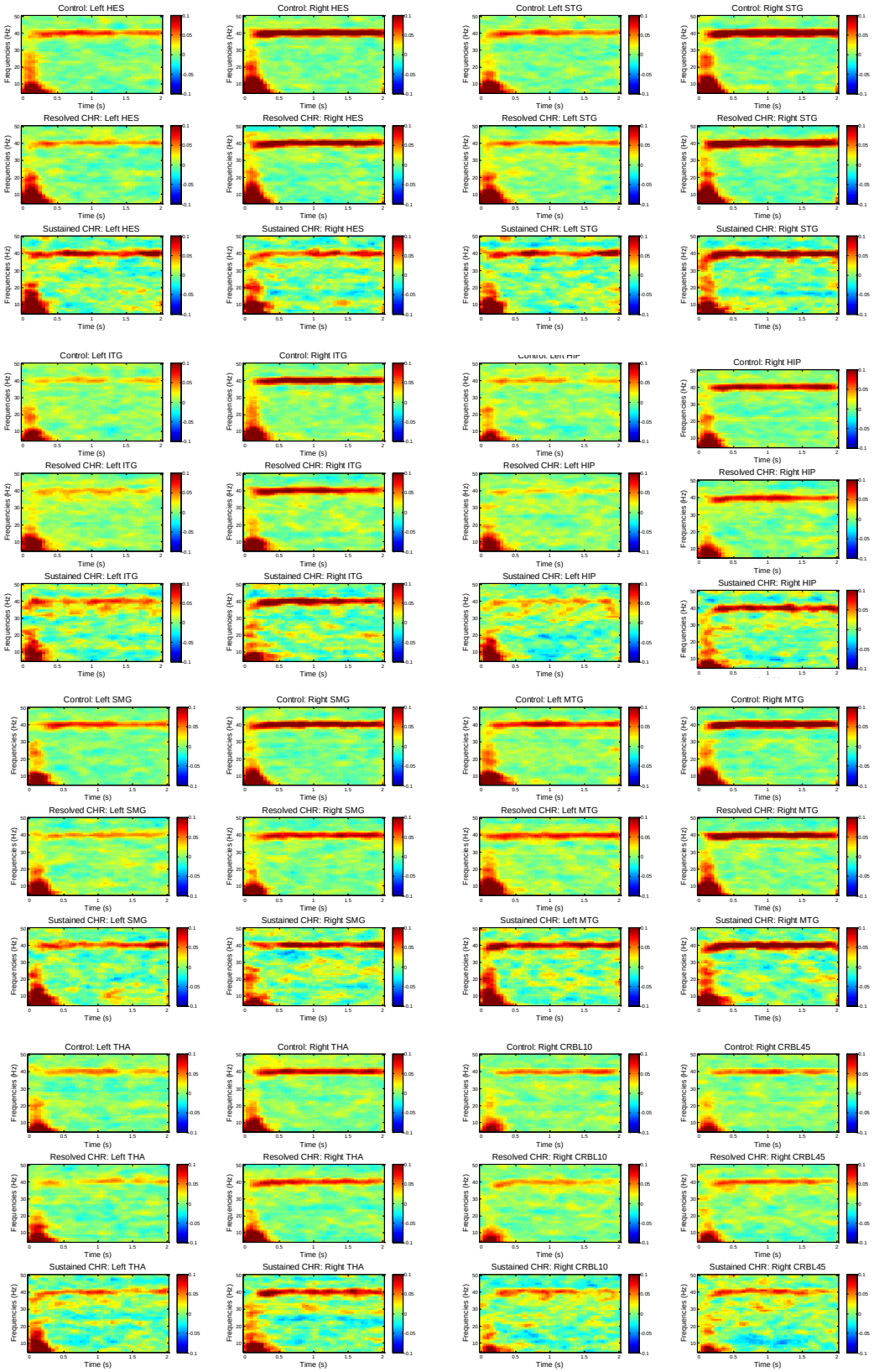

Figure B ITPC plots grouped according to CHR status at 12 months follow-up

Table C Spectral power comparison in controls and GAF groups

Brain region	Group Analysis		Low GAF vs HC			High GAF vs HC			Low vs High GAF		
	F	p	t	p	d	t	p	d	t	p	d
Baseline											
RSMG	2.92	0.05*	-2.39	0.01*	0.46	-0.88	0.20	0.20	1.11	0.13	-0.27
RHES	1.01	0.40	-0.23	0.41	0.04	1.07	0.15	-0.27	1.35	0.10	-0.32
RSTG	0.15	0.88	-0.06	0.47	0.01	0.39	0.35	-0.10	0.61	0.28	-0.14
RMTG	0.59	0.57	-1.09	0.14	0.21	-0.47	0.32	0.11	0.40	0.36	-0.09
RITG	0.02	0.97	0.04	0.48	-0.01	0.21	0.43	-0.06	0.19	0.45	-0.04
RHIP	0.10	0.92	0.08	0.47	-0.03	0.44	0.33	-0.11	0.36	0.37	-0.08
LTHA	1.96	0.15	0.56	0.29	-0.13	-1.44	0.08	0.33	-1.96	0.02*	0.45
RTHA	0.63	0.55	-0.98	0.17	0.18	0.08	0.44	-0.04	0.92	0.18	-0.22
RCRBL45	1.65	0.20	-0.05	0.50	-0.01	1.44	0.08	-0.38	1.84	0.03*	-0.44
12-month Follow-up											
RSMG	2.26	0.12	-0.31	0.38	0.09	-2.18	0.02*	0.55	1.65	0.05*	-0.47
RHES	0.37	0.67	-0.26	0.40	0.11	0.65	0.25	-0.18	-0.83	0.23	0.25
RSTG	0.01	0.99	-0.12	0.50	0.03	-0.12	0.50	0.02	0.00	0.49	0.01
RMTG	0.45	0.68	-0.79	0.23	0.19	-0.67	0.28	0.16	-0.17	0.47	0.05
RITG	0.16	0.86	0.47	0.31	-0.12	-0.11	0.47	0.02	0.54	0.30	-0.15
RHIP	1.56	0.21	1.48	0.07	-0.37	-0.32	0.39	0.07	1.55	0.06	-0.42
LTHA	0.03	0.97	0.02	0.47	-0.02	0.23	0.39	-0.08	-0.18	0.43	0.06
RTHA	0.03	0.97	0.21	0.44	-0.06	0.03	0.48	-0.03	0.17	0.43	-0.03
RCRBL45	0.59	0.55	0.53	0.29	-0.14	1.07	0.15	-0.30	-0.51	0.30	0.16

P<0.05 = * (uncorr)

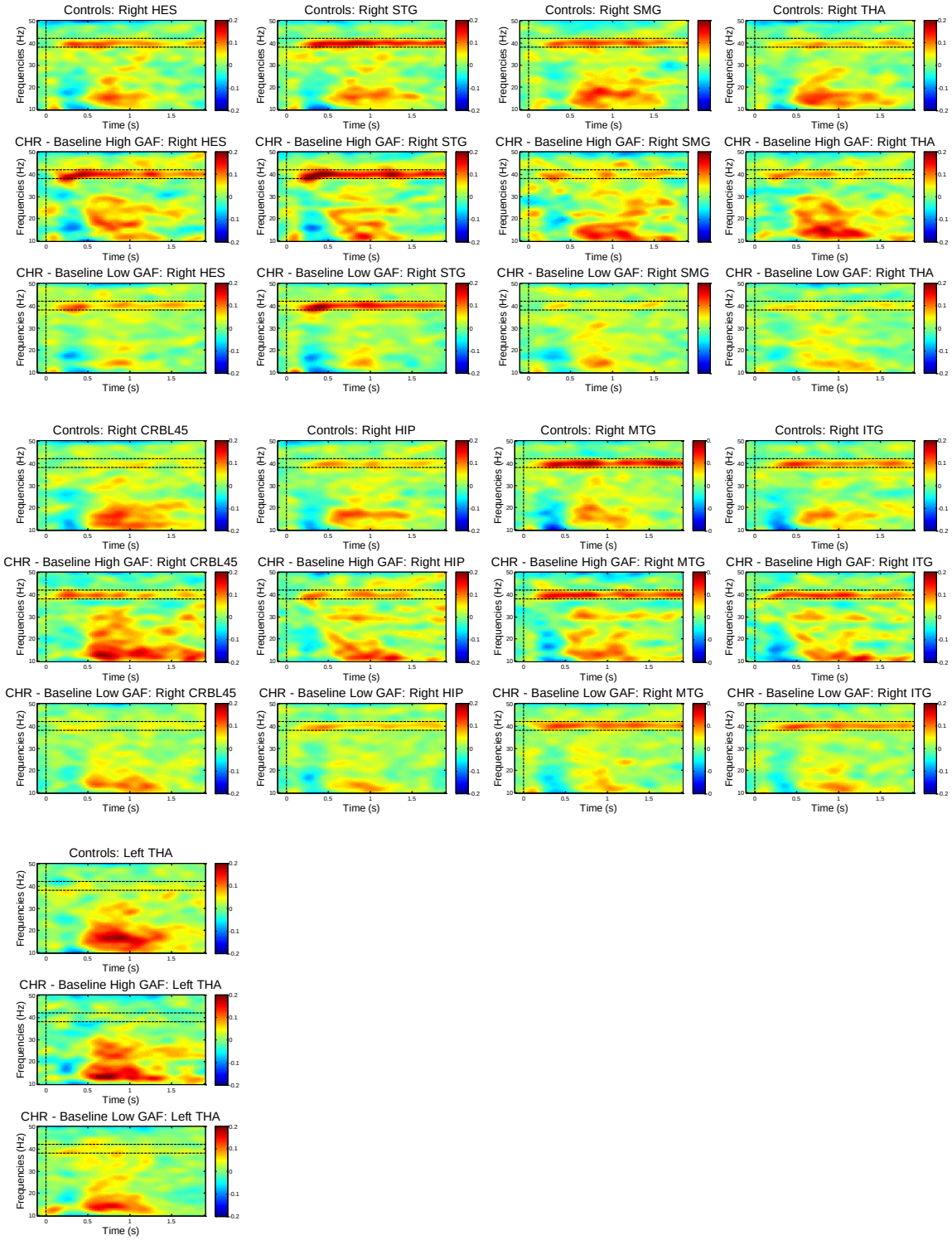

Figure C ASSR time-frequency plots for power ROIs - Grouped according to GAF scores at baseline.

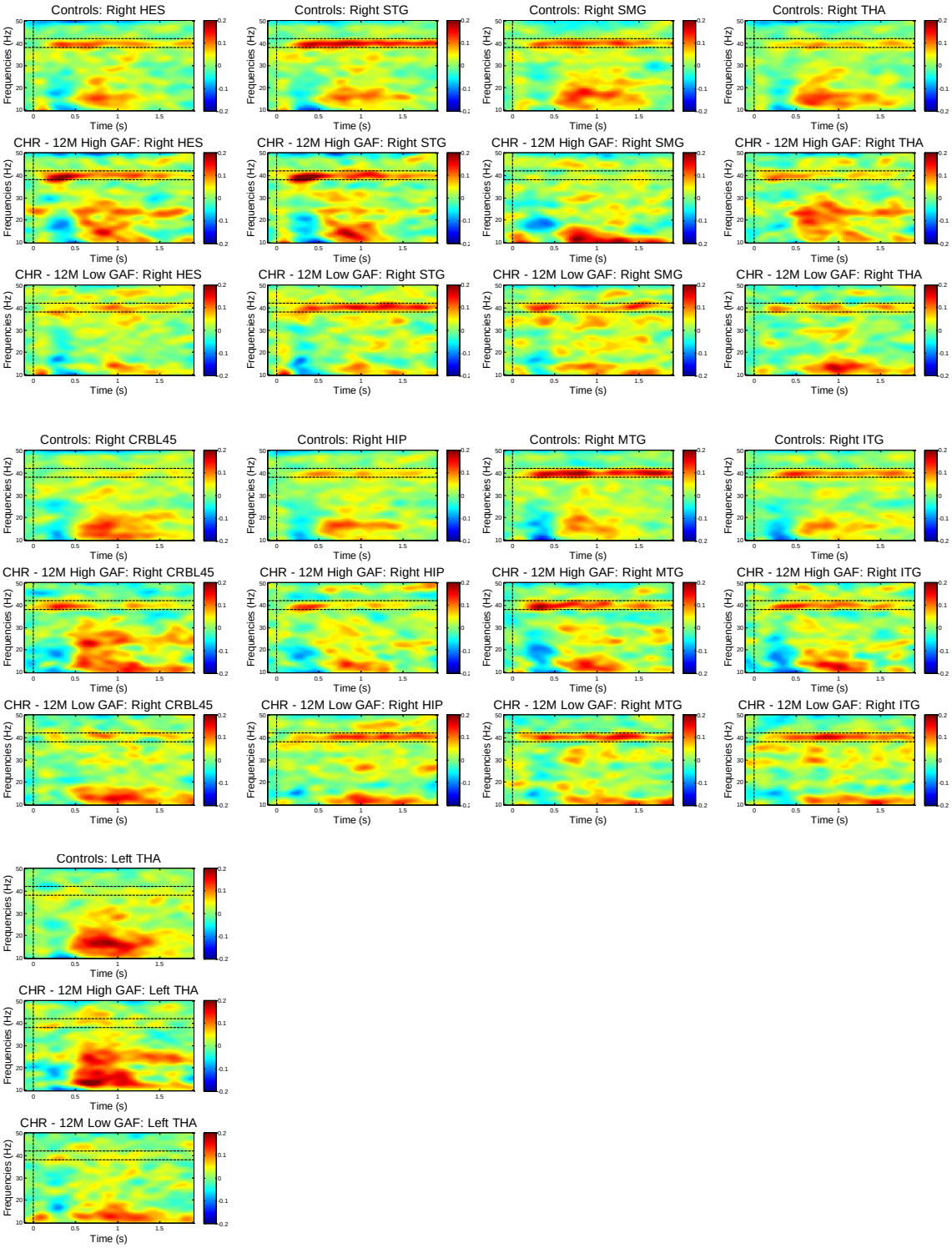

Figure D ASSR time-frequency plots for power ROIs - Grouped according to GAF scores at 12 months follow-up

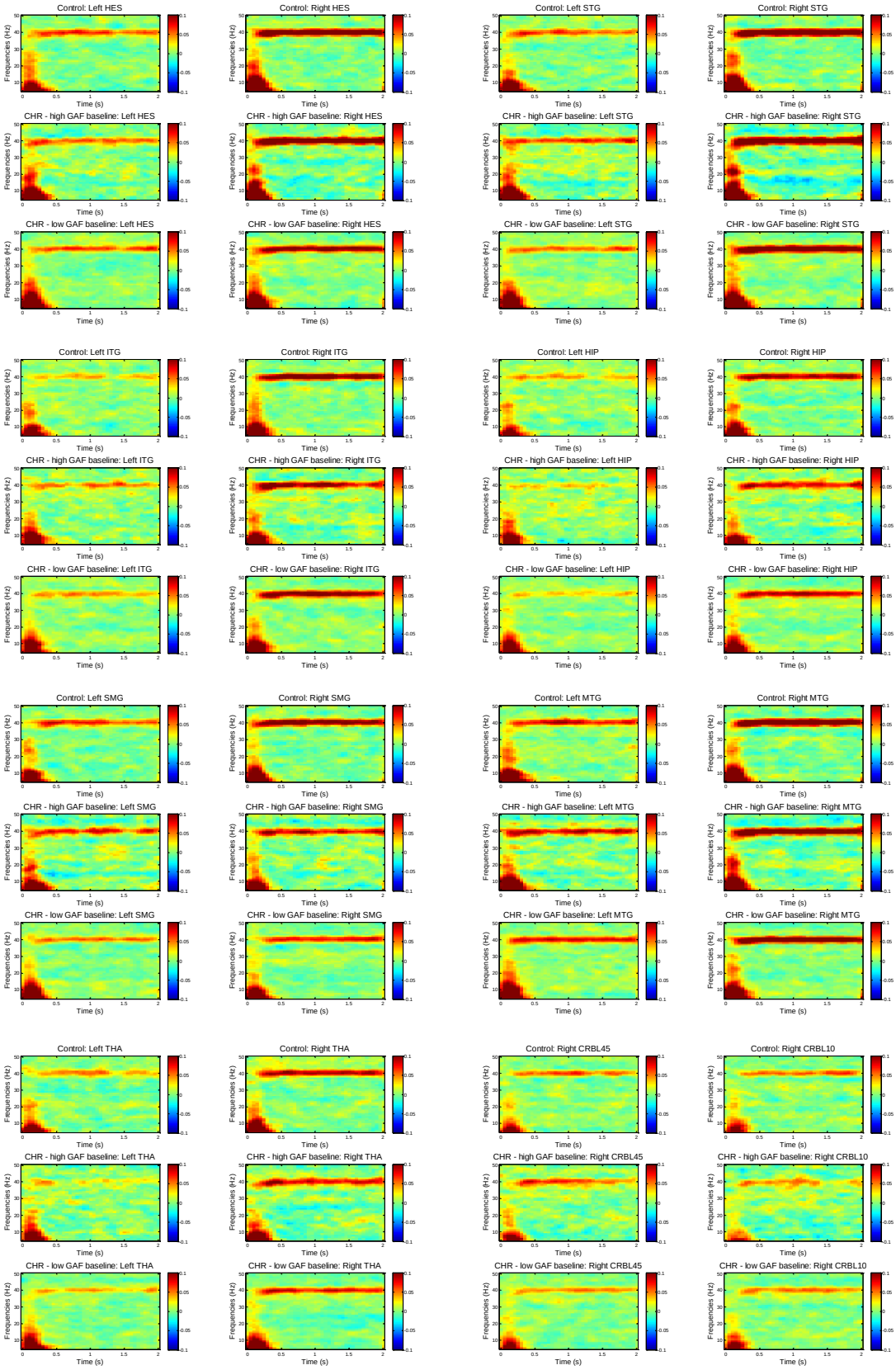

Figure E Plotted ITPC data grouped according to GAF scores at baseline

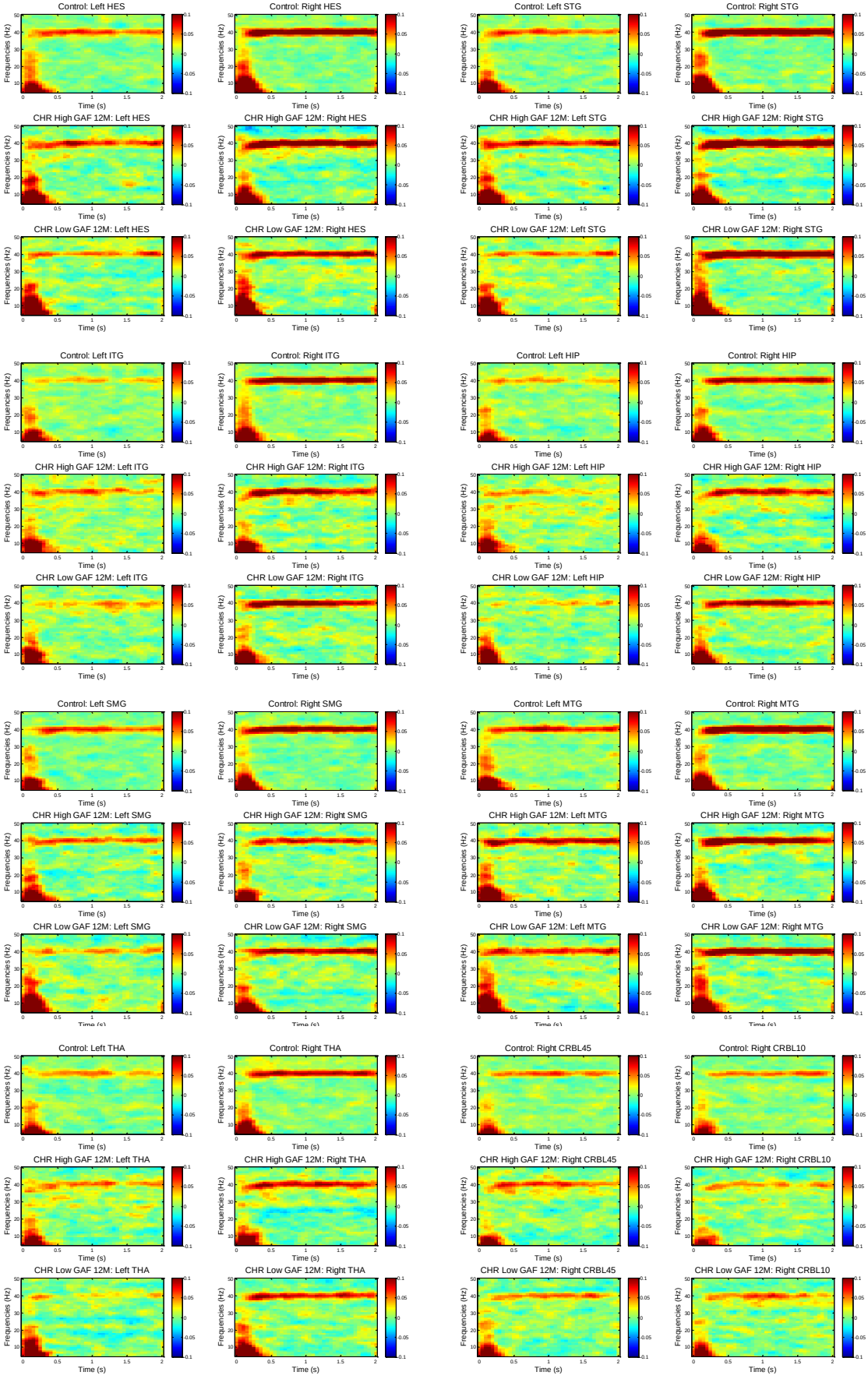

Figure F Plotted ITPC data grouped according to GAF scores at 12 months follow-up

Post-hoc tests from preliminary analyses comparing transitioned participants with non-converters and controls showed that both RSMG spectral power and ITPC in non-transitioned but not in transitioned CHR participants differed significantly from controls. Moreover, spectral power in transitioned CHR participants differed from those who did not transition in the right inferior temporal gyrus (RIFG) and right hippocampus (RHIP) (Table E).

Table E 40 Hz Power in Transitioned CHR vs non-transitioned CHR and Healthy Controls

Brain region	Group Analysis		Transitioned vs HC			Non-transitioned vs HC			Transitioned vs Non-transitioned		
	F	p	t	p	d	t	p	d	t	p	d
RSMG	2.48	0.09	-0.54	0.33	0.28	-2.22	0.02*	0.40	0.19	0.37	-0.10
RHES	0.26	0.78	0.71	0.23	-0.40	0.34	0.40	-0.07	0.58	0.24	-0.31
RSTG	0.62	0.50	0.85	0.11	-0.45	-0.09	0.43	0.01	1.30	0.11	-0.66
RMTG	0.78	0.43	0.07	0.31	-0.05	-1.19	0.11	0.21	0.57	0.23	-0.30
RITG	1.78	0.18	1.66	0.06	-0.87	-0.28	0.37	0.04	1.92	0.05*	-0.96
RHIP	1.62	0.21	1.72	0.06	-0.89	0.01	0.49	-0.01	1.73	0.05*	-0.86
LTHA	0.04	0.97	0.29	0.35	-0.15	0.09	0.48	-0.04	0.23	0.41	-0.10
RTHA	0.32	0.73	0.26	0.38	-0.16	-0.68	0.24	0.11	0.54	0.28	-0.28
RCRBL45	0.42	0.66	0.72	0.21	-0.38	0.54	0.31	-0.12	0.73	0.26	-0.35

P<0.05 = * (uncorr)

Table F ITPC in Transitioned CHR vs non-transitioned CHR and Healthy Controls

Brain region	Group Analysis		Transitioned vs HC			Non-transitioned vs HC			Transitioned vs Non-transitioned		
	F	p	t	p	d	t	p	d	t	p	d
LSMG	0.46	0.62	0.18	0.38	-0.09	-0.87	0.18	0.16	0.52	0.28	-0.27
RSMG	3.77	0.03*	-0.35	0.43	0.18	-2.75	0.00*	0.50	0.61	0.25	-0.31
LHES	0.43	0.67	0.67	0.24	-0.35	-0.34	0.35	0.06	0.97	0.17	-0.50
RHES	0.56	0.56	0.25	0.37	-0.13	-0.96	0.17	0.17	0.59	0.29	-0.30
LSTG	0.04	0.97	0.12	0.38	-0.06	-0.19	0.40	0.04	0.21	0.37	-0.11
RSTG	1.40	0.23	1.19	0.12	-0.62	-0.65	0.24	0.12	1.72	0.06	-0.88
LMTG	0.58	0.56	0.94	0.17	-0.49	0.17	0.43	-0.03	1.13	0.13	-0.58
RMTG	1.07	0.32	0.61	0.24	-0.32	-1.11	0.13	0.20	1.14	0.14	-0.59
LITG	0.92	0.40	-0.23	0.43	0.12	1.22	0.11	-0.22	-0.77	0.23	0.39
RITG	0.96	0.37	0.62	0.25	-0.33	-1.01	0.15	0.18	1.15	0.13	-0.59

LHIP	0.73	0.47	0.20	0.38	-0.11	-1.11	0.13	0.20	0.62	0.21	-0.32
RHIP	1.54	0.20	1.05	0.14	-0.55	-0.93	0.18	0.17	1.73	0.05	-0.89
LTHA	2.10	0.12	0.83	0.20	-0.44	-1.53	0.07	0.28	1.74	0.06	-0.89
RTHA	0.78	0.46	0.45	0.31	-0.24	-1.00	0.15	0.18	0.94	0.17	-0.48
RCRBL45	0.62	0.53	0.68	0.22	-0.35	-0.58	0.27	0.11	1.13	0.13	-0.58
RCRBL10	0.70	0.51	0.78	0.20	-0.41	-0.53	0.30	0.10	1.22	0.13	-0.62

P<0.05 = * (uncorr)

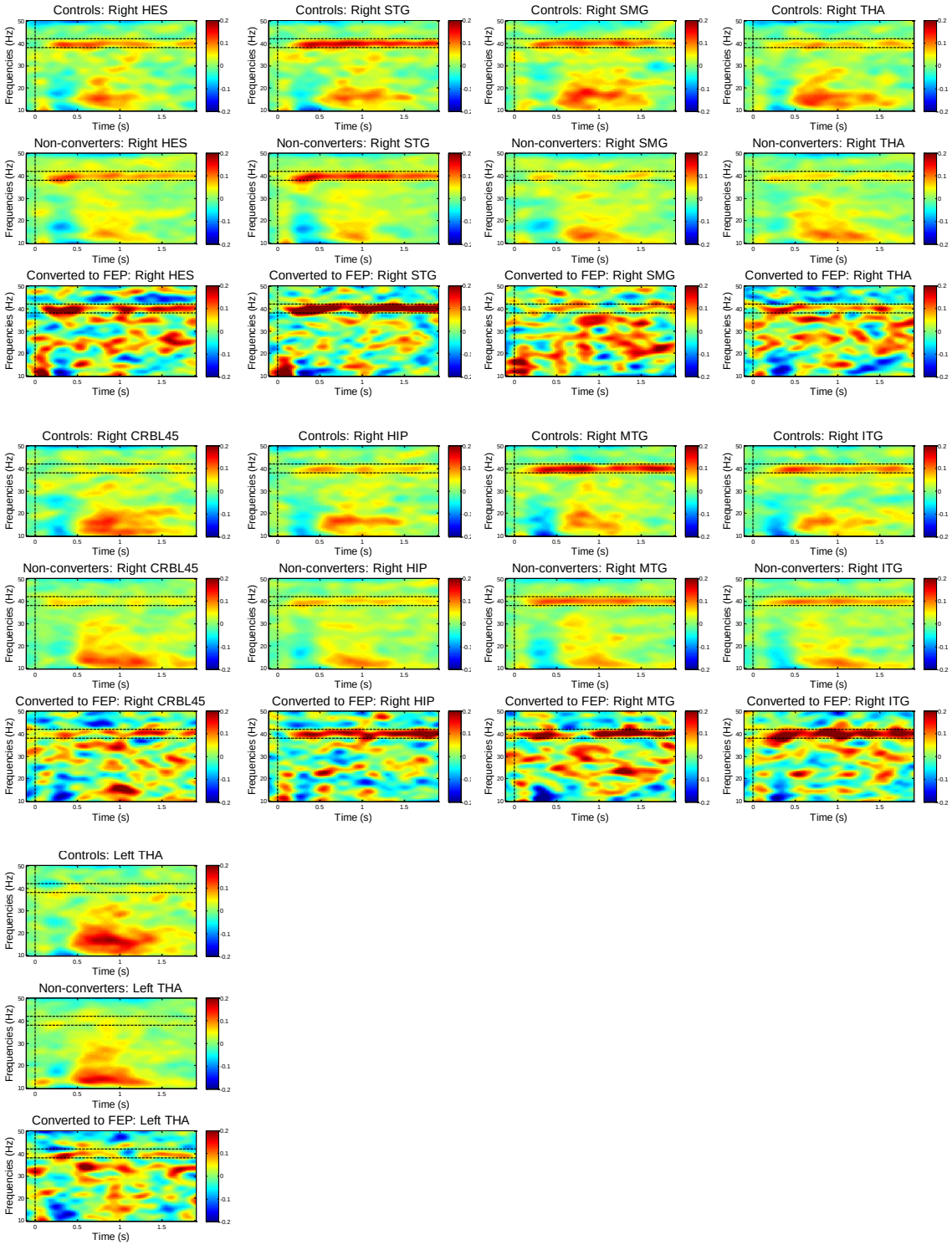

Figure G ASSR time-frequency plots for power ROIs - Grouped according to CHR converters and non-converters

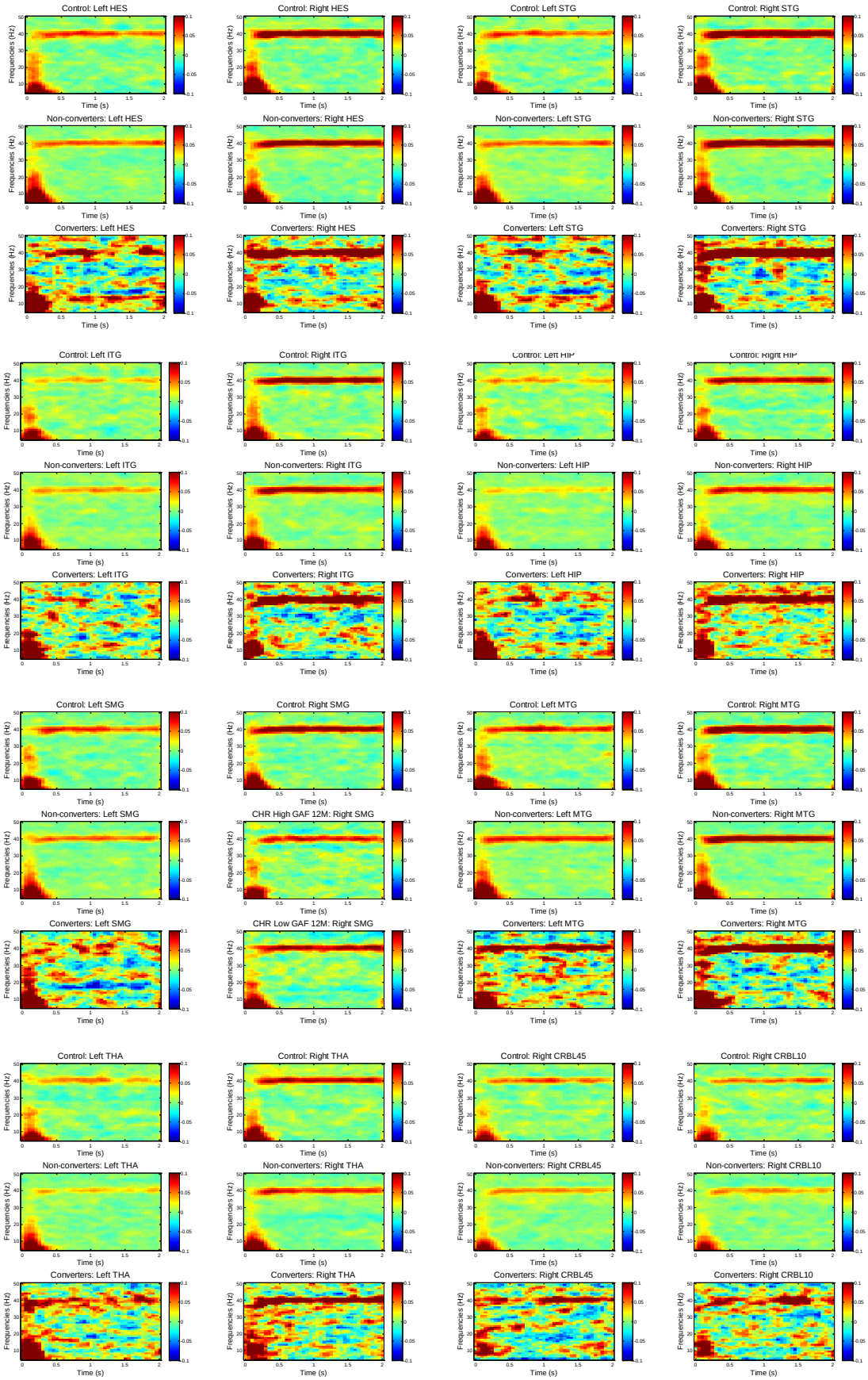

Figure H 40 Hz ITPC data grouped according to psychosis conversion

Bibliography

Addington, J., Cornblatt, B. A., Cadenhead, K. S., Cannon, T. D., McGlashan, T. H., Perkins, D. O., … Heinssen, R. (2011). At clinical high risk for psychosis: Outcome for nonconverters. *American Journal of Psychiatry*, *168*(8), 800–805. https://doi.org/10.1176/appi.ajp.2011.10081191

Adityanjee, A.Aderibigbe, Y., Theodoridis, D., & R.Vieweg, V. (1999). Dementia praecox to schizophrenia:The first 100 years. *Psychiatry and Clinical Neurosciences*, 437–448.

Ahlfors, S. P., Han, J., Belliveau, J. W., & Hämäläinen, M. S. (2010). Sensitivity of MEG and EEG to source orientation. *Brain Topography*, *23*(3), 227–232. https://doi.org/10.1007/s10548-010-0154-x

Andreasen, N. C. (1982). Negative symptoms in schizophrenia. *Arch Gen Psychiatry*, *39*(2), 135. https://doi.org/10.4103/ipj.ipj_30_15

Andreasen, N. C. (1997). The evolving concept of schizophrenia : from Kraepelin to the present and future, *28*, 105–109.

Andreasen, N. C., & Pierson, R. (2008). The Role of the Cerebellum in Schizophrenia. *Biological Psychiatry*, *64*(2), 81–88. https://doi.org/10.1016/j.biopsych.2008.01.003

Andreou, C., Leicht, G., Nolte, G., Polomac, N., Moritz, S., Karow, A., … Mulert, C. (2015). Resting-state theta-band connectivity and verbal memory in schizophrenia and in the high-risk state. *Schizophrenia Research*, *161*(2–3), 299–307. https://doi.org/10.1016/j.schres.2014.12.018

Andreou, C., Nolte, G., Leicht, G., Polomac, N., Hanganu-opatz, I. L., Lambert, M., … Mulert, C. (2015). Increased Resting-State Gamma-Band Connectivity in First-Episode Schizophrenia, *41*(4), 930–939. https://doi.org/10.1093/schbul/sbu121

Angermeyer, M. C., & Kühn, L. (1988). Gender differences in age at onset of schizophrenia. *European Archives of Psychiatry and Neurological Sciences*, *237*, 351–364. https://doi.org/10.1007/BF00380979

Anticevic, A., & Lisman, J. (2017). How Can Global Alteration of Excitation/Inhibition Balance Lead to the Local Dysfunctions That Underlie Schizophrenia? *Biological Psychiatry*, *81*(10), 818–820. https://doi.org/10.1016/j.biopsych.2016.12.006

Attal, Y., & Schwartz, D. (2013). Assessment of Subcortical Source Localization Using Deep Brain Activity Imaging Model with Minimum Norm Operators: A MEG Study. *PLoS ONE*, *8*(3). https://doi.org/10.1371/journal.pone.0059856

Balz, J., Romero, Y. R., Keil, J., Krebber, M., Niedeggen, M., Gallinat, J., & Senkowski, D. (2016). Beta / Gamma Oscillations and Event-Related Potentials Indicate Aberrant Multisensory Processing in Schizophrenia, *7*(December), 1–12. https://doi.org/10.3389/fpsyg.2016.01896

Bambini, V., Arcara, G., Bechi, M., Buonocore, M., Cavallaro, R., & Bosia, M. (2016). The communicative impairment as a core feature of schizophrenia:

Frequency of pragmatic deficit, cognitive substrates, and relation with quality of life. *Comprehensive Psychiatry*, *71*, 106–120. https://doi.org/10.1016/j.comppsych.2016.08.012

Bangert, M., Peschel, T., Schlaug, G., Rotte, M., Drescher, D., Hinrichs, H., … Altenmu, E. (2006). Shared networks for auditory and motor processing in professional pianists : Evidence from fMRI conjunction, *30*, 917–926. https://doi.org/10.1016/j.neuroimage.2005.10.044

Barch, D. M., & Ceaser, A. (2012). Cognition in schizophrenia: core psychological and neural mechanisms. *Trends in Cognitive Sciences*, *16*(1), 27–34. https://doi.org/10.1016/j.tics.2011.11.015

Bardouille, T., & Ross, B. (2008). MEG imaging of sensorimotor areas using inter-trial coherence in vibrotactile steady-state responses. *NeuroImage*, *42*(1), 323–331. https://doi.org/10.1016/j.neuroimage.2008.04.176

Barkley, G. L., & Baumgartner, C. (2003). MEG and EEG in Epilepsy, *20*(3), 163–178.

Barton, K. (2015). Package ‘ MuMIn .’ *CRAN*, (1).

Bartos, M., Vida, I., & Jonas, P. (2007). Synaptic mechanisms of synchronized gamma oscillations in inhibitory interneuron networks. *Nature Reviews Neuroscience*, *8*(1), 45–56. https://doi.org/10.1038/nrn2044

Basar-Eroglu, C., Mathes, B., Khalaidovski, K., Brand, A., & Schmiedt-Fehr, C. (2016). Altered alpha brain oscillations during multistable perception in schizophrenia. *International Journal of Psychophysiology*, *103*, 118–128. https://doi.org/10.1016/j.ijpsycho.2015.02.002

Basar-Eroglu, C., Schmiedt-Fehr, C., Marbach, S., Brand, A., & Mathes, B. (2008). Altered oscillatory alpha and theta networks in schizophrenia, *5*. https://doi.org/10.1016/j.brainres.2008.06.114

Başar, E., & Güntekin, B. (2013). Review of delta, theta, alpha, beta, and gamma response oscillations in neuropsychiatric disorders. *Supplements to Clinical Neurophysiology*. https://doi.org/10.1016/B978-0-7020-5307-8.00019-3

Bastiaansen, M. C. M., & Knösche, T. R. (2000). Tangential derivative mapping of axial MEG applied to event-related desynchronization research. *Clinical Neurophysiology*, *111*(7), 1300–1305. https://doi.org/10.1016/S1388-2457(00)00272-8

Bastos, A. M., & Schoffelen, J.-M. (2016). A Tutorial Review of Functional Connectivity Analysis Methods and Their Interpretational Pitfalls. *Frontiers in Systems Neuroscience*, *9*(January), 1–23. https://doi.org/10.3389/fnsys.2015.00175

Bastos, A. M., Vezoli, J., Bosman, C. A., Schoffelen, J. M., Oostenveld, R., Dowdall, J. R., … Fries, P. (2015). Visual areas exert feedforward and feedback influences through distinct frequency channels. *Neuron*, *85*(2), 390–401. https://doi.org/10.1016/j.neuron.2014.12.018

Bernard, J. A., & Mittal, V. A. (2014a). Cerebellar-motor dysfunction in

schizophrenia and psychosis-risk : the importance of regional cerebellar analysis approaches, *5*(November), 1–14. https://doi.org/10.3389/fpsyt.2014.00160

Bernard, J. A., & Mittal, V. A. (2014b). Dysfunctional Activation of the Cerebellum in Schizophrenia: A Functional Neuroimaging Meta-Analysis. *Clinical Psychological Science*, *3*(4), 545–566. https://doi.org/10.1177/2167702614542463

Bičíková, M., Hampl, R., Hill, M., Řípová, D., Mohr, P., Putz, Z., & Vanuga, P. (2011). Neuro- and immunomodulatory steroids and other biochemical markers in drug-naive schizophrenia patients and the effect of treatment with atypical antipsychotics, *32*(2).

Biomarkers Definitions Working Group, A. (2001). Biomarkers and surrogate endpoints: Preferred definitions and conceptual framework. *Clinical Pharmacology & Therapeutics*, *69*(3), 89–95. https://doi.org/10.1067/mcp.2001.113989

Block, W., Bayer, T. A., Tepest, R., Tra, F., Rietschel, M., Mu, D. J., … Falkai, P. (2000). Decreased frontal lobe ratio of N -acetyl aspartate to choline in familial schizophrenia : a proton magnetic resonance spectroscopy study, *289*, 20–24.

Blüml, S. (2013). Magnetic Resonance Spectroscopy : Basics. In S. Blüml & A. Panigrahy (Eds.), *MR Spectroscopy of Pediatric Brain Disorders* (pp. 11–24). https://doi.org/10.1007/978-1-4419-5864-8

Bobes, J., Garcia-Portilla, M. P., Bascaran, M. T., Saiz, P. A., & Bousoño, M. (2007). Quality of life in schizophrenic patients. *Dialogues in Clinical Neuroscience*, *9*(2), 215–226.

Bodatsch, M., Brockhaus-Dumke, A., Klosterkotter, J., & Ruhrmann, S. (2015). Forecasting psychosis by event-related potentials - Systematic review and specific meta-analysis. *Biological Psychiatry*, *77*(11), 951–958. https://doi.org/10.1016/j.biopsych.2014.09.025

Bodatsch, M., Ruhrmann, S., Wagner, M., Mller, R., Schultze-Lutter, F., Frommann, I., … Brockhaus-Dumke, A. (2011). Prediction of psychosis by mismatch negativity. *Biological Psychiatry*, *69*(10), 959–966. https://doi.org/10.1016/j.biopsych.2010.09.057

Borenstein, M. (2005). CHAPTER 11 Software for Publication Bias. In *PUBLICATION BIAS IN META-ANALYSIS* (pp. 193–220).

Bossong, M. G., Antoniades, M., Azis, M., Samson, C., Quinn, B., Bonoldi, I., … McGuire, P. (2018). Association of Hippocampal Glutamate Levels with Adverse Outcomes in Individuals at Clinical High Risk for Psychosis. *JAMA Psychiatry*. https://doi.org/10.1001/jamapsychiatry.2018.3252

Boutros, N. N., Arfken, C., Galderisi, S., Warrick, J., & Pratt, G. (2009). The Status of Spectral EEG Abnormality as a Diagnostic Test for Schizophrenia, *99*, 225–237.

Bowie, C. R., & Harvey, P. D. (2006). Cognitive deficits and functional outcome in schizophrenia. *Neuropsychiatric Disease and Treatment*, *2*(4), 531–536.

https://doi.org/10.2147/nedt.2006.2.4.531

Bowyer, S. M. (2016). Coherence a measure of the brain networks: past and present. *Neuropsychiatric Electrophysiology*, *2*(1), 1. https://doi.org/10.1186/s40810-015-0015-7

Bowyer, S. M., Gjini, K., Zhu, X., Kim, L., Moran, J. E., Rizvi, S. U., … Boutros, N. N. (2015). Potential Biomarkers of Schizophrenia from MEG Resting-State Functional Connectivity Networks: Preliminary Data. *Journal of Behavioral and Brain Science*, *05*(01), 1–11. https://doi.org/10.4236/jbbs.2015.51001

Brenner, C. a., Sporns, O., Lysaker, P. H., & O'Donnell, B. F. (2003). EEG synchronization to modulated auditory tones in schizophrenia, schizoaffective disorder, and schizotypal personality disorder. *American Journal of Psychiatry*, *160*(12), 2238–2240. https://doi.org/10.1176/appi.ajp.160.12.2238

Brenner, C. a, Krishnan, G. P., Vohs, J. L., Ahn, W.-Y., Hetrick, W. P., Morzorati, S. L., & O'Donnell, B. F. (2009). Steady state responses: electrophysiological assessment of sensory function in schizophrenia. *Schizophrenia Bulletin*, *35*(6), 1065–1077. https://doi.org/10.1093/schbul/sbp091

Brockhaus-Dumke, A., Schultze-lutter, F., Mueller, R., Tendolkar, I., Bechdolf, A., Pukrop, R., … Ruhrmann, S. (2008). Sensory Gating in Schizophrenia : P50 and N100 Gating in Antipsychotic-Free Subjects at Risk , First-Episode , and Chronic Patients. *Biol Psychiatry*, *64*, 376–384. https://doi.org/10.1016/j.biopsych.2008.02.006

Brockhaus-Dumke, A., Tendolkar, I., Pukrop, R., Schultze-Lutter, F., Klosterkötter, J., & Ruhrmann, S. (2005). Impaired mismatch negativity generation in prodromal subjects and patients with schizophrenia. *Schizophrenia Research*, *73*(2–3), 297–310. https://doi.org/10.1016/j.schres.2004.05.016

Brown, M. S., Singel, D., Hepburn, S., & Rojas, D. C. (2013). Increased glutamate concentration in the auditory cortex of persons with autism and first-degree relatives: A 1H-MRS study. *Autism Research*, *6*(1), 1–10. https://doi.org/10.1002/aur.1260

Bubic. (2010). Prediction, cognition and the brain. *Frontiers in Human Neuroscience*, *4*(March), 1–15. https://doi.org/10.3389/fnhum.2010.00025

Burbaeva, G. S., Savushkina, O. K., & Boksha, I. S. (2003). Creatine kinase BB in brain in schizophrenia. *World Journal of Biological Psychiatry*, *4*(4), 177–183. https://doi.org/10.1080/15622970310029916

Cahn, W., Pol, H. E. H., Bongers, M., Schnack, H. G., Mandl, R. C. W., Van Haren, N. E. M., … Kahn, R. S. (2002). Brain morphology in antipsychotic-naïve schizophrenia: A study of multiple brain structures. *British Journal of Psychiatry*, *181*(SUPPL. 43). https://doi.org/10.1192/bjp.181.43.s66

Cannon-Spoor, H. E., Potkin, S. G., & Wyatt, R. J. (1982). Measurement of premorbid adjustment in chronic schizophrenia. *Schizophrenia Bulletin*, *8*(3), 470–484. Retrieved from

http://www.ncbi.nlm.nih.gov/pubmed/7134891

Cannon, T. D., Chung, Y., He, G., Sun, D., Jacobson, A., Van Erp, T. G. M., … Heinssen, R. (2015). Progressive reduction in cortical thickness as psychosis develops: A multisite longitudinal neuroimaging study of youth at elevated clinical risk. *Biological Psychiatry*, *77*(2), 147–157. https://doi.org/10.1016/j.biopsych.2014.05.023

Cannon, T. D., Ph, D., Yu, C., Addington, J., Ph, D., Bearden, C. E., … Cadenhead, K. S. (2016). An Individualized Risk Calculator for Research in Prodromal Psychosis, (October). https://doi.org/10.1176/appi.ajp.2016.15070890

Capizzano, A. A., Toscano, J. L. N., & Ho, B.-C. (2011). Magnetic resonance spectroscopy of limbic structures displays metabolite differences in young unaffected relatives of schizophrenia probands, *131*, 4–10. https://doi.org/10.1016/j.schres.2011.05.024.Magnetic

Cardno, A. G., & Owen, M. J. (2014). Genetic relationships between schizophrenia, bipolar disorder, and schizoaffective disorder. *Schizophrenia Bulletin*, *40*(3), 504–515. https://doi.org/10.1093/schbul/sbu016

Carlén, M., Meletis, K., Siegle, J. H., Cardin, J. A., Futai, K., Vierling-Claassen, D., … Tsai, L. H. (2012). A critical role for NMDA receptors in parvalbumin interneurons for gamma rhythm induction and behavior. *Molecular Psychiatry*, *17*(5), 537–548. https://doi.org/10.1038/mp.2011.31

Carlsson, A., & Lindqvist, M. (1963). Effect of Chlorpromazine or Haloperidol on Formation of 3-Methoxytyramine and Normetanephrine in Mouse Brain. *Acta Pharmacologica et Toxicologica*, *20*(2), 140–144. https://doi.org/10.1111/j.1600-0773.1963.tb01730.x

Carrión, R. E., Ph, D., Cornblatt, B. A., Ph, D., Burton, C. Z., Tso, I. F., … Taylor, S. F. (2017). HHS Public Access, *173*(10), 989–996. https://doi.org/10.1176/appi.ajp.2016.15121565.Personalized

Chan, R. C. K., & Gottesman, I. I. (2008). Neurological soft signs as candidate endophenotypes for schizophrenia: A shooting star or a Northern star? *Neuroscience and Biobehavioral Reviews*, *32*(5), 957–971. https://doi.org/10.1016/j.neubiorev.2008.01.005

Charlson, F. J., Ferrari, A. J., Santomauro, D. F., Diminic, S., Stockings, E., Scott, J. G., … Whiteford, H. A. (2018). Global Epidemiology and Burden of Schizophrenia : Findings From the Global Burden of Disease Study 2016, *44*(6), 1195–1203. https://doi.org/10.1093/schbul/sby058

Chen, G., Zhang, Y., Li, X., Zhao, X., Ye, Q., Lin, Y., … Zhang, X. (2017). Distinct Inhibitory Circuits Orchestrate Cortical beta and gamma Band Oscillations. *Neuron*, *96*(6), 1403–1418.e6. https://doi.org/10.1016/j.neuron.2017.11.033

Chua, S. E., Cheung, C., Cheung, V., Tsang, J. T. K., Chen, E. Y. H., Wong, J. C. H., … McAlonan, G. M. (2007). Cerebral grey, white matter and csf in never-medicated, first-episode schizophrenia. *Schizophrenia Research*, *89*(1–3), 12–21. https://doi.org/10.1016/j.schres.2006.09.009

Chue, P., & Lalonde, J. K. (2014). Addressing the unmet needs of patients with persistent negative symptoms of schizophrenia: Emerging pharmacological treatment options. *Neuropsychiatric Disease and Treatment*, *10*, 777–789. https://doi.org/10.2147/NDT.S43404

Clark, A. (2013). Whatever next? Predictive brains, situated agents, and the future of cognitive science. *Behavioral and Brain Sciences*, *36*(3), 181–204. https://doi.org/10.1017/S0140525X12000477

Colclough, G. L., Woolrich, M. W., Tewarie, P. K., Brookes, M. J., Quinn, A. J., & Smith, S. M. (2016). How reliable are MEG resting-state connectivity metrics? *NeuroImage*, *138*, 284–293. https://doi.org/10.1016/j.neuroimage.2016.05.070

Cousijn, H., Haegens, S., Wallis, G., Near, J., Stokes, M. G., Harrison, P. J., & Nobre, A. C. (2014). Resting GABA and glutamate concentrations do not predict visual gamma frequency or amplitude. *Proceedings of the National Academy of Sciences*, *111*(25), 9301–9306. https://doi.org/10.1073/pnas.1321072111

Creese, I., Burt, D. R., & Snyder, S. H. (1976). Dopamine Receptor Binding Predicts Clinical and Pharmacological Potencies of Antischizophrenic Drugs. *Science*, *192*, 481–484.

Crow, T. J. (1976). Positive and Negative Schizophrenic Symptoms and the Role of Dopamine, (1973).

Da Costa, S., van der Zwaag, W., Marques, J. P., Frackowiak, R. S. J., Clarke, S., & Saenz, M. (2011). Human Primary Auditory Cortex Follows the Shape of Heschl's Gyrus. *Journal of Neuroscience*, *31*(40), 14067–14075. https://doi.org/10.1523/JNEUROSCI.2000-11.2011

Dager, S. R., Oskin, N. M., Richards, T. L., & Posse, S. (2008). Research Applications of Magnetic Resonance Spectroscopy (MRS) to Investigate Psychiatric Disorders. *Top Magn Reson Imaging*, *19*(2), 81–96. https://doi.org/10.1097/RMR.0b013e318181e0be

Dalal, S. S., Osipova, D., Bertrand, O., & Jerbi, K. (2013). Oscillatory activity of the human cerebellum: The intracranial electrocerebellogram revisited. *Neuroscience and Biobehavioral Reviews*, *37*(4), 585–593. https://doi.org/10.1016/j.neubiorev.2013.02.006

Damaraju, E., Allen, E. A., Belger, A., Ford, J. M., McEwen, S., Mathalon, D. H., … Calhoun, V. D. (2014). Dynamic functional connectivity analysis reveals transient states of dysconnectivity in schizophrenia. *NeuroImage: Clinical*, *5*(July), 298–308. https://doi.org/10.1016/j.nicl.2014.07.003

Darvas, F., Pantazis, D., Kucukaltun-Yildirim, E., & Leahy, R. M. (2004). Mapping human brain function with MEG and EEG: Methods and validation. *NeuroImage*, *23*(SUPPL. 1), 289–299. https://doi.org/10.1016/j.neuroimage.2004.07.014

David, O., Kilner, J. M., & Friston, K. J. (2006). Mechanisms of evoked and induced responses in MEG/EEG. *NeuroImage*, *31*(4), 1580–1591. https://doi.org/10.1016/j.neuroimage.2006.02.034

de Paula, A. L. D., Hallak, J. E. C., Maia-de-Oliveira, J. P., Bressan, R. A., & Machado-de-Sousa, J. P. (2015). Cognition in at-risk mental states for psychosis. *Neuroscience and Biobehavioral Reviews*, *57*, 199–208. https://doi.org/10.1016/j.neubiorev.2015.09.006

de Paula, L. A. D., Hallak, J. E. C., Maia-de-oliveira, J. P., Bressan, R. A., & Machado-de-sousa, J. P. (2015). Cognition in at-risk mental states for psychosis. *Neuroscience and Biobehavioral Reviews*, *57*, 199–208.

de Wilde, O. M., Bour, L. J., Dingemans, P. M., Koelman, J. H. T. M., & Linszen, D. H. (2007). A meta-analysis of P50 studies in patients with schizophrenia and relatives: Differences in methodology between research groups. *Schizophrenia Research*, *97*(1–3), 137–151. https://doi.org/10.1016/j.schres.2007.04.028

Di Lorenzo, G., Daverio, A., Ferrentino, F., Santarnecchi, E., Ciabattini, F., & Lisi, G. (2015). Altered resting-state EEG source functional connectivity in schizophrenia : the effect of illness duration, *9*(May), 1–11. https://doi.org/10.3389/fnhum.2015.00234

Do, K. Q., Cuenod, M., & Hensch, T. K. (2015). Targeting Oxidative Stress and Aberrant Critical Period Plasticity in the Developmental Trajectory to Schizophrenia, *41*(4), 835–846. https://doi.org/10.1093/schbul/sbv065

Draganova, R., Ross, B., Wollbrink, A., & Pantev, C. (2008). Cortical steady-state responses to central and peripheral auditory beats. *Cerebral Cortex*, *18*(5), 1193–1200. https://doi.org/10.1093/cercor/bhm153

Duval, S., & Tweedie, R. (2000). Trim and Fill: A Simple Funnel-Plot-Based Method of Testing and Adjusting for Publication Bias in Meta-Analysis. *Biometrics*, *56*(2), 455–463.

Edden, R. a E., Puts, N. a J., Harris, A. D., Barker, P. B., & Evans, C. J. (2013). Gannet: A batch-processing tool for the quantitative analysis of gamma-aminobutyric acid-edited MR spectroscopy spectra. *Journal of Magnetic Resonance Imaging*, *1452*, 1445–1452. https://doi.org/10.1002/jmri.24478

Edgar, J. C., Chen, Y. H., Lanza, M., Howell, B., Chow, V. Y., Heiken, K., … Cañive, J. M. (2014). Cortical thickness as a contributor to abnormal oscillations in schizophrenia? *NeuroImage: Clinical*, *4*, 122–129. https://doi.org/10.1016/j.nicl.2013.11.004

Egerton, A., Modinos, G., Ferrera, D., & McGuire, P. (2017). Neuroimaging studies of GABA in schizophrenia : a systematic review with meta-analysis, *7*(6), e1147-10. https://doi.org/10.1038/tp.2017.124

Egger, M., Smith, G. D., Schneider, M., & Minder, C. (1997). Bias in meta-analysis detected by a simple, graphical test. *BMJ*, *315*(7109), 629 LP-634. https://doi.org/10.1136/bmj.315.7109.629

Engel, A. K., & Fries, P. (2010). Beta-band oscillations-signalling the status quo? *Current Opinion in Neurobiology*, *20*(2), 156–165. https://doi.org/10.1016/j.conb.2010.02.015

Erickson, M. a., Ruffle, A., & Gold, J. M. (2015). A meta-analysis of mismatch negativity in schizophrenia: From clinical risk to disease specificity and

progression. *Biological Psychiatry*. https://doi.org/10.1016/j.biopsych.2015.08.025

Falkenberg, L. E., Westerhausen, R., Specht, K., & Hugdahl, K. (2012). Resting-state glutamate level in the anterior cingulate predicts blood-oxygen level-dependent response to cognitive control. *Proceedings of the National Academy of Sciences*, *109*(13), 5069–5073. https://doi.org/10.1073/pnas.1115628109

Felleman, D. J., & Van Essen, D. C. (1991). Distributed Hierarchical Processing in the Primate Cerebral Cortex. *Cerebral Cortex*, *1*. https://doi.org/10.1093/cercor/1.1.1-a

First, M. B. (2015). Structured Clinical Interview for the *DSM* (SCID). *The Encyclopedia of Clinical Psychology*, 1–6. https://doi.org/10.1002/9781118625392.wbecp351

Fitzsimmons, J., Kubicki, M., & Shenton, M. E. (2013). Review of functional and anatomical brain connectivity findings in schizophrenia, *26*(2), 172–187. https://doi.org/10.1097/YCO.0b013e32835d9e6a

Fletcher, P. C., & Frith, C. D. (2009). Perceiving is believing: A Bayesian approach to explaining the positive symptoms of schizophrenia. *Nature Reviews Neuroscience*, *10*(1), 48–58. https://doi.org/10.1038/nrn2536

Ford, J. M., Dierks, T., Fisher, D. J., Herrmann, C. S., Hubl, D., Kindler, J., … van Lutterveld, R. (2012). Neurophysiological Studies of Auditory Verbal Hallucinations. *Schizophrenia Bulletin*, *38*(4), 715–723. https://doi.org/10.1093/schbul/sbs009

Fries, P. (2015). Rhythms for Cognition: Communication through Coherence. *Neuron*, *88*(1), 220–235. https://doi.org/10.1016/j.neuron.2015.09.034

Fuente-Sandoval, C. De, Leon-Ortiz, P., Favila, R., Stephano, S., & Mamo, D. (2011). Higher Levels of Glutamate in the Associative-Striatum of Subjects with Prodromal Symptoms of Schizophrenia and Patients with First-Episode Psychosis, 1781–1791. https://doi.org/10.1038/npp.2011.65

Fuente-sandoval, C. De, Reyes-madrigal, F., Mao, X., León-ortiz, P., Rodríguez-mayoral, O., Solís-vivanco, R., … Shungu, D. C. (2016). Cortico-Striatal GABAergic and Glutamatergic Dysregulations in Subjects at Ultra-High Risk for Psychosis Investigated with Proton Magnetic Resonance Spectroscopy, *19*, 1–10. https://doi.org/10.1093/ijnp/pyv105

Fusar-Poli, P., Borgwardt, S., Bechdolf, A., Addington, J., Riecher-Rössler, A., Schultze-Lutter, F., … Yung, A. R. (2013). The psychosis at risk state: a comprehensive state-of-the-art review. *JAMA Psychiatry*, *70*(1), 107–120. https://doi.org/10.1001/jamapsychiatry.2013.269.The

Fusar-Poli, P., De Micheli, A., Cappucciati, M., Rutigliano, G., Davies, C., Ramella-Cravaro, V., … McGuire, P. (2017). Diagnostic and Prognostic Significance of DSM-5 Attenuated Psychosis Syndrome in Services for Individuals at Ultra High Risk for Psychosis. *Schizophrenia Bulletin*, *44*(2), 264–275. https://doi.org/10.1093/schbul/sbx055

Fusar-Poli, P., Deste, G., Smieskova, R., Barlati, S., Yung, A. R., Howes, O., …

Borgwardt, S. (2012). Cognitive Functioning in Prodromal Psychosis. *Archives of General Psychiatry*, *69*(6), 562–571. https://doi.org/10.1001/archgenpsychiatry.2011.1592

Fusar-Poli, P., Meneghelli, A., Valmaggia, L., Allen, P., Galvan, F., McGuire, P., & Cocchi, A. (2009). Duration of untreated prodromal symptoms and 12-month functional outcome of individuals at risk of psychosis. *British Journal of Psychiatry*, *194*(02), 181–182. https://doi.org/10.1192/bjp.bp.107.047951

Fusar-Poli, P., Papanastasiou, E., Stahl, D., Rocchetti, M., Carpenter, W., Shergill, S., & McGuire, P. (2015). Treatments of Negative Symptoms in Schizophrenia: Meta-Analysis of 168 Randomized Placebo-Controlled Trials. *Schizophrenia Bulletin*, *41*(4), 892–899. https://doi.org/10.1093/schbul/sbu170

Fusar-Poli, P., Rocchetti, M., Sardella, A., Avila, A., Brandizzi, M., Caverzasi, E., … McGuire, P. (2015). Disorder, not just state of risk: Meta-analysis of functioning and quality of life in people at high risk of psychosis. *British Journal of Psychiatry*, *207*(3), 198–206. https://doi.org/10.1192/bjp.bp.114.157115

Fusar-Poli, P., Schultze-Lutter, F., Cappucciati, M., Rutigliano, G., Bonoldi, I., Stahl, D., … Mcguire, P. (2016). The Dark Side of the Moon: Meta-analytical Impact of Recruitment Strategies on Risk Enrichment in the Clinical High Risk State for Psychosis. *Schizophrenia Bulletin*, *42*(3), 732–743. https://doi.org/10.1093/schbul/sbv162

Fusar-Poli, P., Stone, J. M., Broome, M. R., Valli, I., Mechelli, A., McLean, M. A., … McGuire, P. K. (2011). Thalamic Glutamate Levels as a Predictor of Cortical Response During Executive Functioning in Subjects at High Risk for Psychosis, *68*(9), 881–890. https://doi.org/10.1001/archgenpsychiatry.2011.46

Gaetz, W., Edgar, J. C., Wang, D. J., & Roberts, T. P. L. (2011). Relating MEG measured motor cortical oscillations to resting γ-Aminobutyric acid (GABA) concentration. *NeuroImage*, *55*(2), 616–621. https://doi.org/10.1016/j.neuroimage.2010.12.077

Gaser, C., Nenadic, I., Volz, H. P., Büchel, C., & Sauer, H. (2004). Neuroanatomy of “Hearing Voices”: A Frontotemporal Brain Structural Abnormality Associated with Auditory Hallucinations in Schizophrenia. *Cerebral Cortex*, *14*(1), 91–96. https://doi.org/10.1093/cercor/bhg107

Ghorashi, S., & Spencer, K. M. (2015). Attentional load effects on beta oscillations in healthy and schizophrenic individuals, *6*(October), 1–8. https://doi.org/10.3389/fpsyt.2015.00149

Gifford, G., Crossley, N., Fusar-Poli, P., Schnack, H. G., Kahn, R. S., Koutsouleris, N., … McGuire, P. (2016). Using neuroimaging to help predict the onset of psychosis. *NeuroImage*. https://doi.org/10.1016/j.neuroimage.2016.03.075

Giraldo-Chica, M., & Woodward, N. D. (2017). Review of thalamocortical resting-state fMRI studies in schizophrenia. *Schizophrenia Research*, *180*, 58–63. https://doi.org/10.1016/j.schres.2016.08.005

Goff, D. C., Falkai, P., Fleischhacker, W. W., Girgis, R. R., Kahn, R. M., Uchida, H., … Lieberman, J. A. (2017). The long-term effects of antipsychotic medication on clinical course in schizophrenia. *American Journal of Psychiatry*, *174*(9), 840–849. https://doi.org/10.1176/appi.ajp.2017.16091016

Gold, J. M., Robinson, B., Leonard, C. J., Hahn, B., Chen, S., McMahon, R. P., & Luck, S. J. (2018). Selective attention, working memory, and executive function as potential independent sources of cognitive dysfunction in schizophrenia. *Schizophrenia Bulletin*, *44*(6), 1227–1234. https://doi.org/10.1093/schbul/sbx155

Gomes, F. V, Rincón-Cortés, M., & Grace, A. A. (2016). Neuroscience and Biobehavioral Reviews Adolescence as a period of vulnerability and intervention in schizophrenia : Insights from the MAM model. *Neuroscience and Biobehavioral Reviews*, *70*, 260–270. https://doi.org/10.1016/j.neubiorev.2016.05.030

Gonzalez-Burgos, G., Hashimoto, T., & Lewis, D. A. (2010). Alterations of cortical GABA neurons and network oscillations in schizophrenia. *Current Psychiatry Reports*, *12*(4), 335–344. https://doi.org/10.1007/s11920-010-0124-8

Gonzalez-Burgos, G., & Lewis, D. A. (2012). NMDA receptor hypofunction, parvalbumin-positive neurons, and cortical gamma oscillations in schizophrenia. *Schizophrenia Bulletin*, *38*(5), 950–957. https://doi.org/10.1093/schbul/sbs010

Gonzalez-Liencres, C., Tas, C., Brown, E. C., Erdin, S., Onur, E., Cubukcoglu, Z., … Brüne, M. (2014). Oxidative stress in schizophrenia : a case – control study on the effects on social cognition and neurocognition, 1–9.

Goto, N., Yoshimura, R., Kakeda, S., Moriya, J., Hori, H., Hayashi, K., … Nakamura, J. (2010). No alterations of brain GABA after 6 months of treatment with atypical antipsychotic drugs in early-stage first-episode schizophrenia. *Progress in Neuro-Psychopharmacology and Biological Psychiatry*, *34*(8), 1480–1483. https://doi.org/10.1016/j.pnpbp.2010.08.007

Gottesman, I. I. (1990). Schizophrenics Kill Themselves Too : A Review of Risk Factors for Suicide, *16*(4).

Granger, J. (1969). Investigating Causal Relations by Econometric Models and Cross-spectral Methods Author (s): C . W . J . Granger Published by : The Econometric Society Stable URL : https://www.jstor.org/stable/1912791 to Econometrica. *Econometrica*, *37*(3), 424–438.

Green, M. F., Horan, W. P., & Lee, J. (2015). Social cognition in schizophrenia. *Nature Reviews Neuroscience*, *16*(10), 620–631. https://doi.org/10.1038/nrn4005

Green, M. F., Kern, R. S., Braff, D. L., & Mintz, J. (2000). Neurocognitive deficits and functional outcome in schizophrenia: Are we measuring the "right stuff"? *Schizophrenia Bulletin*, *26*(1), 119–136. Retrieved from http://www.embase.com/search/results?subaction=viewrecord&from=export&id=L30317696%5Cnhttp://sfx.library.uu.nl/utrecht?sid=EMBASE&issn=0586

7614&id=doi:&atitle=Neurocognitive+deficits+and+functional+outcome+in+schizophrenia%3A+Are+we+measuring+the+%27right

Greenhouse, I., Noah, S., Maddock, R. J., & Ivry, R. B. (2016). Individual differences in GABA content are reliable but are not uniform across the human cortex. *NeuroImage*, *139*, 1–7. https://doi.org/10.1016/j.neuroimage.2016.06.007

Grent-'t-Jong, T., Gross, J., Goense, J., Wibral, M., Gajwani, R., Gumley, A. I., & Lawrie, S. M. (2018). alterations in schizophrenia reveal E / I- balance abnormalities across illness- stages, 1–19.

Grent-'t-Jong, T., Rivolta, D., Sauer, A., Grube, M., Singer, W., Wibral, M., & Uhlhaas, P. J. (2016). MEG-measured visually induced gamma-band oscillations in chronic schizophrenia : Evidence for impaired generation of rhythmic activity in ventral stream regions. *Schizophrenia Research*, *176*(2–3), 177–185. https://doi.org/10.1016/j.schres.2016.06.003

Griesmayr, B., Berger, B., Stelzig-Schoeler, R., Aichhorn, W., Bergmann, J., & Sauseng, P. (2014). EEG theta phase coupling during executive control of visual working memory investigated in individuals with schizophrenia and in healthy controls. *Cognitive, Affective, & Behavioral Neuroscience*, *14*(4), 1340–1355. https://doi.org/10.3758/s13415-014-0272-0

Gruetter, R., & Tkáč, I. (2000). Field mapping without reference scan using asymmetric echo-planar techniques. *Magnetic Resonance in Medicine*, *43*(2), 319–323. https://doi.org/10.1002/(SICI)1522-2594(200002)43:2<319::AID-MRM22>3.0.CO;2-1

Grützner, C., Wibral, M., Sun, L., Rivolta, D., Singer, W., Maurer, K., & Uhlhaas, P. J. (2013). Deficits in high- (>60 Hz) gamma-band oscillations during visual processing in schizophrenia. *Frontiers in Human Neuroscience*, *7*(March), 88. https://doi.org/10.3389/fnhum.2013.00088

Gschwandtner, U., Pflüger, M., Aston, J., Borgwardt, S., Drewe, M., & Anita, R. S. (2006). Fine motor function and neuropsychological deficits in individuals at risk for schizophrenia. *Eur Ach Psychiatry Clin Neurosci*, 201–206. https://doi.org/10.1007/s00406-005-0626-2

Guimond, S., Chakravarty, M. M., Bergeron-Gagnon, L., Patel, R., & Lepage, M. (2016). Verbal memory impairments in schizophrenia associated with cortical thinning. *Neuroimage: Clinical*, *11*, 20–29. https://doi.org/10.1016/j.nicl.2015.12.010

Guo, S., Kendrick, K. M., Yu, R., Wang, H. L. S., & Feng, J. (2014). Key functional circuitry altered in schizophrenia involves parietal regions associated with sense of self. *Human Brain Mapping*, *35*(1), 123–139. https://doi.org/10.1002/hbm.22162

Gustavsson, A., Svensson, M., Jacobi, F., Allgulander, C., Alonso, J., Beghi, E., … Olesen, J. (2011). Cost of disorders of the brain in Europe 2010. *European Neuropsychopharmacology*, *21*(10), 718–779. https://doi.org/10.1016/j.euroneuro.2011.08.008

Gutschalk, A., Mase, R., Roth, R., Ille, N., Rupp, Â., Hahnel, S., … Scherg, M.

(1999). Deconvolution of 40 Hz steady-state ® elds reveals two overlapping source activities of the human auditory cortex, *110*, 856–868.

Haining, K., Matrunola, C., Mitchell, L., Gajwani, R., Gross, J., Gumley, A. I., … Uhlhaas, P. J. (2019). Neuropsychological deficits in participants at clinical high risk for psychosis recruited from the community : relationships to functioning and clinical symptoms.

Hamilton, H. K., Ph, D., Williams, T. J., Ph, D., Ventura, J., Ph, D., … Ph, D. (2018). processing deficits in schizophrenia, *175*(3), 275–283. https://doi.org/10.1176/appi.ajp.2017.16111203.Clinical

Hamm, J. P., Bobilev, A. M., Hayrynen, L. K., Hudgens-Haney, M. E., Oliver, W. T., Parker, D. a., … Clementz, B. a. (2015). Stimulus train duration but not attention moderates γ-band entrainment abnormalities in schizophrenia. *Schizophrenia Research*, *165*(1), 97–102. https://doi.org/10.1016/j.schres.2015.02.016

Hamm, J. P., Gilmore, C. S., & Clementz, B. a. (2012). Augmented gamma band auditory steady-state responses: Support for NMDA hypofunction in schizophrenia. *Schizophrenia Research*, *138*(1), 1–7. https://doi.org/10.1016/j.schres.2012.04.003

Hamm, J. P., Gilmore, C. S., Picchetti, N. a M., Sponheim, S. R., & Clementz, B. a. (2011). Abnormalities of Neuronal Oscillations and Temporal Integration to Low and High Frequency Auditory Stimulation in Schizophrenia. *Biol Psychiatry*, *69*(10), 989–996. https://doi.org/10.1016/j.biopsych.2010.11.021.Abnormalities

Hammond, J. C., Shan, D., Meador-Woodruff, J. H., & McCullumsmith, R. E. (2014). Evidence of Glutamatergic Dysfunction in the Pathophysiology of Schizophrenia. In M. Popoli, D. Diamond, & G. Sanacora (Eds.), *Synaptic Stress and Pathogenesis of Neuropsychiatric Disorders* (pp. 265–294). New York, NY: Springer New York. https://doi.org/10.1007/978-1-4939-1056-4_15

Hardingham, G. E., & Do, K. Q. (2016). Linking early-life NMDAR hypofunction and oxidative stress in schizophrenia pathogenesis. *Nature Publishing Group*, 1–9. https://doi.org/10.1038/nrn.2015.19

Harris, A. D., Puts, N. A. J., & Edden, R. A. E. (2015). Tissue correction for GABA-edited MRS: Considerations of voxel composition, tissue segmentation, and tissue relaxations. *Journal of Magnetic Resonance Imaging*, *42*(5), 1431–1440. https://doi.org/10.1002/jmri.24903

Hartmann, J. A., Yuen, H. P., McGorry, P. D., Yung, A. R., Lin, A., Wood, S. J., … Nelson, B. (2016). Declining transition rates to psychotic disorder in "ultra-high risk" clients: Investigation of a dilution effect. *Schizophrenia Research*, *170*(1), 130–136. https://doi.org/10.1016/j.schres.2015.11.026

Hashimoto, K. (2017). *The NMDA receptors*. Springer Nature. https://doi.org/10.1007/978-3-319-49795-2

Hashimoto, T., Volk, D. W., Eggan, S. M., Mirnics, K., Pierri, J. N., Sun, Z., … Lewis, D. A. (2003). Gene Expression Deficits in a Subclass of GABA Neurons

in the Prefrontal Cortex of Subjects with Schizophrenia. *The Journal of Neuroscience*, *23*(15), 6315–6326. https://doi.org/10.1523/JNEUROSCI.23-15-06315.2003

Heinrichs-Graham, E., Kurz, M. J., Gehringer, J. E., & Wilson, T. W. (2017). The functional role of post-movement beta oscillations in motor termination. *Brain Structure and Function*, *222*(7), 3075–3086. https://doi.org/10.1007/s00429-017-1387-1

Henshall, K. R., Sergejew, A. A., Rance, G., McKay, C. M., & Copolov, D. L. (2013). Interhemispheric EEG coherence is reduced in auditory cortical regions in schizo- phrenia patients with auditory hallucinations ☆. *International Journal of Psychophysiology*, *89*(1), 63–71. https://doi.org/10.1016/j.ijpsycho.2013.05.005

Herdman, A. T., Lins, O., Van Roon, P., Stapells, D. R., Scherg, M., & Picton, T. W. (2002). Intracerebral sources of human auditory steady-state responses. *Brain Topography*, *15*(2), 69–86. https://doi.org/10.1023/A:1021470822922

Herdman, A. T., & Stapells, D. R. (2001). Thresholds determined using the monotic and dichotic multiple auditory steady-state response technique in normal-hearing subjects. *Scandinavian Audiology*, *30*(1), 41–49. https://doi.org/10.1080/010503901750069563

Higgins, J. P. T., & Thompson, S. G. (2002). Quantifying heterogeneity in a meta-analysis. *Statistics in Medicine*, *21*(11), 1539–1558. https://doi.org/10.1002/sim.1186

Higuchi, Y., Sumiyoshi, T., Seo, T., Miyanishi, T., Kawasaki, Y., & Suzuki, M. (2013). Mismatch Negativity and Cognitive Performance for the Prediction of Psychosis in Subjects with At-Risk Mental State. *PLoS ONE*, *8*(1). https://doi.org/10.1371/journal.pone.0054080

Hilker, R., Helenius, D., Fagerlund, B., Skytthe, A., Christensen, K., Werge, T. M., … Glenthøj, B. (2018). Heritability of Schizophrenia and Schizophrenia Spectrum Based on the Nationwide Danish Twin Register. *Biological Psychiatry*, *83*(6), 492–498. https://doi.org/10.1016/j.biopsych.2017.08.017

Hillebrand, A., Singh, K. D., Holliday, I. E., Furlong, P. L., & Barnes, G. R. (2005). A New Approach to Neuroimaging With Magnetoencephalography, *211*, 199–211. https://doi.org/10.1002/hbm.20102

Hinkley, L. B. N., Vinogradov, S., Guggisberg, A. G., Fisher, M., Findlay, A. M., & Nagarajan, S. S. (2011). Clinical symptoms and alpha band resting-state functional connectivity imaging in patients with schizophrenia: Implications for novel approaches to treatment. *Biological Psychiatry*, *70*(12), 1134–1142. https://doi.org/10.1016/j.biopsych.2011.06.029

Hirano, Y., Oribe, N., Kanba, S., Onitsuka, T., Nestor, P. G., & Spencer, K. M. (2015). Spontaneous Gamma Activity in Schizophrenia. *JAMA Psychiatry*, *72*(8), 813. https://doi.org/10.1001/jamapsychiatry.2014.2642

Hoff, P. (2015). Bleuler, Eugen (1857-1939). *International Encyclopedia of the Social & Behavioral Sciences: Second Edition*, *2*, 700–702. https://doi.org/10.1016/B978-0-08-097086-8.61009-7

Hoffman, R. E., Hernandez, T., Pittman, B., & Hampson, M. (2011). Elevated Functonal Connectivity Along a Corticostriatal Loop and the Mechanisms of Auditory / Verbal Hallucinations in Patients with Schizophrenia, *69*(5), 407–414. https://doi.org/10.1016/j.biopsych.2010.09.050.ELEVATED

Hoftman, G. D., Volk, D. W., Bazmi, H. H., Li, S., Sampson, A. R., & Lewis, D. a. (2015). Altered Cortical Expression of GABA-Related Genes in Schizophrenia: Illness Progression vs Developmental Disturbance. *Schizophrenia Bulletin*, *41*(1), 180–191. https://doi.org/10.1093/schbul/sbt178

Hong, L. E., Summerfelt, A., McMahon, R. P., Adami, H., Francis, G., Elliott, A., … Thaker, G. K. (2004). Evoked gamma band synchronization and the liability for schizophrenia*1. *Schizophrenia Research*, *70*(2–3), 293–302. https://doi.org/10.1016/j.schres.2003.12.011

Hoogenboom, N., Schoffelen, J.-M., Oostenveld, R., Parkes, L. M., & Fries, P. (2006). Localizing human visual gamma-band activity in frequency, time and space. *NeuroImage*, *29*(3), 764–773. https://doi.org/10.1016/j.neuroimage.2005.08.043

Horovitz, S. G., Skudlarski, P., & Gore, J. C. (2002). Correlations and dissociations between BOLD signal and P300 amplitude in an auditory oddball task: A parametric approach to combining fMRI and ERP. *Magnetic Resonance Imaging*, *20*(4), 319–325. https://doi.org/10.1016/S0730-725X(02)00496-4

Howes, O. D., & Kapur, S. (2009). The dopamine hypothesis of schizophrenia: Version III - The final common pathway. *Schizophrenia Bulletin*, *35*(3), 549–562. https://doi.org/10.1093/schbul/sbp006

Howes, O. D., & McDonald, C. (2004). Pathways to schizophrenia : The impact of environmental factors Pathways to schizophrenia : the impact of environmental factors, *7*(November). https://doi.org/10.1017/S1461145704004122

Howes, O., McCutcheon, R., & Stone, J. (2015). Glutamate and dopamine in schizophrenia: An update for the 21st century. *Journal of Psychopharmacology*, *29*(2), 97–115. https://doi.org/10.1177/0269881114563634

Ising, H. K., Veling, W., Loewy, R. L., Rietveld, M. W., Rietdijk, J., Dragt, S., … Van Der Gaag, M. (2012). The validity of the 16-item version of the prodromal questionnaire (PQ-16) to screen for ultra high risk of developing psychosis in the general help-seeking population. *Schizophrenia Bulletin*, *38*(6), 1288–1296. https://doi.org/10.1093/schbul/sbs068

Isomura, S., Onitsuka, T., Tsuchimoto, R., Nakamura, I., Hirano, S., Oda, Y., … Kanba, S. (2016). Differentiation between major depressive disorder and bipolar disorder by auditory steady-state responses. *Journal of Affective Disorders*, *190*, 800–806. https://doi.org/10.1016/j.jad.2015.11.034

Izhikevich, L., Gao, R., Peterson, E., & Voytek, B. (2018). Measuring the average power of neural oscillations. *BioRxiv*, 441626. https://doi.org/10.1101/441626

Jablensky, A. (2010). The diagnostic concept of schizophrenia: its history, evolution, and future prospects. *Dialogues in Clinical Neuroscience*, *12*(3), 271–287. https://doi.org/10.1097/ALN.0b013e318212ba87

Javitt, D. C. (2009). Sensory Processing in Schizophrenia : Neither Simple nor Intact, *35*(6), 1059–1064. https://doi.org/10.1093/schbul/sbp110

Javitt, D. C., & Sweet, R. A. (2015). Auditory dysfunction in schizophrenia: integrating clinical and basic features. *Nature Reviews Neuroscience*, *16*(9), 535–550. https://doi.org/10.1038/nrn4002

Jensen, J. E., Auerbach, R. P., Pisoni, A., & Pizzagalli, D. A. (2017). Localized MRS reliability of in vivo glutamate at 3 T in shortened scan times: a feasibility study. *NMR in Biomedicine*, *30*(11), 1–9. https://doi.org/10.1002/nbm.3771

Jessen, F., Scherk, H., Träber, F., Theyson, S., Berning, J., Tepest, R., … Block, W. (2006). Proton magnetic resonance spectroscopy in subjects at risk for schizophrenia, *87*, 81–88. https://doi.org/10.1016/j.schres.2006.06.011

Jimenez, A. M., Lee, J., Wynn, J. K., Cohen, M. S., Engel, S. A., Glahn, D. C., … Green, M. F. (2016). Abnormal ventral and dorsal attention network activity during single and dual target detection in schizophrenia. *Frontiers in Psychology*, *7*(MAR), 1–11. https://doi.org/10.3389/fpsyg.2016.00323

Jin, H., & Mosweu, I. (2017). The Societal Cost of Schizophrenia: A Systematic Review. *PharmacoEconomics*, *35*(1), 25–42. https://doi.org/10.1007/s40273-016-0444-6

Kam, J. W. Y., Bolbecker, A. R., Donnell, B. F. O., Hetrick, W. P., & Brenner, C. A. (2013). Resting state EEG power and coherence abnormalities in bipolar disorder and schizophrenia. *Journal of Psychiatric Research*, *47*(12), 1893–1901. https://doi.org/10.1016/j.jpsychires.2013.09.009

Kantrowitz, J. T., & Javitt, D. C. (2010). N-methyl-d-aspartate (NMDA) receptor dysfunction or dysregulation: The final common pathway on the road to schizophrenia? *Brain Research Bulletin*, *83*(3–4), 108–121. https://doi.org/10.1016/j.brainresbull.2010.04.006

Kapur, S. (2003). Psychosis as a State of Aberrant Salience : and Pharmacology in Schizophrenia. *Am J Psychiatry*, (160), 13–23.

Kasai, K., Shenton, M. E., Salisbury, D. F., Hirayasu, Y., Onitsuka, T., Spencer, M. H., … McCarley, R. W. (2003). Progressive Decrease of Left Heschl Gyrus and Planum Temporale Gray Matter Volume in First-Episode Schizophrenia A Longitudinal Magnetic Resonance Imaging Study, *60*, 766–775.

Kay, S. R., Fiszbein, A., & Opler, L. A. (1987). The Positive and Negative Syndrome Scale (PANSS) for Schizophrenia. *Schizophrenia Bulletin*, *13*(2), 261–276. https://doi.org/10.1093/schbul/13.2.261

Keefe, R. S., Bilder, R. M., Davis, S. M., Harvey, P. D., Palmer, B. W., Gold, J. M., … Lieberman, J. A. (2007). Neurocognitive effects of antipsychotic medications in patients with chronic schizophrenia in the CATIE Trial. *Arch Gen Psychiatry*, *64*(6), 633–647. https://doi.org/10.1001/archpsyc.64.6.633

Keefe, R. S. E., Goldberg, T. E., Harvey, P. D., Gold, J. M., Poe, M. P., & Coughenour, L. (2004). The Brief Assessment of Cognition in Schizophrenia: Reliability, sensitivity, and comparison with a standard neurocognitive battery. *Schizophrenia Research*, *68*(2–3), 283–297. https://doi.org/10.1016/j.schres.2003.09.011

Keefe, R. S. E., Silva, S. G., Perkins, D. O., & Lieberman, J. a. (1999). The effects of atypical antipsychotic drugs on neurocognitive impairment in schizophrenia: A review and meta-analysis. *Schizophrenia Bulletin*, *25*(2), 201–222. https://doi.org/10.1093/oxfordjournals.schbul.a033374

Kegeles, L. S., Mao, X., Stanford, a. D., Girgis, R., Ojeil, N., Xu, X., … Shungu, D. C. (2012). Elevated Prefrontal Cortex -Aminobutyric Acid and Glutamate-Glutamine Levels in Schizophrenia Measured In Vivo With Proton Magnetic Resonance Spectroscopy. *Archives of General Psychiatry*, *69*(5), 449–459. https://doi.org/10.1001/archgenpsychiatry.2011.1519

Kelemen, O., Kiss, I., Benedek, G., & Kéri, S. (2013). Perceptual and cognitive effects of antipsychotics in first-episode schizophrenia: The potential impact of GABA concentration in the visual cortex. *Progress in Neuro-Psychopharmacology and Biological Psychiatry*, *47*, 13–19. https://doi.org/10.1016/j.pnpbp.2013.07.024

Keshavan, M. S., Dick, R. M., Diwadkar, V. A., Montrose, D. M., Prasad, K. M., & Stanley, J. A. (2009). Striatal metabolic alterations in non-psychotic adolescent offspring at risk for schizophrenia : A 1 H spectroscopy study. *Schizophrenia Research*, *115*(1), 88–93. https://doi.org/10.1016/j.schres.2009.08.012

Keshavan, M. S., Lawler, A. N., Nasrallah, H. A., & Tandon, R. (2017). New drug developments in psychosis: Challenges, opportunities and strategies. *Progress in Neurobiology*, *152*, 3–20. https://doi.org/10.1016/j.pneurobio.2016.07.004

Keshavan, M. S., Montrose, D. M., Pierri, J. N., & Elizabeth, L. (1997). MAGNETIC RESONANCE IMAGING AND SPECTROSCOPY IN OFFSPRING AT RISK FOR SCI-IIZOPHRENIAz PRELIMINARY STUDIES, *21*(Ix), 1285–1295.

Keshavan, M. S., Reynolds, C. F., Miewald, J. M., Montrose, D. M., Sweeny, J. A., Vasko, R. C., & Kupfer, D. J. (1998). Delta Sleep Deficits in Schizophrenia. *Archives of General Psychiatry*, *55*(May), 443–448. https://doi.org/10.1074/jbc.M314060200

Kew, J. N. C., & Kemp, J. A. (2005). Ionotropic and metabotropic glutamate receptor structure and pharmacology. *Psychopharmacology*, *179*(1), 4–29. https://doi.org/10.1007/s00213-005-2200-z

Kim, M., Lee, T. H., Yoon, Y. B., Lee, T. Y., & Kwon, J. S. (2018). Predicting Remission in Subjects at Clinical High Risk for Psychosis Using Mismatch Negativity. *Schizophrenia Bulletin*, *44*(3), 575–583. https://doi.org/10.1093/schbul/sbx102

Kirihara, K., Rissling, A. J., Swerdlow, N. R., Braff, D. L., & Light, G. a. (2012). Hierarchical Organization of Gamma and Theta Oscillatory Dynamics in Schizophrenia, *71*(10), 873–880.

https://doi.org/10.1016/j.biopsych.2012.01.016.Hierarchical

Kirsch, P., Achenbach, C., Kirsch, M., Heinzmann, M., Schienle, A., & Vaitl, D. (2003). Cerebellar and hippocampal activation during eyeblink conditioning depends on the experimental paradigm: A MEG Study. *Neural Plasticity*, *10*(4), 291–301. https://doi.org/10.1155/NP.2003.291

Kisley, M. A., Noecker, T. L., & Guinther, P. M. (2004). Comparison of sensory gating to mismatch negativity and self-reported perceptual phenomena in healthy adults, *41*, 604–612. https://doi.org/10.1111/j.1469-8986.2004.00191.x

Koenig, T., van Swam, C., Dierks, T., & Hubl, D. (2012). Is gamma band EEG synchronization reduced during auditory driving in schizophrenia patients with auditory verbal hallucinations? *Schizophrenia Research*, *141*(2–3), 266–270. https://doi.org/10.1016/j.schres.2012.07.016

Komek, K., Bard Ermentrout, G., Walker, C. P., & Cho, R. Y. (2012). Dopamine and gamma band synchrony in schizophrenia - insights from computational and empirical studies. *European Journal of Neuroscience*, *36*(2), 2146–2155. https://doi.org/10.1111/j.1460-9568.2012.08071.x

Koshiyama, D., Kirihara, K., Tada, M., Nagai, T., Fujioka, M., Ichikawa, E., … Kasai, K. (2018a). Auditory gamma oscillations predict global symptomatic outcome in the early stages of psychosis: A longitudinal investigation. *Clinical Neurophysiology*, *129*(11), 2268–2275. https://doi.org/10.1016/j.clinph.2018.08.007

Koshiyama, D., Kirihara, K., Tada, M., Nagai, T., Fujioka, M., Ichikawa, E., … Kasai, K. (2018b). Auditory gamma oscillations predict global symptomatic outcome in the early stages of psychosis: A longitudinal investigation. *Clinical Neurophysiology*, *129*(11), 2268–2275. https://doi.org/10.1016/j.clinph.2018.08.007

Koutsouleris, N., Borgwardt, S., Meisenzahl, E. M., Bottlender, R., Moller, H.-J., & Riecher-rossler, A. (2012). Disease Prediction in the At-Risk Mental State for Psychosis Using Neuroanatomical Biomarkers : Results From the FePsy Study, *38*(6), 1234–1246. https://doi.org/10.1093/schbul/sbr145

Koutsouleris, N., Gaser, C., Bottlender, R., Davatzikos, C., Decker, P., Jäger, M., … Meisenzahl, E. M. (2010). Use of neuroanatomical pattern regression to predict the structural brain dynamics of vulnerability and transition to psychosis. *Schizophrenia Research*, *123*(2–3), 175–187. https://doi.org/10.1016/j.schres.2010.08.032

Kraemer, H. C., Kazdin, A. E., Offord, D. R., Kessler, R. C., Jensen, P. S., & Kupfler, D. J. (1997). Coming to terms with the terms of risk, 24–25.

Krause, B., & Kadosh, R. C. (2014). Not all brains are created equal: The relevance of individual differences in responsiveness to transcranial electrical stimulation. *Frontiers in Systems Neuroscience*, *8*(FEB), 1–12. https://doi.org/10.3389/fnsys.2014.00025

Krishna, N., Neill, H. O., Sánchez-Morla, E. M., & Thaker, G. K. (2015). remembered pursuit task is impaired in schizophrenia, *157*(0), 198–203.

https://doi.org/10.1016/j.schres.2014.05.035.Long

Krishnan, G. P., Hetrick, W. P., Brenner, C. a., Shekhar, a., Steffen, a. N., & O'Donnell, B. F. (2009). Steady state and induced auditory gamma deficits in schizophrenia. *NeuroImage*, *47*(4), 1711–1719. https://doi.org/10.1016/j.neuroimage.2009.03.085

Krishnan, G. P., Vohs, J. L., Hetrick, W. P., Carroll, C. a., Shekhar, A., Bockbrader, M. a., & O'Donnell, B. F. (2005). Steady state visual evoked potential abnormalities in schizophrenia. *Clinical Neurophysiology*, *116*(3), 614–624. https://doi.org/10.1016/j.clinph.2004.09.016

Kuhn, A. A., Williams, D., Kupsch, A., Limousin, P., Hariz, M., Schneider, G., … Brown, P. (2004). Event-related beta desynchronization in human subthalamic nucleus correlates with motor performance, *127*(4). https://doi.org/10.1093/brain/awh106

Kwon, J. S., O'Donnell, B. F., Wallenstein, G. V., Greene, R. W., Hirayasu, Y., Nestor, P. G., … McCarley, R. W. (1999). Gamma Frequency–Range Abnormalities to Auditory Stimulation in Schizophrenia. *Ach Gen Psychiatry*, *56*(11), 1001–1005. https://doi.org/10.1016/j.psc.2007.05.001

Lahti, A. C., Weiler, M. A., Michaelidis, T., Parwani, A., & Tamminga, C. A. (2001). Effects of ketamine in normal and schizophrenic volunteers. *Neuropsychopharmacology*, *25*(4), 455–467. https://doi.org/10.1016/S0893-133X(01)00243-3

Lakatos, P., Gross, J., & Thut, G. (2019). Review A new unifying account of the roles of neuronal entrainment. *Current Biology*, *29*(18), 1–16. https://doi.org/10.1016/j.cub.2019.07.075

Larsen, T. K., Moe, L. C., Vibe-Hansen, L., & Johannessen, J. O. (2000). Premorbid functioning versus duration of untreated psychosis in 1 year outcome in first-episode psychosis. *Schizophrenia Research*, *45*(1–2), 1–9. https://doi.org/10.1016/S0920-9964(99)00169-3

Lavoie, S., Jack, B. N., Griffiths, O., Ando, A., Amminger, P., Couroupis, A., … Whitford, T. J. (2018). Impaired mismatch negativity to frequency deviants in individuals at ultra-high risk for psychosis, and preliminary evidence for further impairment with transition to psychosis. *Schizophrenia Research*, *191*, 95–100. https://doi.org/10.1016/j.schres.2017.11.005

Legget, K. T., Hild, A. K., Steinmetz, S. E., Simon, S. T., & Rojas, D. C. (2017). MEG and EEG demonstrate similar test-retest reliability of the 40 Hz auditory steady-state response. *International Journal of Psychophysiology*, *114*, 16–23. https://doi.org/10.1016/j.ijpsycho.2017.01.013

Lehmann, D., Faber, P. L., Pascual-marqui, R. D., Milz, P., Herrmann, W. M., Koukkou, M., … San, C. (2014). Functionally aberrant electrophysiological cortical connectivities in first episode medication-naive schizophrenics from three psychiatry centers, *8*(August), 1–9. https://doi.org/10.3389/fnhum.2014.00635

Leishman, E., O'Donnell, B. F., Millward, J. B., Vohs, J. L., Rass, O., Krishnan, G. P., … Morzorati, S. L. (2015). Phencyclidine Disrupts the Auditory Steady

State Response in Rats. *Plos One*, *10*(8), e0134979. https://doi.org/10.1371/journal.pone.0134979

Leroy, F., Glasel, H., Dubois, J., Hertz-Pannier, L., Thirion, B., Mangin, J.-F., & Dehaene-Lambertz, G. (2011). Early Maturation of the Linguistic Dorsal Pathway in Human Infants. *Journal of Neuroscience*, *31*(4), 1500–1506. https://doi.org/10.1523/JNEUROSCI.4141-10.2011

Leucht, S., Corves, C., Arbter, D., Engel, R. R., Li, C., & Davis, J. M. (2009). Second-generation versus first-generation antipsychotic drugs for schizophrenia: a meta-analysis. *The Lancet*, *373*(9657), 31–41. https://doi.org/10.1016/S0140-6736(08)61764-X

Lewis, D. A. (2011). The chandelier neuron in schizophrenia. *Developmental Neurobiology*, *71*(1), 118–127. https://doi.org/10.1002/dneu.20825

Lewis, D. A., Curley, A. A., Glausier, J. R., & Volk, D. W. (2012). Cortical parvalbumin interneurons and cognitive dysfunction in schizophrenia. *Trends in Neurosciences*, *35*(1), 57–67. https://doi.org/10.1016/j.tins.2011.10.004

Lewis, D. A., Curley, A. A., Glausier, J., & Volk, D. W. (2013). NIH Public Access, *35*(1), 57–67. https://doi.org/10.1016/j.tins.2011.10.004.Cortical

Liddle, E. B., Price, D., Palaniyappan, L., Brookes, M. J., Robson, S. E., Hall, E. L., … Liddle, P. F. (2016). Abnormal salience signaling in schizophrenia: The role of integrative beta oscillations. *Human Brain Mapping*, *37*(4), 1361–1374. https://doi.org/10.1002/hbm.23107

Light, G. a., Hsu, J. L., Hsieh, M. H., Meyer-Gomes, K., Sprock, J., Swerdlow, N. R., & Braff, D. L. (2006). Gamma Band Oscillations Reveal Neural Network Cortical Coherence Dysfunction in Schizophrenia Patients. *Biological Psychiatry*, *60*(11), 1231–1240. https://doi.org/10.1016/j.biopsych.2006.03.055

Lim, A., Hoek, H. W., Deen, M. L., Blom, J. D., Bruggeman, R., Cahn, W., … Wiersma, D. (2016). Prevalence and classification of hallucinations in multiple sensory modalities in schizophrenia spectrum disorders. *Schizophrenia Research*, *176*(2–3), 493–499. https://doi.org/10.1016/j.schres.2016.06.010

Lim, K. O., Lee, T. Y., Kim, M., Chon, M. W., Yun, J. Y., Kim, S. N., & Kwon, J. S. (2018). Early referral and comorbidity as possible causes of the declining transition rate in subjects at clinical high risk for psychosis. *Early Intervention in Psychiatry*, *12*(4), 596–604. https://doi.org/10.1111/eip.12363

Lisman, J. (2012). Excitation, inhibition, local oscillations, or large-scale loops: What causes the symptoms of schizophrenia? *Current Opinion in Neurobiology*, *22*(3), 537–544. https://doi.org/10.1016/j.conb.2011.10.018

Lisman, J. (2016). Low-Frequency Brain Oscillations in Schizophrenia, 2–3. https://doi.org/10.1001/jamapsychiatry.2015.2320.Conflict

Lopes da Silva, F. H. (2010). MEG: An Introduction to Methods. In P. C. Hansen, M. L. Kringelbach, & R. Salmelin (Eds.), *MEG: An Introduction to Methods* (pp. 1–23). https://doi.org/10.1093/acprof:oso/9780195307238.003.0002

Luck, S. J., & Gold, J. M. (2008). The Construct of Attention in Schizophrenia. *Biological Psychiatry*, *64*(1), 34–39. https://doi.org/10.1016/j.biopsych.2008.02.014

Mackay, B. Y. D. M. (1954). TOWARDS AN INFORMATION-FLOW MODEL OF HUMAN BEHAVIOUR, 30–43.

Magistretti, P. J., & Pellerin, L. (1999). Cellular mechanisms of brain energy metabolism and their relevance to functional brain imaging. *Philosophical Transactions of the Royal Society of London.Series B, Biological Sciences*, *354*(1387), 1155–1163. https://doi.org/10.1098/rstb.1999.0471

Maharajh, K., Abrams, D., Rojas, D. C., Teale, P., & Reite, M. L. (2007). Auditory steady state and transient gamma band activity in bipolar disorder. *International Congress Series*, *1300*, 707–710. https://doi.org/10.1016/j.ics.2006.12.073

Maharajh, K., Teale, P., Rojas, D. C., & Reite, M. L. (2010). Fluctuation of gamma-band phase synchronization within the auditory cortex in schizophrenia. *Clinical Neurophysiology*, *121*(4), 542–548. https://doi.org/10.1016/j.clinph.2009.12.010

Maran, M., Grent-'t-Jong, T., & Uhlhaas, P. J. (2016). Electrophysiological insights into connectivity anomalies in schizophrenia: a systematic review. *Neuropsychiatric Electrophysiology*, *2*(1), 6. https://doi.org/10.1186/s40810-016-0020-5

Marenco, S., Meyer, C., Kuo, S., van der Veen, J. W., Shen, J., DeJong, K., … Berman, K. F. (2016). Prefrontal GABA Levels Measured With Magnetic Resonance Spectroscopy in Patients With Psychosis and Unaffected Siblings. *American Journal of Psychiatry*, (15), appi.ajp.2015.1. https://doi.org/10.1176/appi.ajp.2015.15020190

Markov, N. T., Vezoli, J., Chameau, P., Falchier, A., Quilodran, R., Huissoud, C., … Kennedy, H. (2014). Anatomy of hierarchy: Feedforward and feedback pathways in macaque visual cortex. *Journal of Comparative Neurology*, *522*(1), 225–259. https://doi.org/10.1002/cne.23458

Markram, H., Toledo-Rodriguez, M., Wang, Y., Gupta, A., Silberberg, G., & Wu, C. (2004). Interneurons of the neocortical inhibitory system. *Nature Reviews Neuroscience*, *5*(10), 793–807. https://doi.org/10.1038/nrn1519

Marshall, M., Lewis, S., Lockwood, A., Drake, R., Jones, P., & Croudace, T. (2005). Association between duration of untreated psychosis and outcome in cohorts of first-episode patients: a systematic review. *Archives of General Psychiatry*, *62*(9), 975–983. https://doi.org/10.1001/archpsyc.62.9.975

Mason, O., Startup, M., Halpin, S., Schall, U., Conrad, A., & Carr, V. (2004). Risk factors for transition to first episode psychosis among individuals with "at-risk mental states." *Schizophrenia Research*, *71*(2–3), 227–237. https://doi.org/10.1016/j.schres.2004.04.006

McDonald, M., Christoforidou, E., Rijsbergen, N. Van, Gajwani, R., Gross, J., Gumley, A. I., … Uhlhaas, P. J. (2018). Using Online Screening in the General Population to Detect Participants at Clinical High-Risk for Psychosis,

(June), 1–10. https://doi.org/10.1093/schbul/sby069

McGorry, P., Keshavan, M., Goldstone, S., Amminger, P., Allott, K., Berk, M., … Hickie, I. (2014). Biomarkers and clinical staging in psychiatry. *World Psychiatry*, *13*, 211–223.

McGurk, S. R., Coleman, T., Harvey, P. D., White, L., Friedman, J., Parrella, M., … Davis, K. L. (2004). Working Memory Performance in Poor Outcome Schizophrenia : Relationship to Age and Executive Functioning Working Memory Performance in Poor Outcome Schizophrenia : Relationship to Age and Executive Functioning. *Journal of Clinical and Experimental Neuropsychology*, *3395*.

McKenna, M. C. (2007). The glutamate-glutamine cycle is not stoichiometric: Fates of glutamate in brain. *Journal of Neuroscience Research*, *85*(15), 3347–3358. https://doi.org/10.1002/jnr.21444

Meda, S. A., Gill, A., Stevens, M. C., Lorenzoni, R. P., Glahn, D. C., Calhoun, V. D., … Pearlson, G. D. (2012). Differences in Resting-State Functional Magnetic Between Schizophrenia and Psychotic Bipolar Probands and Their Unaffected First-Degree Relatives. *BPS*, *71*(10), 881–889. https://doi.org/10.1016/j.biopsych.2012.01.025

Melloni L., Molina, C., Torres, D., Rodriguez, E., Singer, W., & Pena, M. (2007). Synchronization of Neural Activity across Cortical Areas Correlates with Conscious Perception. *Journal of Neuroscience*, *27*(11), 2858–2865. https://doi.org/10.1523/jneurosci.4623-06.2007

Melynyte, S., Pipinis, E., Genyte, V., Voicikas, A., Rihs, T., & Griskova-Bulanova, I. (2018). 40 Hz Auditory Steady-State Response: The Impact of Handedness and Gender. *Brain Topography*, *31*(3), 419–429. https://doi.org/10.1007/s10548-017-0611-x

Menon, V., Ford, C. A. J. M., Lim, K. O., Glover, G. H., & Pfefferbaum, A. (1997). Combined event-related fMRI and EEG evidence for temporal–parietal cortex activation during target detection. *NeuroReport*, *8*(14), 1–9. Retrieved from papers3://publication/uuid/E50AEA01-1445-41A7-901F-31FD503821B2

Menschikov, P. E., Semenova, N. A., Ublinskiy, M. V, Akhadov, T. A., Keshishyan, R. A., Lebedeva, I. S., … Varfolomeev, S. D. (2016). H MRS and MEGA PRESS Pulse Sequence in the Study of Balance of Inhibitory and Excitatory Neurotransmitters in the Human Brain of Ultra High Risk of Schizophrenia Patients, *468*(1), 168–172. https://doi.org/10.1134/S1607672916030029

Merritt, K., Egerton, A., Kempton, M. J., Taylor, M. J., & Mcguire, P. K. (2016). Nature of Glutamate Alterations in SchizophreniaA Meta-analysis of Proton Magnetic Resonance Spectroscopy Studies, *73*(7), 665–674. https://doi.org/10.1001/jamapsychiatry.2016.0442

Merritt, K., Mcguire, P., & Egerton, A. (2013). Relationship between glutamate dysfunction and symptoms and cognitive function in psychosis, *4*(November), 1–8. https://doi.org/10.3389/fpsyt.2013.00151

Mescher, M., Merkle, H., Kirsch, J., Garwood, M., & Gruetter, R. (1998).

Simultaneous in vivo spectral editing and water suppression. *NMR in Biomedicine*, *11*(6), 266–272. https://doi.org/10.1002/(SICI)1099-1492(199810)11:6<266::AID-NBM530>3.0.CO;2-J

Mescher, M., Tannus, A., O'Neil Johnson, M., & Garwood, M. (1996). Solvent suppression using selective echo dephasing. *Journal of Magnetic Resonance - Series A*, *123*(2), 226–229. https://doi.org/10.1006/jmra.1996.0242

Michalareas, G., Julien, V., Pelt, S. Van, Schoffelen, J., Kennedy, H., Fries, P., … Kennedy, H. (2016). Alpha-Beta and Gamma Rhythms Subserve Feedback and Feedforward Influences among Human Visual Cortical Areas Article Alpha-Beta and Gamma Rhythms Subserve Feedback and Feedforward Influences among Human Visual Cortical Areas. *Neuron*, *89*(2), 1–14. https://doi.org/10.1016/j.neuron.2015.12.018

Mikanmaa, E., Grent-'t-Jong, T., Hua, L., Recasens, M., Thune, H., & Uhlhaas, P. J. (2017). Towards a neurodynamical understanding of the prodrome in schizophrenia. *NeuroImage*, (November), 1–10. https://doi.org/10.1016/j.neuroimage.2017.11.026

Milev, P., Ho, B., Arndt, S., & Andreasen, N. C. (2005). Predictive Values of Neurocognition and Negative Symptoms on Functional Outcome in Schizophrenia: A longitudinal First-Episode Study with 7-Year Follow-Up. *Am J Psychiatry*, (162), 495–506. https://doi.org/10.1176/appi.ajp.162.3.495

Millan, M. J., Andrieux, A., Bartzokis, G., Cadenhead, K., Dazzan, P., Fusar-Poli, P., … Weinberger, D. (2016). Altering the course of schizophrenia: Progress and perspectives. *Nature Reviews Drug Discovery*, *15*(7), 485–515. https://doi.org/10.1038/nrd.2016.28

Millan, M. J., Fone, K., Steckler, T., & Horan, W. P. (2014). Negative symptoms of schizophrenia: Clinical characteristics, pathophysiological substrates, experimental models and prospects for improved treatment. *European Neuropsychopharmacology*, *24*(5), 645–692. https://doi.org/10.1016/j.euroneuro.2014.03.008

Miller, T. J., McGlashan, T. H., Rosen, J. L., Cadenhead, K., Ventura, J., & McFarlane, W. (2003). Prodromal assessment with the structured interview for prodromal syndromes and the scale of prodromal symptoms. *Schizophrenia Bulletin*, *29*, 703–715.

Mittal, V. A., Dean, D. J., Bernard, J. A., Orr, J. M., Pelletier-Baldelli, A., Carol, E. E., … Millman, Z. B. (2014). Neurological soft signs predict abnormal cerebellar-thalamic tract development and negative symptoms in adolescents at high risk for psychosis: A longitudinal perspective. *Schizophrenia Bulletin*, *40*(6), 1204–1215. https://doi.org/10.1093/schbul/sbt199

Modinos, G., Şimşek, F., Azis, M., Bossong, M., Bonoldi, I., Samson, C., … McGuire, P. (2018). Prefrontal GABA levels, hippocampal resting perfusion and the risk of psychosis. *Neuropsychopharmacology*, *43*(13), 2652–2659. https://doi.org/10.1038/s41386-017-0004-6

Modinos, G., Şimşek, F., Horder, J., Bossong, M., Bonoldi, I., Azis, M., … McGuire, P. (2018). Cortical GABA in subjects at ultra-high risk of psychosis:

Relationship to negative prodromal symptoms. *International Journal of Neuropsychopharmacology*, *21*(2), 114–119. https://doi.org/10.1093/ijnp/pyx076

Moghaddam, B., & Javitt, D. (2012). From Revolution to Evolution: The Glutamate Hypothesis of Schizophrenia and its Implication for Treatment. *Neuropsychopharmacology*, *37*(1), 4–15. https://doi.org/10.1038/npp.2011.181

Mohr, F., Hubman, W., Albus, M., Franz, U., Hecht, S., Scherer, J., … Sobizack, N. (2003). Neurological soft signs andneuropsychological performance in patients with first episode schizophrenia. *Psychiatric Research*, *121*, 21–30. https://doi.org/10.1016/S0165-1781

Moncrieff, J., & Leo, J. (2010). A systematic review of the effects of antipsychotic drugs on brain volume. *Psychological Medicine*, *40*(9), 1409–1422. https://doi.org/10.1017/S0033291709992297

Moran, L. V., & Hong, L. E. (2011). High vs Low Frequency Neural Oscillations in Schizophrenia. *Schizophrenia Bulletin*, *37*(4), 659–663. https://doi.org/10.1093/schbul/sbr056

Morrens, M., Docx, L., & Walther, S. (2014). Beyond boundaries : in search of an integrative view on motor symptoms in schizophrenia, *5*(October), 1–4. https://doi.org/10.3389/fpsyt.2014.00145

Morris, B. J., Cochran, S. M., & Pratt, J. A. (2005). PCP: From pharmacology to modelling schizophrenia. *Current Opinion in Pharmacology*, *5*(1), 101–106. https://doi.org/10.1016/j.coph.2004.08.008

Morrison, A. P., & French, P. (2012). Early detection and intervention evaluation for people at risk of psychosis : multisite randomised controlled trial, *2233*(April), 1–14. https://doi.org/10.1136/bmj.e2233

Moskowitz, A., & Heim, G. (2011). Eugen Bleuler's Dementia Praecox or the Group of Schizophrenias (1911): A centenary appreciation and reconsideration. *Schizophrenia Bulletin*, *37*(3), 471–479. https://doi.org/10.1093/schbul/sbr016

Mulert, C., Kirsch, V., Pascual-marqui, R., Mccarley, R. W., & Spencer, K. M. (2011). Long-range synchrony of gamma oscillations and auditory hallucination symptoms in schizophrenia. *International Journal of Psychophysiology*, *79*(1), 55–63. https://doi.org/10.1016/j.ijpsycho.2010.08.004

Mullins, P. G., Mcgonigle, D. J., Gorman, R. L. O., Puts, N. A. J., Vidyasagar, R., Evans, C. J., … Edden, R. A. E. (2014). NeuroImage Current practice in the use of MEGA-PRESS spectroscopy for the detection of GABA. *NeuroImage*, *86*, 43–52. https://doi.org/10.1016/j.neuroimage.2012.12.004

Muthukumaraswamy, S. D., Edden, R. A. E., Jones, D. K., Swettenham, J. B., & Singh, K. D. (2009). Resting GABA concentration predicts peak gamma frequency and fMRI amplitude in response to visual stimulation in humans, *106*(20), 1–6. Retrieved from https://mail.google.com/mail/?ui=2&view=bsp&ver=ohhl4rw8mbn4%5Cnpap

ers3://publication/uuid/1D0BEDB6-7057-469F-8DB3-6D8D898D3611

Näätänen, R., & Kähkönen, S. (2009). Central auditory dysfunction in schizophrenia as revealed by the mismatch negativity (MMN) and its magnetic equivalent MMNm: a review. *The International Journal of Neuropsychopharmacology*, *12*(01), 125. https://doi.org/10.1017/S1461145708009322

Nakagawa, S., & Schielzeth, H. (2013). A general and simple method for obtaining R2 from generalized linear mixed-effects models. *Methods in Ecology and Evolution*, *4*(2), 133–142. https://doi.org/10.1111/j.2041-210x.2012.00261.x

Nakazawa, K., Jeevakumar, V., & Nakao, K. (2017). Spatial and temporal boundaries of NMDA receptor hypofunction leading to schizophrenia. *Npj Schizophrenia*, *3*(1), 7. https://doi.org/10.1038/s41537-016-0003-3

Natsubori, T., Inoue, H., Abe, O., Takano, Y., Iwashiro, N., & Aoki, Y. (2014). Reduced Frontal Glutamate + Glutamine and N -Acetylaspartate Levels in Patients With Chronic Schizophrenia but not in Those at Clinical High Risk for Psychosis or With First-Episode Schizophrenia, *40*(5), 1128–1139. https://doi.org/10.1093/schbul/sbt124

Newsholme, P., Procopio, J., Ramos Lima, M. M., Pithon-Curi, T. C., & Curi, R. (2003). Glutamine and glutamate - Their central role in cell metabolism and function. *Cell Biochemistry and Function*, *21*(1), 1–9. https://doi.org/10.1002/cbf.1003

Ng, F., Berk, M., Dean, O., & Bush, A. I. (2008). Oxidative stress in psychiatric disorders: Evidence base and therapeutic implications. *International Journal of Neuropsychopharmacology*, *11*(6), 851–876. https://doi.org/10.1017/S1461145707008401

Niznikiewicz, M., Donnino, R., McCarley, R. W., Nestor, P. G., Iosifescu, D. V., O'Donnell, B., … Shenton, M. E. (2000). Abnormal angular gyrus asymmetry in schizophrenia. *American Journal of Psychiatry*, *157*(3), 428–437. https://doi.org/10.1176/appi.ajp.157.3.428

O'Donnell, B. F., Vohs, J. L., Krishnan, G. P., Rass, O., Hetrick, W. P., & Morzorati, S. L. (2013). The auditory steady-state response (ASSR), (October 2015), 101–112. https://doi.org/10.1016/B978-0-7020-5307-8.00006-5

Oberhuber, M., Hope, T. M. H., Seghier, M. L., Parker Jones, O., Prejawa, S., Green, D. W., & Price, C. J. (2016). Four Functionally Distinct Regions in the Left Supramarginal Gyrus Support Word Processing. *Cerebral Cortex*, *26*(11), 4212–4226. https://doi.org/10.1093/cercor/bhw251

Ohrmann, P., Siegmund, A., Suslow, T., Pedersen, A., Spitzberg, K., Kersting, A., … Pfleiderer, B. (2007). Cognitive impairment and in vivo metabolites in first-episode neuroleptic-naive and chronic medicated schizophrenic patients: A proton magnetic resonance spectroscopy study. *Journal of Psychiatric Research*, *41*(8), 625–634. https://doi.org/10.1016/j.jpsychires.2006.07.002

Öngür, D., Prescot, A., & Jensen, J. (2009). Creatine abnormalities in

schizophrenia and bipolar disorder. *Psychiatry Research: …*, *172*(1), 44–48. https://doi.org/10.1016/j.pscychresns.2008.06.002.CREATINE

Öngür, D., Prescot, A. P., McCarthy, J., Cohen, B. M., & Renshaw, P. F. (2010). Elevated gamma-aminobutyric acid levels in chronic schizophrenia. *Biological Psychiatry*, *68*(7), 667–670. https://doi.org/10.1016/j.biopsych.2010.05.016

Oostenveld, R., Fries, P., Maris, E., & Schoffelen, J. M. (2011). FieldTrip: Open source software for advanced analysis of MEG, EEG, and invasive electrophysiological data. *Computational Intelligence and Neuroscience*, *2011*. https://doi.org/10.1155/2011/156869

Orrù, G., Pettersson-Yeo, W., Marquand, A. F., Sartori, G., & Mechelli, A. (2012). Neuroscience and Biobehavioral Reviews Using Support Vector Machine to identify imaging biomarkers of neurological and psychiatric disease : A critical review. *Neuroscience and Biobehavioral Reviews*, *36*(4), 1140–1152. https://doi.org/10.1016/j.neubiorev.2012.01.004

Palaniyappan, L., & Liddle, P. F. (2012). Does the salience network play a cardinal role in psychosis? An emerging hypothesis of insular dysfunction. *Journal of Psychiatry and Neuroscience*, *37*(1), 17–27. https://doi.org/10.1503/jpn.100176

Pantelis, C., Velakoulis, D., Mcgorry, P. D., Wood, S. J., Suckling, J., Phillips, L. J., … Mcguire, P. K. (2003). @ Neuroanatomical abnormalities before and after onset of psychosis : a cross-sectional and longitudinal MRI comparison lpfymtllin sycboiic disoiSers oufs ^ f ^ sycK ^ s are essential for an understanding of develop the disorder had less grey matter in th, *361*, 281–288.

Pantev, C., Roberts, L. E., Elbert, T., Ross, B., & Wienbruch, C. (1996). Tonotopic organization of the sources of human auditory steady-state responses. *Hear Res*, *101*(1–2), 62–74. https://doi.org/10.1016/S0378-5955(96)00133-5

Parker, S. (2006). Identification of young people at risk of psychosis. *Advances in Psychiatric Treatment*, *12*(4), 249–255. https://doi.org/10.1192/apt.12.4.249

Pascual-Marqui, R. D., Lhmann, D., Koukkou, M., Kochi, K., Anderer, P., Saletu, B., … Kinoshita, T. (2011). Assessing interactions in the brain with exact low-resolution electromagnetic tomography. *Phil. Trans. R. Soc. A (2011)*, 3768–3784. https://doi.org/10.1098/rsta.2011.0081

Pascual-Marqui, R. D., Michel, C. M., & Lehmann, D. (1994). Low resolution electromagnetic tomography : a new method for localizing electrical activity in the brain. *International Journal of Psychophysiology*, *8760*(94).

Pastor, M. A., Artieda, J., Arbizu, J., Marti-climent, J. M., Pen, I., & Masdeu, J. C. (2002). Activation of Human Cerebral and Cerebellar Cortex by Auditory Stimulation at 40 Hz, *22*(23), 10501–10506.

Patel, R., Jayatilleke, N., Broadbent, M., Chang, C.-K., Foskett, N., Gorrell, G., … Stewart, R. (2015). Negative symptoms in schizophrenia: a study in a large

clinical sample of patients using a novel automated method. *BMJ Open*, *5*(9), e007619. https://doi.org/10.1136/bmjopen-2015-007619

Patterson, J. V., Hetrick, W. P., Boutros, N. N., Jin, Y., Sandman, C., Stern, H., … Bunney, W. E. (2008). P50 sensory gating ratios in schizophrenics and controls: A review and data analysis. *Psychiatry Research*, *158*(2), 226–247. https://doi.org/10.1016/j.psychres.2007.02.009

Paus, T. (2005). Mapping brain maturation and cognitive development during adolescence. *Trends in Cognitive Sciences*, *9*(2), 60–68. https://doi.org/10.1016/j.tics.2004.12.008

Phillips, K. G., & Uhlhaas, P. J. (2015). Neural oscillations as a translational tool in schizophrenia research: Rationale, paradigms and challenges. *Journal of Psychopharmacology*, *29*(2), 155–168. https://doi.org/10.1177/0269881114562093

Picard, H., Amado, I., Mouchet-Mages, S., Olié, J. P., & Krebs, M. O. (2008). The role of the cerebellum in schizophrenia: An update of clinical, cognitive, and functional evidences. *Schizophrenia Bulletin*, *34*(1), 155–172. https://doi.org/10.1093/schbul/sbm049

Pinheiro, J., Bates, D., DebRoy, S., & RCoreTeam. (2011). Package ‘ nlme .’ *CRAN*, *3.1-98*.

Poels, E. M. P., Kegeles, L. S., Kantrowitz, J. T., Javitt, D. C., Lieberman, J. A., Abi-dargham, A., & Girgis, R. R. (2014). Glutamatergic abnormalities in schizophrenia : A review of proton MRS fi ndings. *Schizophrenia Research*, *152*(2–3), 325–332. https://doi.org/10.1016/j.schres.2013.12.013

Popov, T. G., Rockstroh, B. S., Popova, P., Carolus, A. M., & Miller, G. A. (2014). Dynamics of alpha oscillations elucidate facial affect recognition in schizophrenia, 364–377. https://doi.org/10.3758/s13415-013-0194-2

Pratt, J., Dawson, N., Morris, B. J., Grent-’t-Jong, T., Roux, F., & Uhlhaas, P. J. (2017). Thalamo-cortical communication, glutamatergic neurotransmission and neural oscillations: A unique window into the origins of ScZ? *Schizophrenia Research*, *180*, 4–12. https://doi.org/10.1016/j.schres.2016.05.013

Premoli, I., Bergmann, T. O., Fecchio, M., Rosanova, M., Biondi, A., Belardinelli, P., & Ziemann, U. (2017). NeuroImage The impact of GABAergic drugs on TMS-induced brain oscillations in human motor cortex. *NeuroImage*, *163*(March), 1–12. https://doi.org/10.1016/j.neuroimage.2017.09.023

Radeloff, D., Ciaramidaro, A., Siniatchkin, M., Hainz, D., Schlitt, S., Weber, B., … Freitag, C. M. (2014). Structural alterations of the social brain: A comparison between schizophrenia and autism. *PLoS ONE*, *9*(9), 1–9. https://doi.org/10.1371/journal.pone.0106539

Ramantani, G., Boor, R., Paetau, R., Ille, N., Feneberg, R., Rupp, A., … Bast, T. (2006). MEG versus EEG: Influence of background activity on interictal spike detection. *Journal of Clinical Neurophysiology*, *23*(6), 498–508. https://doi.org/10.1097/01.wnp.0000240873.69759.cc

Ramyead, A., Kometer, M., Studerus, E., Koranyi, S., Ittig, S., Gschwandtner,

U., … Riecher-Rössler, A. (2015). Aberrant Current Source-Density and Lagged Phase Synchronization of Neural Oscillations as Markers for Emerging Psychosis. *Schizophrenia Bulletin*, *41*(4), 919–929. https://doi.org/10.1093/schbul/sbu134

Ramyead, A., Studerus, E., Kometer, M., Uttinger, M., Gschwandtner, U., Fuhr, P., & Riecher-Rössler, A. (2016). Prediction of psychosis using neural oscillations and machine learning in neuroleptic-naïve at-risk patients. *World Journal of Biological Psychiatry*, *17*(4), 285–295. https://doi.org/10.3109/15622975.2015.1083614

Rass, O., Forsyth, J., & Krishnan, G. (2012). Auditory Steady State Response in the Schizophrenia, First- Degree Relatives, and Schizotypal Personality Disorder. *Schizophrenia Research*, *136*, 143–149. https://doi.org/10.1016/j.schres.2012.01.003.Auditory

Rass, O., Krishnan, G., Brenner, C. a., Hetrick, W. P., Merrill, C. C., Shekhar, A., & O'Donnell, B. F. (2010). Auditory steady state response in bipolar disorder: Relation to clinical state, cognitive performance, medication status, and substance disorders. *Bipolar Disorders*, *12*(8), 793–803. https://doi.org/10.1111/j.1399-5618.2010.00871.x

Rauschecker, J. P., & Scott, S. K. (2009). Maps and streams in the auditory cortex : nonhuman primates illuminate human speech processing, *12*(6), 718–725. https://doi.org/10.1038/nn.2331

Raznahan, A., Lee, Y., Stidd, R., Long, R., Greenstein, D., Clasen, L., … Giedd, J. N. (2010). Longitudinally mapping the influence of sex and androgen signaling on the dynamics of human cortical maturation in adolescence. *Proceedings of the National Academy of Sciences*, *107*(39), 16988–16993. https://doi.org/10.1073/pnas.1006025107

Rebollo, B., Perez-zabalza, M., Ruiz-mejias, M., Perez-mendez, L., & Sanchez-vives, M. V. (2018). N EUROSCIENCE Beta and Gamma Oscillations in Prefrontal Cortex During NMDA Hypofunction : An In Vitro Model of Schizophrenia Features. *Neuroscience*, *383*, 138–149. https://doi.org/10.1016/j.neuroscience.2018.04.035

Reyes, S. A., Lockwood, A. H., Salvi, R. J., Coad, M. Lou, Wack, D. S., & Burkard, R. F. (2005). Mapping the 40-Hz auditory steady-state response using current density reconstructions. *Hearing Research*, *204*(1–2), 1–15. https://doi.org/10.1016/j.heares.2004.11.016

Rice, D. M., Potkin, S. G., Jin, Y., Isenhart, R., Heh, C. W. C., Sramek, J., … Sandman, C. A. (1989). EEG alpha photic driving abnormalities in chronic schizophrenia. *Psychiatry Research*, *30*(3), 313–324. https://doi.org/10.1016/0165-1781(89)90022-X

Richards, T. L., Gates, G. a, Gardner, J. C., Merrill, T., Hayes, C. E., Panagiotides, H., … Rubel, E. W. (1997). Functional MR spectroscopy of the auditory cortex in healthy subjects and patients with sudden hearing loss. *AJNR. American Journal of Neuroradiology*, *18*(4), 611–620.

Riečanskỳ, I., Kašpárek, T., Řehulová, J., Katina, S., & Přikryl, R. (2010). Aberrant EEG responses to gamma-frequency visual stimulation in

schizophrenia. *Schizophrenia Research*, *124*(1–3), 101–109. https://doi.org/10.1016/j.schres.2010.06.022

Riecher-Rössler, A., Gschwandtner, U., Aston, J., Borgwardt, S., Drewe, M., Fuhr, P., … Stieglitz, R. D. (2007). The Basel early-detection-of-psychosis (FEPSY)-study - Design and preliminary results. *Acta Psychiatrica Scandinavica*, *115*(2), 114–125. https://doi.org/10.1111/j.1600-0447.2006.00854.x

Riley, E. M., McGovern, D., Mockler, D., Doku, V. C. K., Óceallaigh, S., Fannon, D. G., … Sharma, T. (2000). Neuropsychological functioning in first-episode psychosis - Evidence of specific deficits. *Schizophrenia Research*, *43*(1), 47–55. https://doi.org/10.1016/S0920-9964(99)00177-2

Ripke, S., Neale, B. M., Corvin, A., Walters, J. T. R., Farh, K.-H., Holmans, P. a., … O'Donovan, M. C. (2014). Biological insights from 108 schizophrenia-associated genetic loci. *Nature*, *511*, 421–427. https://doi.org/10.1038/nature13595

Roa Romero, Y., Keil, J., Balz, J., Niedeggen, M., Gallinat, J., & Senkowski, D. (2016). Alpha-Band Oscillations Reflect Altered Multisensory Processing of the McGurk Illusion in Schizophrenia. *Frontiers in Human Neuroscience*, *10*(February), 1–12. https://doi.org/10.3389/fnhum.2016.00041

Roach, B. J., Ford, J. M., Hoffman, R. E., & Mathalon, D. H. (2013). Converging Evidence for Gamma Synchrony Deficits in Schizophrenia. *Suppl Clin Neurophysiol*, *62*, 163–180.

Rojas, D., Teale, P., Maharajh, K., Kronberg, E., Youngpeter, K., Wilson, L., … Hepburn, S. (2011). Transient and steady-state auditory gamma-band responses in first-degree relatives of people with autism spectrum disorder. *Molecular Autism*, *2*(1), 11. https://doi.org/10.1186/2040-2392-2-11

Rorden, C., & Brett, M. (2000). Stereotaxic display of brain lesions. *Behavioural Neurology*, *12*(4), 191–200. https://doi.org/10.1155/2000/421719

Rosburg, T., Trautner, P., Elger, C. E., & Kurthen, M. (2009). NeuroImage Attention effects on sensory gating — Intracranial and scalp recordings. *NeuroImage*, *48*(3), 554–563. https://doi.org/10.1016/j.neuroimage.2009.06.063

Rosenberg, M. D., Finn, E. S., Scheinost, D., Papademetris, X., Shen, X., Constable, R. T., … Haven, N. (2016). A neuromarker of sustained attention from whole-brain functional connectivity. *Nature Neuroscience*, *19*(1), 165–171. https://doi.org/10.1038/nn.4179.A

Ross, B., Herdman, A. T., & Pantev, C. (2005). Right hemispheric laterality of human 40 Hz auditory steady-state responses. *Cerebral Cortex*, *15*(12), 2029–2039. https://doi.org/10.1093/cercor/bhi078

Rössler, W., Joachim Salize, H., Van Os, J., & Riecher-Rössler, A. (2005). Size of burden of schizophrenia and psychotic disorders. *European Neuropsychopharmacology*, *15*(4), 399–409. https://doi.org/10.1016/j.euroneuro.2005.04.009

Rowland, L. M., Kontson, K., West, J., Edden, R. A., Zhu, H., Wijtenburg, S. A.,

… Barker, P. B. (2013). In vivo measurements of glutamate, GABA, and NAAG in schizophrenia. *Schizophrenia Bulletin*, *39*(5), 1096–1104. https://doi.org/10.1093/schbul/sbs092

Rudy, B., Fishell, G., Lee, S. H., & Hjerling-Leffler, J. (2011). Three groups of interneurons account for nearly 100% of neocortical GABAergic neurons. *Developmental Neurobiology*, *71*(1), 45–61. https://doi.org/10.1002/dneu.20853

Rueckert, L., & Grafman, J. (1996). Sustained attention deficits in patients with right frontal lesions, *34*(96), 953–963.

Ruhrmann, S., Schultze-Lutter, F., & Klosterkötter, J. (2010). Probably at-risk, but certainly ill - Advocating the introduction of a psychosis spectrum disorder in DSM-V. *Schizophrenia Research*, *120*(1–3), 23–37. https://doi.org/10.1016/j.schres.2010.03.015

Rummel-Kluge, C., Komossa, K., Schwarz, S., Hunger, H., Schmid, F., Lobos, C. A., … Leucht, S. (2010). Head-to-head comparisons of metabolic side effects of second generation antipsychotics in the treatment of schizophrenia: A systematic review and meta-analysis. *Schizophrenia Research*, *123*(2–3), 225–233. https://doi.org/10.1016/j.schres.2010.07.012

Salisbury, D. F., Shenton, M. E., Griggs, C. B., Bonner-Jackson, A., & McCarley, R. W. (2003). Mismatch Negativity in Chronic Schizophrenia and First-Episode Schizophrenia. *Archives of General Psychiatry*, *59*(8), 686. https://doi.org/10.1001/archpsyc.59.8.686

Schaefer, J., Giangrande, E., Weinberger, D. R., & Dickinson, D. (2013). The global cognitive impairment in schizophrenia: Consistent over decades and around the world. *Schizophrenia Research*, *150*(1), 42–50. https://doi.org/10.1016/j.schres.2013.07.009

Schäppi, L., Stegmayer, K., Viher, P. V., & Walther, S. (2018). Distinct associations of motor domains in relatives of schizophrenia patients-different pathways to motor abnormalities in schizophrenia? *Frontiers in Psychiatry*, *9*(APR), 1–12. https://doi.org/10.3389/fpsyt.2018.00129

Schneider, M., & Koch, M. (2005). Deficient social and play behavior in juvenile and adult rats after neonatal cortical lesion: Effects of chronic pubertal cannabinoid treatment. *Neuropsychopharmacology*, *30*(5), 944–957. https://doi.org/10.1038/sj.npp.1300634

Schoffelen, J. M., & Gross, J. (2009). Source connectivity analysis with MEG and EEG. *Human Brain Mapping*, *30*(6), 1857–1865. https://doi.org/10.1002/hbm.20745

Schretlen, D. J., Cascella, N. G., Meyer, S. M., Kingery, L. R., Testa, S. M., Munro, C. A., … Pearlson, G. D. (2007). Neuropsychological Functioning in Bipolar Disorder and Schizophrenia. *Biological Psychiatry*, *62*(2), 179–186. https://doi.org/10.1016/j.biopsych.2006.09.025

Schultz, S. H., North, S. W., & Shields, C. G. (2007). Schizophrenia: A Review. *American Family Physician (AAFP)*. Retrieved from http://www.aafp.org/afp/2007/0615/p1821.html

Schultze-Lutter, F. (2009). Subjective symptoms of schizophrenia in research and the clinic: The basic symptom concept. *Schizophrenia Bulletin*, *35*(1), 5–8. https://doi.org/10.1093/schbul/sbn139

Selemon, L. D., & Zecevic, N. (2015). Schizophrenia : a tale of two critical periods for prefrontal cortical development. *Translational Psychiatry*, *5*(8), e623-11. https://doi.org/10.1038/tp.2015.115

Senkowski, D., & Gallinat, J. (2015). Dysfunctional prefrontal gamma-band oscillations reflect working memory and other cognitive deficits in schizophrenia. *Biological Psychiatry*, *77*(12), 1010–1019. https://doi.org/10.1016/j.biopsych.2015.02.034

Seth, A. K., Barrett, A. B., & Barnett, L. (2015). Granger Causality Analysis in Neuroscience and Neuroimaging. *Journal of Neuroscience*, *35*(8), 3293–3297. https://doi.org/10.1523/JNEUROSCI.4399-14.2015

Shad, M. U., Keshavan, M. S., Steinberg, J. L., Mihalakos, P., Thomas, B. P., Motes, M. A., … Tamminga, C. A. (2012). Neurobiology of self-awareness in schizophrenia: An fMRI study. *Schizophrenia Research*, *138*(2–3), 113–119. https://doi.org/10.1016/j.schres.2012.03.016

Sheehan, D. V, Lecrubier, Y., Sheehan, K. H., Amorim, P., Janavs, J., Weiller, E., … Dunbar, G. C. (1998). The Mini-International Neuropsychiatric Interview (M.I.N.I): The development and validation of a structured diagnostic psychiatric interview for DSM-IV and ICD-10. *The Journal of Clinical Psychiatry*. US: Physicians Postgraduate Press.

Sheffield, J. M., & Barch, D. M. (2016). Cognition and resting-state functional connectivity in schizophrenia. *Neuroscience and Biobehavioral Reviews*, *61*, 108–120. https://doi.org/10.1016/j.neubiorev.2015.12.007

Sheitman, B. B., Kraus, J. E., Bodfish, J. W., & Carmel, H. (2004). Are the negative symptoms of schizophrenia consistent with an autistic spectrum illness? *Schizophrenia Research*, *69*(1), 119–120. https://doi.org/10.1016/S0920-9964(03)00177-4

Shen, H., Wang, L., Liu, Y., & Hu, D. (2010). Discriminative analysis of resting-state functional connectivity patterns of schizophrenia using low dimensional embedding of fMRI. *NeuroImage*, *49*(4), 3110–3121. https://doi.org/10.1016/j.neuroimage.2009.11.011

Shergill, S. S., Murray, R. M., & McGuire, P. K. (1998). Auditory hallucinations: A review of psychological treatments. *Schizophrenia Research*, *32*(3), 137–150. https://doi.org/10.1016/S0920-9964(98)00052-8

Shin, Y. W., O'Donnell, B. F., Youn, S., & Kwon, J. S. (2011). Gamma oscillation in schizophrenia. *Psychiatry Investigation*, *8*(4), 288–296. https://doi.org/10.4306/pi.2011.8.4.288

Shrivastava, A., McGorry, P., Tsuang, M., Woods, S., Cornblatt, B., Corcoran, C., & Carpenter, W. (2011). "Attenuated psychotic symptoms syndrome" as a risk syndrome of psychosis, diagnosis in DSM-V: The debate. *Indian Journal of Psychiatry*, *53*(1), 57. https://doi.org/10.4103/0019-5545.75560

Shungu, D. C., Mao, X., Gu, M., Milak, M. S., Weiduschat, N., Mayer, D., …

Kegeles, L. S. (2013). 'Glx' Measured by J-editing/MEGA-PRESS is Primarily 'Pure' Glutamate…Or is it? *Proc. Intl. Soc. Mag. Reson. Med.*, *21*, 4346.

Siegel, M., Donner, T. H., & Engel, A. K. (2012). Spectral fingerprints of large-scale neuronal interactions. *Nature Reviews Neuroscience*, *13*(2), 121–134. https://doi.org/10.1038/nrn3137

Sies, H. (1996). PHYSIOLOGICAL SOCIETY SYMPOSIUM : IMPAIRED ENDOTHELIAL AND SMOOTH MUSCLE CELL FUNCTION IN OXIDATIVE STRESS OXIDATIVE STRESS : OXIDANTS AND ANTIOXIDANTS.

Sigurdsson, T. (2016). Neural circuit dysfunction in schizophrenia: Insights from animal models. *Neuroscience*, *321*, 42–65. https://doi.org/10.1016/j.neuroscience.2015.06.059

Simon, A. E., Grädel, M., Cattapan-Ludewig, K., Gruber, K., Ballinari, P., Roth, B., & Umbricht, D. (2012). Cognitive functioning in at-risk mental states for psychosis and 2-year clinical outcome. *Schizophrenia Research*, *142*(1–3), 108–115. https://doi.org/10.1016/j.schres.2012.09.004

Singh, I., & Rose, N. (2009). Biomarkers in psychiatry, *460*(July).

Sivarao, D. V. (2015). The 40-Hz auditory steady-state response: a selective biomarker for cortical NMDA function. *Annals of the New York Academy of Sciences*, *1344*(1), 27–36. https://doi.org/10.1111/nyas.12739

Sivarao, D. V., Chen, P., Senapati, A., Yang, Y., Fernandes, A., Benitex, Y., … Ahlijanian, M. K. (2016). 40 Hz Auditory Steady-State Response Is a Pharmacodynamic Biomarker for Cortical NMDA Receptors. *Neuropsychopharmacology*, *41*(9), 2232–2240. https://doi.org/10.1038/npp.2016.17

Sivarao, D. V., Frenkel, M., Chen, P., Healy, F. L., Lodge, N. J., & Zaczek, R. (2013). MK-801 disrupts and nicotine augments 40 Hz auditory steady state responses in the auditory cortex of the urethane-anesthetized rat. *Neuropharmacology*, *73*, 1–9. https://doi.org/10.1016/j.neuropharm.2013.05.006

Skosnik, P. D., Krishnan, G. P., & Donnell, B. F. O. (2007). The effect of selective attention on the gamma-band auditory steady-state response, *420*, 223–228. https://doi.org/10.1016/j.neulet.2007.04.072

Sohal, V. S., Zhang, F., Yizhar, O., & Deisseroth, K. (2009). Parvalbumin neurons and gamma rhythms enhance cortical circuit performance. *Nature*, *459*(7247), 698–702. https://doi.org/10.1038/nature07991

Solis-Escalante, T., Müller-Putz, G. R., Pfurtscheller, G., & Neuper, C. (2012). Cue-induced beta rebound during withholding of overt and covert foot movement. *Clinical Neurophysiology*, *123*(6), 1182–1190. https://doi.org/10.1016/j.clinph.2012.01.013

Sommer, I. E. C., Diederen, K. M. J., Blom, J. D., Willems, A., Kushan, L., Slotema, K., … Kahn, R. S. (2008). Auditory verbal hallucinations predominantly activate the right inferior frontal area. *Brain*, *131*(12), 3169–3177. https://doi.org/10.1093/brain/awn251

Spellman, T. J., & Gordon, J. A. (2015). Synchrony in schizophrenia: A window into circuit-level pathophysiology. *Current Opinion in Neurobiology*, *30*, 17–23. https://doi.org/10.1016/j.conb.2014.08.009

Spencer, K. M. (2008). Visual Gamma Oscillations in Schizophrenia: Implications for Understanding Neural Circuitry Abnormalities. *Clinical EEG and Neuroscience*, *39*(2), 65–68. https://doi.org/10.1177/155005940803900208

Spencer, K. M. (2012). Baseline gamma power during auditory steady-state stimulation in schizophrenia. *Frontiers in Human Neuroscience*, *5*(January), 1–7. https://doi.org/10.3389/fnhum.2011.00190

Spencer, K. M., Niznikiewicz, M. a, Nestor, P. G., Shenton, M. E., & McCarley, R. W. (2009). Left auditory cortex gamma synchronization and auditory hallucination symptoms in schizophrenia. *BMC Neuroscience*, *10*(1), 85. https://doi.org/10.1186/1471-2202-10-85

Spencer, K. M., Salisbury, D. F., Shenton, M. E., & McCarley, R. W. (2008). γ-Band Auditory Steady-State Responses Are Impaired in First Episode Psychosis. *Biological Psychiatry*, *64*(5), 369–375. https://doi.org/10.1016/j.biopsych.2008.02.021

Steinmann, S., Leicht, G., Ertl, M., Andreou, C., Polomac, N., Westerhausen, R., … Mulert, C. (2014). Conscious auditory perception related to long-range synchrony of gamma oscillations. *NeuroImage*, *100*, 435–443. https://doi.org/10.1016/j.neuroimage.2014.06.012

Stephan, K. E., Friston, K. J., & Frith, C. D. (2009). Dysconnection in Schizophrenia : From Abnormal Synaptic Plasticity to Failures of Self-monitoring, *35*(3), 509–527. https://doi.org/10.1093/schbul/sbn176

Stone, J. M., Morrison, P. D., & Pilowsky, L. S. (2007). Glutamate and dopamine dysregulation in schizophrenia - A synthesis and selective review. *Journal of Psychopharmacology*, *21*(4), 440–452. https://doi.org/10.1177/0269881106073126

Sullivan, E. M., Timi, P., Hong, L. E., & O'Donnell, P. (2015). Effects of NMDA and GABA-A Receptor Antagonism on Auditory Steady-State Synchronization in Awake Behaving Rats. *International Journal of Neuropsychopharmacology*, *18*(7), pyu118-pyu118. https://doi.org/10.1093/ijnp/pyu118

Sun, D., van Erp, T. G. M., Thompson, P. M., Bearden, C. E., Daley, M., Kushan, L., … Cannon, T. D. (2009). Elucidating a Magnetic Resonance Imaging-Based Neuroanatomic Biomarker for Psychosis: Classification Analysis Using Probabilistic Brain Atlas and Machine Learning Algorithms. *Biological Psychiatry*, *66*(11), 1055–1060. https://doi.org/10.1016/j.biopsych.2009.07.019

Tada, M., Nagai, T., Kirihara, K., Koike, S., Suga, M., Araki, T., … Kasai, K. (2016). Differential Alterations of Auditory Gamma Oscillatory Responses Between Pre-Onset High-Risk Individuals and First-Episode Schizophrenia, (March), 1027–1035. https://doi.org/10.1093/cercor/bhu278

Tan, H.-R. M., Gross, J., & Uhlhaas, P. J. (2015a). MEG—measured auditory

steady-state oscillations show high test–retest reliability: A sensor and source-space analysis. *NeuroImage*, *122*, 417–426. https://doi.org/10.1016/j.neuroimage.2015.07.055

Tan, H.-R. M., Gross, J., & Uhlhaas, P. J. (2015b). MEG—measured auditory steady-state oscillations show high test–retest reliability: A sensor and source-space analysis. *NeuroImage*, *122*, 417–426. https://doi.org/10.1016/j.neuroimage.2015.07.055

Tandon, N., Bolo, N. R., Sanghavi, K., Mathew, I. T., Francis, A. N., Stanley, J. A., & Keshavan, M. S. (2013). Brain metabolite alterations in young adults at familial high risk for schizophrenia using proton magnetic resonance spectroscopy. *Schizophrenia Research*, *148*(1–3), 59–66. https://doi.org/10.1016/j.schres.2013.05.024

Tandon, R., Gaebel, W., Barch, D. M., Bustillo, J., Gur, R. E., Heckers, S., … Carpenter, W. (2013). De fi nition and description of schizophrenia in the DSM-5, *150*, 3–10. https://doi.org/10.1016/j.schres.2013.05.028

Tandon, R., Keshavan, M. S., & Nasrallah, H. a. (2008). Schizophrenia, “just the facts” what we know in 2008. 2. Epidemiology and etiology. *Schizophrenia Research*, *102*(1–3), 1–18. https://doi.org/10.1016/j.schres.2008.04.011

Tauscher, J., Fischer, P., Neumeister, A., & Rappelsberger, P. (1998). Low Frontal Electroencephalographic Coherence in Neuroleptic-Free Schizophrenic Patients, *3223*(97).

Taylor, S. F., & Tso, I. F. (2014). GABA abnormalities in schizophrenia: A methodological review of in vivo studies. *Schizophrenia Research*, *167*(1–3), 84–90. https://doi.org/10.1016/j.schres.2014.10.011

Tayoshi, S., Nakataki, M., Sumitani, S., Taniguchi, K., Shibuya-Tayoshi, S., Numata, S., … Ohmori, T. (2010). GABA concentration in schizophrenia patients and the effects of antipsychotic medication: A proton magnetic resonance spectroscopy study. *Schizophrenia Research*, *117*(1), 83–91. https://doi.org/10.1016/j.schres.2009.11.011

Teale, P., Collins, D., Maharajh, K., Rojas, D. C., & Kronberg, E. (2009). are Different in Schizophrenia. *October*, *42*(4), 1481–1489. https://doi.org/10.1016/j.neuroimage.2008.06.020.Cortical

Teale, P., Collins, D., Maharajh, K., Rojas, D. C., Kronberg, E., & Reite, M. (2008). Cortical source estimates of gamma band amplitude and phase are different in schizophrenia. *NeuroImage*, *42*(4), 1481–1489. https://doi.org/10.1016/j.neuroimage.2008.06.020

Théberge, J., Al-Semaan, Y., Williamson, P. C., Menon, R. S., Neufeld, R. W. J., Rajakumar, N., … Drost, D. J. (2003). CONTRAlign: Discriminative training for protein sequence alignment. *Glutamate and Glutamine in the Anterior Cingulate and Thalamus of Medicated Patients With Chronic Schizophrenia and Healthy Comparison Subjects Measured With 4.0-T Proton MRS*, *3909 LNBI*, 160–174. https://doi.org/10.1007/11732990_15

Thuné, H., Recasens, M., & Uhlhaas, P. J. (2016). The 40-Hz Auditory Steady-State Response in Patients With Schizophrenia. *JAMA Psychiatry*, *73*(11),

1145–1153. https://doi.org/10.1001/jamapsychiatry.2016.2619

Tlumak, A. I., Rubinstein, E., & Durrant, J. D. (2007). Meta-analysis of variables that affect accuracy of threshold estimation via measurement of the auditory steady-state response (ASSR). *International Journal of Audiology*, *46*(11), 692–710. https://doi.org/10.1080/14992020701482480

Todorovic, A., Schoffelen, J., Ede, F. Van, Maris, E., & De, F. P. (2016). Temporal Expectation and Attention Jointly Modulate Auditory Oscillatory Activity in the Beta Band. *PLoS ONE*, *10*(3), 1–16. https://doi.org/10.7910/DVN/27955

Torrey, E. F. (2007). Schizophrenia and the inferior parietal lobule. *Schizophrenia Research*, *97*(1–3), 215–225. https://doi.org/10.1016/j.schres.2007.08.023

Tsuchimoto, R., Kanba, S., Hirano, S., Oribe, N., Ueno, T., Hirano, Y., … Onitsuka, T. (2011). Reduced high and low frequency gamma synchronization in patients with chronic schizophrenia. *Schizophrenia Research*, *133*(1), 99–105. https://doi.org/10.1016/j.schres.2011.07.020

Tzourio-Mazoyer, N., Landeau, B., Papathanassiou, D., Crivello, F., Etard, O., Delcroix, N., … Joliot, M. (2002). Automated anatomical labeling of activations in SPM using a macroscopic anatomical parcellation of the MNI MRI single-subject brain. *NeuroImage*, *15*(1), 273–289. https://doi.org/10.1006/nimg.2001.0978

Uddin, L. Q., Molnar-Szakacs, I., Zaidel, E., & Iacoboni, M. (2006). rTMS to the right inferior parietal lobule disrupts self-other discrimination. *Social Cognitive and Affective Neuroscience*, *1*(1), 65–71. https://doi.org/10.1093/scan/nsl003

Uhlhaas, P. J. (2013). Dysconnectivity, large-scale networks and neuronal dynamics in schizophrenia. *Current Opinion in Neurobiology*, *23*(2), 283–290. https://doi.org/10.1016/j.conb.2012.11.004

Uhlhaas, P. J., Gajwani, R., Gross, J., Gumley, A. I., Lawrie, S. M., & Schwannauer, M. (2017). The Youth Mental Health Risk and Resilience Study (YouR-Study). *BMC Psychiatry*, *17*(1), 1–8. https://doi.org/10.1186/s12888-017-1206-5

Uhlhaas, P. J., Linden, D. E. J., Singer, W., Haenschel, C., Lindner, M., Maurer, K., & Rodriguez, E. (2006). Dysfunctional Long-Range Coordination of Neural Activity during Gestalt Perception in Schizophrenia, *26*(31), 8168–8175. https://doi.org/10.1523/JNEUROSCI.2002-06.2006

Uhlhaas, P. J., & Singer, W. (2010). Abnormal neural oscillations and synchrony in schizophrenia. *Nature Reviews Neuroscience*, *11*(2), 100–113. https://doi.org/10.1038/nrn2774

Uhlhaas, P. J., & Singer, W. (2011). The Development of Neural Synchrony and Large-Scale Cortical Networks During Adolescence: Relevance for the Pathophysiology of Schizophrenia and Neurodevelopmental Hypothesis. *Schizophrenia Bulletin*, *37*(3), 514–523. https://doi.org/10.1093/schbul/sbr034

Uhlhaas, P. J., & Singer, W. (2014). Oscillations and Neuronal Dynamics in Schizophrenia: The Search for Basic Symptoms and Translational Opportunities. *Biological Psychiatry*, *77*(12), 1001–1009. https://doi.org/10.1016/j.biopsych.2014.11.019

Van Der Meer, L., De Vos, A. E., Stiekema, A. P. M., Pijnenborg, G. H. M., Van Tol, M. J., Nolen, W. A., … Aleman, A. (2013). Insight in schizophrenia: Involvement of self-reflection networks? *Schizophrenia Bulletin*, *39*(6), 1352–1362. https://doi.org/10.1093/schbul/sbs122

van Kerkoerle, T., Self, M. W., Dagnino, B., Gariel-Mathis, M.-A., Poort, J., van der Togt, C., & Roelfsema, P. R. (2014). Alpha and gamma oscillations characterize feedback and feedforward processing in monkey visual cortex. *Proceedings of the National Academy of Sciences*, *111*(40), 14332–14341. https://doi.org/10.1073/pnas.1402773111

van Lutterveld, R., Hillebrand, A., Diederen, K. M. J., Daalman, K., Kahn, R. S., Stam, C. J., & Sommer, I. E. C. (2012). Oscillatory cortical network involved in auditory verbal hallucinations in Schizophrenia. *PLoS ONE*, *7*(7). https://doi.org/10.1371/journal.pone.0041149

Van Veen, B. D., Van Drongelen, W., Yuchtman, M., & Suzuki, A. (1997). Localization of brain electrical activity via linearly constrained minimum variance spatial filtering. *IEEE Transactions on Biomedical Engineering*, *44*(9), 867–880. https://doi.org/10.1109/10.623056

Vierling-Claassen, D., Siekmeier, P., Stufflebeam, S., & Kopell, N. (2008). Modeling GABA alterations in schizophrenia: A link between impaired inhibition and altered gamma and beta range auditory entrainment. *Journal of Neurophysiology*, *99*(5), 2656–2671. https://doi.org/10.1152/jn.00870.2007

Vines, B. W., Schnider, N. M., & Schlaug, G. (2006). Testing for causality with transcranial direct current stimulation: pitch memory and the left supramarginal gyrus, *17*(10), 1047–1050. https://doi.org/10.1097/01.wnr.0000223396.05070.a2.Testing

Vohs, J. L., Chambers, R. A., O'Donnell, B. F., Krishnan, G. P., & Morzorati, S. L. (2012). Auditory steady state responses in a schizophrenia rat model probed by excitatory/inhibitory receptor manipulation. *International Journal of Psychophysiology*, *86*(2), 136–142. https://doi.org/10.1016/j.ijpsycho.2012.04.002

Vrba, J., & Robinson, S. E. (2000). The effect of environmental noise of magnetometer- and gradiometer-based {M}{E}{G} systems. *Biomag 2000, 12th Int. Conf. on Biomagnetism, Aug 13 to 17, 2000, Helsinki Univ. of Technology, Espoo, Finland*, 3–6.

Wacongne, C. (2016). A predictive coding account of MMN reduction in schizophrenia. *Biological Psychology*, *116*, 68–74. https://doi.org/10.1016/j.biopsycho.2015.10.011

Wagner, J., Wessel, J. R., Ghahremani, A., & Aron, A. R. (2017). Establishing a Right Frontal Beta Signature for Stopping Action in Scalp EEG: Implications for Testing Inhibitory Control in Other Task Contexts. *Journal of Cognitive*

Neuroscience, *30*(1), 107–118. https://doi.org/10.1162/jocn_a_01183

Wang, J., Wang, J., Tang, Y., Zhang, T., Cui, H., Xu, L., … Zhang, J. (2016). Reduced γ-Aminobutyric Acid and Glutamate+Glutamine Levels in Drug-Naïve Patients with First-Episode Schizophrenia but Not in Those at Ultrahigh Risk. *Neural Plasticity*, *2016*. https://doi.org/10.1155/2016/3915703

Ward, L. M. (2003). Synchronous neural oscillations and cognitive processes. *Trends in Cognitive Sciences*, *7*(12), 553–559. https://doi.org/10.1016/j.tics.2003.10.012

Wibral, M., Rahm, B., Rieder, M., Lindner, M., Vicente, R., & Kaiser, J. (2011). Transfer entropy in magnetoencephalographic data: Quantifying information flow in cortical and cerebellar networks. *Progress in Biophysics and Molecular Biology*, *105*(1–2), 80–97. https://doi.org/10.1016/j.pbiomolbio.2010.11.006

Wijtenburg, S. A., Yang, S., Fischer, B. A., & Rowland, L. M. (2015). In vivo assessment of neurotransmitters and modulators with magnetic resonance spectroscopy : Application to schizophrenia. *Neuroscience and Biobehavioral Reviews*, *51*, 276–295. https://doi.org/10.1016/j.neubiorev.2015.01.007

Wilson, T. W., Hernandez, O. O., Asherin, R. M., Teale, P. D., Reite, M. L., & Rojas, D. C. (2008). Cortical Gamma Generators Suggest Abnormal Auditory Circuitry in Early-Onset Psychosis, *18*(2), 371–378. https://doi.org/10.1093/cercor/bhm062.Cortical

Wilson, T. W., Rojas, D. C., Reite, M. L., Teale, P. D., & Rogers, S. J. (2007). Children and Adolescents with Autism Exhibit Reduced MEG Steady-State Gamma Responses. *Biological Psychiatry*, *62*(3), 192–197. https://doi.org/10.1016/j.biopsych.2006.07.002

Winterer, G., Coppola, R., Egan, M. F., Goldberg, T. E., & Weinberger, D. R. (2003). Functional and Effective Frontotemporal Connectivity and Genetic Risk for Schizophrenia. https://doi.org/10.1016/S0006-3223(03)00532-8

Wittorf, A., Wiedemann, G., Buchkremer, G., & Klingberg, S. (2007). Prediction of community outcome in schizophrenia 1 year after discharge from inpatient treatment. *European Archives of Psychiatry and Clinical Neuroscience*, *258*(1), 48–58. https://doi.org/10.1007/s00406-007-0761-z

Wong, D., Schranz, A. L., & Bartha, R. (2018). Optimized in vivo brain glutamate measurement using long - echo - time semi - LASER at 7 T, (July), 1–13. https://doi.org/10.1002/nbm.4002

Wood, S. J., Berger, Q., Velakoulis, D., Phillips, L. J., Mcqorry, P. D., Yung, A. R., … Pantelis, C. (2003). Proton Magnetic Resonance Spectroscopy in First Episode Psychosis and Ultra High-Risk Individuals, 831–844.

Wood, S. J., Kennedy, D., Phillips, L. J., Seal, M. L., Yücel, M., Nelson, B., … Pantelis, C. (2010). Hippocampal pathology in individuals at ultra-high risk for psychosis : A multi-modal magnetic resonance study. *NeuroImage*, *52*(1), 62–68. https://doi.org/10.1016/j.neuroimage.2010.04.012

Woodward, N. (2014). Resting-State Networks In Schizophrenia ., (November).

https://doi.org/10.2174/1568026611212210011

Wróbel, A. (2000). Beta activity : attention Andrzej Wróbel a carrier for visual. *Acta Neurobiol Exp (Wars)*, *60*(2), 247–260.

Wu, C., & Sun, D. (2015). GABA receptors in brain development, function, and injury. *Metabolic Brain Disease*, *30*(2), 367–379. https://doi.org/10.1007/s11011-014-9560-1

Wynn, J. K., Ph, D., Light, G. A., Ph, D., Breitmeyer, B., Ph, D., … Ph, D. (2005). Event-Related Gamma Activity in Schizophrenia Patients During a Visual Backward-Masking Task, (December), 2330–2336.

Yang, L. H., Wonpat-Borja, A. J., Opler, M. G., & Corcoran, C. M. (2010). Potential stigma associated with inclusion of the psychosis risk syndrome in the DSM-V: An empirical question. *Schizophrenia Research*, *120*(1–3), 42–48. https://doi.org/10.1016/j.schres.2010.03.012

Ying, J., Zhou, D., Lin, K., & Gao, X. (2015). Network Analysis of Functional Brain Connectivity Driven by Gamma-Band Auditory Steady-State Response in Auditory Hallucinations. *Journal of Medical and Biological Engineering*, *35*(1), 45–51. https://doi.org/10.1007/s40846-015-0004-0

Yoo, S. Y., Yeon, S., Choi, C., Kang, D., Lee, J., & Young, N. (2009). Proton magnetic resonance spectroscopy in subjects with high genetic risk of schizophrenia : Investigation of anterior cingulate , dorsolateral prefrontal cortex and thalamus. *Schizophrenia Research*, *111*(1–3), 86–93. https://doi.org/10.1016/j.schres.2009.03.036

Yoon, J. H., Maddock, R. J., Rokem, A., Silver, M. A., Minzenberg, M. J., Ragland, J. D., & Carter, C. S. (2010). GABA Concentration Is Reduced in Visual Cortex in Schizophrenia and Correlates with Orientation-Specific Surround Suppression. *Journal of Neuroscience*, *30*(10), 3777–3781. https://doi.org/10.1523/JNEUROSCI.6158-09.2010

Yung, A. R., Yuen, H. P., Berger, G., Francey, S., Hung, T. C., Nelson, B., … McGorry, P. (2007). Declining transition rate in ultra high risk (prodromal) services: Dilution or reduction of risk? *Schizophrenia Bulletin*, *33*(3), 673–681. https://doi.org/10.1093/schbul/sbm015

Yung, A. R., Yuen, H. P., McGorry, P. D., Phillips, L. J., Kelly, D., Dell'Olio, M., … Buckby, J. (2005). Mapping the onset of psychosis: the Comprehensive Assessment of At-Risk Mental States. *The Australian and New Zealand Journal of Psychiatry*, *39*(11–12), 964–971. https://doi.org/10.1111/j.1440-1614.2005.01714.x

Yung, A. R., Yuen, H. P., Phillips, L. J., Francey, S., & McGorry, P. D. (2003). Mapping the onset of psychosis: The comprehensive assessment of at risk mental states (CAARMS). *Schizophrenia Research*, *60*(1), 30–31. https://doi.org/10.1016/S0920-9964(03)80090-7

Zhang, Y., Chen, Y., Bressler, S. L., & Ding, M. (2008). Response preparation and inhibition: The role of the cortical sensorimotor beta rhythm. *Neuroscience*, *156*(1), 238–246. https://doi.org/10.1016/j.neuroscience.2008.06.061

Zhang, Z., & Sun, Q. Q. (2011). *The Balance Between Excitation And Inhibition*

And Functional Sensory Processing In The Somatosensory Cortex. *International Review of Neurobiology* (Vol. 97). Elsevier Inc. https://doi.org/10.1016/B978-0-12-385198-7.00012-6

Zhou, T. H., Mueller, N. E., Spencer, K. M., Mallya, S. G., Lewandowski, K. E., Norris, L. A., … Hall, M. H. (2018). Auditory steady state response deficits are associated with symptom severity and poor functioning in patients with psychotic disorder. *Schizophrenia Research*, *201*, 278–286. https://doi.org/10.1016/j.schres.2018.05.027

Zoefel, B., & VanRullen, R. (2017). Oscillatory mechanisms of stimulus processing and selection in the visual and auditory systems: State-of-the-art, speculations and suggestions. *Frontiers in Neuroscience*, *11*(MAY), 1–13. https://doi.org/10.3389/fnins.2017.00296